The impact of sex and species of cells in herpes simplex virus infection

Yeu-Yang Tseng

April 2019

A thesis submitted for the degree of Doctor of Philosophy of The Australian National University

Declaration

The work in this thesis was performed at the Australian National University. To the best of my knowledge, this thesis contains no material, which has been accepted for the award of any other degree or diploma in any university. It does not contain material previously published or written by another person, except where reference is made in the text.

Yeu-Yang Tseng
April 2019

Acknowledgment

I still remember the first day I arrived in Canberra carrying a feminine suitcase (thanks my dear mom) alone in a bloody cold winter (2015). After wolfed down tasteless instant noodles, my supervisor Professor David Tscharke rescued me from my pity and uninhabited room by taking me to purchase basic life needs. This is how David is important for me during my PhD journey. Without his invaluable guidance and sometimes crazy ideas, this project would never have been accomplished. His door is always open to his students for scientific discussion. It is hard to express how grateful I am for having him as my PhD supervisor. I am really glad to have him as my supervisor as well as a friend.

My deep appreciation also goes to all the members of my supervisory panel, Dr. Si Ming Man, Dr. Gaétan Burgio and Dr. Michael Frese for their suggestion and support. They are not just like distant relatives turning up once a year at a family event during Christmas holidays. We discussed how to improve this project and shared ideas quite often. I would like to especially thank Dr. Si Ming Man for putting every effort into modifying my two manuscripts. I need to thank the other fantastic collaborator, Dr. Zhi-Ping Feng who transferred my wet-lab life into a semi-dry one. With her insight and expertise, we would be able to analyse our big data accurately and efficiently. I also thank all the members of the Tscharke lab: Stewart Smith, Inge Flesch, Tiffany Russell, Thilaga Velusamy, Anjali Gowripalan, Matthew Witney, Navneet Singh and Sherin. Their friendships and having morning tea together are the base for me to survive in this process.

Warm encouragements from Taiwan are always the cure for my homesickness. Dr. Wei-Li Hsu and Dr. Jui-Hung Shien are as supportive as they used to be since my college time. My sincere thanks also extend to Messi Chou and Strawberry Liao for talking nonsense with me and occupying my cherished times. It is my pleasure to meet Eden Chen in the toughest time in my life and I am profoundly grateful for you being understanding, supportive and always there.

Thank you my buddies in Canberra, George Yu and Aaron Sung, for doing grocery shopping every week with and fooling around the Australia together. Of course, I did not forget my dad and my brother who lured me with irresistibly sponsored (i.e. free) flight tickets to coming home and picked me up all the time at the airport in Taiwan.

Abstract

Herpes simplex virus type I (HSV-1) is a large, enveloped DNA virus which belongs to the Herpesviridae family. HSV-1 is a highly infectious human pathogen that contacts mucosal surfaces to initiate infection and causes a range of diseases from mild cold sores to keratitis and encephalitis. A growing number of studies point to a sex difference in the prevalence and severity of viral infections. However, the role for sex in herpes infection is unclear due to the complexity of factors involving in the manifestation of HSV diseases. Furthermore, many primary infections are asymptomatic, contributing to the difficulty of studying HSV infections in humans. The neurotropic properties of HSV make it harder to reach information from infected humans for investigating the immune mechanisms controlling reactivation of latent infection within sensory ganglia or central nervous system. Therefore, mouse models have been used extensively to understand multiple aspects of HSV pathogenesis. However, the molecular basis underpinning cross-species differences between humans and mice in response to HSV-1 infection is unknown. In this thesis, we asked whether these two factors, sex and species, may influence HSV-1 replication. Much progress towards these goals has been made using reductionist approaches such as *in vitro* cell cultures and in many situations this is the only way that cell-intrinsic mechanisms can be dissected.

We demonstrated that HSV-1 can adapt to specific sex and generate different mutations due to selective pressure derived from different sexes. Next, profiling of male and female transcriptomic programs revealed that the cytosolic sensing pathway is induced to a greater degree in female primary mouse skin cells (female cells), correlating with higher yields of infectious virions in male counterparts (male cells). In addition, female cells distinctively reactivated *Xist*, a critical component of X-inactivation, to silence the expression of the transcriptional repressor on the X chromosome, which thereby maintained higher innate immune responses and further explains the different growth phenotypes in HSV-1 replication between the two sexes. Collectively, we propose a model in which HSV-1 triggers a sex-specific regulation of antiviral response in the cytosolic sensing signalling via the control of *Xist*.

During investigation of the sex difference, we coincidently found that viperin, an interferon-stimulated gene (ISG), is upregulated in mouse but not in all tested human cells, which is related to previous findings in the field and encouraged us to comprehensively study human-mouse differences in HSV-1 infection. We show that the growth kinetics of HSV-1 differed substantially in human and mouse cells. A

computational pipeline was developed to analyse the cross-species RNA sequencing data, revealing over 60% of differentially regulated pathways between these two hosts in cell cultures. Strikingly, mouse cells upregulated more genes in the antiviral pathway driven by ISGs. To identify the key factor that influences the cross-species difference, we identified that Janus kinase 1 (Jak1) is essential for contributing to the human-mouse difference in HSV-1 replication. Lastly, we utilized virus mutants to show that HSV-1 vhs plays an important role to regulate JAK1 expression and therefore activation between human and mouse cells.

In summary, this thesis has expanded our understanding on basic differences of cell cultures that sex and species can affect scientific interpretations in virus infection. Furthermore, the results presented in this study provide rich resources to translate data between the two sexes or mouse experiments into the human disease.

Table of contents

List of figures

List of tables

Abbreviation

aa	Amino acids
ANOVA	A one-way analysis of variance
ANU	The Australian National University
APS	Ammonium Persulphate
ASFV	African swine fever virus
BSA	Bovine serum albumin
Casp8	Inhibiting caspase 8
cGAS	Cyclic guanosine monophosphate-adenosine monophosphate synthase
CHIKV	Chikungunya virus
CMC	Carboxymethylcellulose
CMV IE	Cytomegalovirus immediate-early
CNS	Central nervous system
CPE	Cytopathic effect
CPM	Counts per million
CRISPR	Clustered regularly spaced palindromic repeats
CT	Threshold cycle
DAI	The DNA-dependent activator of IRFs
DAPI	4,6-diamidino-2-phenylindole
DC	Dendritic cells
DENV	Dengue virus
DMEM	Dulbecco's modified Eagle medium
DMSO	Dimethyl sulfoxide
DNA	Deoxyribonucleic acid
dNTP	Deoxynucleotide triphosphate
DRG	Dorsal root ganglia
dsRNA	double-stranded RNA
E; β	Early
EBV	Epstein-Barr virus
ECL	Enzyme-linked chemiluminescence
EDTA	Ethylenediaminetetraacetic acid
EEEV	Equine encephalitis virus
eIF2α	Eukaryotic initiation factor 2α
ELISA	Enzyme-linked immunosorbent assay
ER	Endoplasmic reticulum
FBS	Foetal bovine serum
FDR	False discovery rate
Female cells	Primary mouse skin female cells

gB	Glycoprotein B
GBP	The guanylate nucleotide binding protein
gD	Glycoprotein D
gE	Glycoprotein E
GFP	Green fluorescent protein
gH	Glycoprotein H
GO	Gene ontology
HCF-1	Host cell factor 1
HCMV	Human cytomegalovirus
HCV	Hepatitis C virus
HDAC	Histone deacetylase
HFF	Primary human foreskin fibroblast cells
HHV8	The eighth human herpesvirus
HIV	Human immunodeficiency virus
HRP	Horseradish peroxidase
HSE	Herpes simplex encephalitis
HSV	Herpes simplex virus
ICP	Infected cell protein
IE; α	Immediate-early
IFI16	IFN-inducible protein 16
IFIT1	IFN-induced protein 65
IFITM1	IFN-induced transmembrane protein
IFN	Interferon
IFNAR	Type I IFN receptor
Ig	Immunoglobulin
IKK	Inhibitor of κB kinase
IL	Interleukin
INDELs	Small insertions and deletions
IRF1	Interferon regulatory factor 1
IRF3	Interferon regulatory factor 3
IRF7	Interferon regulatory factor 7
IRF9	Interferon regulatory factor 9
IR_L	Internal long repeats
IR_S	Internal short repeats
ISG	Interferon-stimulated gene
ISG15	IFN-stimulated protein
ISGF3	Interferon-stimulated gene factor 3
ISREs	IFN-stimulated response elements
JAK1	Janus kinae 1
JCSMR	John Curtin School of Medical Research

JEV	Japanese encephalitis virus
JNK	Jun amino-terminal kinase
kb	kilobase
kDa	kilodalton
KEGG	Kyoto Encyclopedia of Genes and Genomes
KSHV	Kaposi's sarcoma-associated herpesvirus
L; γ	Late
LAT	Latency associated transcript
LB	Luria-Bertani
LPS	Lipopolysaccharide
Male cells; MF	Primary mouse skin male cells
MAPK	Mitogen-activated protein kinase
MDA5	Melanoma differentiation-associated gene 5
MEM	Minimum essential medium
MHC	Major histocompatibility complex
miRNA	microRNA
MLKL	Mixed lineage kinase-like protein
MOI	Multiplicity of infection; plaque forming unit/cell
mRNA	messenger RNA
MX1	Myxovirus resistance 1
MX2	Myxovirus resistance 2
MyD	The myeloid differentiation primary response
NFκB	Nuclear factor kappa B
NK	Natural killer
NLRs	Nod-like receptors
NS	Non-structural
Oct-1	Octamer binding protein 1
ORFs	Open reading frames
pi	Post infection
PAMPs	Pathogen-associated molecular patterns
PBMC	Peripheral blood mononuclear cells
PBS	Phosphate buffered saline
PCA	Principal coordinate analysis
PE	Phycoerythrin
PFA	Paraformaldehyde
PFU	Plaque forming unit
PKR	Protein kinase R
PML	Promyelocytic leukemia protein
PRRs	Pathogen-recognition receptors
PRV	Pseudorabies virus

qPCR	Quantitative PCR
RABV	Rabies virus
RHIM	The RIP homotypic interaction motif
RIG-I	Retinoic acid-inducible gene I
RIN	RNA integrity number
RIP	Receptor-interacting proteins
RL	Long repeat
RLRs	RIG-I-like receptors
Rnaes L	Ribonuclease L
RNA-seq	RNA sequencing
ROAST	Rotation gene sets analysis
RPKM	Reads per kilobase of transcript per million mapped reads
r_{max}	maximum radius
rpm	Revolutions per minute
rRNA	Ribosomal RNA
RSAD2	Radical S-adenosyl methionine domain containing 2
RT	Reverse transcriptase
SAM	S-adenosyl-L-methionine
SDS	Sodium dodecyl sulphate
SDS-PAGE	Tris-glycine Sodium dodecyl sulfate polyacrylamide gel electrophoresi
SEM	Standard error of the mean
SINV	Sindbis virus
siRNA	Small interfering RNA
SNPs	Single nucleotide polymorphism
SOC	Super optimal broth with catabolite repression medium
STAT1	Signal transducer and activator of transcription 1
STAT2	Signal transducer and activator of transcription 2
STING	Stimulator of interferon genes
TAE	Tris-Acetate-EDTA
TAP	Transporter associated with antigen presentation
TBK1	TANK-binding kinase 1
TCR	α/β T-Cell receptors
TEMED	N-N-N'-N'-tetramethylethylenediamine
TFP	Mitochondrial trifunctional protein
TG	Trigeminal ganglia
Th1	T helper cell type 1
TIR	Toll/IL-1 receptor
TLR	Toll-like receptor
TNF-α	Tumour necrosis factor α
TRAF6	TNF receptor-associated factor 6

TRIF	TIR-domain-containing adapter-inducing interferon-β
TR_L	Terminal long repeats
TR_S	Terminal short repeats
UL	Unique long region of the HSV-1 genome
US	Unique short region of the HSV-1 genome
VACV	Vaccinia virus
vhs	virion host shutoff protein
vIRF1	The viral interferon regulatory factor 1
VP	Virion protein
VSV	Vesicular stomatitis virus
VZV	Varicella zoster virus
WB	Western blotting
WNV	West Nile virus
WR	Vaccinia virus strain Western Reserve
ZIKV	Zika virus
Δ	Deletion
5dl1.2	ICP27 null mutant
ΔSma	vhs function mutant
LJS1	ICP27/vhs double mutant
siControl	control siRNA
EIAV	Equine infectious anaemia virus
CTL	Cytotoxic T lymphocytes
GSEA	Gene set enrichment analysis
MEFs	Mouse embryonic fibroblasts
SVV	Simian varicella virus
eIFs	Eukaryotic initiation factors
UTRs	Untranslated regions

Chapter 1. Introduction

1.1 Herpes simplex virus

The herpes simplex virus (HSV) belongs to the family *Herpesviridae* and subfamily *Alphaherpesvirinae*. All viruses within the *Herpesviridae* share similar characteristics, such as particle morphology and have a large double-stranded (ds) DNA genome (Roizmann et al., 1992; Davison et al., 2009). Herpesviruses are classified as well by their similarities in gene arrangement and, particularly, by sequence similarity in the proteins that they encode. Thus, predicted protein sequence similarlity is certainly is an important defining characteristic of the alphaherpesviruses as well as all mammalian and avian herpesviruses. Viruses within the *Alphaherpesvirinae* can cause diseases in a wide range of animals, including humans, non-human primates, birds and fish (Davison, 2002). HSV-1 infection cycle occurs in lytic, latent and reactivation phases (Section 1.1.3). During the latent phase, there is no detectable infectious virus, whereas during lytic or reactivation phases, HSV-1 is transmissible (Stevens and Cook, 1971; Koelle and Corey, 2008).

1.1.1 HSV-1 virion and genome

The three-dimensional capsid structure has been investigated by electron cryomicroscopy at 8.5 angstrom resolution (Zhou et al., 2000). HSV-1 particles are approximately 150-200 nm in diameter (Grunewald et al., 2003). The outer surface of the nucleocapsid is icosahedral and is made up of 162 capsomeres. A lipid envelope containing glycoprotein spikes surrounds the capsid. The HSV-1 nucleocapsid is surrounded by a tegument and enclosed in an envelope formed from host cytoplasmic membranes. There are 11 different HSV-1 glycoproteins that protrude through the HSV-1 envelope (van Genderen et al., 1994; Grunewald et al., 2003).

The dsDNA genome is tightly packed into the nucleocapsid (Booy et al., 1991). The genome of HSV-1 is around 153 kb and has approximately 68% GC content. During HSV-1 infection, the virus expresses at least 74 proteins, although it has been speculated that there are about 94 putative open reading frames (ORFs) in the HSV-1 genome (Rajcani et al., 2004; McGeoch et al., 2006). The HSV-1 genome can be mainly divided into two major segments: unique long (UL) and unique short (US) regions (Figure 1-1). The UL region encodes around 56 distinct genes and the U_S region contains at least 12 ORFs (McGeoch et al., 1988; Watson et al., 2012). Each region is flanked by a pair of inverted repeats, named internal repeats (IR_L or IR_S), that are located at the junction between UL and US, as well as terminal repeats (TR_L or TR_S)

that are located at both ends of the genome. Two functional origins of replication are present, Ori_L in the middle of UL and two copies of Ori_S in the IR_S and TR_S, respectively (Stow, 1982). Additionally, the "a" sequence is a short repeat found at each terminus of the genome and also located as an inverted copy at the junction of the IR_L and IR_S components (Wagner and Summers, 1978).

Figure 1-1. Schematic diagram of HSV-1 genome. The HSV-1 genome can be majorly classified into two unique linked segments named UL and US. TR_L and IR_L are inverted repeats flanking UL and IR_S and TR_S are inverted repeats flanking US. The "a" region is a terminal redundancy found at the genome termini.

1.1.2 HSV-1 epidemiology and diseases

1.1.2.1 HSV-1 epidemiology

HSV-1 is one of the most wide-spread human pathogens. The seroprevalence rates are approximately 90% worldwide and around 76.5% in Australia (Wentworth and Alexander, 1971; Cunningham et al., 2006). Interestingly, age, sex and demography may influence prevalence of the disease (Howard et al., 2003). Earlier studies reported that the HSV-1 prevalence among females in Australia is higher than among males (Roest et al., 2001). One study reported that the HSV-1 prevalence among females was 80%, which was significantly higher than the prevalence in males (71%) (Cunningham et al., 2006). More recent global estimates of the prevalence and incidence HSV-1 infections have suggested that the prevalence varies widely by region and there is no statistically significant difference in prevalence between males and females among all age groups (Looker et al., 2015a). Contradictory conclusions among these publications may be due to different sample sizes, sample selection criteria and laboratory detection methods. Nevertheless, the high HSV-1 prevalence together with the broad spectrum and severity of HSV diseases highlights the importance of investigating the pathogenesis of HSV-1 so as to relieve the substantial medical burden resulting from HSV diseases.

1.1.2.2 Oral herpes

HSV-1 transmission primarily occurs via damaged skin or mucosal surfaces. Oral herpes infection is mainly transmitted by oral-to-oral contact through HSV-1 virions in saliva. Both primary lytic HSV-1 infection and subsequent reactivation events can be asymptomatic or symptomatic, depending on a range of factors, presumably including the immunological status of the host (Bustamante and Wade, 1991; Ramchandani et al., 2016).

The vast majority of symptomatic oral herpes manifest as mild cold sores and fever blisters, typically occurring around the mouth (Fatahzadeh and Schwartz, 2007). Symptoms often start with small blisters which eventually break open and produce sores and then heal themselves within a few weeks (Johnston and Corey, 2016). Mild or asymptomatic HSV-1 infection is most common.

1.1.2.3 Ocular herpes

Another major clinical problem caused by HSV-1 infections that involve the eye. Ocular herpes generally affects the top layer of the cornea and is usually cleared without any permanent problems. However, stromal keratitis is developed when the lesion gets into the layers of the cornea. This may result in scarring and loss of vision, especially with recurrent diseases (Chernakova et al., 2014; Zhu and Zhu, 2014). Recurrent ocular herpes is a major problem and a reason for repeated corneal transplants (Remeijer et al., 2009; Al-Dujaili et al., 2011).

1.1.2.4 Genital herpes

HSV-1 can also be transmitted to the genital area. Importantly, an increase in the frequency of genital herpes caused by HSV-1, compared with HSV-2 infection, has been reported over the past decades (Reina et al., 2005; Wald, 2006). Individuals who already have HSV-1 oral herpes are unlikely to be subsequently infected with genital herpes. However, it is possible to have concurrent oral and genital infections with an identical strain of HSV-1 in humans (Embil et al., 1981). Genital HSV affects approximately 20-65% of pregnant women and most of them are unaware of the infection (Corey and Wald, 2009). Additionally, the increased incidence of HSV-1 isolated from genital herpes lesions could be explained by the lower prevalence of HSV-1 among children, leaving them susceptible to HSV-1 later in life (Gutierrez, 2007). There is an increased prevalence of oral-genital contact, rather than genital-genital sex, among adolescents, thus raising the risk of transmission of genital HSV-1 (Wald, 2006).

1.1.2.5 Neonatal herpes

Transmission of HSV diseases to neonates is the most severe consequence of maternal genital herpes. Around 0.2-0.39% of all pregnant women shed HSV in the genital tract near the time of delivery, regardless of previous history of recurrent HSV infection (Pinninti and Kimberlin, 2014). Neonatal herpes can also happen after contact with people with cold sores soon after birth. Although neonatal HSV infections remain uncommon, there is only a 40% survival rate in untreated cases (Corey and Wald, 2009).

1.1.2.6 Herpes simplex Encephalitis

Severe manifestations, such as encephalitis may occur in some cases (Burcea et al., 2015; Slifer and Jennings, 2015). In addition, HSV-1 can affect the central nervous

system, resulting in herpes simplex encephalitis (HSE) (Whitman et al., 1946). HSE prevalence is 2 cases per million people per year of HSE and is responsible for about 10% of the 20,000 annual viral encephalitis cases in the United States (Levitz, 1998; Kuroda, 2015). HSE is associated with more than 50% mortality in untreated cases and most of the patients are affected by reactivation of an earlier infection (Whitley, 1988; Steiner and Benninger, 2013; Singh et al., 2016).

1.1.3 HSV-1 life cycle

The HSV-1 life cycle can generally be divided into three stages: lytic infection, latency and reactivation (Figure 1-2). The virus initiates replication in mucous membranes or the epidermis of broken skin as a primary infection site (Boehmer and Nimonkar, 2003; Rahn et al., 2017). At these peripheral sites, HSV-1 gains access to the termini of nerves, followed by retrograde transport to neuronal cell bodies. The virus is capable of traveling back to skin during lytic infection and thus, infecting more cells near primary infection sites and causing larger skin lesions (Thompson and Sawtell, 2000; Shimeld et al., 2001). With the spread of lesions on the skin surface, it is likely that more innervating axonal endings are infected. Hence, virus replication in primary sensory neurons contributes to the initial lesion size and subsequently, the spread of virus within peripheral neurons (Smith, 2012).

The adaptive immune response can clear HSV-1 primary lytic infection in the peripheral sites and ganglia within a few days (Simmons et al., 1992; Chew et al., 2009). However, during latent infection, HSV can deposit its genome within neurons and thus, establish a lifelong latent infection (Stevens, 1975; Rock and Fraser, 1983; Hill et al., 1996; Nicoll et al., 2012). Latency is considered to occur when there is a stable reservoir of viral DNA without producing infectious virus (Lachmann, 2003; Grinde, 2013). Only when certain environmental or physiological stimuli occur, such as stress or immunosuppression, will the virus reactivate and return to the lytic cycle, thereby producing progeny virions. During the reactivation phase of infection, HSV-1 progeny travels down the axon towards the skin and manifests at the initial site of infection. (Fraser and Valyi-Nagy, 1993; Suzich and Cliffe, 2018).

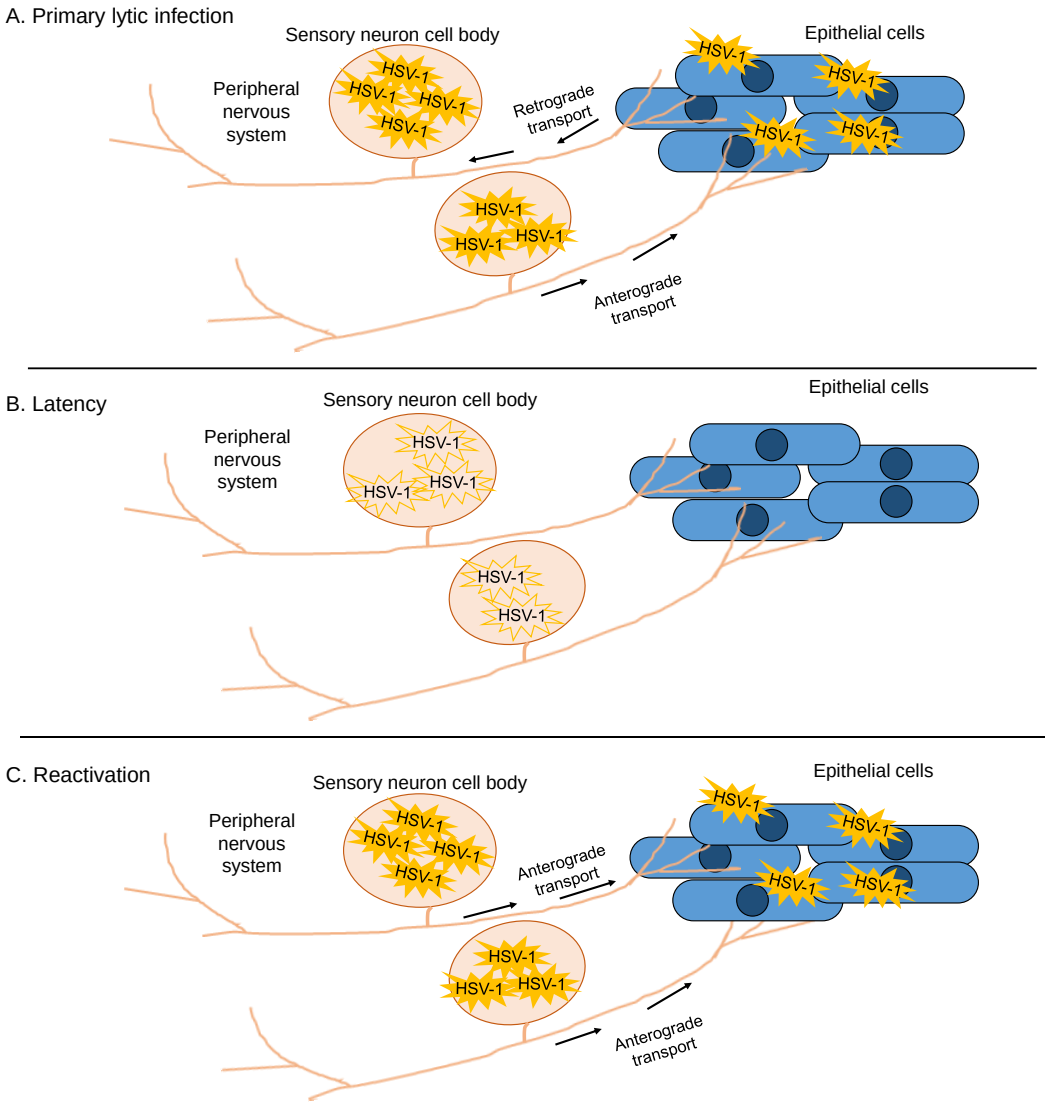

Figure 1-2. HSV-1 life cycle (primary lytic infection, latency and reactivation). (A) The primary lytic infection occurs at the periphery and is initiated in the epithelial cells where HSV-1 replicates to produce viral progeny. Viral infection within the cell body is productive (filled star). Virus can enter the nerve endings innervating the primary infection site. (B) Latency is established by some viruses persist in the sensory neurons without production of infectious virus (unfilled star). (C) While latency is disrupted with a certain stimulus, HSV-1 can reactivate and initiate productive infection in both the primary infection site and neurons.

1.1.4 HSV-1 gene expression

During lytic infection, HSV-1 gene expression occurs in an ordered and time-dependent cascade. All HSV-1 protein-coding genes can be classified into three categories: immediate-early (IE or α), early (E or β or delayed early) and late (L or γ) genes (Honess and Roizman, 1974; Lehman and Boehmer, 1999; Weller and Coen, 2012). The late genes are the final group of genes in the cascade. Late gene expression peaks between six and twelve hours post-infection (Stingley et al., 2000; Harkness et al., 2014). HSV-1 transcripts are encoded by the host cell RNA polymerase II transcription machinery, and contain 5' 7-methyl G caps as well as 3' polyadenylation. Expression is regulated by viral proteins that either enhance or suppress the machinery (Ben-Zeev and Asher Y'Becker, 1976; Beck and Millette, 1982).

1.1.4.1 HSV-1 gene expression and virus replication during lytic infection

Upon the binding of HSV-1 particles to receptors on the cell surface, the viral envelope fuses with the cell membrane and the viral nucleocapsid enters into the cytoplasm. It is transported along cytoplasmic microtubules with the help of the motor protein complex (Dohner et al., 2002). The HSV-1 capsid is transported to the nuclear pore and the viral DNA genome is released into the nucleus in an importin-dependent manner (Sodeik et al., 1997; Ojala et al., 2000). Transcription of initial HSV-1 genes is controlled by the viral transactivator VP16 acting on the RNA pol II machinery, a late viral protein packaged into virion as a tegument component, interacting with the cellular proteins octomer binding protein (Oct1) and host cell factor (HCF). The VP16-Oct1-HCF interactions induce RNA polymerase II-dependent transcription (Triezenberg et al., 1988a; Stern and Herr, 1991; Wilson et al., 1993). There are five IE proteins expressed by HSV-1, including ICP0, ICP4, ICP22, ICP27 and ICP47. IE genes, such as ICP0 and ICP4, are expressed within one to two hours post-infection (Harkness et al., 2014). ICP0 acts to inhibit the cellular innate immune response and ICP4 is a primary viral transcription factor that can negatively regulate the expression of IE genes and stimulate the expression of early genes (Persson et al., 1985; Cai and Schaffer, 1992; Yang and Courtney, 1995). IE protein synthesis is followed by early gene expression between four and seven hours post-infection (Harkness et al., 2014). In general, the products of early genes are essential for replication of the viral genome (Honess and Roizman, 1974; Challberg, 1986). Both ICP4 and ICP27 also have the ability to promote transcription of late genes, which mainly encode structural proteins of HSV-1 or those assisting viral assembly (Pizer et al., 1986; Newcomb et al., 2006).

The late genes are the final class of genes in the HSV-1 gene expression cascade. HSV-1 late genes predominantly functions in viral assembly and release of infectious particles. They mainly encode structural proteins and many of which form a part of the virion with other functions, such as the immunomodulatory protein ICP34.5 and the virion host shut-off protein (vhs) (Smiley, 2004; Wilcox and Longnecker, 2016). The late genes are subdivided into two classes (γ1 and γ2) based on the requirement for DNA replication (Gruffat et al., 2016). Expression of the γ1 genes follows that of the early genes and expression of the γ2 genes is dependent on the completion of lytic DNA amplification. In addition to the TATA box, the presence of initiator elements which overlap the initiation start site, plays an essential role for the regulation of late genes (Steffy and Weir, 1991; Guzowski and Wagner, 1993).

At least three HSV-1 proteins, such as ICP4, ICP27 and ICP8, are required for the proper expression of the γ1 and γ2 genes. ICP4 interacts with initiator elements in late promoters and transactivates late gene expression (Grondin and DeLuca, 2000; Zabierowski and DeLuca, 2004). In addition to ICP4, ICP27 has been found to regulate the late viral gene, including gC and UL47 (Jean et al., 2001). The ability of ICP27 to promote late gene expression has found to be at the mRNA transcription level, as ICP27 interacts directly with the C-terminal domain of RNA polymerase II (Sandri-Goldin and Mendoza, 1992; Zhou and Knipe, 2002). Furthermore, HSV-1 early protein ICP8, a single stranded DNA-binding protein, plays a role in late viral gene expression (Gruffat et al., 2016). Both the accumulation of late gC mRNA and late protein synthesis in cells expressing a dominant negative form of ICP8 indicates ICP8 has inhibitory effects on late viral gene expression (Gao and Knipe, 1991; Chen and Knipe, 1996).

At least seven HSV-1 proteins, including UL6, UL15, UL17, UL25, UL28, UL32 and UL33, support the excision of unit-length genomes and their subsequent encapsidation (Preston et al., 1983; Beard et al., 2002). The mature virion is transported out of the cell by exocytosis (Homa and Brown, 1997). The capsid acquires its first envelope when it buds through the inner nuclear membrane, but it will lose the first envelope while leaving the nucleus (Homa and Brown, 1997). In the cytosol, the virus gains its final envelope studded with viral glycoproteins from cytoplasmic vesicles through the ER-Golgi intermediate compartment membranes (Homa and Brown, 1997; Baines, 2011). After the mature virus exits the cell through fusion with the plasma membrane, HSV-1 spreads to and infects other susceptible cells, such as epithelial cells or neurons innervating the primary site of infection.

1.1.4.2 Latency-associated transcripts and lytic genes in latency

It has been proposed that during latent infection, DNA remains in a non-replicating and quiescent state in the neuronal nuclei until receiving outside stimulation to reactivate (Perng and Jones, 2010; Thellman and Triezenberg, 2017). Latency-associated transcripts (LATs) are transcribed from a locus within the repeat regions flanking the HSV-1 UL sequence. This transcription produces an 8.3 kb transcript. Subsequently, the LAT undergoes sequential splicing events to produce a 2.0kb, then a 4.5kb stable intron (Zabolotny et al., 1997). Functionally, LATs have an anti-apoptotic function and a role in epigenetically regulating lytic genes (Gupta et al., 2006; Bloom et al., 2010). In addition, several microRNA (miRNA) sequences have been identified within LATs (Cui et al., 2006; Umbach et al., 2008; Jurak et al., 2010). Despite LAT's various functions and its abundance during latent infection, it is generally accepted that LATs are not the key gene to establish latency, maintain latency or induce reactivation (Javier et al., 1988; Sedarati et al., 1989; Steiner et al., 1989). Originally, it was widely agreed that HSV-1 gene expression is silent during latency. However, with the improvement of experimental methods, recent reports have indicated that spontaneous molecular reactivations and certain viral transcripts can be detected during latency (Feldman et al., 2002; Ma et al., 2014). For example, transcripts of the IE gene ICP4 are found in the ratio of one to seven molecules of RNA in latently-infected cells, as compared to the viral genome in 20% of ganglia (Kramer and Coen, 1995; Feldman et al., 2002). Furthermore, several studies have revealed that lytic gene expression in HSV-1 latency is correlated with host gene regulation (Nicoll et al., 2016; Russell and Tscharke, 2016; Cliffe and Wilson, 2017). This also indicates that managing HSV latency engages active cellular responses to viral activity (Ma et al., 2014; Russell and Tscharke, 2016). Nevertheless, there is still debate over gene expression during reactivation. This situation may occur because the various models of reactivation are triggered by different cellular stimuli and popular models employ rodents or rodent neurons that may not reflect the natural virus-host interaction (Du et al., 2011; Webre et al., 2012).

1.2 Recognition of HSV-1 in host cells

During the initial microbial infection, host cells utilise pathogen-recognition receptors (PRRs) to sense pathogen-associated molecular patterns (PAMPs). PAMPs are microbe-derived molecules of pathogens such as nucleic acids, proteins and lipids (Akira and Hemmi, 2003; Akira and Takeda, 2004). The recognition of PAMPs by PRRs results in activation of signalling pathways that work to control microbial replication (Akira et al., 2006). Multiple mechanisms of nucleic acid sensing exist to

trigger innate immune responses against HSV-1. Therefore, HSV-1 has evolved strategies to counteract host sensors and the cellular signalling pathway (Ma and He, 2014).

1.2.1 Toll-like receptors (TLRs)

The first discovered and well-characterised PRRs were the Toll-like receptor (TLRs) (Medzhitov et al., 1997). TLRs are located in the plasma membrane and endosomal vesicles. TLRs bind with microbial elements and can induce early antiviral cellular responses and stimulate the secretion of mediators to activate nearby cells (Kawai and Akira, 2011). The role of each TLR in HSV-1 infection remains controversial and likely contributes to virus control in a cell-specific manner. Three TLRs have been found to be important in HSV-1 infection, namely TLR2, TLR3 and TLR9 and each of them will be discussed below.

1.2.1.1 TLR2

TLR2 is the predominant sensor located on the plasma membrane that engages in antiviral defences (Beutler, 2009). TLR2 has been shown to be capable of detecting a broad range of herpesviruses, including HSV-1, cytomegalovirus (CMV), Epstein-Barr virus (EBV) and varicella-zoster virus (VZV) (Aravalli et al., 2005; Wang et al., 2005; Szomolanyi-Tsuda et al., 2006; Gaudreault et al., 2007). The activation of TLR2 by HSVs is primarily induced by the binding of viral envelope glycoproteins (gH/gL) to TLR2. Downstream signalling after receptor ligation induces nuclear factor kappa-light-chain-enhancer of activated B cells (NF-κB) activation, type I interferon (IFN) production and interleukin-10 (IL-10) secretion (Gianni et al., 2013; Cheshenko et al., 2014). Yet, the specific downstream consequence of inducing TLR2 is virus strain- and infection route-dependent. Only certain laboratory strains and clinical isolates of HSV-1 lead to the TLR2-dependent pathway (Sato et al., 2006). Sensing intraperitoneal and ocular HSV-1 infection via TLR2 can be detrimental to the host due to severe inflammatory responses with excessive secretion of cytokines in the brain. Reduced mortality and proinflammatory cytokine production have been observed in TLR2-deficient neonatal and adult mice infected with HSV-1 (Kurt-Jones et al., 2004; Finberg et al., 2005; Kurt-Jones et al., 2005).

1.2.1.2 TLR3

TLR3 is an endosomal TLR and well-studied for its ability to recognise dsRNA, and thus, induce expression of type I IFN and inflammatory cytokines (Jensen and Thomsen, 2012; Perales-Linares and Navas-Martin, 2013). During HSV-1 infection, viral dsRNA is detectable and serves as the ligand for TLR3, although the mechanism is still unclear (Jacquemont and Roizman, 1975; Hayashi et al., 2006). Several reports have used that deletion or mutation of TLR3, resulting in defective signalling to study its function. For example, a single amino acid substitution (P554S) impairs the dsRNA binding activity and dimerization of TLR3, which was associated with the development of herpes simplex encephalitis (Zhang et al., 2007; Guo et al., 2011). However, the deficiency in TLR3 in patients did not increase the susceptibility for other viral infection and the efficiency of spread of HSV-1 in the periphery (Zhang et al., 2007; Guo et al., 2011). Together, this suggests that TLR3 may be dispensable for antiviral responses in the skin in humans. Similarly, the type I IFN signalling mediated by TLR3 in HSV is cell-specific. For example, when stimulated with dsRNA or HSV, human TLR3-deficient peripheral blood mononuclear cells (PBMC) and leukocytes still generate type I IFN (Guo et al., 2011). However, this was not observed in human fibroblasts (Guo et al., 2011). In addition to IFN signalling, TLR3 has been shown to be upstream of the activation of several transcription factors, including NF-κB, Jun amino-terminal kinase (JNK) and p38, both in immortalised and in primary human corneal epithelial cells (Li et al., 2006). In the murine model, HSV replicates more efficiently in TLR3-deficient neurons and astrocytes, indicating that TLR3 is essential for the intrinsic immunity of type I IFN to HSV-1 in the central nervous system (Lafaille et al., 2012; Reinert et al., 2012). However, TLR3 signalling is not required for type I IFN production in murine macrophages during HSV-1 infection (Malmgaard et al., 2004). These results indicate the redundant role of TLR3 in various cell types and suggest that there may be a human-mouse difference in the utilisation of TLR3 as an antiviral factor against HSV-1 infection.

1.2.1.3 TLR9

TLR9 is one of the endosomally localised PPRs, just like TLR3, 7 and 8 (Yang et al., 2005). In mice, TLR9 is broadly expressed in different cell types, while its expression is restricted to dendritic cells (DCs) and B cells in humans (Takeuchi and Akira, 2010). TLR9 recognizes CpG-rich DNA, which is abundant in the HSV genome and is assumed to be the most potent stimulator of innate immune responses (Bauer et al., 2001; Chockalingam et al., 2009). The previous literature has shown that $TLR9^{-/-}$ mice are more susceptible to HSV-1 infection (Lima et al., 2010; Boivin et al., 2012). Further, macrophages derived from these mice have a defective ability to produce inflammatory

cytokines when treated with CpG DNA (Zolini et al., 2014). In addition, mice pre-treated with a TLR9 agonist intranasally were reported to have higher survival rates and reduced HSV viral loads in the brain (Boivin et al., 2008). TLR9 signalling causes the activation of interferon regulatory factor 7 (IRF7), leading to the expression of type I IFN in both human and mouse DCs (Lund et al., 2003; Lim et al., 2007). In agreement with this, reduced type I IFN produced from pDCs and impaired nature killer (NK) cell activation in TLR9-deficeint mice has been shown (Lund et al., 2003). However, other studies have indicated that the role of TLR9 *in vivo* is dose-dependent and TLR9 did not contribute to virus control in the corneal infection model when mice were infected with high doses of HSV-1 (Wuest et al., 2006). Moreover, previous data have revealed that even in epithelial cells that are deficient in TLR9, the DNA-dependent immune responses can still be induced, implying that multiple mechanisms of DNA sensing exist and that the role of TLR9 is redundant (Conrady et al., 2012).

1.2.2 Cytosolic DNA sensors

Since HSV fuses its envelope with the plasma membrane and the capsid is released directly into the cytoplasm, cytosolic sensors are also activated during HSV infection (Unterholzner et al., 2010). The accumulation of viral nucleic acids in the cytoplasm, including both DNA and RNA as well as commonly observed PAMPs, contributes to innate immune recognition (Ablasser et al., 2009).

1.2.2.1 DNA-dependent activator of IRFs (DAI)

DAI was the first identified DNA sensor in the cytosol and also the first one found to recognise HSV-1 (Takaoka et al., 2007). DAI has the ability to recognize cytoplasmic DNA and depletion of DAI correlates with increased HSV replication *in vitro* (Pham et al., 2013). Although DAI was initially characterized for its ability to directly interact with DNA, recent evidence from HSV1, VACV and MCMV indicates that newly synthesized transcripts during infection are the most likely PAMP for DAI under natural conditions. When small interfering RNA (siRNA) was used to reduce the expression level of DAI, IFN responses were restricted in HSV-1 infection (Takaoka et al., 2007). However, other studies have revealed that cells derived from DAI-deficient mice, including macrophages and mouse embryonic fibroblasts, respond normally to DNA viruses and immunostimulatory DNA (Ishii et al., 2006; Wang et al., 2008b; Furr et al., 2011). These findings indicate that DAI may act specifically in certain cell types or have redundancy in detection of HSV genome.

1.2.2.2 Cyclic guanosine monophosphate-adenosine monophosphate (cGAMP) synthase (cGAS)

Another cytosolic DNA sensor, cGAS, interacts with DNA through its amino-terminal domain and can detect HSV genomes (Ablasser et al., 2013; Li et al., 2013; Xiao and Fitzgerald, 2013). While responding to DNA, cGAS can produce cGAMP which activates stimulator of interferon genes (STING)-dependent IFN production through direct interaction in macrophages and lung fibroblasts (Li et al., 2013). The depletion of cGAS results in reduced IFN levels, interferon-stimulated gene (ISG) expression and IRF3 activation during HSV-1 infection (Schoggins et al., 2014). Consistent with observations *in vitro*, $cGAS^{-/-}$ mice were found to be more vulnerable to HSV-1 infection (Li et al., 2013).

1.2.2.3 IFN-inducible protein 16 (IFI16)

IFI16 is a member of the pyrin and HIN-domain (PYHIN) family and is a microbial DNA sensor that participates in the IRF3-mediated pathway (Schattgen and Fitzgerald, 2011; Orzalli et al., 2012). Lack of IFI16 expression in mouse macrophages and human fibroblasts leads to a reduction in IRF3 and NF-κB activation (Diner et al., 2015; Orzalli et al., 2015). IFI16 senses DNA through a sequence-independent mechanism and is localised in both the nucleus and the cytoplasm, dependent on the cell type (Li et al., 2012). The cellular location of IFI16 may support different strategies to recognise viral DNA. While normally the nucleocapsid protects the HSV-1 DNA through cytoplasmic transit to the nucleus. The nucleocapsid can be subject to proteosomal degradation. The release of HSV genome DNA into the cytoplasm after degradation of the viral capsid is critical for IFI16 to detect HSV-1 in human macrophages (Horan et al., 2013). Moreover, nuclear IFI16 recognises HSV-1 infection upon release of encapsidated viral DNA into the nucleus during HSV-1 replication in human fibroblasts. This is inhibited by the viral nuclear ICP0 protein by promoting IFI16 degradation (Orzalli et al., 2012). A previous study has also shown that IFI16 may play an essential role in controlling HSV-1 infection *in vivo* as higher HSV-1 titres were detected in the corneal tissue of IFI16-deficient mice as compared to wild-type mice (Conrady et al., 2012).

1.2.3 Retinoic acid-inducible gene I (RIG-I)-like receptors (RLRs)

RNA polymerase III plays an essential role in linking DNA sensing to RNA recognition. Although RNA polymerase III does not directly sense DNA, it produces ligands to stimulate cytosolic RNA sensors. RNA polymerase III resides in the cytosol and

transcribes AT-rich DNA into the uncapped 5'-triphosphate form of dsRNA that can be recognised by cytosolic RNA sensors (Ablasser et al., 2009; Valentine and Smith, 2010). Consequently, the recognition of RNA results in the induction of type I IFN, the secretion of cytokines and the stimulation of ISGs via several signalling pathways (Chiu et al., 2009). RIG-I-like receptors, namely cytosolic RNA sensors, include RIG-I and melanoma differentiation-associated gene 5 (MDA5). RLRs are expressed in most cell types and can be directly induced by IFN treatment (Szabo et al., 2012). RIG-I preferentially senses short dsRNA (<300 bp) having a 5' triphosphate (5'-ppp), and MDA5 recognises long dsRNA (>1000 bp). Although RLRs were initially discovered for their role in detecting RNA, later studies showed that they also function to directly sense DNA (Cheng et al., 2007; Chow et al., 2018). There is a predicted helicase-like domain in RIG-I that can interact with B form DNA. In addition to B form DNA, RIG-I can bind to other immunogenic DNAs, such as HSV-1 genome DNA and synthetic stimulatory DNA (Choi et al., 2009). The RNA-RLR pathway has been found to activate IRF3 and NF-κB, while the DNA-RLR pathway primarily induces expression of IRF3 and therefore type I IFN and ISGs (Choi et al., 2009).

Knockdown studies of RIG-I or MDA5 with siRNA in macrophages indicated that MDA5, rather than RIG-I, is the major mediator recognising HSV-1 due to the strikingly reduced IFN-β and IFN-λ levels with cells lacking MDA5 expression (Melchjorsen et al., 2010). MDA5 and its adaptor protein mitochondrial antiviral signalling protein (MAVS) are required for producing IFNs in primary human macrophages during HSV-1 infection (Melchjorsen et al., 2010). Upon stimulation of type I IFN receptor (IFNAR) knockout cells with foreign DNA, overexpression of RIG-I and MDA5 in these cells was found to selectively rescue high level of type I IFN mRNA expression, in the absence of signalling from the association between IFN and its receptors (Choi et al., 2009). Therefore, these studies provide evidence that RLRs are critical for type I IFN expression in an IFNAR-independent manner.

1.3 Downstream signalling pathways after sensing HSV-1

Both membrane-bound receptors (e.g., TLRs) and cytosolic sensors (e.g., DAI, cGAS, RLRs) signal through adaptors to transduce their signals to the nucleus (Figure 1-3). The myeloid differentiation primary response (MyD) 88 and TIR-domain-containing adapter-inducing interferon-β (TRIF) are two primary adaptors interacting with the intracellular domain of TLR (Takeda and Akira, 2004; Piras and Selvarajoo, 2014). MyD88 associates with the cytoplasmic fragments of TLRs via interaction between individual Toll/IL-1 receptor (TIR) domains and this process further induces expression

of inflammatory cytokines such as tumour necrosis factor (TNF)-α, IL-1, IL-6 and IFN-γ through activation of transcriptional factors NF-κβ and IRF3 (Takeuchi et al., 2000; Akira et al., 2001). TRIF has a major role in TLR3-, TLR4-dependent and MyD88-independent signalling which elicits expression of IFNs and numerous ISGs through activation of IRF3, TANK-binding kinase 1 (TBK1) and IKKε (Kawai et al., 2001; Doyle et al., 2002). As for RLRs, RIG-I and MDA5 recognise cytosolic nucleic acid ligands and then signal to the adaptor protein, MAVS (Reikine et al., 2014; Wu and Hur, 2015). Signals from RLRs are then transferred to TBK1 and IκB kinases, leading to the phosporylation of several transcription factors, including IRF3, IRF7 and NF-κB (Melchjorsen et al., 2010; Xing et al., 2012a). After activation, NF-κB and IRFs are translocated into the nucleus and transactivate the expression of type I IFN, as well as other inflammatory cytokines and ISGs (Schneider et al., 2014; Chen et al., 2015a). Moreover, Wang et al. showed that high levels of activated IRF3 expression are sufficient for induction of IFN-β in NF-κB knockout MEFs, indicating IRF3 can induce type I IFN transcription independent of NF-κB (Wang et al., 2010b; Wang et al., 2010c). In the DNA sensing pathway, STING is an essential adaptor protein involved in the regulation of signal transduction, either by directly binding to exogenous DNA or via receiving signals from other sensors like cGAS and IFI16 (Barber, 2014; Bhat and Fitzgerald, 2014; Hansen et al., 2014). Activated STING recruits TBK1 and IRF3 to from a complex. The formation of this complex promotes phosphorylation of both TBK1 and IRF3, resulting in an increase in the expression of type I IFN and ISGs (Ishikawa et al., 2009; Ishikawa and Barber, 2011; Tanaka and Chen, 2012). Lastly, cell death is a downstream consequence of PRR activation and HSV-1 employs ICP6 to block both caspase 8 (Casp 8) and Z-DNA Binding Protein 1 activation in human cells (Guo et al., 2018).

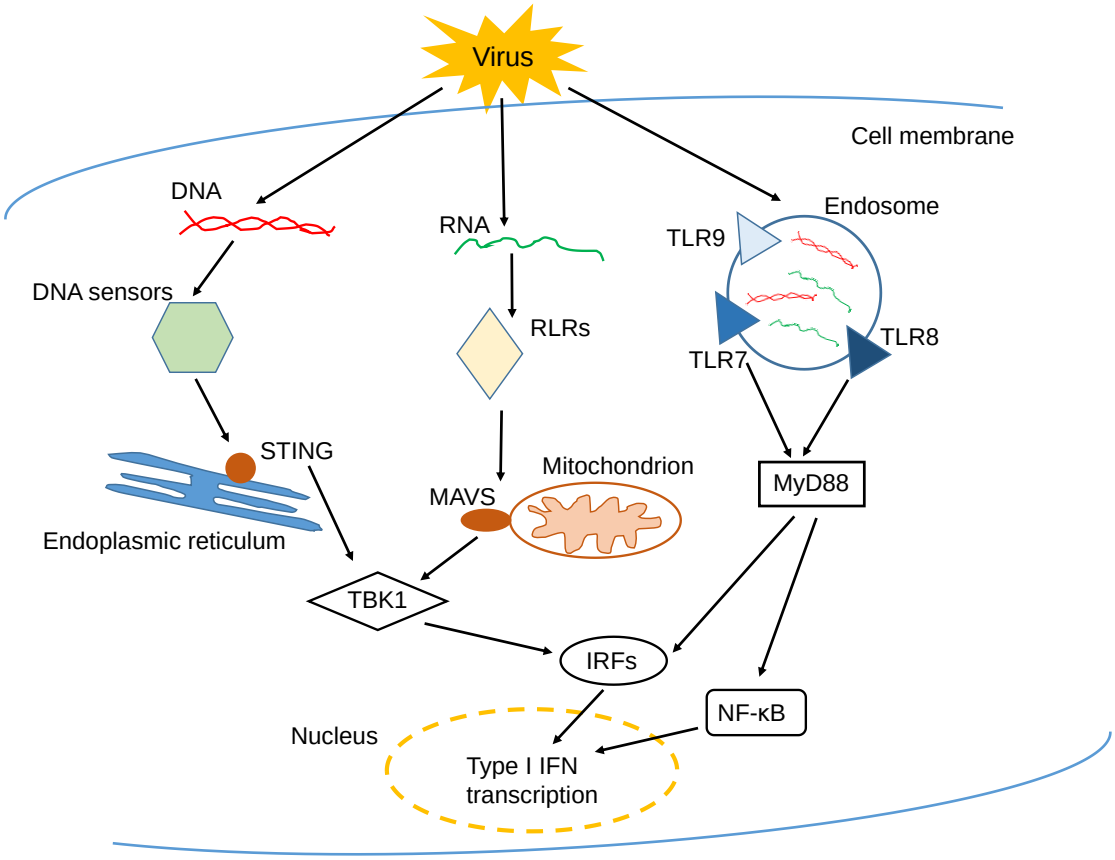

Figure 1-3. Nucleic acid recognition pathways. Pathogen-derived RNA or DNA is sensed via TLR and/or nucleic acid-sensors. Upon endosomal translocation, viral RNA and DNA are recognized by endosomally expressed TLR7, TLR8 and TLR9. The adaptor molecule MyD88 is essential for driving the production of type I IFNs. Viral RNA is also sensed by RLRs through MAVS, a CARD-containing adaptor protein. RLRs/MAVS then interacts with TBK1 and activates IRFs. Viral DNA can be recognised by DNA sensors. Upon DNA stimulation, STING translocates from the membrane of endoplasmic reticulum the cytoplasmic punctate structure, where it interacts with TBK1 and then activates IRFs to trigger type I IFN production.

1.3.1 Canonical IFN signalling pathway

After viral PAMPs are sensed by various host PRRs and the antiviral signal is transduced to transcription factors that promote IFN production (Su et al., 2016). IFN is secreted from the producing cell and acts in an autocrine and paracrine manner to amplify cell-intrinsic antiviral responses and ultimately reduce virus replication. Secreted IFNs bind to IFNAR, a heterodimeric transmembrane receptor, and this interaction actives receptor-associated protein tyrosine kinases such as Janus kinase 1 (JAK1) and tyrosine kinase 2 (TYK2) (Krishnan et al., 1997; Schindler et al., 2007). Diverse pathways downstream can be induced, leading to multiple biological effects. In canonical IFN signalling, phosphorylated JAK1 and TYK2 further phosphorylate the signal transducer and activator of transcription 1 (STAT1) and STAT2 proteins, resulting in dimerization, nuclear translocation and association with IRF9 to form the ISG factor3 (ISGF3) complex (Levy et al., 1989). ISGF3 interacts with specific DNA sequences, known as IFN-stimulated response elements (ISREs), in numerous ISGs. Thus, this step activates the transcription of ISGs. Several hundred ISRE-driven ISGs have been found to be induced by viral infections (Schoggins et al., 2011; MacMicking, 2012). In addition to the canonical IFN signalling pathway, type I IFN can activate STAT homodimers which interact with a distinct gamma-activated sequence, commonly related to IFN-γ-mediated signalling (Ahmed and Johnson, 2006).

IFN responses have been shown to have an important role in combating HSV-1 infection. The expression of IFNs has been shown to correlate with resistance to HSV infection *in vivo* (Wrzos et al., 1990; Halford et al., 1997). The presence of IFN expression and functional IFNAR is required to control virus spread from peripheral sites to the central nervous system by reducing virus replication in trigeminal ganglia (Leib et al., 1999; Luker et al., 2003). Additionally, more severe skin lesions, characterised by extensive oedema and loss of lymphatics, occur in IFNAR-deficient mice, compared with wild-type mice, during HSV-1 infection (Bryant-Hudson et al., 2013). IFNs activate various ISGs to protect the host from HSV-1 lytic infection (Su et al., 2016). For example, ISG15-deficient mice had increased susceptibility to HSV-1 infection (Lenschow et al., 2007). Moreover, promyelocytic leukemia protein (PML), another ISG, was found to mediate the anti-HSV state induced by exogenous IFNs, which counteracts the activity of ICP0 (Chee et al., 2003; Everett et al., 2006). IFNs not only restrict lytic infection of HSV1, but also control HSV-1 latency. Supplementation with IFN-γ was found to control HSV-1 reactivation in *ex vivo* trigeminal ganglion cultures (Liu et al., 2001).

1.3.2 IFN-independent mechanisms

Aside from IFN induction, entry of certain pathogens into the cell at the initial stage of infection can stimulate host cell innate responses through IRFs, in the absence of IFNs. Activated IRFs act as transcriptional activators to upregulate expression of a subset of ISGs (Nicholl et al., 2000; Mossman et al., 2001). The activation of IRF family members, especially IRF1 and IRF3, directly induces this response in epithelial cells and fibroblasts (Chin and Cresswell, 2001; Collins et al., 2004; Stirnweiss et al., 2010). Mossman et al. (Mossman et al., 2001) used an HSV-1 mutant, which cannot induce a functional level of IFN expression, together with other soluble cytokines as a model to investigate antiviral activity in an IFN-independent manner. The data indicated that HSV-1-infected cells can induce an IFN-independent antiviral state and induce expression of ISGs, including myxovirus resistance 1 (MX1), MX2, IFN-stimulated protein (ISG15), IFN-induced protein 65 (IFIT1), IFN-induced transmembrane protein (IFITM1) and OAS family members (OAS2 and OAS3) (Mossman, 2002). Another study also showed that HSV-1 virions can activate ISG15, ISG54, IFI56, MX1 and IFITM1 expression in the absence of protein synthesis and *de novo* viral gene expression (Nicholl et al., 2000). These antiviral responses are not dependent on IFN itself or JAK/STAT signaling components that are triggered by IFN in human fibroblasts (Nicholl et al., 2000). Therefore, despite the importance of IFN being shown, IFN-independent pathways are likely to remain important in some cell types.

1.4 Regulation of viperin and its role in innate antiviral responses

The ISGs mentioned in the previous section were not investigated in this thesis. However, due to our experimental results (Section 4.2), we chose to examine viperin. For this reason, this molecule is introduced here in detail. Viperin is an ISG, encoded by radical S-adenosyl methionine domain containing 2 (RSAD2) gene, with broad spectrum inhibition of virus replication, including both DNA and RNA viruses (Seo et al., 2011a; Helbig and Beard, 2014). However, due to limited studies, the mechanism and whether viperin is essential for controlling HSV-1 infection remains unclear. Viperin was initially identified as an ISG in human macrophages and a cytomegalovirus-inducible gene in human fibroblasts (Zhu et al., 1997; Chin and Cresswell, 2001). Therefore, viperin is also known as cytomegalovirus-induced gene 5 (cig5). The viperin protein is highly conserved across species from humans to fish (Duschene and Broderick, 2012). Human viperin is composed of 361 amino acids with a predicated molecular size of 42 kDa (Figure 1-4). Viperin is divided into three distinct domains: an N-terminal domain that has varied length and sequence between species, a

highly conserved central domain with a motif containing cysteine residues (CxxxCxxC) and a C-terminal domain that shows similarity across species. An amphipathic helix located from residue 9 to 42 in the N-terminus of viperin can associate with the cytosolic surface of the endoplasmic reticulum (Hinson and Cresswell, 2009b). The N-terminus is also capable of interacting with lipid droplets (Hinson and Cresswell, 2009a). Motifs homologous to the radical S-adenosyl-L-methionine (SAM) domain were shown in the central domain. The interaction between these motifs and iron-sulphur clusters, a characteristic function of radical SAM enzymes, has been shown (Shaveta et al., 2010). The role of the conserved C-terminus is not yet clearly defined, but it appears to act as a necessary fragment for suppression of replication of viruses in the Flaviviridae, such as dengue virus (DENV) and Zika virus (ZIKV) (Jiang et al., 2008; Helbig et al., 2013).

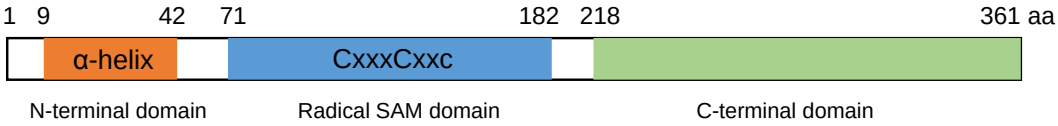

Figure 1-4. Schematic diagram of known domains in viperin. The N-terminal domain (9-42 aa) is important for localization of viperin to the cytosolic surface of the endoplasmic reticulum. The central domain (71-182 aa) is conserved and contains a binding motif with cysteine residues. The C-terminal domain (218-361 aa) is relatively highly conserved.

Viperin expression is induced by all types of IFNs (α, β and γ), as well as some microbial PAMPs, dsRNA, dsDNA and lipopolysaccharide (LPS) (Severa et al., 2006; Hinson et al., 2010). Viperin induction can generally be divided into two major routes: IFN-mediated and IFN-independent pathways (Boudinot et al., 2000). The induction of viperin expression in an interferon-dependent manner occurs after the ligation of PAMPs with PRRs and subsequent downstream IFN production. One consequence of IFN-stimulation is the assembly of ISGF3, a multi-protein complex with DNA binding functionality, within the cytoplasm and ISGF3 translocation to the nucleus. Within the nucleus, ISGF3 binds to the internal ribosome entry site within the viperin promoter, thus inducing viperin expression. (Severa et al., 2006). Viperin expression can also be regulated in an IFN-independent manner. Studies with several viruses, such as human cytomegalovirus (HCMV), Japanese encephalitis virus (JEV) and vesicular stomatitis virus (VSV), show upregulated viperin expression in infected cells independently of IFNs (Boudinot et al., 2000; Boehme et al., 2004; Chan et al., 2008). Mechanistically, IFN-independent viperin induction occurs after the ligation of viral dsRNA and RLRs, subsequent recruitment to peroxisomal MAVS and IRF1/3-dependent ISG expression (DeFilippis et al., 2006; Dixit et al., 2010; Stirnweiss et al., 2010). During reovirus and influenza virus infection, peroxisomal MAVS was found to produce rapid IFN-independent viperin expression early after infection, while mitochondrial MAVS activated an IFN-dependent expression of viperin to maintain a stable antiviral environment with delayed kinetics in the presence of IFNs (Dixit et al., 2010).

Viperin has been shown to inhibit DNA and RNA viruses by diverse mechanisms. In Herpesviridae, viperin affects replication of both HCMV and HSV in different ways. Envelope glycoprotein B (gB) from HCMV can directly induce expression of different ISGs, including viperin (Chin and Cresswell, 2001; Boehme et al., 2004). Human fibroblasts expressing viperin show a reduction in HCMV production, indicating that viperin is a potential antiviral against HCMV (Chin and Cresswell, 2001). HCMV vMIA protein can interact with viperin, resulting in the redistribution of viperin from endoplasmic reticulum to mitochondria. The iron-sulphur binding motifs in the central domain of viperin play an essential role in associating with mitochondrial trifunctional protein (TFP). This interaction then leads to cytoskeleton disruption and enhancement of HCMV infectivity (Chin and Cresswell, 2001; Seo et al., 2011b). Ectopically expressed viperin did not inhibit the replication of wild-type virus in HEK239 cells (Shen et al., 2014). Reduced virus replication was found only where the virus did not express UL41 due to that UL41 reduces accumulation of viperin mRNA (Shen et al., 2014).

1.5 Herpesviral proteins that evade DNA sensing and the IFN pathway

As a large virus with a slow replication rate compared to those of RNA viruses *in vivo*, it is essential for HSV-1 to establish infection within the first few replication cycles (Rathinam and Fitzgerald, 2011; Christensen and Paludan, 2017). In order to evade sensing from host cells and the subsequent innate immune responses, HSV-1 has evolved various viral proteins (Friedman, 2003; Su et al., 2016). Different viral proteins can aim redundantly at the same signalling pathway, and these gene products can also be multifunctional (Wadd et al., 1999; Smith et al., 2005; Kawaguchi, 2013).

1.5.1 ICP0

ICP0, an IE protein of HSV-1, is a strong inhibitor of TLR-mediated cellular signalling. Daubeuf et al. reported that ICP0 binds to ubiquitin-specific-processing protease 7 (USP7) and USP7 is then translocated from the nucleus to cytoplasm (Daubeuf et al., 2009). Within the cytoplasm, USP7 deubiquitinates TNF receptor-associated factor 6 (TRAF6) and inhibitor of κB kinase (IKK), leading to the reduced activation of mitogen-activated protein kinase (MAPK) via TLR signalling (Daubeuf et al., 2009). Others have shown that ICP0 inhibits TLR2 signalling by targeting the adapter protein MyD88 for degradation, abolishing NF-κB signalling (van Lint et al., 2010). Another function of ICP0 is the inhibition of expression of ISGs (Lanfranca et al., 2014). For instance, the RING finger domain of ICP0 has been found to interact with IRF3 and IRF7, disrupting induction of ISG expression (Lin et al., 2004). It has also been reported that ICP0 sequestered nuclear IRF3, promoting IRF3 degradation, and thus suppressing transcription of IFN-β and ISGs (Melroe et al., 2007). Additional studies have shown that in human foreskin fibroblasts, nuclear localisation of ICP0 is critical for inhibition of the IFI16-induced IRF3 signalling pathway through degradation of IFI16. (Paladino et al., 2010).

1.5.2 ICP27

Another IE protein of HSV-1, ICP27, has been found to be involved in a wide range of HSV-1 biological functions, such as viral gene expression, virion release and the export of viral mRNA (Sekulovich et al., 1988; Tian et al., 2013; Park et al., 2015). In addition, it induces host-cell shutoff by decreasing cellular mRNA stability and inhibiting host splicing machinery (Hardwicke and Sandri-Goldin, 1994). In addition to these broad antiviral activities, ICP27 helps HSV-1 to evade type I IFN signalling through

inhibition of the activation of IRF3 and STAT1 (Melchjorsen et al., 2006; Johnson et al., 2008). Melchjorsen et al. showed that ICP27-deletion in HSV-1 led to higher levels of IRF3, NF-κB and cytokine production in infected human monocyte-derived macrophages and dendritic cells, as compared to wild-type virus (Melchjorsen et al., 2006). These data indicate that ICP27 protein mediated suppression of cytokine expression through effects on IRF3 and NF-κB in HSV-1 infection. Another report found that ICP27 is necessary for blocking STAT1 phosphorylation at early infection time points, preventing nuclear translocation (Johnson et al., 2008). A recent study discovered a new role of HSV-1 ICP27 in regulating the cGAS/STING pathway (Christensen et al., 2016). An interaction between ICP27 and the STING-TBK1 complex inhibited TBK1-mediated phosphorylation of IRF3 and induction of ISGs (Christensen et al., 2016). Thus, ICP27 may play a key role in suppressing IFN and IFN-independent responses to HSV-1 infection.

1.5.3 ICP34.5

ICP34.5, a neurovirulence factor of HSV-1, is well known for its regulation of innate antiviral responses in host cells (Melchjorsen et al., 2009; Rosato and Leib, 2015). HSV-1 ICP34.5 has been found to recruit protein phosphatase 1 to dephosphorylate eukaryotic translation initiation factor 2 (eIF2α). This process blocks the translational arrest effect of eIF2α, thus supporting virus replication in infected cells (He et al., 1997). Furthermore, ICP34.5 directly interacts with beclin1 to prevent autophagy, which functions to deliver viral molecules to endosomes (Orvedahl et al., 2007; Into et al., 2012). Hence, the inhibition of autophagy by ICP34.5 may offset the recognition of viral DNA and RNA by endosomal TLRs. In addition, ICP34.5 controls the activity of TBK1 (Verpooten et al., 2009). The interaction between ICP34.5 and TBK1 prevents TBK1 associating with IRF3, thus inhibiting subsequent expression of IFNs and ISGs (Ma et al., 2012). In agreement with this finding, levels of IRF3 phosphorylation and type I IFN were found to be higher in cells infected with the ICP34.5-deletion virus compared with wild-type HSV-1 (Verpooten et al., 2009). ICP34.5 has also been identified as suppressing NF-κB signalling by dephosphorylating IKK, resulting in decreased inflammatory cytokine production (Jin et al., 2011).

1.5.4 virion host shutoff (vhs; UL41)

HSV-1 encodes a ribonuclease, UL41, also referred to as the virion host shutoff protein (vhs). HSV-1 vhs is a component of the tegument and digests both host and viral mRNAs after viral entry. This restricts translation of host mRNA contributing to the

shutdown of cell-intrinsic immune responses (Smiley, 2004). In the absence of vhs, HSV-1 is attenuated with reduced infection in corneal *in vivo* (Strelow and Leib, 1995). However, the consequence of a lack of vhs activity in cell culture is dependent on cell type (Dauber et al., 2011). With respect to cytosolic sensing, in cells infected with a vhs null mutant, viral RNA accumulated, acting as an increased pathogen signal (Pasieka et al., 2008). Concurrently, vhs is critical for reducing the activation of the RNA-sensing pathways via MyD88- and TLR3-independent pathways in both human and mouse DCs (Cotter et al., 2010). However, the target of vhs is not the TLR agonist for these sensors, indicating that an inhibitory effect may occur at some point upstream of the pathway (Cotter et al., 2010). Another study has showed that vhs selectively suppresses expression of several components in the nucleic acid-sensing pathway in epithelial cells, including TLR2, TLR3 RIG-I and MDA5 (Yao and Rosenthal, 2011). HSV-1 vhs also reduces signalling by the cGAS/STING-mediated pathway by reducing mRNA and subsequent protein levels of cGAS (Su and Zheng, 2017). In terms of IFN responses, vhs-null HSV-1 shows a growth deficit with smaller plaques, and as expected, increased sensitivity to the effect of IFNs (Read et al., 1993; Pasieka et al., 2008). When compared to wild-type HSV, the vhs mutant was found to cause greater activation of IRF3. HSV-1 vhs has also been found to disrupt IFN-related antiviral immunity by targeting multiple proteins, such as dsRNA-activated protein kinase (PKR), ribonuclease L (RNase L) and JAK1 due to its ribonuclease activity (Murphy et al., 2003; Chee and Roizman, 2004; Duerst and Morrison, 2004). Pasieka et al. (Pasieka et al., 2008) revealed that the presence of vhs activity affects the phosphorylation of eIF2α in a PKR-dependent manner because the phosphorylation of eIF2α is increased during HSV-1 infection lacking vhs function as compared to wild-type virus. Further, another study indicated that downregulation of JAK1 and STAT2 occur in cells infected with wild-type HSV-1, but both JAK1 and STAT2 expression are restored in cells infected with vhs-defective virus, suggesting that the vhs protein is involved in counteracting the JAK/STAT2-mediated IFN signalling pathway (Chee and Roizman, 2004). Taken together, the results summarized above indicate that vhs has multiple mechanisms by which if interferes with cytosolic sensing and IFN signalling pathways.

1.5.5 Us3

Us3, a multifunctional serine/threonine kinase, participates in the egress of viral particles from the nucleus, the regulation of the cytoskeleton and the inhibition of apoptosis (Leopardi et al., 1997; Mettenleiter, 2002; Kato et al., 2011). Us3-deletion HSV-1 mutant triggers activation of IRF3, secretion of type I IFN and expression of

TLR3, indicating that Us3 interrupts the TLR3 pathway and its downstream expression of IFNs (Piroozmand et al., 2004; Peri et al., 2008). Moreover, Us3 interferes with TLR2 signalling, inhibiting the TLR2-associated NF-κB pathway and the subsequent induction of cytokines (Sen et al., 2013).

1.5.6 Us11

HSV-1 Us11 also plays an important role during the capsid assembly and egress process (Mettenleiter, 2002). Studies have shown that Us11 inhibits the RNase L antiviral pathway and PKR-mediated protein synthesis (Poppers et al., 2000; Khoo et al., 2002; Sanchez and Mohr, 2007; Lussignol et al., 2013). An association has been reported between the C-terminal RNA-binding domain of Us11 and endogenous RIG-I and MDA5. This association prevents RIG-I and MDA5 from binding to their adapter protein MAVS, resulting in downregulation of the RLR signalling pathway (Xing et al., 2012b).

1.5.7 Other HSV-1 inhibitors

HSV-1 serine protease VP24 has been shown to occlude both the interferon stimulatory DNA- and cGAS/STING-mediated IFN signalling pathway by interfering with IRF3 promoter activation, without blocking the function of the NF-κB promoter (Zhang et al., 2016). Mechanistically, VP24 prevents the association between IRF3 and TBK1 through physical interaction of VP24 with IRF3. This interaction inhibits the phosphorylation and dimerization of IRF3 (Zhang et al., 2016). In addition, both HSV-1 UL24 and UL36 inhibit the cGAS/STING-induced DNA sensing pathway by interfering the NF-κB activation (Xu et al., 2017; Ye et al., 2017). UL24 inhibits the interferon stimulatory DNA- and cGAS/STING-mediated NF-κB signalling pathway, which is correlated with reduced production of IFNs and IL-6. These data suggest that UL24 blocks cGAS/STING-mediated NF-κB activation via the interaction between UL24 and endogenous p65 and p50 proteins. This association decreases p65 and p50 translocation, thus affecting NF-κB transcription (Xu et al., 2017). Ubiquitin-specific protease UL36 is another protein interrupting cGAS/STING-mediated NF-κB signalling (Ye et al., 2017). Overexpression of UL36 reduces cGAS/STING-induced IFNs and activation of the NF-κB promoter by restraining IκBα degradation through the deubiquitinase activity of UL36 and this blocks the activation of NF-κB (Ye et al., 2017).

1.6 The effect of sex on the immune system

Sex refers to biological characteristics that determine male and female, such as reproductive organs, arrangement of chromosomes and sex hormones. The physiological differences arising from sex may affect the control and clearance of microbes, and the difference in anatomical structure between the two sexes can influence exposure and transmission of infectious diseases (Guerra-Silveira and Abad-Franch, 2013; Nhamoyebonde and Leslie, 2014). Based on available literature reviews, in general, the prevalence of infections are usually higher among males than females. However, females face more severe disease outcomes associate with immunopathology, suggesting that sex differences matter in the pathogenesis of infectious diseases (Fischer et al., 2015; Klein et al., 2015).

1.6.1 Mechanisms of sex differences in immune responses

1.6.1.1 Sex steroids

Several mechanisms have been proposed to underline differences in immune function between the sexes (Klein et al., 2015; Ghosh and Klein, 2017; Roved et al., 2017). The most well-established hypothesis is the action of sex steroids (De Leon-Nava et al., 2009; Guerra-Silveira and Abad-Franch, 2013). Specifically, estrogen and testosterone affect the function of the immune cells (Fish, 2008; Xia et al., 2009). These steroid hormones bind to their receptors in the cytoplasm and form the steroid-receptor complex that move to the nucleus and associate with hormone response elements in the promoter regions of sets of genes in DCs, macrophages and lymphocytes (Sakabe et al., 1990; De Leon-Nava et al., 2009). Direct interactions between sex steroids and their respective receptors further modulate cellular signalling via IRFs and NF-κB (Hewagama et al., 2009). Therefore, the production of different cytokines and chemokines is differentially regulated between the two sexes (Hewagama et al., 2009).

1.6.1.2 Incomplete X chromosome inactivation

Another mechanism for the sex-based differences in immunological reactions involves the sex chromosomes (Migeon, 2007). Females possess two X chromosomes, one from each parent, while males have only one X chromosome from the mother. Compared to the Y chromosome, which only carries about 100 genes, the X chromosome harbours approximately 1100 genes and some of them play crucial roles to mediating immune responses, such as TLRs and interleukin receptors (Libert et al., 2010). During the early stage of embryogenesis in females, gene expression from one of the X chromosomes is

shut down to avoid a double dosage of these proteins in females (Brown et al., 1991). This process is called X chromosome inactivation and is driven by the long non-coding RNA *Xist*. (Senner and Brockdorff, 2009; Pontier and Gribnau, 2011). This process generates cellular mosaicism in females, which means that the X chromosome from paternal or maternal origin is expressed in different cells (Migeon, 2007). As a result, deleterious mutations cause whole cell populations in males to lose their functions, but only around half of the cells are affected in females. Cellular mosaicism not only protects females against the consequence of disadvantageous gene mutations, but also supports the ability of females to counteract various microbial infections by adding diversity. However, the disadvantage may be that females are at higher risk than males of developing immunopathology resulting from excessive and prolonged activation of the immune system (Klein, 2012). In addition to cellular mosaicism, some immune-related genes have been found to be expressed at a higher level in females, as compared to males, due to incomplete X-inactivation (Wang et al., 2016b). For example, TLR7, which is encoded by a gene on the X chromosome, is present in females at a higher level than males owing to incomplete X-inactivation. Greater TLR7 expression has been noted in a large proportion of DCs, B lymphoctyes and monocytes (Souyris et al., 2018a; Souyris et al., 2018b). These findings suggest that overexpression of TLR7 is a potential factor to the risk of systemic lupus erythematosus, an autoimmune disease with strong female bias (Subramanian et al., 2006; Deane et al., 2007).

1.6.1.3 X chromosome encoded miRNAs

In addition to incomplete X chromosome inactivation, it is proposed that the X chromosome contains a high intensity of miRNAs which are involved in modulating immune responses (Pinheiro et al., 2011; Bianchi et al., 2012). For instance, mir-223 has the ability to downregulate LPS-induced IFN signalling in splenic lymphocytes and can also inhibit TLR4- or TLR3-triggered inflammatory responses (O'Neill et al., 2011; He et al., 2014). Moreover, previous studies have shown that both mir-351 and mir-448 expression can be induced by IFN-β, and subsequently act to inhibit HCV replication (Pedersen et al., 2007; Pinheiro et al., 2011; Shrivastava et al., 2015). To date, there are no reports suggesting that spontaneous mutations in these miRNAs can influence sex differences in immune reactions, but many researchers still believe that dysregulation of miRNAs expression on the X chromosome may partly explain differences in immunity between the sexes (Pinheiro et al., 2011).

1.6.2 Sex-specific differences in HSV-1 infection

Sexual dimorphism in immune responses has been observed during herpesvirus infection. Several studies have reported that mortality rates are higher in male mice when they are infected with HSV-1 by the corneal route or intranasal injection (Han et al., 2001; Lundberg et al., 2003; Brown et al., 2004). In contrast, Geurs et al. (Geurs et al., 2012) showed that in systemic viral infections, female mice are more susceptible to large dsDNA viruses such as HSV-1 and CMV due to differential regulation of IFNAR signalling between the two sexes. The inconsistent results described above may be explained by different infection routes, strains of HSV-1 and mice, which have been noted to exhibit variation in HSV-1 pathogenesis (Perng et al., 2001; Kastrukoff et al., 2012; Wang et al., 2013a).

Female mice infected by HSV-1 intraperitoneally produce more antibodies than their male counterparts, and castration significantly enhances antibody production in male mice due to the effect of sex hormones (Knoblich et al., 1983). In addition, $CD4^+$ T cell activity and glycoprotein D (gD)-dependent humoral immune responses are higher in females than in males during clinical trials of the HSV-1 vaccine (Zhang et al., 2008). This observation is correlated with results from the gD-based HSV-2 vaccine which showed a significant sex-bias in protection and there was 73% efficacy in females but only 11% in males (Stanberry et al., 2002). Similar results have been reported for other members of the herpesvirus family. For example, serological screening of EBV antibodies via indirect immunofluorescence or by enzyme-linked immunosorbent assay (ELISA) has indicated that males are more likely to be EBV-seronegative than females in a prevelance study (Wagner et al., 1994). Women infected with CMV can also produce a higher number of IL-2-secreting cells and greater levels of INFs and IL-2 compared to similarly infected men (Villacres et al., 2004). In summary, these results suggest that there are sex differences in host immune responses to herpesviruses whereby females may display more protective responses than males, but the mechanisms behind this remain poorly understood.

1.7 Differences between mouse and human immunity

Over the past century, mice have developed into the premier mammalian model system for biomedical research because they have many similarities to humans in terms of anatomy, physiology and genetics (Emes et al., 2003). Mice and humans share around 95% similarity in their genomes and have many genetic diseases in common. Additionally, only about 300 genes are unique to one species or the other (Guigo et al., 2003; Cheng et al., 2014). However, there remain significant differences between mice and humans in terms of their innate and adaptive immune systems (Haley, 2003). This

section describes broad differences in immunity between these two species at the beginning (Section 1.7.1), including innate immune responses and antiviral ISGs, and then illustrates human-mouse differences in HSV-1 infection in Section 1.7.2.

1.7.1 Cytokines and innate immune responses

1.7.1.1 Cytokines

The expression and function of cytokines and innate proteins may be different in different species. For instance, IL-13 induces switching expression of the Ig isotype in B lymphocytes in humans, from IgM to IgE, but not in mice (Tangye et al., 2002; Kracker and Radbruch, 2004). Moreover, the signals leading to the development of Th cells in $CD4^+$ T cells are different between mice and humans. In humans, type I IFNs promote Th1 development and can activate STAT4 by gathering the IFNAR complex dependent on STAT2. However, the C-terminal domain of the STAT2 protein in mice has been altered due to a minisatellite insertion in this gene. This further disturbs the ability of STAT2 to activate STAT4 (Farrar et al., 2000). In addition, Th2 cells release IL-10 in mice, while in humans, IL-10 is produced by Th1 and Th2 cells (Del Prete et al., 1993). Lastly, mouse IL-7 and IL-7 receptors are essential for differentiation of immature T cells and B cells. However, deficiency of IL-7 receptors causes the arrest of T-cell development, but not B-cell development, in humans (Peschon et al., 1994; Roifman et al., 2000).

1.7.1.2 TLRs

Recent studies indicate that TLR orthologues are differently expressed in mice and humans, including the expression of varied TLR transcripts in different cell types and differing functions on cellular activation (Bryant and Monie, 2012). For example, TLR2 mRNA is low or undetectable in mouse blood cells. However, constitutive levels of TLR2 expression have been shown in peripheral blood leukocytes in humans (Matsuguchi et al., 2000; Zarember and Godowski, 2002). Furthermore, during proinflammatory stimuli, the mouse TLR2 promoter is active and induced rapid TLR2 expression in macrophages. By contrast, it is difficult to activate TLR2 promoters of human monocytic cell lines by LPS (Musikacharoen et al., 2001; Haehnel et al., 2002). Other studies have also found that TLR9 is expressed on all mouse myeloid cells, plasmacytoid DCs and B cells, whereas in humans, TLR9 is primarily located on plasmacytoid DCs and B cells (Kadowaki et al., 2001; An et al., 2002).

1.7.1.3 MX proteins

1.7.1.3.1 Cellular localization of MX proteins

A typical example of a human-mouse difference in ISGs is the MX proteins. MX proteins, belonging to the family of interferon-induced GTPases, act differently during virus infection in mice and humans. Both human and mouse MX1 proteins are able to reduce viral protein expression in influenza (Pavlovic et al., 1992). However, the distinct cellular distribution of MX1 provides different strategies to inhibit virus replication. Human MX1 protein accumulates in the cytoplasm and has been found to interfere in both influenza viral protein synthesis and genome amplification (Zurcher et al., 1992a). An explanation for this is that the MX1 protein probably intercepts the intracytoplasmic transport of viral mRNA or the translocation of newly synthesised viral proteins to the nucleus. In contrast, mouse MX1 is primarily localised in the nucleus (Stranden et al., 1993). Nuclear localisation of mouse MX1 is essential to counteracting influenza virus infection, based on the data showing that cytoplasmic variants of mouse MX1 protein were inefficient in inhibiting both influenza virus and VSV (Zurcher et al., 1992c).

1.7.1.3.2 Antiviral activity of MX proteins

Further, the primary influenza viral transcript levels of the three polymerase genes PB1, PB2 and PA were found to be significantly lower in stably transfected cell lines expressing MX1 protein (Verhelst et al., 2012). These results suggest that mouse MX1 inhibits the mRNA synthesis of the influenza virus dependent on the location of the MX1 protein in the cells. In addition to restricting replication of RNA viruses, the cytoplasmic human MX1 protein has been found to have broad antiviral activities against large DNA viruses, such as African swine fever virus (ASFV) and HSV (Netherton et al., 2009; Ku et al., 2011). Another member of the MX family has also been reported to show human-mouse differences. Mouse MX2 has been shown to reside in the cytoplasm and exhibit antiviral activity against VSV and Hantaan virus (Zurcher et al., 1992b; Jin et al., 2001). However, no antiviral activity has been discovered in human MX2 protein to date.

1.7.2 Human-mouse differences in HSV-1 infection

1.7.2.1 IFN-stimulated genes

In the innate immune responses, several genes, including *Mda5*, *Mx2* and members in the guanylate nucleotide binding protein (*Gbp*), are upregulated in mouse embryonic fibroblasts, but these genes are significantly downregulated by HSV-1 infection in primary human fibroblasts (Pasieka et al., 2006; Peng et al., 2008). In addition to the human-mouse difference in the expression level of innate proteins, a controversial relationship between MX1 and HSV-1 has been identified. Originally, human MX1 protein was reported to have no ani-HSV-1 activity when MX1-transfected mouse 3T3 cells were infected (Pavlovic et al., 1990). Later, another study showed that HSV-1 titres were decreased in human HEK293 cells transiently overexpressed with MX1 (Ku et al., 2011). These contradictory results may be due to the use of different cell types and methods to express the MX1 protein or to a difference between species.

1.7.2.2 Necroptosis

HSV-1 suppresses necroptosis in human cells (Guo et al., 2015b; Guo et al., 2018), but it induces necroptosis in mouse cells (Dufour et al., 2011a; Dufour et al., 2011b; Yu and He, 2016). Necroptosis is a mechanism to eliminate pathogens in infected cells by disrupting cellular membrane in a programmed manner, thus distinct from necrosis (Du et al., 2013; Yu and He, 2016). Necroptosis occurs when Casp8 and apoptosis is inhibited, but the cell death pathways are activated by stimuli, such as viral nucleic acids and viral proteins (Orzalli and Kagan, 2017). When Casp8 is inhibited, TNF signalling induces the formation of a protein complex known as the necrosome, which includes receptor interacting protein-1 and -3 (RIP1 and RIP3) (Holler et al., 2000; Cho et al., 2009). Activated RIP3 recruits and phosphorylates mixed lineage kinase-like (MLKL), and MLKL forms a pore-like structure on the cell membrane, resulting in cell lysis and membrane leakage (Orzalli and Kagan, 2017; Nailwal and Chan, 2019).

Host cells use this strategy to overcome both DNA and RNA virus infection (Galluzzi et al., 2017). This is because necroptosis mediates the release of intracellular damage-associated molecular patterns, including IL-1, uric acid and DNA, leading to the recruitment of proinflammatory cell types to sites of infection (Huang et al., 2015; Nogusa et al., 2016). HSV-1 ICP6 normally blocks apoptosis and necroptosis in human cells and that just the opposite is seen in mice (Huang et al., 2015; Yu et al., 2015). HSV-1 can inhibit apoptosis and Casp8 activity, resulting in necroptosis as an alternative death pathway during HSV-1 infection in human cells (Dufour et al., 2011a; Dufour et al., 2011b). Additionally, HSV-1 replication in RIP3 knockout mouse cells was elevated because necroptosis does not correctly proceed (Huang et al., 2015). Furthermore, the RIP homotypic interaction motif (RHIM) domain of the UL39 protein

in both HSV-1 and HSV-2 associates with RHIM domain in the RIP1/3 complex, triggering necroptosis in HSV-1-infected mouse cells (Yu et al., 2015). RHIM domains of RIP1 and RIP3 are required for the interaction with the UL39 protein (Huang et al., 2015). On the contrary, the UL39 protein cannot induce necroptosis in human cells (Guo et al., 2015b). The UL39 protein was found to be sufficient to interrupt the RIP1-RIP3 association in a UL39- and RHIM-dependent manner, protecting human cells from HSV-1 induced necroptosis (Guo et al., 2015b). The data above suggest that the sequence of the RHIM domain in the UL39 protein and RIPs may determine whether the interaction is pro-necroptotic or anti-necroptotic in different species. HSV-1 has evolved a method to evade necroptosis-mediated antiviral signalling in humans, but sequence differences between human and mouse proteins which interact with UL39 result in species-specific discrepancies.

1.8 Aims of this thesis

Species and sex differences are either ignored or poorly studied in HSV-1 infection. Both of these factors are amenable to characterisation by RNA sequencing analysis, leading to further dissection. Thus, the aims of this thesis were:

1. To determine whether there are sex-related differences in virus replication and transcriptional regulation during HSV-1 infection of cells in cultures (Chapter 3).

2. To discover potential antiviral factors acting as an ideal marker for the sex-specific responses (Chapter 4).

3. To examine potential mechanisms that drive sex-specific responses in HSV-1-infected cells (Chapter 5)

4. To characterise the pathways that are differentially regulated between primary human and mouse skin cells (Chapter 6).

5. To identify key genes in the host and virus that contribute to the human-mouse differences in HSV-1 replication (Chapter 6).

Chapter 2. Materials and Methods

2.1 Materials

2.1.1 Buffers and solvents

EDTA: 0.5 M ethylenediaminetetraacetic acid in deionised water (pH 8.0).

1x TAE buffer: 1 mM EDTA (pH 8.0), 20 mM glacial acetic acid and 40 mM Tris base in deionised water.

1x ThermoPol buffer: Diluted from 10x ThermoPol buffer (New England Biolabs) in deionised water.

TE buffer: 1 mM EDTA and 10 mM Trizma base (pH 8.0) in deionised water.

1x T4 DNA ligase buffer: Diluted from 10x T4 DNA ligase buffer (New England Biolabs) in deionised water.

RSB buffer: 1.5 mM magnesium chloride (Ajax FineChem), 10 mM potassium chloride (Sigma-Aldrich) and 10 mM Trizma base (Sigma-Aldrich) in deionised water.

PBS: Phosphate-buffered saline obtained from Sigma-Aldrich.

PBS-T: PBS with 0.1% Tween-20 detergent.

FACS-PBS: PBS with 2% foetal bovine serum (FBS; Serana, Australia).

1 M Tris, pH 6.8: 1 M Trizma base (Sigma-Aldrich) in deionised water (pH 6.8).

1.5M Tris, pH 8.8: 1 M Trizma base (Sigma-Aldrich) in deionised water (pH 8.8).

Cycloheximide: 100 mg/mL cycloheximide (Sigma-Aldrich).

Acetone (Merck).

Dimethyl sulfoxide (DMSO) (Sigma-Aldrich).

Ethanol (Merck).

Methanol (Merck).

Nuclease free water (Ambion).

Sterile water (Baxter healthcare).

2.1.2 Media for cell culture

CMC-MEM: 0.4% (w/v) medium viscosity sodium carboxymethyl cellulose (CMC; Sigma) in Minimum Essential Medium (MEM) supplemented with 2 mM L-glutamine and 2% FBS.

DMEM: Dulbecco's modified eagle medium (DMEM; Invitrogen), supplemented with 2 mM L-glutamine (Life Technologies) and 2% (v/v) or 10% (v/v) FBS (Serana, Australia).

MEM: Minimum essential medium (MEM; Invitrogen) supplemented with 5 mM HEPES (Life Technologies), 2 mM L-glutamine (Invitrogen), 50 μM 2-mercaptoethanol (Gibco) and 2% (v/v) or 10% (v/v) FBS (Serana, Australia).

2.1.3 Media for bacterial culture

Luria-Bertani (LB) medium: 5 g yeast extract (Bacto), 10 g sodium chloride (Merck) and 10 g tryptone (Bacto) in 1 L deionised water.

LB-agar plates: 10 g tryptone (Bacto), 5 g yeast extract (Bacto), 10 g sodium chloride (Sigma-Aldrich) and 15 g Bacto-agar (Bacto) in 1 L deionised water. To make LB-agar plates with antibiotics, ampicillin (Sigma-Aldrich) or kanamycin (Sigma-Aldrich) was added to a final concentration of 100 μg/ml before pouring.

SOC medium: Super optimal broth with catabolite repression (SOC) medium (Invitrogen).

Antibiotics: 100 μg/ml ampicillin (Sigma-Aldrich) or 100 μg/ml kanamycin (Sigma-Aldrich) in deionised water .

60% (v/v) Glycerol: 60% (v/v) glycerol (Sigma-Aldrich) in deionised water.

2.1.4 Reagents for molecular biology

10% SDS: 10% (w/v) sodium dodecyl sulfate (SDS; Sigma-Aldrich).

Bovine Serum Albumin (BSA; Sigma-Aldrich).

Transfer buffer: 6 g/L Trizma base (Sigma-Aldrich), 3 g/L glycine (Bacto) and 10% (v/v) methanol (Merck) in deionised water.

1x Laemmli buffer: 3 g/L Trizma base (Sigma-Aldrich), 19 g/L glycine and 1% (v/v) SDS with the pH adjusted to 8.3.

40% Acrylamide/Bis solution: 40% acrylamide and bis acrylamide (29:1) solution (Biorad).

Tween 20 (Sigma).

Bromophenol blue (Biorad).

Tetramethylethylenediamine (N-N-N'-N'-tetramethylethylenediamine; TEMED; Biorad).

10% ammonium persulfate: 10% (w/v) ammonium persulfate (APS; Biorad) in deionised water.

5x Western blot loading buffer: 15 ml stock solution containing 3 ml 20% SDS, 3.75 ml Tris buffer (1 M, pH 6.8), 9 mg bromphenol blue, 2.4 ml 2-mercaptoethanol, 4.5 ml glycerol.

Tris-glycine Sodium dodecyl sulfate polyacrylamide gel electrophoresis (SDS-PAGE): Recipes for stacking and resolving gels for SDS-PAGE are described in Table 2-1 and Table 2-2.

Table 2-1. Resolving gel for Tris-glycine SDS-PAGE in 10 ml.

	10%	12%	15%
Deionised water	4.8 ml	4.3 ml	3.5 ml

40% acrylamide/bis solution	2.5 ml	3.0 ml	3.8 ml
1.5 M Tris, pH 8.8	2.5 ml	2.5 ml	2.5 ml
10% APS	100 µl	100 µl	100 µl
10% SDS	100 µl	100 µl	100 µl
TEMED	4 µl	4 µl	4 µl

Table 2-2. 5% (v/v) stacking gel for Tris-glycine SDS-PAGE in 4 ml.

Deionised water	2.9 ml
40% acrylamide/bis solution	0.5 ml
1 M Tris, pH 6.8	0.5 ml
10% APS	40 µl
10% SDS	40 µl
TEMED	4 µl

Protein marker: Prestained protein ladder (10 to 180 kDa; Thermo Scientific).

Nitrocellulose membrane (NC membrane): 0.20 µm pore-size nitrocellulose membrane (Biorad).

Enzyme-linked chemiluminescence (ECL) substrate: Clarity Western ECL substrate (Biorad) and Amersham ECL prime Western blotting detection reagent (GE Healthcare).

Agarose for DNA gel electrophoresis: 1.0% or 2.0% (w/v) UltraPure Agarose (Life Technologies) in 1x TAE Buffer.

Plasmid miniPrep kit (Favorgen).

Plasmid midiPrep kit (Invitrogen).

Gel and PCR clean-up kit: Wizard SV gel and PCR clean-up system (Promega).

qPCR mastermix: 2x Power SYBR green master mix (Applied Biosystems).

Qubit assays: Qubit RNA HS assay (Life Technologies).

Bioanalyser: Agilent 2100 Bioanalyser (Agilent Technologies).

High Sensitivity DNA Kit: Agilent High Sensitivity DNA kit (Agilent Technologies).

RNA analysis kit: Agilent RNA 6000 Nano kit (Agilent Technologies).

Whole transcriptome analysis (RNA-Seq) kit: TruSeq stranded total RNA library preparation kit (Illumina).

Whole genome sequencing kit: Nextera XT DNA library preparation kit (Illumina).

Big Dye terminator: Big Dye terminator for DNA sequencing (Life Technologies) with 5x reaction buffer supplied by Biomolecular Resource Facility, John Curtin School of Medical Research, ANU.

DNA markers: 100 bp (New England Biolabs) and 1 kb DNA markers (New England Biolabs).

6x DNA gel loading buffer (New England Biolabs).

Deoxyribonucleotide triphosphate mix: 10 mM deoxyribonucleotide triphosphate (dNTP) mix (Bioline).

siRNAs.

Table 2-3. siRNAs used in this thesis.

Ref_mRNA_ID	Gene_Symbol	Assay ID	Source
NM_001290729	Taf1	503338	Thermo Scientific
NM_001079513	Zbtb33	SASI_Mm02_00293002	Sigma-Aldrich
NM_001113354	Phf8	SASI_Mm02_00307463	Sigma-Aldrich
NM_027382	Hdac8	SASI_Mm01_00107278	Sigma-Aldrich
NM_007922	Elk1	SASI_Mm01_00163817	Sigma-Aldrich
NM_008224	Hcfc1	SASI_Mm01_00051349	Sigma-Aldrich
NM_008390	Irf1	SASI_Mm01_00151781	Sigma-Aldrich
NM_016849	Irf3	SASI_Mm02_00323626	Sigma-Aldrich
NM_016850	Irf7	SASI_Mm01_00188289	Sigma-Aldrich
NM_020256	Zbtb33	SASI_Mm01_00171874	Sigma-Aldrich
NR_001463	Xist	SASI_Mm02_00352381	Sigma-Aldrich
NM_021384	Viperin	SASI_Mm01_00031984	Sigma-Aldrich
NM_006777	Zbtb33	SASI_Hs01_00199087	Sigma-Aldrich
NR_001564	Xist	SASI_Hs02_00375151	Sigma-Aldrich

NM_080657	Viperin	SASI_Hs02_00362416	Sigma-Aldrich
Universal negative control	NA	SIC001	Sigma-Aldrich

In-Fusion HD cloning kit (Clontech).

Phusion DNA polymerase: Phusion DNA polymerase (New England Biolabs).

Taq DNA Polymerase: Taq DNA Polymerase (New England Biolabs).

Restriction enzymes: Various restriction endonucleases (New England Biolabs).

DNA gel staining solution: GelRed staining solution (Biotium), 1 in 10,000 diluted in deionised water.

Lipofectamine transfection kit: Lipofectamine 2000 (Life Technologies).

Nucleofector transfection kit: Nucleofector kits for primary fibroblasts (Lonza).

Nuclear and cytoplasmic extraction reagents: Nuclear extraction kit (Abcam; ab113474).

Paraformaldehyde: 16% paraformaldehyde (PFA) in deionised water (Electron Microscopy Sciences).

cDNA synthesis kit: SuperScript VILO cDNA synthesis kit (Life Technologies).

DNase: DNase I, RNase free (Ambion).

Phenol:chloroform: Phenol:chloroform:isoamyl alcohol (25:24:1 ratio; Sigma-Aldrich).

IGEPAL: IGEPAL CA-630 (Sigma-Aldrich).

RNA extraction kits: Two RNA isolations kits were used: the RNAqueous micro kit (Ambion) for small scale RNA isolation from sorted cells and the TRIzol reagent (Invitrogen) for medium scale RNA extraction from cultured cells.

T4 DNA ligase: 400 units/µl T4 DNA ligase (New England Biolabs).

Sodium acetate: 3 M sodium acetate (Merck) in deionised water.

2.1.5 Reagents for cell culture and virology

Crystal violet staining solution: 2.5% (v/v) crystal violet (Sigma-Aldrich) in 20% (v/v) ethanol.

Collagenase solution: 0.5% (w/v) Type IV Collagenase (at least 160 units/ml; Worthington) in deionised water.

Trypsin: 0.05% (w/v) trypsin with 0.53 mM EDTA (Invitrogen).

Foetal bovine serum (Serana, Australia).

100x MEM NEAA: MEM Non-Essential Amino Acids Solution (NEAA; Gibco), diluted as appropriate.

2-Mercaptoethanol: 55 mM 2-Mercaptoethanol in Dulbecco's Phosphate Buffered Saline (DPBS; Gibco).

Penicillin streptomycin solution: Penicillin streptomycin solution (10,000 U/ml; Gibco), diluted as appropriate.

Geneticin solution: Geneticin solution (50 mg/ml; G418; Gibco), diluted as appropriate.

2.1.6 Reagents for infection of mice

Avertin: 2.5% (v/v) 2-methyl-butanol (Sigma-Aldrich) and 12.5 mg/ml 2,2,2-tribromoethanol (Sigma-Aldrich) in deionised water.

Veet depilatory cream: Veet depilatory cream for sensitive skin (Reckitt Benckiser).

2.1.7 Plasmids

All plasmids in this thesis were isolated using a MiniPrep or MidiPrep kit (Section 2.2.2.1). Plasmids used during this thesis are listed in Table 2-4. Plasmids produced during this thesis are described in Table 2-5.

Table 2-4. Plasmids used in this thesis.

Plasmid name	Description	Source
pSSmCB	The plasmid contains an mCherry gene under the control of the Vaccinia virus (VACV) strong synthetic promoter.	(Dobson et al., 2014)
lentiCRISPR v2	The plasmid contains two expression cassettes, hSpCas9 and the chimeric guide RNA. It can be digested by the *B*smBI restriction enzyme and a pair of annealed oligos can be cloned into the single guide RNA scaffold.	A gift from Dr. Gaétan Burgio (Burgio, 2018)
p3x FLAG-CMV-14	The plasmid encodes three adjacent FLAG epitopes downstream of the multiple cloning sites. It is used to establish expression of transient or stable intracellular C-terminal 3x FLAG fusion proteins in mammalian cells.	A gift from Professor Wei-Li Hsu (Tseng et al., 2015)

Table 2-5. Plasmids generated in this thesis.

Plasmid name	Description
lentiCRISPRmCherry	lentiCRISPR v2 vector with the coding sequence of the mCherry fluorescent protein under the control of the EFS-NS promoter.
p3xFLAG-viperin	p3xFLAG-CMV-14 with the full-length coding sequence of mouse viperin fusion with three adjacent FLAG epitopes.
p3xFLAG-viperin-Δ9-42	p3xFLAG-CMV-14 with the mouse viperin deleted of 9 to 42 amino acid residues fusion with three adjacent FLAG epitopes.
p3xFLAG-viperin-Δ71-182	p3xFLAG-CMV-14 with the mouse viperin deleted of 71 to 182 amino acid residues fusion with three adjacent FLAG epitopes.
p3xFLAG-viperin-Δ218-361	p3xFLAG-CMV-14 with the mouse viperin deleted of 218 to 361 amino acid residues fusion with three adjacent FLAG epitopes.
lentiCRISPRmCherry-Mb21d1 (cGAS)	Contains a guide RNA designed to target the Mb21d1 (cGAS) coding sequence inserted into lentiCRISPRmCherry.
lentiCRISPRmCherry-Ifih1 (Mda5)	Contains a guide RNA designed to target the Ifih1 (Mda5) coding sequence inserted into lentiCRISPRmCherry.
lentiCRISPRmCherry-Ddx58 (Rig-I)	Contains a guide RNA designed to target the Ddx58 (Rig-I) coding sequence inserted into lentiCRISPRmCherry.
lentiCRISPRmCherry-Tbk1	Contains a guide RNA designed to target the Tbk1 coding sequence inserted into lentiCRISPRmCherry.

lentiCRISPRmCherry-Tlr3	Contains a guide RNA designed to target the Tlr3 coding sequence inserted into lentiCRISPRmCherry.
lentiCRISPRmCherry-Tlr4	Contains a guide RNA designed to target the Tlr4 coding sequence inserted into lentiCRISPRmCherry.
lentiCRISPRmCherry-Zbtb33	Contains a guide RNA designed to target the Zbtb33 coding sequence inserted into lentiCRISPRmCherry.
lentiCRISPRmCherry-Rsad2 (Viperin)	Contains a guide RNA designed to target the Rsad2 (viperin) coding sequence inserted into lentiCRISPRmCherry.
lentiCRISPRmCherry-human-Mx1	Contains a guide RNA designed to target the human Mx1 coding sequence inserted into lentiCRISPRmCherry.
lentiCRISPRmCherry-human-Jak1	Contains a guide RNA designed to target the human Jak1 coding sequence inserted into lentiCRISPRmCherry.
lentiCRISPRmCherry-mouse-Mx1	Contains a guide RNA designed to target the mouse Mx1 coding sequence inserted into lentiCRISPRmCherry.
lentiCRISPRmCherry-mouse-Jak1	Contains a guide RNA designed to target the mouse Jak1 coding sequence inserted into lentiCRISPRmCherry.
p3xFLAG-HSV-1-VP16	p3xFLAG-CMV-14 with the coding sequence of HSV-1 VP16
p3xFLAG- HSV-1-ICP34.5	p3xFLAG-CMV-14 with the coding sequence of HSV-1 ICP34.5

2.1.8 Oligodeoxynucleotides

Oligodeoxynucleotides used in this thesis were synthesised and purified by Sigma-Aldrich and are listed in Table 2-6, Table 2-7, Table 2-8 and Table 2-9. Working stocks of 10 pmol/µl (10 µM) were prepared in deionised water and stored at -20°C. Primer sets for qPCR for the detection of human or mouse genes (Table 2-7) were acquired from the GETprime online tool (http://bbcftools.epfl.ch/getprime/). Guide RNA (Table 2-8) was designed based on the ATUM CRISPR gRNA design tool (https://www.atum.bio/eCommerce/cas9/input).

Table 2-6. Oligodeoxynucleotides used for InFusion and ligation-based cloning.

Primer name	Sequence (5'-3')
IF-mCherry-F	CGCCACCCGCGACGACGTCATGGTGAGCAAGGGCGAGGA
IF-mCherry-R	CGGCCCTGGGGACGTCGTCTTACTTGTACAGCTCGTCC
viperin-*K*pnI-F	TCAAGGTACCATGCTAGTGCCCACT

viperin-*X*baI-R	CGTATCTAGAGCACCAGTCCAGCTTCAG
Δ9-42 viperin-*K*pnI-F	TCAAGGTACCATGCTAGTGCCCACTGCTCTAGCT GGGAAGGAACAGCCACAGGT
Δ71-182 viperin-F	ACTCAGCGCACAACCGATGAACAGGTTAAT
Δ71-182 viperin-R	ATTAACCTGTTCATCGGTTGTGCGCTGAGT
Δ218-361 viperin-*X*baI-R	CGTATCTAGACTTGAAAGCCACCTTGT
HSV-1-VP16-*H*indIII-F	TCCGAAGCTTATGGACCTCTTGGTCGACG
HSV-1-VP16-*X*baI-R	CGCGTCTAGAGTACCCACCGTACTCGTCA

Table 2-7. Oligodeoxynucleotide primers used for qPCR.

Primer name	Sequence (5'-3')
mouse-Mb21d1 (cGAS)-F	CATGTGAAGATTTCTGCTCCT
mouse-Mb21d1 (cGAS)-R	TCACAAGATAGAAAGCACCTG
mouse-Ifih1 (Mda5)-F	CTGTGACCACAGAATCAGAC
mouse-Ifih1 (Mda5)-R	TGTTGCTGTTATGTCCAAGAC
mouse-Ddx58 (Rig-I)-F	AATTTGGAAAGACGGTTCACC
mouse-Ddx58 (Rig-I)-R	GTCAGGAACAGGTTGTGGT
mouse-Tbk1-F	GAAGAGTGGATGAGAAAGATGC
mouse-Tbk1-R	TTCCTCTTCGATATCGAAACAC
mouse-Rsad2 (Viperin)-F	CTCAAACAGGCTGGTTTGG
mouse-Rsad2 (Viperin)-R	CTTGCCCAAGTATTCACCC
mouse-Irf1-F	AAACCAAGAGGAAGCTGTG
mouse-Irf1-R	GGTCATCAGGTAGGGTAGAG
mouse-Irf3-F	CTACACTCTGTGGTTCTGC
mouse-Irf3-R	GTAGGAACAACCTTGACCA
mouse-Irf7-F	CTTGGATCTACTGTGGGCC
mouse-Irf7-R	CTTGCCAGAAATGATCCTGG
mouse-Zbtb33-F	AGTAACAACACAGCAACACAG
mouse-Zbtb33-R	TCACTTCCGAAATAGCAACAG
mouse-Xist-F	AGACTACAGGATGAATTTGGAG
mouse-Xist-R	ACTCTTCACTCCTCTAAATCCA
human-Rsad2 (Viperin)-F	GTGGTTCCAGAATTATGGTGAG
human-Rsad2 (Viperin)-R	ATAAGGACATTGACTTCCTCGT
human-Zbtb33-F	GAGCGACGTTTAAAGAAGGG
human-Zbtb33-R	TTCTACTCTCCATGCCTGC
human-Xist-F	CGGGTCTCTTCAAGGACATTTAGCC

human-Xist-R	GCACCAATACAGAGGAATGGAGGG
human-Tbk1-F	GGAAACAGTTATTATCGCTGAC
human- Tbk1-R	AGGCAGAGTTTCTTGTAACTC
human-Jak1-F	TCAGCATTAACAAGCAGGAC
human-Jak1-R	AGGGACACAAAGGACAAGG
human-Mx1-F	TAATAAAGCCCAGAATGCCA
human-Mx1-R	TTAGAGTCAGATCCGGGAC
human-Mx2-F	TTGAGATCATCGTGCATCAG
human-Mx2-R	GGATAATTTCCATGGCTTTCTG
human-Eif2ak2-F	ACATACCGTCAGAAGCAGG
human-Eif2ak2-R	GAAATGTAAACCTCCTATCATGTGG
human-Mapk1-F	CTATTTGCTTTCTCTTCCACAC
human-Mapk1-R	CAATAAGTCCAGAGCTTTGGA
human-Stat2-F	GCTATGATGGAGAAGCTGG
human-Stat2-R	CTGGATCTTATATCGGAAGCAG
mouse-Jak1-F	TATCTGTTTGCACAGGGAC
mouse-Jak1-R	TATCATGTCCGTCTTGCTC
mouse-Mx1-F	TGCTGTACTGCTAAGTCCA
mouse-Mx1-R	GAAGTGAAGTCGGATCAGG
mouse-Mx2-F	CACATCTGTAAATCTCTTCCTCTG
mouse-Mx2-R	TACCGTACTTCTGCAGCTC
mouse-Eif2ak2-F	GCTCGTCTATGACAAGTAATGG
mouse-Eif2ak2-R	CGAGACCGTTCGTAAACAC
mouse-Mapk1-F	GATCTCAAGATCTGTGACTTTGG
mouse-Mapk1-R	TACGTACTCTGTCAAGAACCC
mouse-Stat2-F	TGATCTCTAACAGACAGGTGG
mouse-Stat2-R	CTGCATTCACTTCTAAGGACTC
mouse-18srRNA-F	GCAATTATTCCCCATGAACG
mouse-18srRNA-R	GGCCTCACTAAACCATCCAA
human-18srRNA-F	CTACCACATCCAAGGAAGCA
human-18srRNA-R	TTTTTCGTCACTACCTCCCCG

Table 2-8. Oligodeoxynucleotides used for cloning guide RNA into lentiCRISPRmCherry vector.

Oligo name	Sequence (5'-3')
gRNA-Mb21d1 (cGAS)-F	CACCGGCGGACGGCTTCTTAGCGCG
gRNA-Mb21d1 (cGAS)-R	AAACCGCGCTAAGAAGCCGTCCGCC
gRNA- Ifih1 (Mda5)-F	CACCGCAGCAGCAGTTCTGCCGCGC
gRNA- Ifih1 (Mda5)-R	AAACGCGCGGCAGAACTGCTGCTGC
gRNA-Ddx58 (Rig-I)-F	CACCGCTGACTGCCTCCGTCGGCGT
gRNA-Ddx58 (Rig-I)-R	AAACACGCCGACGGAGGCAGTCAGC
gRNA-Tbk1-F	CACCGTTAGACCCTTCGAGGGGCCT
gRNA-Tbk1-R	AAACAGGCCCCTCGAAGGGTCTAAC
gRNA-Rsad2 (Viperin)-F	CACCGTGTCATTAATCGCTTCAACG
gRNA-Rsad2 (Viperin)-R	AAACCGTTGAAGCGATTAATGACAC

gRNA-Tlr3-F	CACCGCTTTCACACGTGCAGTCGAA
gRNA-Tlr3-R	AAACTTCGACTGCACGTGTGAAAGC
gRNA-Tlr4-F	CACCGCACGTCCATCGGTTGATCTT
gRNA-Tlr4-R	AAACAAGATCAACCGATGGACGTGC
gRNA-Zbtb33-F	CACCGACCGAAAATTCCGGGCCCAT
gRNA-Zbtb33-R	AAACATGGGCCCGGAATTTTCGGTC
gRNA-human-Jak1-F	CACCGCACTGACTGCTCATTGTCGT
gRNA-human-Jak1-R	AAACACGACAATGAGCAGTCAGTGC
gRNA-human-Mx1-F	CACCGAGCCCAGAATGCCATCGCCG
gRNA-human-Mx1-R	AAACCGGCGATGGCATTCTGGGCTC
gRNA-mouse-Jak1-F	CACCGTACAGACTGTTCGTTGTCAT
gRNA-mouse-Jak1-R	AAACATGACAACGAACAGTCTGTAC
gRNA-mouse-Mx1-F	CACCGGCCTGCCATCGCTGTCATTG
gRNA-mouse-Mx1-R	AAACCAATGACAGCGATGGCAGGCC

Table 2-9. Oligodeoxynucleotides used for Sanger sequencing.

Primer name	Sequence
hU6	GAGGGCCTATTTCCCATGATT
CMVIE	CGCAAATGGGCGGTAGGCGTG

2.1.9 Escherichia coli strains

In this thesis, two strains of E. coli were utilised, including α-Select Chemically Competent Cells (Gold Efficiency, Bioline) and One Shot Stbl3 Chemically Competent E. coli (Invitrogen). α-Select cells were generally used for cloning most vectors. Stbl3 cells were used to reduce the frequency of homologous recombination of long terminal repeats in lentiviral expression vectors.

2.1.10 Mice

Six-week-old male or female specific pathogen-free C57BL/6 mice were obtained from the Australian Phenomics Facility (Canberra, Australia). All mice were maintained in the containment suite at the John Curtin School of Medical Research, ANU. All experiments were approved by the ANU Animal Ethics and Experimentation Committee under protocol A2014/025 and A2017/39.

For preparation of primary mouse skin fibroblasts, three-day-old C57BL/6, Balb/c or IFNAR knockout mice (a gift from Dr. Si Ming Man) (Man et al., 2015) were obtained from the Australian Phenomics Facility (Canberra, Australia). Further details on the preparation of the primary mouse skin fibroblasts are provided in Section 2.2.18.

2.1.11 Cells

The cells used in this thesis are listed in Table 2-10. Cells were maintained in culture flasks at 37°C with 5% CO_2 and were subcultured twice a week as described in Section 2.2.17.

Table 2-10. Cells used in this thesis.

Cell	Origin	Property	Split ratio	Sex
HEK293	Human embryonic kidney cells transformed with human adenovirus 5 DNA	Adherent	1 in 12	Female
HFF	Human foreskin fibroblasts	Adherent	1 in 8	Male
MRC5	Human lung fibroblasts	Adherent	1 in 8	Male
Male cells (MF)	Mouse skin fibroblasts	Adherent	1 in 6	Male
Female cells	Mouse skin fibroblasts	Adherent	1 in 6	Female
$IFNAR^{-/-}$ (Male)	Mouse skin fibroblasts	Adherent	1 in 6	Male
$IFNAR^{-/-}$ (Female)	Mouse skin fibroblasts	Adherent	1 in 6	Female
HeLa	Human cervical cancer cells	Adherent	1 in 10	Female
Vero	African green monkey kidney epithelial cells	Adherent	1 in 8	Female
V27	Vero cells that were stably transfected to contain the HSV ICP27 gene preceded by the neo gene conferring resistance to Geneticin	Adherent	1 in 8	Female
BSC-1	African green monkey kidney epithelial cells	Adherent	1 in 6	NA
M2-10B4	Mouse bone marrow/stroma fibroblasts	Adherent	1 in 8	Female

2.1.12 Viruses

Viruses used in this thesis are listed in Table 2-11. 5dl1.2, ΔSma and LJS1 were gifts from Professor James Smiley, Department of Medical Microbiology and Immunology, University of Alberta, Edmonton, Canada (Corcoran et al., 2006). All viruses were grown and titres were determined in Vero cells, except 5dl1.2 and LJS1, for which V27 cells were used.

Table 2-11. Viruses used in this study.

Virus name	Description	Reference
HSV-1 KOS	Wild-type HSV-1 strain KOS	(Smith, 1964)

HSV-1 pICP47	HSV-1 strain KOS expressing an GFP/Cre cassette under the control of the ICP47 promoter from the UL3/UL4 intergenic region	(Russell and Tscharke, 2016)
5dl1.2 (HSV-1 ICP27 mutant)	HSV-1 strain KOS containing ICP27 null mutant	(McCarthy et al., 1989)
ΔSma (HSV-1 vhs mutant)	HSV-1 strain KOS containing a 588-nucleotide deletion in the UL41 gene (vhs)	(Read et al., 1993)
VACV Western Reserve (WR)	Wild-type Vaccinia strain WR	(Parker et al., 1941)
CPXV	Cowpox virus strain Brighton Red	A gift from Dr. Klaus Früh (Alzhanova et al., 2014)
MCMV	Murine cytomegalovirus strain Smith	A gift from Dr. Si Ming Man (Man et al., 2016)

2.1.13 Antibodies

The commercially available antibodies used in this study are listed in Table 2-12. All the antibodies were used to perform Western blotting. Anti-rabbit IgG-horseradish peroxidase (HRP) or anti-mouse IgG-horseradish peroxidase (HRP) was used as the secondary antibody for Western blotting. Other antibodies were used as the first antibodies.

Table 2-12. Antibodies used in this thesis.

Name	Host	Source
Anti-rabbit IgG-HRP	Goat	Abcam (ab97051)
Anti-mouse IgG-HRP	Goat	Abcam (ab6789)
Anti-mouse-MB21D1 (cGAS)	Rabbit	Cell Signalling (#31659)
Anti-mouse-IFIH1 (MDA5)	Rabbit	Abcam (ab69983)
Anti-mouse-DDX58 (RIG-I)	Rabbit	Cell Signalling (#3743)
Anti-mouse-TBK1	Rabbit	Cell Signalling (#3504)
Anti-mouse-TBK1p	Rabbit	Cell Signalling (#5483)
Anti-mouse-IRF1	Rabbit	Abcam (ab186384)
Anti-mouse-IRF3	Rabbit	Cell Signalling (#4302)
Anti-mouse-IRF7	Rabbit	Abcam (ab62505)
Anti-mouse-RSAD2 (Viperin)	Mouse	Abcam (ab107359)
Anti-mouse-β-CATENIN	Rabbit	Cell Signalling (#9582)
Anti-mouse-ZBTB33	Mouse	Abcam (ab12723)

Anti-human/mouse-JAK1	Rabbit	Cell Signalling (#3344)
Anti-human/mouse-JAK1p	Rabbit	Cell Signalling (#74129)
Anti-FLAG	Mouse	Sigma (F3165)
Anti-GAPDH	Rabbit	Cell Signalling (#5174)
Anti-HSV1 gB	Mouse	Abcam (ab6506)

2.2 Methods

2.2.1 Growth and maintenance of bacteria

E.coli was grown in liquid LB or on LB-agar plates supplemented with the appropriate antibiotics at 37ºC overnight. Bacterial stocks were stored in glycerol solution (600 µl of overnight culture in 400µl 60% glycerol) at -80 ºC.

2.2.2 DNA extraction and purification

2.2.2.1 Plasmid DNA isolation

Most plasmid DNA was extracted from 1.5 ml of overnight liquid bacterial cultures using the Favorgen plasmid MiniPrep kit according to the manufacturer's instructions. DNA was eluted in 40 µl of elution buffer.

If a large amount of DNA was required, plasmid DNA was isolated from 200 ml of liquid bacterial cultures using the Invitrogen MidiPrep kit according to the manufacturer's instructions. DNA was eluted in 1 ml of elution buffer.

2.2.2.2 PCR products and purification of linearized plasmids

PCR products and linearized plasmids obtained from restriction enzyme digestion were purified using the Wizard SV gel and a PCR clean-up kit from Promega, according to the manufacturer's instructions. The DNA was eluted in 40 µl of elution buffer.

In some experiments, DNA was isolated from an agarose gel to ensure that PCR products and linearized plasmids of the desired size were extracted. DNA fragments of the correct size were excised from the gel. Wizard SV gel and a PCR clean-up kit was used to purify DNA fragments from the agarose gel, according to the manufacturer's instructions.

2.2.2.3 Extraction of HSV genomic DNA for whole genome sequencing (WGS)

To generate HSV-1 DNA for use in WGS, male or female cells at 80% confluence were infected with the indicated viruses at an multiplicity of infection (MOI) of 0.01 for 48 hours. The cells were collected by centrifuging at 2,000 rpm (r_{max}: 207.8 mm) for 10 minutes at 4^{o}C and the supernatant was stored on ice. The harvested cells were lysed with RSB buffer with 0.5% (v/v) IGEPAL and were incubated for 10 minutes on ice. The cellular debris was pelleted by centrifuging at 2,000 rpm (r_{max}: 207.8 mm) for 10 minutes at 4°C. All of the collected supernatants were pooled and pelleted by centrifuging at 14,000 rpm (r_{max}: 63 mm) for 90 minutes at 4°C. The pellet was resuspended in 0.5 ml TE buffer with 50 µg/ml proteinase K, and was incubated for 5 minutes at room temperature. An equal volume of phenol:chloroform was added into this sample. The mixture was gently inverted until evenly mixed, and was then centrifuged at 14,000 rpm (r_{max}: 63 mm)for 10 minutes. The aqueous phase was again extracted with phenol:chloroform two times. The final aqueous phase was precipitated with a 0.1 volume of 3 M sodium acetate and two volumes of 100% ethanol. The DNA was collected by centrifuging at 14,000 rpm (r_{max}: 63 mm) for 30 minutes and the pellet was washed with 70% ethanol. The final pellet was resuspended in 100 µl TE buffer.

2.2.3 Polymerase chain reaction

Standard PCR was performed primarily for molecular cloning in this study. Phusion high-fidelity DNA polymerase (New England Biolabs) was used according to the manufacturer's instructions. PCRs were performed in 20 µl or 50 µl reaction volume using an ABI Veriti 96-well Thermocycler. The final reaction contained 1x Phusion HF buffer, 1 unit Phusion high-fidelity DNA polymerase, 200 µM dNTPs, 0.5 µM forward primer, 0.5 µM reverse primer and 2 µl template DNA (either purified plasmids (Section 2.2.2) or diluted cDNA reversely transcribed from RNA of male mouse skin fibroblasts (Section 2.2.4) in a 20 µl reaction. In this study, Phusion HF buffer was replaced with the Phusion GC buffer while amplifying HSV-1 gene. The samples were run on a PCR machine using the following conditions:

a. Initial denaturation: 98^{o}C for 5 minutes
b. Amplification
    30 cycles of
        Denaturation: 98^{o}C for 10 seconds
        Annealing: 60-65^{o}C for 30 seconds (depending on T_m of primers)
        Extension: 72^{o}C for 30 seconds per kb
c. Final extension: 72^{o}C for 10 minutes

d. Hold at 4°C

2.2.4 RNA isolation

2.2.4.1 Total RNA isolation from sorted cells

For sorted cells, RNA was extracted using the RNAqueous micro kit (Ambion). Sorted cells (Section 2.2.27) were mixed with 200 µl of the lysis buffer immediately to protect the RNA from degradation. RNA was extracted from the mixture following the manufacturer's instructions. DNase treatment was performed post-elution by incubating samples with DNase I and 1x DNase I buffer (Ambion) at 37°C for 30 minutes. Samples were stored at -80°C until required.

2.2.4.2 Total RNA isolation from cultured cells

For general cultured cells, RNA was isolated using the TRIzol reagent (Invitrogen). Cells were harvested and collected by centrifugation at 1,200 rpm (r_{max}: 207.8 mm) for 10 minutes. The supernatant was then removed and 1 ml of the TRIzol reagent was added into every 1 x 10^6 cells. After incubation of the mixture at room temperature for 5 minutes, RNA was isolated according to the manufacturer's instructions. Briefly, an equal volume of phenol:chloroform was added into this mixture and the mixture as gently inverted to evenly mix the samples. The two phases were then separated by centrifugation at 14,000 rpm (r_{max}: 63 mm) for 10 minutes. The aqueous phase was extracted with phenol:chloroform one more time. The resulting aqueous phase was precipitated with isopropanol (0.5 ml of isopropanol per 1 ml TRIzol reagent). The RNA was collected by centrifuging at 14,000 rpm (r_{max}: 63 mm) for 30 minutes and the pellet was washed with 70% ethanol. The final pellet was resuspended in 50 µl TE buffer.

2.2.5 Determining nucleic acid quantity

For general determination of DNA or RNA concentration, 2 µl of sample was measured by Nanodrop spectrophotometer (Thermo Scientific). To obtain a more accurate concentration of nucleic acid for use in qPCR analysis, a Qubit fluorometer (Life Technologies) was applied. For detecting RNA intact number before constructing RNAseq libraries or DNA library size distributions, the Agilent RNA 6000 Nano Kit (Agilent Technologies) or the Agilent High Sensitivity DNA Kit (Agilent Technologies) was used following the manufacturer's instructions.

2.2.6 cDNA synthesis

cDNA was synthesised using the SuperScript VILO cDNA synthesis kit (Invitrogen) according to the manufacturer's instructions. Briefly, 100, 300 or 500 ng of RNA was mixed with 4 µl of 5x VILO Reaction Mix and 2 µl of 10x SuperScript III Enzyme, and was filled up to 20 µl with nuclease-free water. The reaction was performed by incubation at 25°C for 10 minutes and then at 42°C for 60 minutes, followed by termination at 85°C for 5 minutes.

2.2.7 Construction of standard curve for qPCR analysis

p3xFLAG-viperin plasmid was isolated as described in Section 2.2.2.1. DNA quantity was measured by Qubit assay (Life Technologies), as mentioned in Section 2.2.5. The mass in nanograms was converted to copy numbers based on the formula below:

$$\text{Number of copies (molecules)} = \frac{\text{X ng} * 6.0221*10^{23}\ \text{molecules/mole}}{(\text{N} * 660\ \text{g/mole}) * 1*10^{9}\ \text{ng/g}}$$

X: amount of DNA (ng);
N: length of dsDNA;
660 g/mole: average mass of 1 bp dsDNA.

The DNA was diluted in 10-fold serial dilutions to the desired concentration in order to construct the standard curve.

2.2.8 qPCR analysis

Human or mouse qPCR primer sets were designed by the GETprime online tool to amplify specific transcripts (http://bbcftools.epfl.ch/getprime/). Samples were diluted 1:3, 1:5 or 1:10 with nuclease-free water before performing qPCR on a 7900HT Fast Real-Time PCR System (Applied Biosystems). The qPCR reaction was performed by mixing 0.5 µM forward primer, 0.5 µM reverse primer, appropriated diluted sample and 5 µl of 2x Power SYBR green PCR master mix (Applied Biosystems) in 10 µl total volume. The qPCR assays were performed using the following program:

a. Initial denaturation: 95ºC for 10 minutes
b. Amplification and detection
    40 cycles of
        Denaturation: 95ºC for 15 seconds
        Annealing and Extension: 60ºC for 30 seconds
c. Dissociation curves detection
    1 cycle of
        Denaturation: 95ºC for 15 seconds
        Annealing: 60ºC for 15 seconds
        Extension: 95ºC for 15 seconds

Dissociation curves were run to determine the accuracy of the amplified products. Sequence Detection System v2.4 software from Applied Biosystems was used to analyse Ct and Tm values. Expression levels of each gene were normalised to 18srRNA and then differential expressions were determined by the $2^{-\Delta\Delta Ct}$ method.

2.2.9 Restriction enzyme digestion

Restriction enzyme digestion was used to linearize plasmids for cloning. Digests were performed according to the manufacturer's instructions (New England Biolabs). In brief, each restriction digestion reaction contained 1x NEBuffer, 100 ng/µl purified plasmids and 0.2 unit/µl restriction enzymes, in a total volume of 20 µl. The reactions were incubated at the recommended temperature overnight.

2.2.10 Agarose gel electrophoresis

To visualise the resulting DNA fragments digested by restriction enzymes or the PCR products, the DNA fragments were separated by running gel electrophoresis on 0.8, 1.0 or 2.0% agarose TAE gels in 1x TAE buffer. DNA ladder was loaded into the first well of each gel and used to indicate a molecular size. DNA was mixed with 6x DNA loading dye and the mixture was loaded into the wells. Gels were run at 110 V for 30 minutes using horizontal electrophoresis apparatuses (Bio-Rad). Gels were stained after electrophoresis with GelRed staining solution (Biotium) for 20 minutes. DNA fragments were visualised and photographed using the Gel Doc XR System (Biorad).

2.2.11 Annealing of single-stranded oligonucleotides

Oligonucleotides shown in Table 2-8 were annealed with their complementary oligonucleotides to generate short double-stranded DNA inserts encoding guide RNA for cloning into lentiCRISPRmCherry vectors (Section 2.2.12). Briefly, 1 µl (100 µM) of each complementary single-stranded oligonucleotide was mixed with 1.5 µl of 10x T4 DNA ligase buffer and 8.5 µl deionised water. The sample was then incubated at 95°C for 5 minutes, followed by ramping down to 25ºC at 5ºC/min. The annealed oligonucleotides were then stored at 4°C before use.

2.2.12 Molecular cloning

Two different methods were used for construction of plasmids in this thesis: standard ligation of digested, amplified or annealed DNA and InFusion cloning (Clontech).

2.2.12.1 Ligation for molecular cloning

T4 DNA ligase and its buffer, both obtained from New England Biolabs, were used to ligate linearized plasmids with annealed oligonucleotides (Section 2.2.11 and Table 2-13) or PCR products after restriction digest with enzymes producing complementary overhanging sequences (Table 2-14).

For ligation of annealed oligonucleotides with linearized plasmids, the annealed oligonucleotides from Section 2.2.11 were diluted into sterile water at a 1:100 ratio. Briefly, a 12 µl reaction contained 1 µl of the diluted oligonucleotides, 50 ng of *B*smBI digested plasmid, two units of T4 DNA ligase and 1x T4 DNA ligase buffer. The reaction was incubated at 16ºC for two hours and was then used for transformation (Section 2.2.13). Plasmids generated by this method are shown in Table 2-13.

For ligation of PCR products after enzyme digestion with linearized plasmids (Table 2-14), the reaction contained 50 ng of vector DNA, a 2:1 molar ratio of insert to vector DNA, two units of T4 DNA ligase and 1x T4 DNA ligase buffer in a total volume of 12 µl. The reaction was incubated at room temperature for 16 hours and was then used for transformation (Section 2.2.13). DNA fragments of viperin with deletion of residues 71 to 182 were built by overlap extension PCR (Heckman and Pease, 2007). In short, two separate rounds of PCRs were applied to produce the upstream or downstream sequences of the deletion region from p3xFLAG-viperin plasmids. Afterwards, products of the two separate PCR reactions having 15-bp overlaps were then used as the template for the next round of PCR using the outermost primers to construct the

final insert DNA fragments. These insert fragments were digested by corresponding restriction enzymes and ligated with the linearized p3xFLAG-CMV-14 vector.

Table 2-13. Plasmids constructed by ligation of annealed oligonucleotides.

Plasmid produced	Restriction enzyme (s)	Vector details	Insert details	
		Parental plasmid	oligo 1	oligo 2
lentiCRISPRmCherry-Mb21d1 (cGAS)	*B*smBI	lentiCRISPRmCherry	gRNA-Mb21d1 (cGAS)-F	gRNA-Mb21d1 (cGAS)-R
lentiCRISPRmCherry-Ifih1 (Mda5)	*B*smBI	lentiCRISPRmCherry	gRNA- Ifih1 (Mda5)-F	gRNA- Ifih1 (Mda5)-R
lentiCRISPRmCherry-Ddx58 (Rig-I)	*B*smBI	lentiCRISPRmCherry	gRNA-Ddx58 (Rig-I)-F	gRNA-Ddx58 (Rig-I)-R
lentiCRISPRmCherry-Tbk1	*B*smBI	lentiCRISPRmCherry	gRNA-Tbk1-F	gRNA-Tbk1-R
lentiCRISPRmCherry-Tlr3	*B*smBI	lentiCRISPRmCherry	gRNA-Tlr3-F	gRNA-Tlr3-R
lentiCRISPRmCherry-Tlr4	*B*smBI	lentiCRISPRmCherry	gRNA-Tlr4-F	gRNA-Tlr4-R
lentiCRISPRmCherry-Zbtb33	*B*smBI	lentiCRISPRmCherry	gRNA-Zbtb33-F	gRNA-Zbtb33-R
lentiCRISPRmCherry-Rsad2 (Viperin)	*B*smBI	lentiCRISPRmCherry	gRNA-Rsad2 (Viperin)-F	gRNA-Rsad2 (Viperin)-R
lentiCRISPRmCherry-human-Jak1	*B*smBI	lentiCRISPRmCherry	gRNA-human-Jak1-F	gRNA-human-Jak1-R
lentiCRISPRmCherry-human-Mx1	*B*smBI	lentiCRISPRmCherry	gRNA-human-Mx1-F	gRNA-human-Mx1-R
lentiCRISPRmCherry-mouse-Jak1	*B*smBI	lentiCRISPRmCherry	gRNA-mouse-Jak1-F	gRNA-mouse-Jak1-R
lentiCRISPRmCherry-mouse-Mx1	*B*smBI	lentiCRISPRmCherry	gRNA- mouse -Mx1-F	gRNA- mouse -Mx1-R

Table 2-14. Plasmids constructed by ligation of products of restriction digest.

Plasmid produced	Restriction enzyme (s)	Vector details	Insert details		
		Parental plasmid	Template DNA	Forward primer	Reverse primer
p3xFLAG-viperin	*K*pnI and *X*baI	p3xFLAG-CMV-14	MF cDNA	viperin-*K*pnI-F	viperin-*X*baI-R
p3xFLAG-viperin-Δ9-42	*K*pnI and *X*baI	p3xFLAG-CMV-14	p3xFLAG-viperin	Δ9-42 viperin-*K*pnI-F	viperin-*X*baI-R
p3xFLAG-viperin-Δ71-182	*K*pnI and *X*baI	p3xFLAG-CMV-14	p3xFLAG-viperin	viperin-*K*pnI-F and Δ71-182 viperin-F	viperin-*X*baI-R and Δ71-182 viperin-R
p3xFLAG-viperin-Δ218-361	*K*pnI and *X*baI	p3xFLAG-CMV-14	p3xFLAG-viperin	viperin-*K*pnI-F	Δ218-361 viperin-*X*baI-R

p3xFLAG-HSV-1-VP16	*H*indIII and *X*baI	p3xFLAG-CMV-14	HSV-1 genomic DNA	HSV-1-VP16-*H*indIII-F	HSV-1-VP16-*X*baI-R
p3xFLAG-HSV-1-ICP34.5	*H*indIII and *X*baI	p3xFLAG-CMV-14	Synthesized by GenScript		

2.2.12.2 In-Fusion cloning

In-Fusion cloning is a ligation-independent cloning method which was applied to directly insert PCR products into a linearized vector by recombination. The plasmids that were generated using the In-Fusion cloning method are shown in Table 2-15. In brief, the insert used for In-Fusion cloning was amplified by PCR from plasmid DNA using a high fidelity polymerase. These primers had 15 nucleotide extensions at their 5' end homologous to the vector sequence.

In this thesis, a 2:1 molar ratio of insert to vector was used in a total volume of 10 µl containing 1x In-Fusion reaction buffer, 1 µl In-Fusion enzyme and deionised water. The reaction was performed by incubating at 37°C for 15 minutes, followed by 50°C for 15 minutes, and was then used for transformation (Section 2.2.13).

Table 2-15. Plasmids constructed by In-Fusion cloning.

Plasmid produced	Restriction enzyme (s)	Vector details	Insert details		
		Parental plasmid	Template DNA	Forward primer	Reverse primer
lentiCRISPRmCherry	Tth111I	lentiCRISPR v2	pSSmCB	IF-mCherry-F	IF-mCherry-R

2.2.13 Transformation

In total, 3 µl of In-Fusion reaction or 10 µl ligation mixture was mixed with 50 µl of α-Select Chemically Competent *E. coli* (Bioline) or 50 µl of One Shot Stbl3 competent cells (Invitrogen). The reaction was incubated on ice for 30 minutes and was then heat shocked at 42°C using a water bath for 90 seconds, followed by incubation on ice for 2 minutes. Next, 900 µl SOC medium was added into the transformed cells and the mixture was incubated at 37°C with shaking for one hour. Then, 200 µl of the transformed cells were plated onto LB-agar plates with the appropriate antibiotics (100 µg/ml of ampicillin or 100 µg/ml of kanamycin) and incubated at 37°C overnight. Plasmids from colonies were isolated (Section 2.2.2.1) for confirmation by restriction digest of plasmid DNA and Sanger sequencing (Section 2.2.14).

2.2.14 Sanger sequencing

Sanger sequencing reactions were performed using Big Dye Terminator (Life Technologies). Each 20 µl reaction contained 1 µl Big Dye terminator, 3.5 µl reaction buffer, 3.2 pmol appropriate primer and template DNA (150-300 ng of purified plasmid). Primers used Sanger sequencing in this thesis are shown in Table 2-9 and Table 2-16. The PCR conditions for Sanger DNA sequencing are described below:

a. Initial denaturation: 94°C for 5 minutes
b. Amplification and detection
    30 cycles of:
        Denaturation: 96°C for 10 seconds
        Annealing: 50°C for 5 seconds
        Extension: 60°C for 4 minutes
c. Hold at 4°C

DNA products from Sanger sequencing reactions were precipitated by adding 80 µl of solution containing 3.75 µl sodium acetate (3M), 62.5 µl 100% ethanol and 13.75 µl deionised water. After incubation at room temperature for 15 minutes, samples were centrifuged at 14,000 rpm (r_{max}: 63 mm) for 20 minutes and then washed with 250 µl 70% ethanol. The extension products were air dried and sent to the Biomolecular Resource Facility (John Curtin School of Medical Research, ANU) for sequencing.

Table 2-16. Primers used in Sanger sequencing.

Primer name	Used to sequence
hU6	lentiCRISPRmCherry; lentiCRISPRmCherry-Mb21d1 (cGAS); lentiCRISPRmCherry-Ifih1 (Mda5); lentiCRISPRmCherry-Ddx58 (Rig-I); lentiCRISPRmCherry-Tbk1; lentiCRISPRmCherry-Tlr3; lentiCRISPRmCherry-Tlr4; lentiCRISPRmCherry-Zbtb33; lentiCRISPRmCherry-Rsad2 (Viperin); lentiCRISPRmCherry-human-Mx1; lentiCRISPRmCherry-human-Jak1; lentiCRISPRmCherry-mouse-Mx1; lentiCRISPRmCherry-mouse-Jak1
CMVIE	p3xFLAG-viperin; p3xFLAG-viperin-Δ9-42; p3xFLAG-viperin-Δ71-182; p3xFLAG-viperin-Δ218-361; p3xFLAG-HSV-1-VP16

2.2.15 RNA sequencing (RNA-seq)

HFF, MRC5, male and female cells were infected with HSV-1 pICP47 at an MOI of 0.5. Four or eight hours post-infection, GFP-positive cells were collected by FACS Aria II (BD Biosciences; Section 2.2.27). Total RNA was extracted from sorted cells using an RNAqueous micro total RNA isolation kit (Ambion), according to the manufacturer's instructions (Section 2.2.4). RNA concentrations were first detected using a Nanodrop spectrophotometer (Thermo Scientific; Section 2.2.5) and then RNA integrities were checked using an Agilent 2100 Bioanalyzer (Agilent Technologies; Section 2.2.5). Only those samples with an RNA integrity number (RIN) greater than 8.5 were kept for RNA-seq library preparation.

The TruSeq stranded total RNA library kit (Illumina) was used for library preparation with 1 μg RNA as input for each sample in this study, according to the manufacturer's instructions. Both cytoplasmic and mitochondrial rRNAs were removed using the Ribo Zero Gold kit (Illumina). In order to minimise PCR bias, only eight cycles were run to enrich fragment-ligated adaptors. The PCR conditions are shown below:

a. Initial denaturation: 98^{o}C for 30 seconds
b. Amplification
    8 cycles of
        Denaturation: 98^{o}C for 10 seconds
        Annealing: 60^{o}C for 30 seconds
        Extension: 72^{o}C for 30 seconds
c. Final extension: 72^{o}C for 5 minutes
d. Hold at 4°C

Before mixing barcoded libraries in equimolar concentrations, these libraries were analysed for length and concentration using the Agilent 2100 Bioanalyzer (Agilent Technologies). A NextSeq 500 system was executed in the high output stage to produce 400 million single-end reads of length 1x 75 bps in a lane.

2.2.16 Viral whole genome sequencing

In order to identify genotype differences in serial passage viruses (Section 2.2.23), WGS was applied for detection of single nucleotide polymorphism (SNPs) or small insertions and deletions (INDELs) in the HSV-1 genome. Briefly, 1 ng of viral DNA (Section 2.2.2.3) was used as the input for the Nextera XT DNA library preparation kit

(Illumina), following the manufacturer's guide. This kit uses an engineered transposome to tagment dsDNA and then these fragments are tagged with adapter sequences. Eight cycles of PCR were used to amplify the insert DNA and the thermocycler conditions are shown below:

a. Initial denaturation: 95ºC for 30 seconds
b. Amplification
    8 cycles of
        Denaturation: 95ºC for 10 seconds
        Annealing: 55ºC for 30 seconds
        Extension: 72ºC for 30 seconds
c. Final extension: 72ºC for 5 minutes
d. Hold at 4°C

This PCR step also added index adapter sequences on both ends of the DNA, which enables sequencing of pooled libraries on Illumina sequencing platforms. A MiSeq system (Illumina) was performed to produce 50 million pair-end reads of length 2x 300 bps in a lane.

2.2.17 Maintenance of mammalian cells

Details of the mammalian cells used during this study are provided in Table 2-10. All cell cultures were incubated at 37ºC with 5% CO_2. Cells were subcultured two times a week at a certain ratio (Table 2-10). To subculture mammalian cells from a culturing flask, media were removed and washed with PBS. The cells were then treated with 0.05% trypsin (Invitrogen) in PBS at 37ºC until the cells detached. After removing the residual trypsin by aspiration, the cells were diluted in appropriate culture media and then transferred into new culturing flasks (Nunc) or plates (Corning). Cell numbers were counted using a hemocytometer after staining with trypan blue solution.

2.2.18 Preparation of mouse skin fibroblasts

Three-day-old C57BL/6, Balb/c or IFNAR knockout mice (a gift from Dr. Si Ming Man) (Man et al., 2015) were obtained from the Australian Phenomics Facility (Canberra, Australia). In general, three male and three female mice were ordered every time, and each mouse was treated as a different biological replicate. Mice were culled by decapitation at the time they arrived. Each mouse was skinned immediately after decapitation and the skin was placed in a separate petri dish with 2 ml PBS. These skins

were minced with a scalpel until the pieces were around 1 mm in size. Next, 5 ml of 0.5% (w/v) collagenase (Worthington) was added into each of the petri dishes. Samples were collected into falcon tubes, mixed gently, and then incubated at 37ºC for 20 minutes. Samples were pelleted by centrifugation at 800 rpm (r_{max}: 207.8 mm) for five minutes and then washed with PBS once. After the residual supernatant was removed, 5 ml 0.05% trypsin (Invitrogen) was added into each tube and then incubated at 37ºC for 20 minutes. Cells and debris were collected by centrifugation at 800 rpm (r_{max}: 207.8 mm) for five minutes, then were resuspended in 6 ml of appropriate medium and cells from each mouse were placed in separate 25 cm^2 flasks (Nunc).

The original cell culture medium was removed and replaced with mouse skin fibroblast medium (DMEM with 10% FBS, 1% MEM NEAA, 1% penicillin streptomycin solution and 2 mM L-glutamine) once every day for the first three days. Cells were split and transferred into 75 cm^2 flasks at day four post-processing. After transferring mouse fibroblasts into 75 cm^2 flasks, cells were cultured as described in Section 2.2.17. Mouse skin fibroblasts can generally be subcultured 10-12 times with normal abilities of differentiation and replication. All experiments were approved by the ANU Animal Ethics and Experimentation Committee under protocol A2014/025 and A2017/39.

2.2.19 Transfection

2.2.19.1 Lipofectamine method

HEK293 cells were transfected with plasmid DNA using Lipofectamine 2000 at a 1:2 ratio of DNA (μg) to Lipofectamine solution (μl). For each well to be transfected in the24-well plate, DNA and Lipofectamine were added to 80 μl of DMEM without FBS, mixed evenly, and then incubated for 20 minutes at room temperature. After cell culture medium was removed and replaced with 300 μl of DMEM without FBS, the transfection mix was then dripped on HEK293 cell monolayers at around 80% confluence. After six hours incubation at 37ºC with 5% CO_2, the transfection mix was removed and replaced with 500 μl of DMEM with 10% FBS.

2.2.19.2 Nucleofector ion method

A Nucleofector transfection kit (Lonza) was employed to transfect plasmid DNA or siRNA into cells, according to the manufacturer's guide. In brief, medium was removed from cells and then cells were washed once with PBS. For harvesting, the cells were then treated with 0.05% trypsin at 37ºC until detached. Appropriate medium with FBS

was added into the flasks to neutralise the trypsinisation reaction and the cell density was determined using a hemocytometer. Next, 1 x 10^6 of each cell was pelleted by centrifugation at 500 rpm (r_{max}: 207.8 mm) for 10 minutes at room temperature and then was resuspended in the solution containing 82 µl of basic Nucleofector solution for mammalian fibroblasts (Lonza), 18 µl supplement (Lonza) and 2 µg plasmid DNA or 50 pmol siRNA. The mixture was placed into the supplied certified cuvettes and transfected using the U-023 program in the Nucleofector 2b Device (Lonza). Once the program was finished, 500 µl of the culture medium was added into the cuvette and the sample was gently transferred into a well of the six-well plate. The transfected cells were incubated at 37°C with 5% CO_2 until analysis.

2.2.20 Preparation of HSV-1 stock

To prepare a HSV-1 master stock, a 75 cm^2 flask of confluent Vero cells was infected with HSV-1 (MOI around 0.01) in 4 ml of MEM without FBS and these cells were then incubated at 37°C with 5% CO_2 for one hour. The inoculum was replaced with 8 ml MEM with 2% FBS and incubated at 37°C with 5% CO_2 for four days. Cells were then collected by centrifugation at 800 rpm (r_{max}: 207.8 mm) for 5 minutes at 4°C. The supernatant was kept and centrifuged at 14,000 rpm (r_{max}: 152.5 mm) for 90 minutes at 4°C to harvest the supernatant-associated virus. In the meantime, the cell pellet was resuspended in a total volume of 500 µl MEM without FBS (cell-associated virus), and the cell pellet was then sonicated for 60 seconds at ~80% power. The cells were pelleted by centrifugation at 800 rpm (r_{max}: 207.8 mm) for 10 minutes at 4°C. The supernatant containing the cell-associated virus was then kept and pooled with the supernatant-associated virus. This master stock was titrated as described in Section 2.2.21.

To prepare a working stock, three 175 cm^2 flasks were infected with the master stock at an MOI of 0.01 in 8 ml of MEM without FBS and they were then incubated at 37°C with 5% CO_2 for one hour. The inoculum was replaced with 16 ml MEM with 2% FBS and incubated at 37°C with 5% CO_2 for three days or until full cytopathogenic effect was observed. The virus working stock was harvested as described for the master stock. Working stocks were aliquoted into 50 µl and titrated before use.

2.2.21 Plaque assays for the titration of HSV-1, VACV, CPXV and MCMV

Plaque assays were used to determine viral titres of new virus stocks, serial passages of viruses, samples from growth curves or organs from infected mice. For all HSV-1 viruses, except 5dl1.2, the titres were determined on confluent Vero cells. Titres of

5dl1.2 were measured on V27 cell monolayers. For VACV and CPXV, viral titres were determined by plaque assays in BSC-1 cells. Titres of MCMV were determined by plaque assays in M2-10B4 cells.

Duplicate 10-fold serial dilutions of samples were prepared in MEM without FBS. Medium was removed from two six-well plates with confluent Vero, V27, BSC-1 or M2-10B4 cell monolayers and 0.5 ml of the virus dilutions was added to the wells and incubated for 90 minutes at 37ºC with 5% CO_2. Plates were gently rocked every 15 minutes to ensure the monolayer remained covered by inoculum during infection. After incubation for 60 minutes, the infectious medium was removed and replaced with 2 ml of MEM with 2% FBS and 0.4% CMC (CMC-MEM) in each well. For plaque formation, the cells were incubated at 37ºC with 5% CO_2 for 72 hours. Medium was then aspirated and the cells were stained with 1 ml crystal violet solution for 10 minutes at room temperature. The crystal violet staining solution was removed and the plates were air dried. The stained plates were counted using a light microscope at 10x magnification. The number of plaques was counted and the titre in plaque forming unit (PFU) per ml was calculated according to the dilution factor and duplicate titrations were then averaged. If duplicates differed by more than two-fold, the titration was repeated.

2.2.22 Virus growth curves

2.2.22.1 Single step growth curves

Confluent monolayers of HFF, MRC5, male or female cells in six-well plates were infected with the virus at an MOI of 5 in 500 µl of MEM without FBS for one hour at 37ºC with 5% CO_2. The inoculum was then removed and the cell monolayer was washed once with 1 ml PBS, then 1 ml of MEM with 2% FBS was added into each well. 0 hour post-infection (hpi) samples were harvested immediately after the fresh medium was added. Other samples were collected by scraping using cell lifters (Corning) and harvested into existing medium at 2, 6, 12 and 24 hpi. These samples were frozen, and thawed three times and then titrated as described in Section 2.2.21.

2.2.22.2 Multiple step growth curves

Confluent monolayers of HFF, MRC5, male or female cells in six-well plates were infected with the virus at an MOI of 0.01 in 500 µl of MEM without FBS for one hour at 37ºC with 5% CO_2. After adsorption for one hour, the infectious medium was

removed and the cell monolayers were washed with 1 ml PBS. Next, 1 ml of MEM with 2% FBS was added into each well. 0 hpi samples were harvested immediately after the fresh medium was added. At 0, 2, 4, 6, 12 and 24 hpi, the samples were harvested as described for the single step growth curve in Section 2.2.22.1. For very low MOI infections with HSV-1 in male and female cells, MOIs of 0.001, 0.0003 and 0.0001 were used for infection and samples were collected at 24, 48, 72 and 96 hpi. Determination of viral titres was performed using plaque assays (Section 2.2.21).

2.2.23 Serial passage of viruses

HSV-1 pICP47 recombinant virus or VACV strain WR was blindly passaged in mouse skin fibroblasts acquired from male or female C57BL/6 mice. Male passage virus means that the virus was blindly passaged only in male cells and female passage virus means that the virus was continuously grown in female cells. Cross passage virus was first propagated in male cells and then cultured in female cells for the next round.

2.2.23.1 Serial passage of HSV-1

For passaging of HSV-1, mouse skin fibroblasts were obtained from three individual three-day-old male or female C57BL/6 mice. Next, 1 x 10^6 of male or female cells were seeded into each well of a six-well plate. Cells were infected with HSV-1 pICP47 recombinant virus at an MOI of 0.01 for the first passage. After incubation for 48 hours at 37^{o}C with 5% CO_2, the cells were scraped from the surface of the well with cell lifters (Corning), and were submitted to three freezing/thawing cycles. Then, 2 µl of the harvested virus was used to infect a new well of the six-well plate seeded with male or female cells in 10 ml 2% FBS DMEM. This process was repeated up to 30 times.

2.2.23.2 Serial passage of VACV

For passaging of VACV, mouse skin fibroblasts were obtained from three individual three-day-old male or female C57BL/6 mice. Next, 1 x 10^6 male or female cells were seeded into each well of the six-well plate. Cells were then infected with VACV strain WR virus at an MOI of 0.01 for the first passage. The following steps were the same as described for the serial passage of HSV-1 in Section 2.2.23.1.

2.2.24 Western blotting (WB)

The cells were harvested by scraping using cell lifters (Corning) and were then centrifuged at 800 rpm (r_{max}: 207.8 mm) for 10 minutes at room temperature. The cell pellet was resuspended in appropriate 5x Western blot loading buffer (Section 2.1.4) and incubated at 95^{o}C in the heat block for 15 minutes. Samples were then stored at -20^{o}C until required.

2.2.24.1 Protein gel electrophoresis

A Mini-PROTEAN Tetra Cell chamber (Biorad), a vertical mini gel electrophoresis system was used to perform protein electrophoresis and transfer. The Mini-PROTEAN Tetra Cell chamber was first assembled by casting with Tris-glycine SDS-PAGE gels and then filling the wells with an appropriate volume of 1x Laemmli buffer (Section 2.1.4). Boiled samples were then loaded into the wells of Tris-glycine SDS-PAGE gels (Table 2-1 and Table 2-2). Appropriate protein ladders (Section 2.1.4) were used to indicate molecular size and estimate mass. Gels were run at 100 V for 20 minutes, followed by 120 V for 80 minutes to separate the proteins.

2.2.24.2 Transfer

The Mini-PROTEAN Tetra Cell chamber was set with Mini Trans-Blot Module (Biorad) and filled with an appropriate volume of transfer buffer (Section 2.1.4). Before inserting the assembled gel holder cassette into the electrode module, the correct direction for arranging the protein gels, NC membranes, filter papers (Biorad) and fibre (Biorad) was checked. The transferring procedure ran at 250 mA for two hours at 4^{o}C.

2.2.24.3 Immunoblotting

After transfer (Section 2.2.24.2), the membrane was blocked with 10 ml of 5% skim milk or 3% BSA in PBS-T on the shaker at 37^{o}C for two hours. Following this, immune staining was performed with diluted antibodies (Table 2-17). Primary antibodies were diluted with 5% skim milk in PBS-T and then incubated with the membrane overnight at 4^{o}C. Appropriate secondary antibodies were applied and incubated with the membrane for two hours at room temperature. Washing with PBS-T was performed three times between each step. An ECL substrate (Biorad; GE Healthcare) was used to treat the NC membranes. The signal was detected using an ImageQuant LAS 4000 system (GE Healthcare).

Table 2-17. Dilution factors for antibodies used in this study.

Name	Dilution	Primary/Secondary
Anti-rabbit IgG-HRP	1:10000	Secondary
Anti-mouse IgG-HRP	1:10000	Secondary
Anti-mouse-MB21D1 (cGAS)	1:5000	Primary
Anti-mouse-IFIH1 (MDA5)	1:1000	Primary
Anti-mouse-DDX58 (RIG-I)	1:1000	Primary
Anti-mouse-TBK1	1:5000	Primary
Anti-mouse-TBK1p	1:1000	Primary
Anti-mouse-IRF1	1:500	Primary
Anti-mouse-IRF3	1:500	Primary
Anti-mouse-IRF7	1:500	Primary
Anti-mouse-RSAD2 (Viperin)	1:500	Primary
Anti-mouse-β-CATENIN	1:2000	Primary
Anti-mouse-TLR3	1:500	Primary
Anti-mouse-TLR4	1:500	Primary
Anti-mouse-ZBTB33	1:500	Primary
Anti-human/mouse-JAK1	1:1000	Primary
Anti-human/mouse-JAK1p	1:500	Primary
Anti-FLAG	1:5000	Primary
Anti-GAPDH	1:5000	Primary

2.2.25 Fluorescence microscopy

For this assay, 1 x 10^6 male or female cells were transfected with 2 µg of p3xFLAG-viperin or empty p3xFLAG vectors using a Nucleofector transfection kit (Section 2.2.19.2). Cells were then seeded on the coverslips in the 12-well plate. After 24 hours -transfection, cells were infected with HSV-1 pICP47 recombinant virus at an MOI of 1 for eight hours. Cells were then fixed with 4% PFA for 20 minutes and then washed with PBS three times. To visualise the nucleus, cells were stained with 4,6-diamidino-2-phenylindole (DAPI) for 10 minutes and mounted onto slides and they were then observed with confocal microscopy.

2.2.26 Quantification of fluorescent protein expression by flow cytometry

Flow cytometry was used to measure the expression of fluorescent proteins in cells being transfected or infected with a plasmid or virus that can express GFP or mCherry. Cells were harvested by trypsinisation as described in Section 2.2.17. Approximately 8 x 10^5 cells were transferred to an 1.5 ml microcentrifuge tube and were collected by centrifugation at 800 rpm (r_{max}: 207.8 mm) for 10 minutes. After washing with FACS-

PBS, the cells were fixed by 1% PFA for 20 minutes at room temperature. The cells were centrifuged at 800 rpm (r_{max}: 207.8 mm) for 10 minutes, washed once with FACS-PBS and resuspended in 100 µl of FACS-PBS. In general, at least 10,000 events were collected. An LSR-II (BD Biosciences) or an Accuri C6 (BD Biosciences) flow cytometer was used to acquire data in this study. The data acquired by the flow cytometer was analysed using FlowJo 10.1 software (Tree Star). Appropriate gates were applied to individual experiments when analysing the data (Figure 2-1).

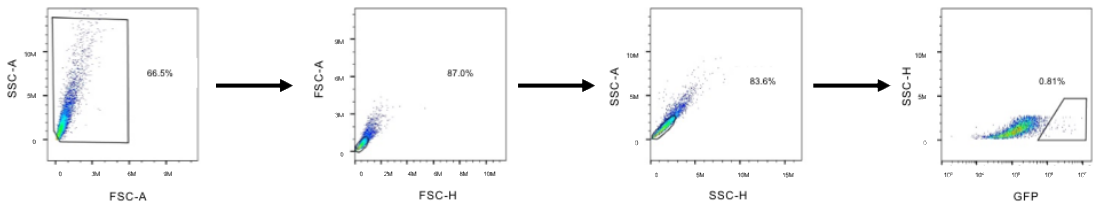

Figure 2-1. Gating strategy to identify GFP+ cells after HSV-1 infection. Mouse skin fibroblasts were infected with HSV-1 pICP47 recombinant virus at an MOI of 0.0001 for 72 hours. Cells were harvested, fixed with 4% paraformaldehyde and analysed by flow cytometry. To identify GFP^+ cells, events were first selected based on the forward scatter (FSC) and side scatter (SSC) parameters. Next, singlets were gated according to height (H) and area (A) parameters of FSC and then SSC. Lastly, GFP^+ events were gated on a GFP x SSC-H plot.

2.2.27 Sorting cells

A FACS Aria II cell sorter (BD Biosciences) was used to collect GFP-positive cells that were infected with HSV-1 pICP47 recombinant virus. Cells were harvested by typsinisation as described in Section 2.2.17. Approximately 2 x 10^6 cells were transferred to a 15 ml Falcon tube and were centrifuged at 800 rpm (r_{max}: 207.8 mm) for 10 minutes. Cells were washed once with FACS-PBS and then resuspended in 500 µl of appropriate culture medium. The samples were filtered using a cell strainer (Falcon) to obtain a single-cell suspension, before being subjected to cell sorting. The purity of the sorted cells was remeasured immediately after the sorting procedure by a FACS Aria II cell sorter (BD Biosciences).

2.2.28 Infection of mice with HSV-1

Six-week-old male or female C57BL/6 mice were obtained from the Australian Phenomics Facility (Canberra, Australia) and were kept until eight-week old before they were used. Mice were infected with 1 x 10^8 PFU of HSV-1 by tattooing on the flank. Avertin, an injectable anaesthetic agent, was used in this study to anesthetise mice through intraperitoneal injection using a 1 ml syringe (BD Biosciences) and a 26G x 1/2" needle (BD Biosciences). Under anaesthesia, the hair on the left flank was trimmed from the dorsal to ventral midline using clippers and then depilated with Veet (Reckitt Benckiser) to remove all hair. A 5 x 5 mm area of skin of the left flank, located above the tip of the spleen, was marked. After a tattoo needle was dipped in virus solution (1 x 10^8 PFU/ml) in DMEM without FBS, mice were then tattooed for 20 seconds using a Swiss rotary tattoo machine (Pullman Tools). Tissue was wrapped around the body of each mouse to maintain adequate body temperature until the mouse had regained consciousness. The development of lesions was also monitored from day one post-infection until an endpoint in each experiment.

2.2.29 Collection and titration of organs from HSV-1-infected mice

Mice were euthanised by asphyxiation with CO_2 and all samples were collected on day two post-infection. A 1 cm^2 region of skin was collected from mice infected by tattoo (Section 2.2.27) and was harvested into 500 µl of MEM with 2% FBS. The dorsal root ganglions (DRGs) located at the ipsilateral side, referring to spinal levels T8 to T12, were isolated using curved forceps and then pooled into 500 µl of MEM with 2% FBS.

Organs in MEM with 2% FBS were homogenised by using tissue grinders (Wheaton) and were subjected to three freezing/thawing cycles before titration (Section 2.2.21).

2.2.30 Statistical analyses

Statistical analyses were performed using GraphPad Prism 7 software. The difference between tested groups was considered to be statistically significant when p-value <0.05. In all figures, single, double and triple asterisks indicate p-values <0.05, <0.01 and <0.001, respectively. When two groups of samples were compared, the unpaired Student's t-test was used to compare the difference between the two means. If more than two sample groups were to be compared, one-way analysis of variance (ANOVA) was used and then Tukey's post-tests were performed for multiple pairwise comparisons. Two-way ANOVA was performed to compare growth kinetics of multiple viruses across different infection times or passages, followed by Tukey's post-tests for pairwise comparisons. If more than two factors were involved in the experiment, a linear model was employed to determine significant differences using the lm() function in R, a free software program for statistical computing and graphics (https://www.r-project.org/).

2.2.31 Bioinformatics analysis

2.2.31.1 Viral genome assembly pipeline

The quality of the resulting reads from Section 2.2.16 were first checked by FastQC (version 0.11.4), a quality control tool for high-throughput sequence data. Illumina adapters generated by the library preparation protocol, and reads that were shorter than 50 bp or with a quality lower than 20, were removed using the BBMap tools (https://sourceforge.net/projects/bbmap/?source=navbar). The remaining reads were uploaded to the VirAmp server via a Galaxy interface (http://viramp.com/) (Wan et al., 2015). To remove reads from the host genome, Burrows-Wheeler Aligner (BWA) (Li and Durbin, 2009) was used to map reads against the mouse genome (mm10). Unmapped reads were then performed with pair-end *de novo* assembly pipeline via VirAMP. In general, each sample, including parent virus (i.e., HSV-1 pICP47 recombinant virus) and three biological replicates from p10 and p30 of the male, female or cross passage virus (Section 2.2.23), was assembled into large and continuous contigs based on different k-mers and then combined into a dataset using the Velvet package (Zerbino and Birney, 2008). After the *de novo* assembly step, AMOScmp was used to orient the resulting contigs by aligning to a reference genome (HSV-1 strain

KOS; Gene Bank accession number: JQ673480) and then a new draft genome was created by connecting every contig from multiple alignments (Treangen et al., 2011). Next, SSPACE was applied for assembly correction and expansion by aligning paired-ends back to the contigs assembled by AMOScmp (Boetzer et al., 2011; Boetzer and Pirovano, 2014). SSPACE then searched for unmapped reads located near the edge of the gap and estimated the placement of these reads into the gap regions. Further, the spacing between reads was utilised to scaffold contigs to form an intact sequence for the final genome assembly. This rescues the information loss in the digital normalisation and coverage reduction at the beginning of the VirAmp pipeline. A final single linear sequence was created from a set of contigs generated by SSPACE via alignment to the reference genome and then production of a linear genome. Finally, variation analysis was performed using the MUMmer package to identify SNPs/INDELs between the parent virus and serial passage viruses (Delcher et al., 2003; Marcais et al., 2018).

2.2.31.2 Differentially regulated transcripts between sexes

The raw reads of male and female cells from three individual mice produced in Section 2.2.15 were sorted by barcodes and then trimmed for adapters and low quality reads using Trimmomatic (Bolger et al., 2014). The reads were then mapped against the mouse genome (mm10) using the TopHat2 aligner which uses Bowtie2 as its core read-alignment engine and has an algorithm to assign reads that span introns in the presence of alternative splicing events and isoforms (Kim et al., 2013). The number of reads generated from a transcript was calculated by Cufflinks using reads per kilobase of transcript per million mapped reads (RPKM) (Trapnell et al., 2012). Differentially regulated genes were then identified using the Cuffdiff package which quantifies expression of each transcript in the triplicates of male and female cells. Variation in each transcript across the replicates was used to test the statistical significance of observed changes in expression between HSV-1-infected and uninfected samples (Garber et al., 2011; Trapnell et al., 2012). A false discovery rate (FDR) smaller than 0.05 and a p-value smaller than 0.05 were defined as a significant difference based on the Cuffdiff outputs (Trapnell et al., 2010; Trapnell et al., 2013). The $\log_2$ fold change was measured by comparing the average expression of infected triplicates at 4 or 8 hpi to uninfected counterparts in male and female cells, respectively.

Significantly upregulated or downregulated transcripts at 4 or 8 hpi in male and female cells were compiled into different lists for biological process gene ontology (GO) enrichment classification and Kyoto Encyclopedia of Genes and Genomes (KEGG)

pathways analysis via the DAVID online database (https://david.ncifcrf.gov/) (Huang et al., 2007; Huang da et al., 2009). An FDR smaller than 0.05 and a p-value smaller than 0.05 was classified as differential regulation. Upregulated or downregulated GO terms in male or female cells at one and/or more time points were combined into other lists and further visualised using REVIGO (http://revigo.irb.hr/) (Supek et al., 2011).

2.2.31.3 Cross-species analysis of RNA-seq data

The raw reads of triplicates of HFF, MRC5 and male cells from three individual mice generated in Section 2.2.15 were first allocated by barcodes to separate libraries, then Illumina adapters were trimmed and reads with low quality scores were discarded via Trimmomatic as described in Section 2.2.31.2 (Bolger et al., 2014). The remaining reads were further mapped to the human (hg38) or mouse (mm10) genome, depending on the species of cells, using the TopHat2 mapper (Trapnell et al., 2012; Kim et al., 2013). Raw counts of each gene were calculated by the featureCounts package and were then transferred into counts per million (CPM) (Liao et al., 2014). Genes with low raw counts (<3) were removed and the TMM method was used to normalise libraries through the edgeR package (Robinson et al., 2010). After generating raw counts and normalisation, initial Ensembl gene IDs were converted into gene symbols in both human and mouse samples. Only shared human and mouse orthologous genes were kept for further analysis. The cross-species difference at the gene level was analysed by the limma and edgeR packages (Smyth, 2004; Robinson et al., 2010; Ritchie et al., 2015; Law et al., 2016). In brief, the voom method, a linear modelling strategy, was applied to estimate the mean-variance relationship of counts, produce a precision weight for each sample and introduce these into the limma empirical Bayes analysis procedure to identify significant differences (Law et al., 2014). A $\log_2$ fold change more than 1 and a p-value smaller than 0.05 between infected samples and mock samples were the designated criteria to acquire differentially regulated genes. Differentially regulated genes at 4 or 8 hpi in HFF, MRC5 and male cells were combined into lists as inputs for GO enrichment analysis via g:Profiler (http://biit.cs.ut.ee/gprofiler/index.cgi). Specific regulated GO terms between HFF and MRC5 or male cells at 4 and/or 8 hpi were compiled and were further visualised by REVIGO (http://revigo.irb.hr/) (Supek et al., 2011).

At the pathway level, rotation gene sets analysis (ROAST) was performed based on the expression levels of each gene in human or mouse samples between infection time points of 4 or 8 hpi and mock groups (Wu et al., 2010). Differentially regulated pathways were defined by those pathways that had both a p-value and an FDR smaller

than 0.05 in the REACTOME database (Wu et al., 2010). Reference gene lists were based on the human or mouse C2 curated gene sets in the Molecular Signatures Database v6.0 (http://software.broadinstitute.org/gsea/msigdb/index.jsp).

2.2.31.4 HSV-1 gene expression analysis

Unmapped reads in Section 2.2.31.2 and Section 2.2.31.3 were mapped against the modified HSV-1 genome (Gene Bank accession number: JQ673480) with only one copy of the terminal repeats (TR_L and TR_S) preserved. Raw counts of each viral gene were calculated by the featureCounts package and were transferred into CPM and normalised by the TMM method in each library, as described in Section 2.2.31.3 (Liao et al., 2014). Differential viral gene expression was analysed by a generalised linear model built in edgeR. The cutoff of differential expression was set to a p-value smaller than 0.05 and a $\log_2$ fold change more than 1.5. Finally, for visualisation, an HSV-1 genome coverage plot was constructed via the Gviz package in R, following the users guide (Hahne and Ivanek, 2016).

Chapter 3. Does the sex of cells play a role during HSV-1 infection in vitro?

3.1 Introduction

Sex differences in the prevalence and intensity of viral infections are illustrated by a growing body of literature (Fischer et al., 2015; Klein and Flanagan, 2016). Males and females deploy distinct responses to diverse viruses, including influenza virus, HIV and herpesviruses (Klein, 2012). However, the mechanisms that underlie differences between the sexes are complicated and can involve genetic, hormonal and behavioural factors (Roved et al., 2017). The immune system has evolved to provide a balance between proinflammatory and anti-inflammatory reactions, and thereby, determines the outcome of viral infection (Rouse and Sehrawat, 2010). Generally, females generate higher innate and higher adaptive immune responses compared with males, which accelerates virus clearance but may be detrimental through the development of immunopathology (de Jong et al., 2006). For example, during influenza virus infection, females induce greater proinflammatory responses, such as TNF-α, IL-6 and activation of NF-κB signalling, which sometimes correlates with elevated morality in females (Walsh et al., 2011). Conversely, in males, multiple depressive effects on the immune system during microbial infections have been discovered (Ghosh and Klein, 2017). Nonetheless, it is clear that specific differences in immune responses between the sexes are dependent on the microbe, as not every infection leads to increased overall susceptibility in one sex over the other. Thus, including sex as a criteria in studies is critical for improving our knowledge base on immunity to infections in general.

To date, the available evidence on whether a particular sex is more susceptible to HSV-1 infection in animal models is inconsistent. The best controlled studies of the role of sex on HSV-1 infection have been done in mouse models. Male mice show less limb paralysis than female mice following intravenous inoculation with HSV-1, despite female mice consistently generating more antibodies (Knoblich et al., 1983; Yirrell et al., 1987). Likewise, greater mortality is observed in female mice during systemic viral infection, such as with intraperitoneal injection (Han et al., 2001; Geurs et al., 2012). By contrast, mortality is higher in male 129/SvEv wild-type, IFN-γ knockout and IFN-γ receptor knockout strains when inoculated with HSV-1 via the corneal route. It also varies according to infection routes and strains of mice. Therefore, although several studies suggest that sex can influence HSV-1 pathogenesis, sex-based differences in HSV-1 infection remain ill-defined.

In this chapter, we addressed whether there is a sex difference during HSV-1 infection from various perspectives focusing on cell-intrinsic effects in culture. First of all, we

examined growth kinetics of HSV-1 in male and female primary mouse skin fibroblasts (referred to hereafter as male and female cells), in a single- or multi-step growth experiment. We then tested if HSV-1 can adapt to sex using a serial passage method in a cell-based system. Furthermore, whole genome sequencing (WGS) was employed to identify SNPs/INDELs in these sex-adapted HSV-1 genomes. Next, we investigated whether sex-adapted HSV-1 generates different pathogenesis in the flank zosteriform mouse model. Finally, in order to identify potential mechanisms driving the sex difference in HSV-1 infection, RNA-seq was applied to comprehensively investigate transcriptional differences between HSV-1-infected male and female cells.

3.2 Results

3.2.1 Single- and multi-step growth curves of HSV-1 pICP47 recombinant virus in male and female mouse skin fibroblasts

In order to understand whether sex affects general virus replication, both single- and multi-step growth curves were constructed. Primary skin fibroblasts were considered suitable host cells as skin is the major location where HSV-1 invades and initiates infection. Likewise, primary cells with few mutations are considered to be closer to the cells infected *in vivo*, compared with cell lines. The use of primary cells also allows replicates to be cultures from individual mice and not simply replicate infection of the same batches of cells. HSV-1 pICP47 recombinant virus was selected to conduct this experiment as it can express the GFP protein, which is a marker for downstream cell sorting enabling collection of the infected cell population post-infection (Section 2.2.27). It has also been recently plaque purified in the lab. HSV-1 pICP47 contains a GFP/Cre cassette driven by an ICP47 promoter, inserted into the UL3 and UL4 intergenic region of HSV-1 strain KOS (Russell and Tscharke, 2016). Male and female cells were infected with HSV-1 pICP47 virus at an MOI of 10 for generating one-step growth curves or at an MOI of 0.01, 0.001, 0.0003 and 0.0001 for producing multi-step growth curves. Viral titres were determined at indicated time points and are shown in Figure 3-1. Male and female cells produced similar viral yields when infected with HSV-1 pICP47 recombinant virus during one-cycle replication (Figure 3-1A). However, when the cells were exposed to very low amounts of virus, HSV-1 replicated more efficiently in male cells compared to female cells. There were significant differences in growth between male and female cells during HSV-1 infection at an MOI of 0.0003 and 0.0001 (Figure 3-1D and Figure 3-E), which was consistent with a larger infected population detected by flow cytometry in male cells compared to female cells (Figure 3-2). There was no significant difference in the size of plaques on male and

female cells at 96 hpi (Figure 3-3), indicating different viral yields between male and female cells is not dependent on the cell-to-cell spread.

3.2.2 HSV-1 but not VACV strain WR can adapt to sex

As shown in Section 3.2.1, HSV-1 replicates differently in male and female cells after very low multiplicity infections where virus can continue to spread throughout the culture period. Thus, we speculated that the cells of male and female mice might exert different selective pressure on virus replication over multiple rounds of growth. To date, most studies examining the experimental evolution of viruses have focused on RNA viruses with high mutation rates (Montville et al., 2005; Vignuzzi et al., 2006). Less is known about the adaptive strategies of large dsDNA viruses, such as herpesviruses and poxviruses, but adaptation is possible (Lynch, 2010; Elde et al., 2012). In this section, an experimental evolution method was applied to investigate whether HSV-1 can adapt to sex using serial infections at relatively small population sizes. Essentially, male or female cells were infected with HSV-1 pICP47 recombinant virus at a low MOI (0.01 PFU/cell) in three independent cultures. Forty-eight hours post-infection, the virus was collected and then repeatedly propagated in male cells (male passage virus), female cells (female passage virus) or between these two types of cells (cross passage virus) for 30 rounds (Section 2.2.23 and Figure 3-4).

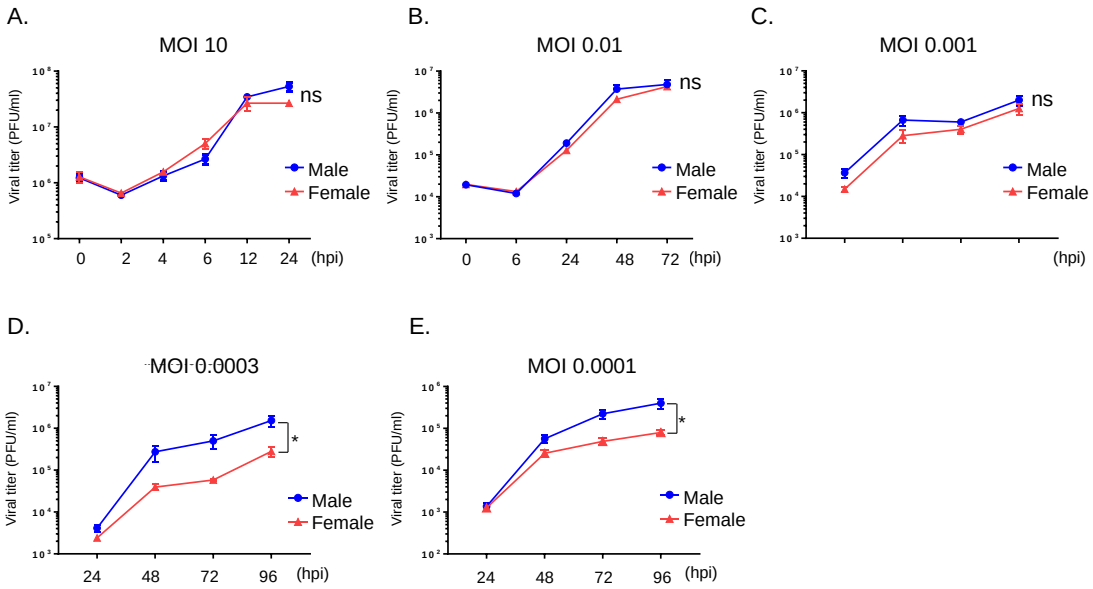

Figure 3-1. Different growth phenotypes of HSV-1 pICP47 recombinant virus in male and female primary mouse fibroblasts (male and female cells). Confluent monolayers of male and female cells were infected with HSV-1 pICP47 recombinant virus at an MOI of (A) 10, (B) 0.01, (C) 0.001, (D) 0.0003 or (E) 0.0001. After an hour of absorption, the inoculum was replaced with 2 ml MEM with 2% FBS. A 0 hpi sample was harvested immediately after the addition of fresh media. The samples were collected at indicated time points and viral titres were determined by plaque assays. The data are expressed as mean ± SEM of cultures from three individual mice. Two-way ANOVA with Tukey's post-tests was performed to test differences between means in titres over time between male and female cells, where significance is denoted by * (p-value <0.05). ns, no significant difference.

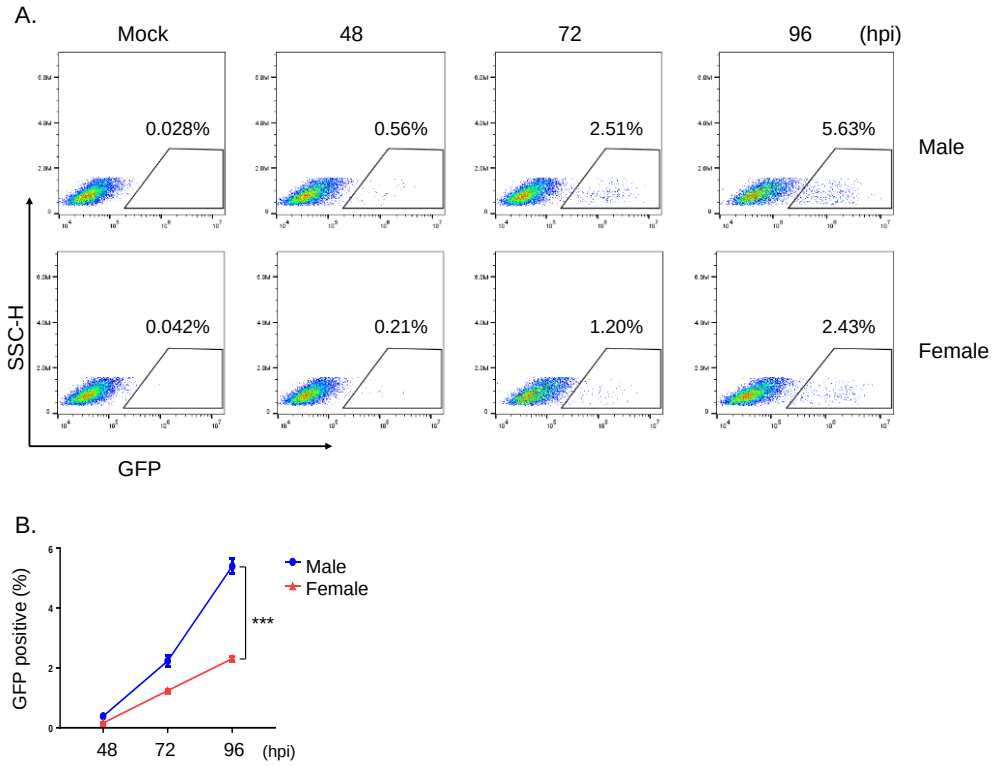

Figure 3-2. A higher percentage of infected cells (GFP-positive) in male than in female cultures during low MOI infection with HSV-1 pICP47 recombinant virus. Monolayers of male or female cells were infected with HSV-1 pICP47 recombinant virus at an MOI of 0.0001 or mock infected with PBS. At 48, 72 and 96 hpi, cells were harvested, fixed with 4% paraformaldehyde at room temperature for 20 minutes and resuspended in the FACS-PBS for flow cytometry analysis. (A) Representative flow cytometry plots from one of three independent experiments showing the percentage of GFP expression. (B) The data are presented as mean ± SEM of cultures from three individual mice. Two-way ANOVA with Tukey's post-tests was used to test differences between means in GFP percentage over time between male and female cells. *** p-value <0.001.

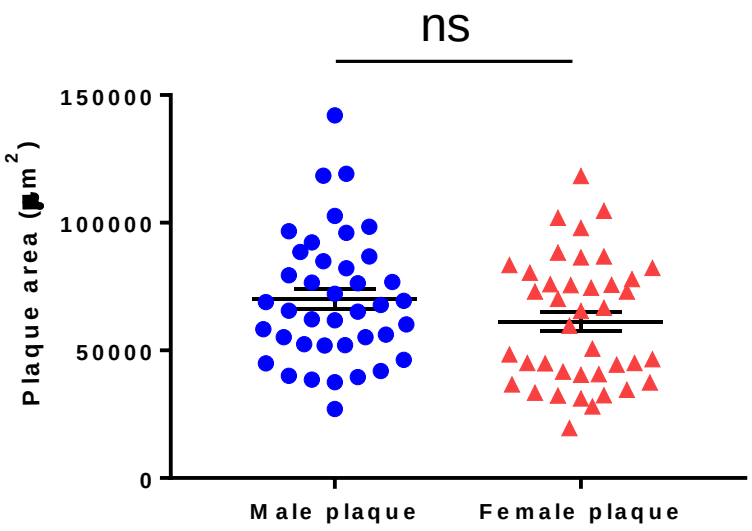

Figure 3-3. Size of plaques formed by HSV-1 in male and female cells at 96 hpi. Monolayers of male or female cells from three individual mice were infected with HSV-1 pICP47 recombinant virus at an MOI of 0.0001 for 96 hr. Plaques were crystal violet stained and the area of plaques produced on male and female cells were measured using ImageJ (n=40). Statistical significance was determined using Student's t-test. ns, not significant difference.

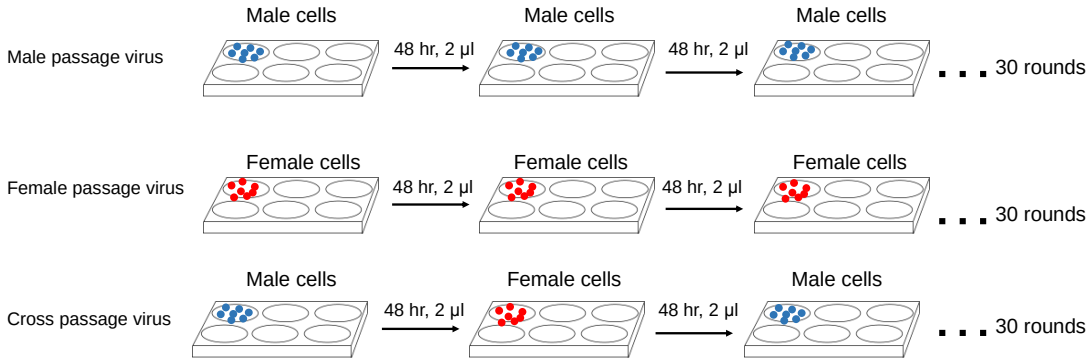

Figure 3-4. Flow chart of experimental evolution of HSV-1 in mouse skin fibroblasts. Male or female cells from three individual mice were infected with HSV-1 pICP47 recombinant virus at an MOI of 0.01 for the first passage. After 48 hours, the cell pellet was resuspended in 200 µl of DMEM without FBS, followed by three freeze/thaw cycles. Next, 2 µl of this harvested virus was used to infect fresh monolayers of male or female cells in 2 ml of DMEM with 2% FBS. Male passage virus indicates that the virus was passaged only in male cells and female passage virus indicates that the virus was continuously grown in female cells. Cross passage virus indicates that the virus was first propagated in male cells and then cultured in female cells in the next round. The serial passage was repeated 30 rounds for each male, female and cross passage virus. Blue and red dots reflect male and female cells, respectively.

After serial passage of HSV-1 pICP47 recombinant virus to obtain male passage virus, female passage virus and cross passage virus, the indicated passage number of each virus was used to infect fresh male and female cells from another three individual mice at an MOI of 0.01 for another 48 hours. Then viral yields were measured to examine the replication properties of these viruses (Figure 3-5). Vero cells were used here to

Male passage viruses consistently produced higher viral titres in male cells than in female cells after 10 serial passages (Figure 3-6A). Female passage viruses initially seemed to produce greater viral titres in male cells, although there was no significant difference due to large variation among each replicate. This phenomenon was reversed after approximately 10 rounds of passages that female passage viruses began to grow more efficiently in female cells compared with male cells (Figure 3-6B). By contrast, cross passage viruses generated similar viral yields in male and female cells, indicating that inconsistent evolution pressure from the different sexes cannot lead to a virus lineage specifically adapted to male or female cells (Figure 3-6C). Finally, increased viral titres were observed in all cultures over time, suggesting that HSV-1 also adapted to mouse skin fibroblasts during the experiment (Figure 3-6).

As each mouse strain is unique and different from other strains in many respects (Casellas, 2011; Hunter, 2012; Walkin et al., 2013), it is necessary to understand whether HSV-1 male and female passage viruses harbour similar replication properties in other mouse strains. Therefore, instead of using male and female cells derived from C57BL/6, which have been utilised for most experiments in this study, mouse skin fibroblasts prepared from three individual male and female BALB/c were infected with male passage viruses or female passage viruses from 30 passages at an MOI of 0.01 for 48 hours. Viral titres were then determined by plaque assays. In line with what was found in C57BL/6 cells, male passage viruses exhibited titres about 5-10-fold higher in male BALB/c skin fibroblasts than in female skin fibroblasts (Figure 3-7). HSV-1 female passage viruses produced more infectious viruses in female than in male BALB/c skin fibroblasts. However, there was no difference in growth phenotype between male and female BALB/c skin fibroblasts when the cells were inoculated with cross passage viruses. Collectively, the data in BALB/c skin fibroblasts (Figure 3-7) are in agreement with the finding in C57BL/6 skin fibroblasts (Figure 3-6).

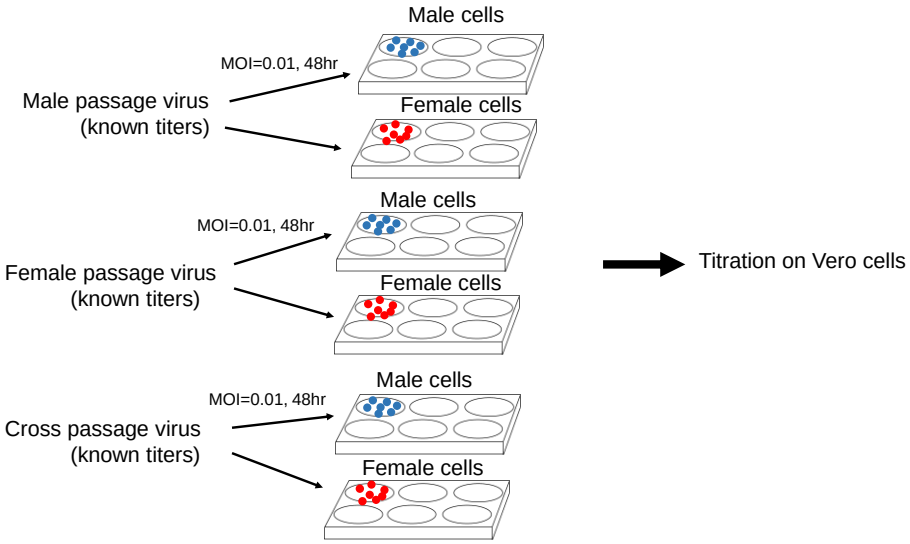

Figure 3-5. A method to determine the growth phenotypes of male, female and cross passage viruses in male and female skin fibroblasts. First, to determine the viral titres from serial passage viruses, male, female and cross passage viruses from each passage were titrated using plaque assays on Vero cells. Then male and female cells from three individual mice (independent of the initial cultures) were then infected with male, female and cross passage virus at an MOI of 0.01 for 48 hours. The progeny were then titrated on Vero cells to investigate whether HSV-1 gains or loses fitness in cells of a particular sex after serial passages, because the parental HSV-1 was made and titrated on Vero cells. Blue and red dots indicate male and female cells, respectively.

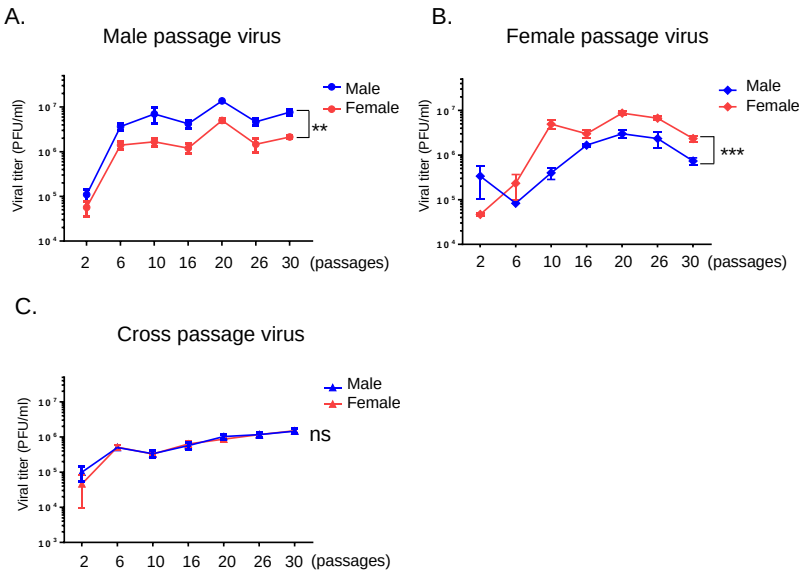

Figure 3-6. HSV-1 can adapt to sex. (A) Male, (B) female or (C) cross passage viruses at indicated passages were used to infect monolayers of male and female cells from three individual mice at an MOI of 0.01. After 48 hours of infection, cell lysates were collected and the viral titres were determined on Vero cells. Error bars are mean ± SEM. Two-way ANOVA with Tukey's post-tests was performed to test differences between means in titres over time between male and female cells, where significance is indicated by ** and *** (p-value <0.01 and p-value <0.001). ns, no significant difference.

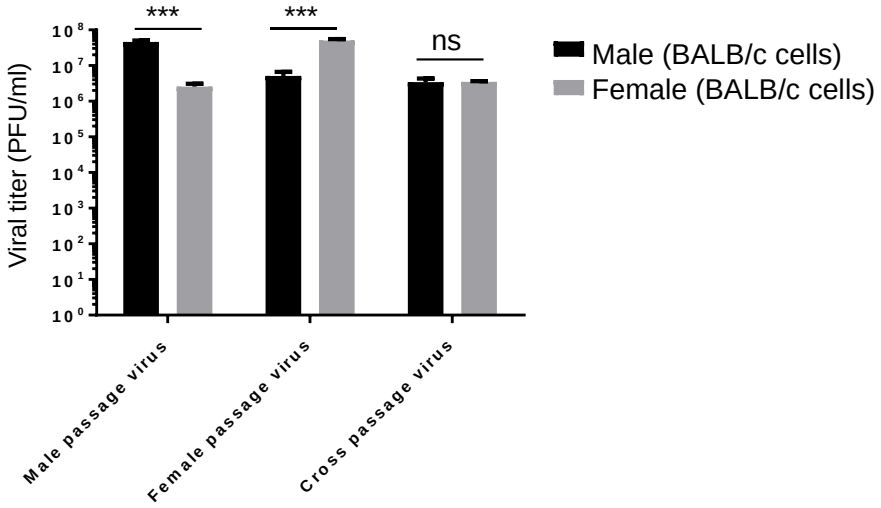

Figure 3-7. Growth phenotypes of sex-adapted HSV-1 in male and female cells derived from BALB/c mice. Male and female cells were derived from three individual BALB/c mice and then infected with passage 30 male passage virus, female passage virus and cross passage virus at an MOI of 0.01 for 48 hours. Cell lysates were collected and viral titres were determined by plaque assays. Error bars are mean ± SEM. The data were compared using one-way ANOVA with Tukey's post-tests (*** p-value <0.001; ns, no significant difference).

In order to investigate whether the sex adaptation is specific for HSV-1, or whether it can be applied to other large dsDNA viruses, VACV strain WR was selected as another candidate to perform serial passages in male and female cells based on the same experimental evolution protocol for HSV-1 (Section 2.2.23 and Figure 3-4). After 30 blind passages, VACV appeared to adapt to mouse cells since viral yields reached a peak at 20 passages after rising with increasing passage times (Figure 3-8). However, unlike HSV-1, each biological replicate of VACV from 30 passages showed a similar growth phenotype in male and female cells.

Taken together, it appears that HSV-1 can adapt to the sex of host cells, and thereby, generate different replication abilities in male and female mouse skin fibroblasts prepared from both C57BL/6 and BALB/c mice. Although HSV-1 and VACV are large dsDNA viruses and both can adapt to mouse cells, only HSV-1 adapted to the sex of cells in our experiments.

3.2.3 Replication of sex-adapted HSV-1 *in vivo*

Next, to understand whether *in vitro* growth phenotypes observed in the sex-adapted HSV-1 (Section 3.2.2) also occurs in live animals, mouse flank skin infection model was applied to investigate the replication of sex-adapted HSV-1 *in vivo* (Robinson and Dover 1972; Blyth et al., 1984). Briefly, eight-week-old male and female C57BL/6 mice were anesthetised and then infected by tattoo infection with male, female or cross passage viruses (Russell et al., 2015). The mice were culled at two days post-infection and their skin and DRGs were collected and processed as described in Section 2.2.29. Viral titres were then measured by plaque assays. In skin, male passage viruses produced more infectious virus in male mice than in female mice (Figure 3-9A). In line with this, female passage viruses replicated more efficiently in the skin of female mice. These results are correlated with what was illustrated in Section 3.2.2. However, although there was a similar trend discovered in the DRGs, it was not statistically significant (Figure 3-9B). With respect to cross passage viruses, these replicated comparably between male and female mice in both skin and DRGs. Taken together, it shows that the sex-adapted HSV-1 generated by serial passages in male or female cells also shows different replication phenotypes in the skin of male and female mice infected via tattoo infection.

3.2.4 Genetic changes in sex-adapted HSV-1

To determine the genetic basis of HSV-1 sex adaptation, paired-end deep sequencing of parental HSV-1 and each replicate of virus from 10 and 30 passages (p10 and p30), including parental HSV-1 pICP47 virus, male, female and cross passage viruses, was performed to acquire approximately 2,000-fold genome coverage. Herpesviruses are difficult to sequence due to their high GC-content (60-70%) and palindromic sequences which result in the formation of a stable hairpin structures (Brown, 2007; Ouyang et al., 2012; Lee et al., 2015). For the purpose of resolving uncertainties associated with these limitations, several computational and statistical methods have been developed for studying the genetic heterogeneity of the herpesviral population (Renner and Szpara, 2018). Szpara and colleagues, a research team specialising in evolution and diversity of herpesviral genomes, have developed a viral *de novo* assembly workflow specifically for herpesviruses both in a web-based and Unix command-line interface (Parsons et al., 2015; Wan et al., 2015). Herein, this multi-step herpesviral genome assembly pipeline established by Szpara's group, VirAmp, was applied to analyse the genetic differences between the parental and sex-adapted HSV-1 (Section 3.2.2) (Wan et al., 2015).

In brief, HSV-1 genomic DNA was isolated as described in Section 2.2.2.3 and elsewhere (Russell and Tscharke, 2016). An Illumina Nextera XT library kit was then employed to construct WGS libraries using 10 ng of input HSV-1 DNA. Next, a 300-bp paired-end run was carried out on the Illumina Miseq platform. After removing adaptors and reads with low quality scores, the entire VirAmp pipeline was operated. HSV-1 genomes were assembled *de novo* by Velvet; these assemblers used the de Bruijn graph algorithm and then variation analysis was conducted using the MUMmer package to identify SNPs and INDELs between the parental HSV-1 recombinant virus and each sex-adapted virus (Kurtz et al., 2004; Zerbino and Birney, 2008). The details of the genome assembly pipeline are shown in Section 2.2.31.1. The number of SNPs/INDELs in each biological replicate of HSV-1 male passage virus, female passage virus or cross passage virus from 30 passages was combined accordingly and is shown in a boxplot (Figure 3-10A). Slightly more SNPs/INDELs were found in the female passage viruses compared with the male passage viruses and cross passage viruses, although there was no statistically significant difference. SNPs/INDELs identified at least two times in triplicates of male passage viruses, female passage viruses or cross passage viruses were defined as mutations derived from the selective pressure during serial passages. These mutations from male passage viruses, female passage viruses or cross passage viruses were calculated and are presented in a Venn diagram (Figure 3-10B). As expected, cross passage viruses rarely produced unique mutations and most of the mutations were also found in male or female passage viruses.

On the contrary, the populations of male and female passage viruses contained relatively more unique mutations, which indicates that consistent pressure from each specific sex introduces the potential for fitness advantages for HSV-1.

HSV-1 US3 may contain hot spots for mutations during serial passages in mouse skin fibroblasts, as all male, female and cross passage viruses had SNPs in the US3 gene. HSV-1 US3 is a multifunctional protein that regulates various cellular and viral functions by phosphorylating a number of protein substrates, blocking apoptosis and modulating host immune systems (Leopardi et al., 1997; Cartier et al., 2003; Wang et al., 2013b). In both p10 and p30, male and cross passage populations shared the same mutation C456Y in the US3 region. Female passage viruses specifically gained a 341 G-to-R AA substitution, which had already been modified since p10 and was maintained until p30. These data indicate that US3 is a prime target for HSV-1 adaptation in experimental evolution and can be quickly modified after only 10 serial passages. Likewise, female passage viruses also had a second unique mutation that emerged by p10, namely US8 (S477L).

Unique genetic changes (identified at least two times in triplicates and not shared with other conditions) associated with male (blue), female (red) and cross (yellow) passage viruses resulting after 10 and 30 passages are shown in Figure 3-11. Additionally, details of the nucleotide (NT) and deduced amino acid (AA) changes in these sex-adapted HSV-1 viruses (identified at least two times in triplicates), relative to the parental virus, are listed in Table 3-1 and Table 3-2. In 30 passages, both male and female passage viruses exhibited NT changes in the UL48 gene that encodes VP16. VP16 is a key transcriptional activator of HSV-1 lytic infection to initiate immediate early gene expression via the assembly of a transcriptional regulatory complex (Ace et al., 1988; Ace et al., 1989; Arnosti et al., 1993). Correspondingly, the identified AA sequences revealed that these NT changes led to a 67 D-to-N and a 344 L-to-F AA substitution in male and female passage viruses, respectively. Furthermore, selective pressure from both male and female sexes caused NT changes in HSV-1 glycoproteins. Male passage viruses contained an INDEL (T132H) that may disrupt the structure of UL22 (glycoprotein H; gH) due to this mutation leads to a predicted frameshift and may generate truncated gH protein. Based on our preliminary alignment result, this predicted frameshift caused an early termination at 143 AA and may use another reading frame to make the other truncated form of gH protein (from 271 to 839 AA) (data not shown). UL22 is an essential component for the cell-to-cell spread of virions and for the penetration of virions into cells (Westra et al., 1997). Another mutation (S477L) was found in female passage viruses in US8 (glycoprotein E; gE). This is involved in the

promotion of cell-to-cell spread at basolateral surfaces of epithelial cells and functions as an Fc receptor (Baucke and Spear, 1979; Dingwell et al., 1994).

Lastly, few SNPs and INDELs were identified across all triplicates in male, female and cross passage viruses at intergenic regions in the HSV-1 genome, such as RL2/RL1 (124544 A to AA) and UL25/UL26 (50732 T to nT) (Table 3-1 and Table 3-2). This suggests that these INDELs may be involved in the adaptation of HSV-1 to mouse skin fibroblasts, although they did not directly affect coding regions of these genes and did not influence potential transcriptional regulatory factors, such as the TATA-box sequence. The mechanism behind this is not clear and needs more invstigation to see whether there are unidentified *cis*-acting signals regulating transcription termination, and reinitiation at a downstream gene. All mutations mentioned in Section 3.2.4 need to be confirmed by Sanger sequencing using a set of sequencing additives for high GC rich and repeated regions in HSV-1 genome in the future (Kieleczawa and Mazaika, 2010; Riet et al., 2017).

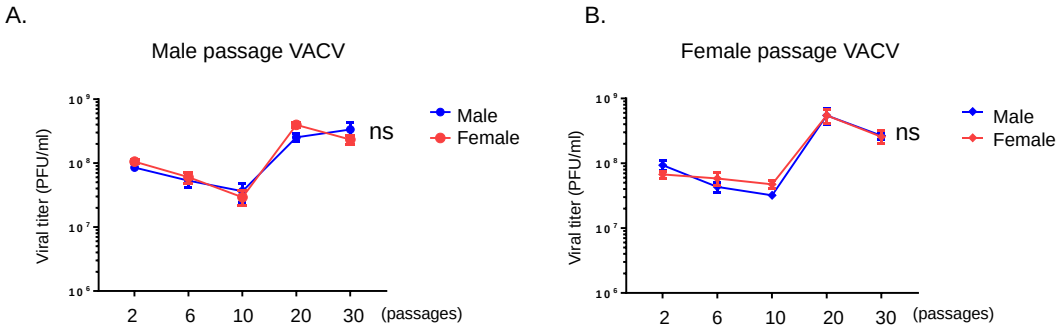

Figure 3-8. Vaccinia viruses do not adapt to the sex of cells in culture. (A) Male and (B) female passage vaccinia viruses at indicated passages were used to infect fresh monolayers of male and female cells from three individual mice at an MOI of 0.01. After 48 hours of infection, cell lysates from male and female cells were collected and the viral titres were determined on BSC-1 cells. Error bars are mean ± SEM. Two-way ANOVA with Tukey's tests was performed to test differences between means in titres over time between male and female cells. ns, no significant difference.

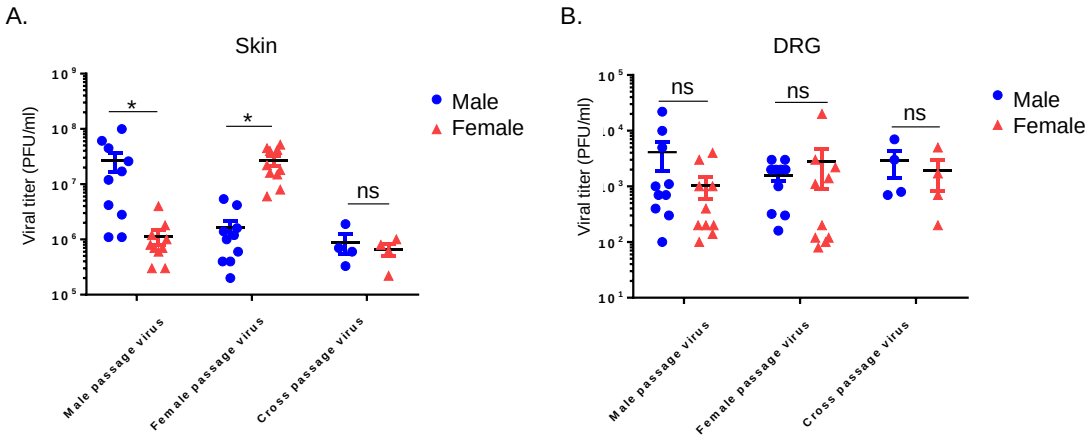

Figure 3-9. Different growth phenotypes of the sex-adapted HSV-1 pICP47 recombinant viruses after flank infection. C57BL/6 mice were infected by tattoo with 1×10^8 PFU/mL male passage virus (n=10 in male mice; n=10 in female mice), female passage virus (n=10 in male mice; n=10 in female mice) or cross passage virus (n=4 in male mice; n=4 in female mice). Two days post-infection, mice were culled and then skin and DRG (from spinal levels L1 to T5) were harvested for determining viral yields on Vero cells. Data are pooled from two independent experiments. Each dot represents one mouse and the black bar represents the mean ± SEM. Statistical significance was determined by one-way ANOVA with Tukey's post-tests for pairwise comparisons. * p-value <0.05 and ns, no significant difference.

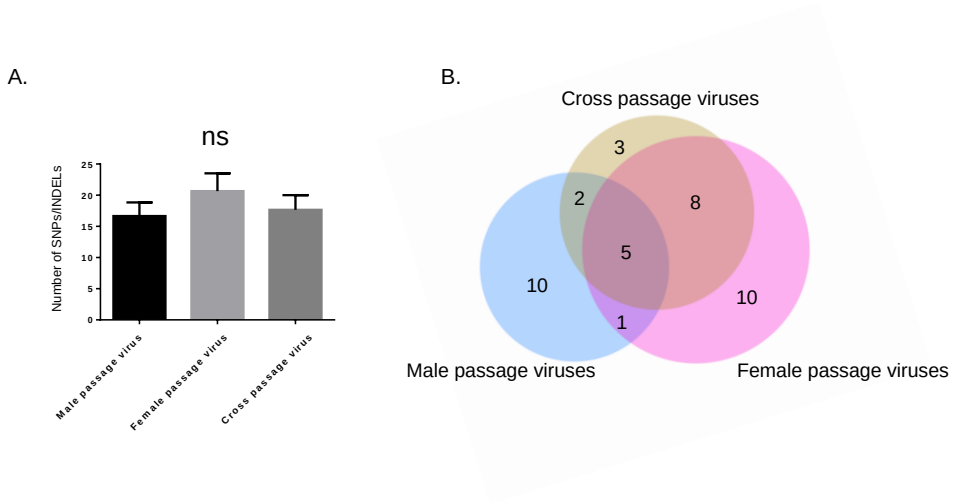

Figure 3-10. Number of mutations in the sex-adapted HSV-1 pICP47 recombinant virus. (A) Number of SNPs and INDELs from each of the three biological replicates of male, female and cross passage viruses were counted and mean ± SEM are shown in the bar chart. One-way ANOVA with Tukey's tests was used to test differences between means. (B) Identical SNPs or INDELs (identified at least two times in triplicates) between each sex-adapted HSV-1 pICP47 recombinant virus were calculated and are shown in the three-way Venn diagram. Blue, male passage virus; pink, female passage virus; yellow, cross passage virus.

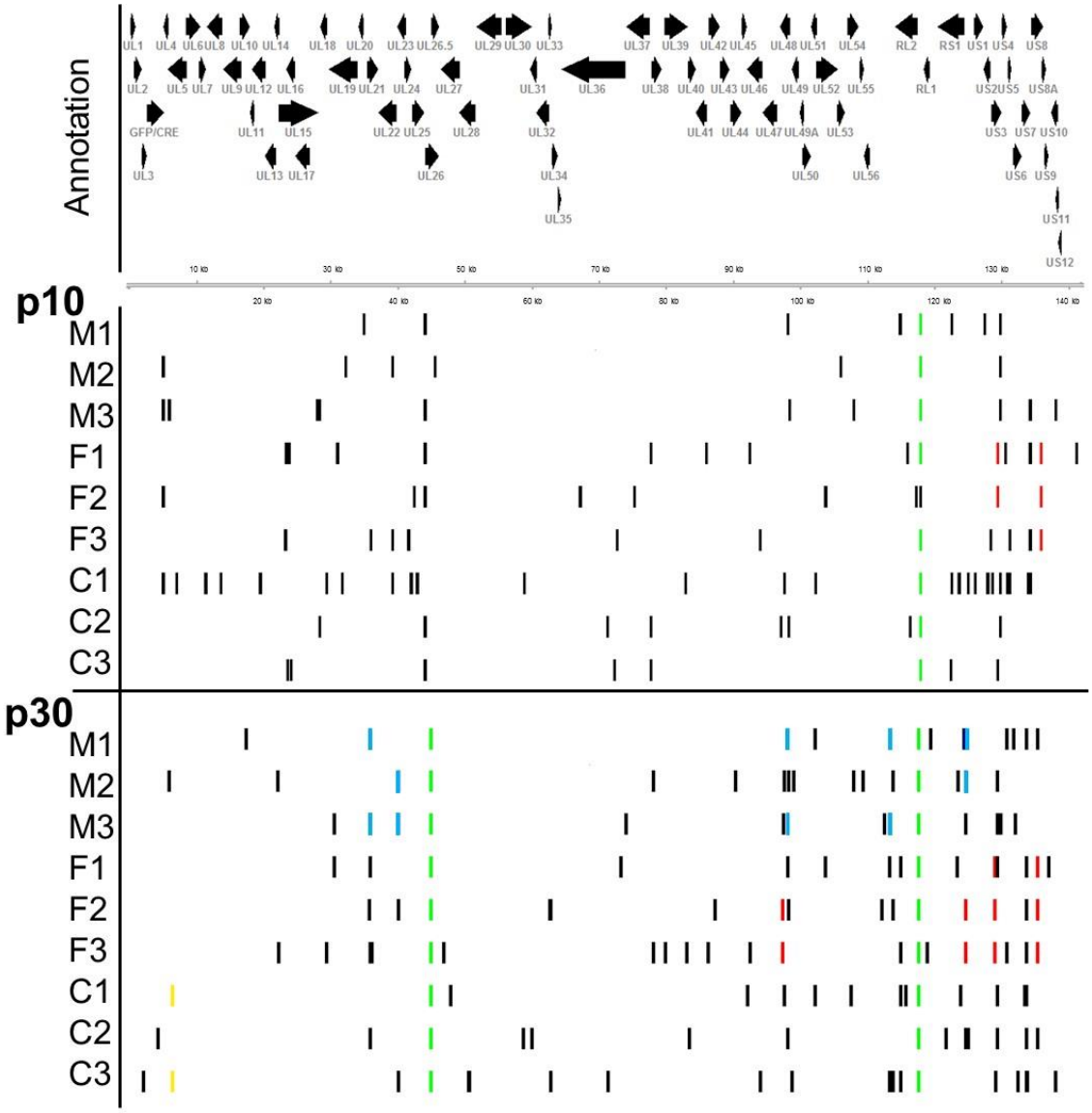

Figure 3-11. Location of SNPs and INDELs to the culture condition in the sex-adapted HSV-1 pICP47 recombinant viruses. The position of SNPs or INDELs in passage 10 (p10) and 30 (p30) is shown relative to a map of HSV-1 genes. The HSV-1 modified genome is annotated with each HSV-1 gene and shown without the long and short terminal repeats, as sequences in these two regions are represented in the internal repeats. Black and green lines indicate mutations found in a single virus and identical mutations across all viruses, respectively. Blue, red and yellow lines show culture-specific mutations in male, female or cross passage viruses (identified at least two times in triplicates and not shared with other conditions), respectively. M1, M2, M3, biological replicates 1-3 of male passage virus; F1, F2, F3, biological replicates 1-3 of female passage virus; C1, C2, C3, biological replicates 1-3 of cross passage virus.

Table 3-1. Details of mutations (identified at least two times in three isolates) in the sex-adpated HSV-1 in passage 10.

Viruses	SNP/INDEL	Gene name	NT[1] change	AA[2] change	Unique mutation[3]
Male passage virus					
	INDEL	RL2/RL1	124544 A -> AA	NA	No
	SNP	US3	136446 G -> A	C456Y	No
Female passage virus					
	INDEL	UL25/UL26	50732 T -> nT[4]	NA	No
	INDEL	RL2/RL1	124544 A -> AA	NA	No
	SNP	US3	136100 G -> A	G341R	Yes
	SNP	US8	142514 C -> T	S477L	Yes
Cross passage virus					
	INDEL	UL25/UL26	50732 T -> nT	NA	No
	INDEL	RL2/RL1	124544 A -> AA	NA	No
	SNP	US3	136446 G -> A	C456Y	No

1: nucleotide

2: amino acid

3: mutations identified at least two times in three isolates and unique in the culture

4: multiple T

Table 3-2. Details of mutations (identified at least two times in three isolates) in the sex-adpated HSV-1 in passage 30.

Viruses	SNP/INDEL	Gene name	NT[1] change	AA[2] change	Unique mutation[3]
Male passage virus					
	SNP	UL20/21	41598 G -> A	NA	Yes
	INDEL	UL22	45930 T -> TG	T132H*	Yes
	INDEL	UL25/UL26	50732 T -> nT[4]	NA	No
	SNP	UL48	104801 C -> T	D67N	Yes
	INDEL	UL56/RL2	120203 CCC -> C	NA	Yes
	INDEL	RL2/RL1	124544 A -> AA	NA	No
	INDEL	RS1/US1	131692 CC -> C	NA	Yes
	SNP	US3	136446 G -> A	C456Y	No
Female passage virus					
	INDEL	UL25/UL26	50732 T -> nT	NA	No
	SNP	UL48	103968 C -> A	L344F	Yes
	SNP	RL2	123396 A -> C	V204R	No
	SNP	RL2	123397 C -> G	C203S	No
	SNP	RL2	123400 A -> T	R202R	No
	INDEL	RL2/RL1	124544 A -> AA	NA	No
	SNP	RS1/US1	131693 C -> .	NA	Yes
	SNP	US3	136100 G -> A	G341R	Yes
	INDEL	US7/US8	140910 CC -> C	NA	No
	SNP	US8	142514 C -> T	S477L	Yes
Cross passage virus					
	INDEL	UL3/UL4	11725 GG -> G	NA	Yes
	INDEL	UL25/UL26	50732 T -> nT	NA	No
	SNP	RL2	123396 A -> C	V204R	No
	SNP	RL2	123397 C -> G	C203S	No
	SNP	RL2	123400 A -> T	R202R	No
	INDEL	RL2/RL1	124544 A -> AA	NA	No
	SNP	US3	136446 G -> A	C456Y	No
	INDEL	US7/US8	140910 CC -> C	NA	No

1: nucleotide

2: amino acid

3: mutations identified at least two times in three isolates and unique in the culture

4: multiple T

*: predicted frameshift

3.2.5 Investigation of mechanisms driving the different growth of HSV-1 in male and female cells

Based on the previous data in Sections 3.2.1-3.2.3, HSV-1 gained different mutations in the HSV-1 genome after serial passage on male and female cells and these viruses have sex-specific growth phenotypes *in vitro* and *in vivo*. In addition, HSV-1 replicates more efficiently in male cells compared to female cells after very low inoculum of HSV-1 (Figure 3-1). These observations suggested that male and female cells respond distinctively to HSV-1 infection. However, the mechanism that counteracts HSV-1 infection or drives the evolution of HSV-1 in each specific sex is unknown. Herein, RNA-seq was employed to comprehensively understand transcriptomic regulation, which may provide further information about how male and female cells respond differentially to HSV-1.

3.2.5.1 Infection rate of HSV-1 pICP47 recombinant virus in male and female cells

Before performing RNA-seq analysis, a suitable MOI and suitable infection time points needed to be selected. The use of a high MOI to ensure all cells are infected, may also overwhelm cells with excessive viral particles and risks destroying the cells before adequate evidence of host gene modulation has accumulated. Thus, the use of a low MOI was preferred in this study. The other factor in our experimental design was to ensure we could observe expression of all HSV-1 genes, including IE, early and late genes of HSV-1. Late genes of HSV-1 are predominantly expressed at least 4 hpi, with most transcription occurring between 6 and 12 hours post-infection (Stingley et al., 2000; Harkness et al., 2014). Hence, 4 and 8 hpi were selected as time points in the experiments. To test these conditions, we examined the percentage of infected cells in male and female cells at 4 and 8 hpi after infection with an MOI of 0.5 with HSV-1 pICP47 by flow cytometry. Four hours post-infection with HSV-1 pICP47 recombinant virus at an MOI of 0.5, around 75% of cells were GFP-positive in male and female cells (Figure 3-12). On the other hand, at 8 hpi, the percentage of GFP-positive cells increased to about 85-90% in both male and female cells (Figure 3-12). There was no significant difference in infection rate between male and female cells during an MOI of 0.5 infection with HSV-1 pICP47 virus at 4 and 8 hpi.

3.2.5.2 Design of the RNA-seq experiment to investigate transcription in the HSV-1 infected male and female cells

We considered using the same MOI that we showed a growth difference for HSV-1 between male and female cells (MOI <0.0003), but too few cells would be infected and this was not practical for use in the RNA-seq methods available at the time. Further, in the virus adaptation experiment (Section3.2.2), we used a higher MOI (starting with 0.01) and the male and female cells drove selection of virus variants. Therefore, it is reasonable to suggest that as long as the MOI is not too high (MOI <1) it should be possible to probe gene expression differences between male and female cells. An MOI of 0.5 was chosen as we reasoned that it would not be so high that any subtle cellular responses would be rapidly overwhelmed. In addition, at this MOI, HSV-1 replicated similarly between male and female cells (Figure 3-12), which means that differences in host response would not be simply due to the infection proceeding more quickly in cells of one sex, compared with the other. However, this infection condition left around 10-15% of uninfected cells and thus we decided to use a GFP-expressing virus and cell sorting to exclude uninfected cells in the design of our RNA-seq experiment. In order to collect HSV-1-infected cell populations, triplicates of male and female cells derived from different individual mice were separately infected with HSV-1 pICP47 recombinant virus at an MOI of 0.5 for four and eight hours. Following this, GFP-positive cells were sorted using flow cytometry. Representative plots showing the gating strategy for separation of infected and non-infected cells can be found in Figure 3-13. GFP-positive cells indicated HSV-1-infected populations and the signal detected in the phycoerythrin (PE) channel was used as a proxy for autofluorescence. The purity of sorted cells was re-analysed by flow cytometry and GFP percentage was around 95-98%. Total RNA was then extracted from sorted cells at indicated time points for library preparation. And RNA-seq was performed using the Illumina platform as described in Section 2.2.15.

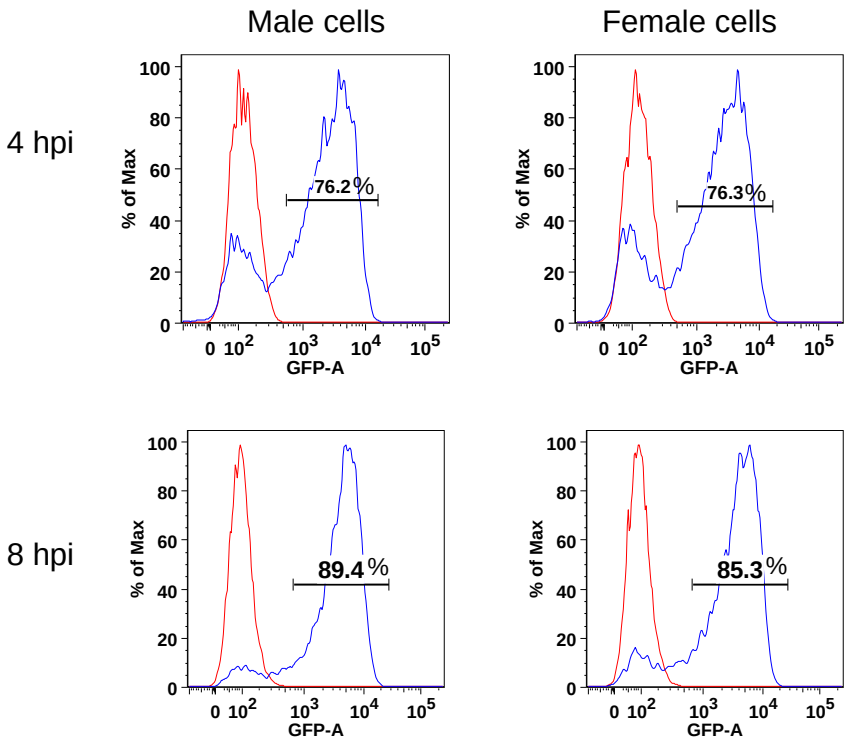

Figure 3-12. The infectivity of HSV-1 in male and female cells. Male and female cells from three individual mice were infected with HSV-1 pICP47 recombinant virus at an MOI of 0.5 for four or eight hours. Representative flow cytometric histograms from three independent experiments show the levels and percentage of GFP expression. Blue lines represent cells infected with HSV-1 pICP47 recombinant virus . Red lines represent mock infection.

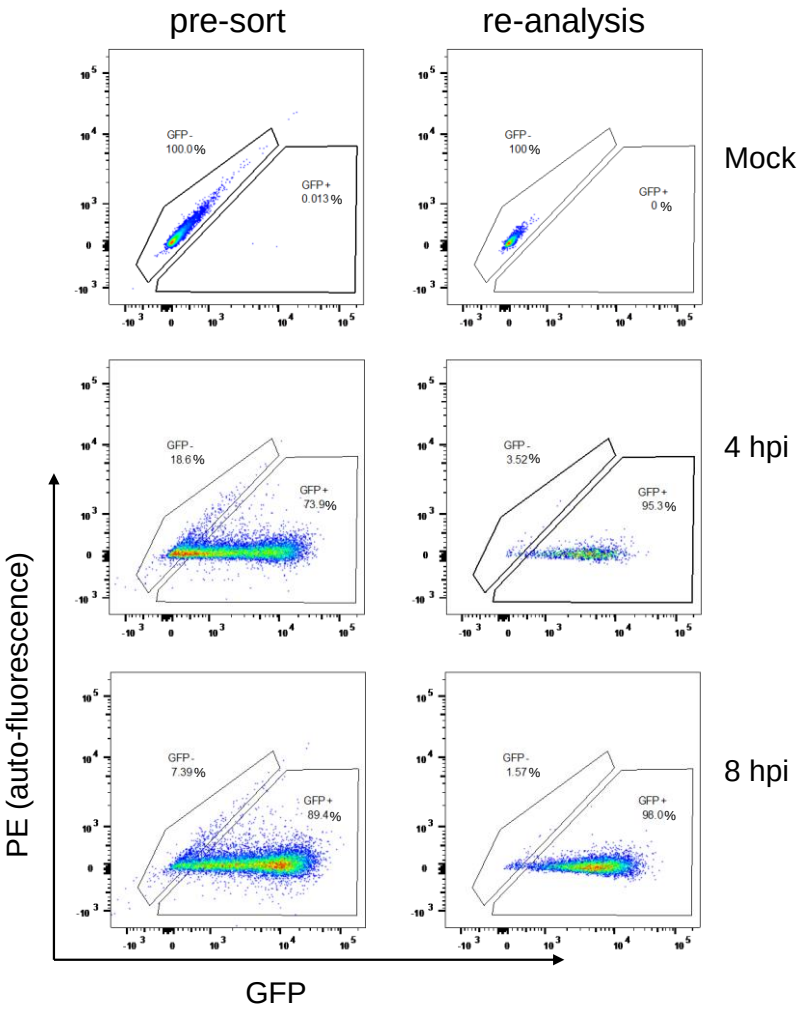

Figure 3-13. Strategy for separation of HSV-1-infected and non-infected cells. Representative flow cytometric plots show the gating strategy and the purity of cells post-sorting. The GFP-positive population was sorted from infected samples at 4 and 8 hpi. The PE channel was applied as a proxy for cellular autofluorescence. The proportions of GFP-positive (GPF +) and negative cells (GPF -) are indicated by percentages. Pre-sort represents cells before sorting and re-analysis represents cells after sorting.

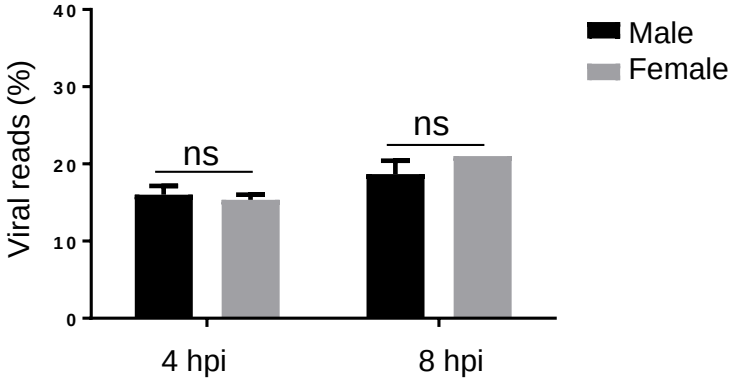

Figure 3-14. Percentage of raw reads mapped to the HSV-1 genome. Male and female cells from three individual mice were infected with HSV1 pICP47 recombinant virus at an MOI of 0.5. At 4 and 8 hpi, total RNA was extracted from sorted GFP-positive cells and then transcribed into cDNA libraries following the manufacturer's guide. Samples were subjected to an Illumina sequencing platform and the conditions are described in Section 2.2.15. After filtering reads with low quality scores and removing adapters, the resulting reads were mapped to a modified HSV-1 genome having only one long and short repeat, using the TopHat2 aligner. Percentage of viral reads relative to the total number of reads is shown. One-way ANOVA with Tukey's tests was used to test differences between means. Error bars are mean ± SEM. ns, no significant difference.

3.2.5.3 Comparison of HSV-1 transcription between male and female cells

Reads resulting from the RNA-seq experiment described in Section 3.2.5.2 were first processed and mapped to the mouse genome. The unmapped reads were then aligned to the modified sequences of the HSV-1 KOS strain. Details of the analysis of HSV-1 gene expression are provided in Section 2.2.31.4. The percentage of total reads aligned to the viral genome is shown in Figure 3-14. At 4 hpi, around 15% of total reads were viral reads in HSV-1-infected male and female cells. Viral reads accounted for about 20% of all reads at 8 hpi in these two cell types. There was no significant difference in the percentage of reads aligned to the virus between male and female cells at either 4 or 8 hpi. The expression of each HSV-1 gene at four and eight hpi was plotted in a heat map (Figure 3-15). Individual replicates of male or female cells were grouped together and then clustered based on infection time, indicating that each replicate acts comparably and time point post-infection was more important than the sex of cells in classifying expression of HSV-1 transcripts. Investigation of differential expression of HSV-1 genes between the two sexes revealed that none were statistically significant (data not shown). This is consistent with the finding that HSV-1 replication was similar for male and female cells at MOIs from 0.001 to 10 (Figure 3-1).

3.2.5.4 Differentially regulated host transcription between male and female cells during HSV-1 infection

In addition to investigating viral gene expression during HSV-1 infection in male and female cells, overall transcriptional regulation in the host was examined to determine whether males and females respond differently to HSV-1 infection. Reads that had been mapped against the mouse genome in Section 3.2.5.3 were further analysed for differential transcript expression between male and female cells using the Cufflinks package, as described in Section 2.2.31.2 (Trapnell et al., 2012). To visualise the transcriptional relatedness and reproducibility of each RNA-seq sample, principal coordinate analysis (PCA) was used. Each infection condition, including mock, 4 hpi and 8 hpi, was grouped into a defined cluster within the PCA plot (Figure 3-16). Infected samples were broadly mapped into the 4 hpi or 8 hpi clusters. Major transcriptional differences were observed between mock and 8 hpi, for cells of both sex. In the PCA plot, more male samples can be differentiated from female ones at 8 hpi, compared to 4 hpi or mock, indicating there were more differences between male and female cells at eight hours post-infection (Figure 3-16).

Next, the correlation of baseline mRNA expression between male and female cells (i.e. from the mock infection) was examined. The Pearson's correlation coefficient of 0.98 indicates that these two cells had very similar baseline mRNA expression prior to HSV-1 infection for most genes, although there were several outliers (Figure 3-17). Gene expression of 34,618 transcripts are shown in a heatmap (Figure 3-18) and they were further analysed for differential regulation compared to mock in male and female cells in HSV-1 infection (Figure 3-19 and Figure 3-20). Each replicate was clustered together first and then grouped by infection condition based on the Pearson's correlations and unsupervised hierarchical clustering. The results indicate that every replicate subjected to RNA-seq showed reproducible characteristics and there were more significant differences between individual infection times than the sex of cells (Figure 3-18). This was similar to viral transcription observed in Figure 3-15.

Although most genes had similar expression levels before infection between male and female cells (Figure 3-17), there were some sex-specific transcripts. Therefore, to investigate regulation due to HSV-1 infection, we used $\log_2$ fold changes (4 hpi or 8 hpi relative to mock) to normalize the original differences between male and female cells. The correlation of host transcriptional regulation by infection between the sexes was relatively high at 4 hpi (0.87) (Figure 3-19A), but it dropped to 0.72 at 8 hpi, suggesting that RNA regulation by infection diverged more between male and female cells at this time point as infection progressed (Figure 3-19B).

Differentially regulated transcripts at 4 and 8 hpi were evaluated as pairwise comparisons relative to mock ($\log_2$ fold change >1 or <1 and false discovery rate <0.05) in male and female cells. When comparing up- and downregulated differential gene regulation by infection between male and female cells at 4 and 8 hpi, the overall response to early HSV-1 infection was quite similar between the two sexes and more distinctively regulated transcripts were found at 8 hpi (Figure 3-20). In HSV-1-infected male or female cells, there were around 4,500 to 5,000 upregulated or downregulated transcripts at 4 and 8 hpi, respectively. Although HSV-1 infection induced comparable numbers of differentially regulated transcripts between male and female cells, these genes were not all shared. The two sexes shared 85.0-91.4% and 87.1-92.0% similarities in up- and downregulated transcripts, respectively, at 4 hpi and this decreased to 77.2-81.4% and 81.8-84.8%, respectively, at 8 hpi.

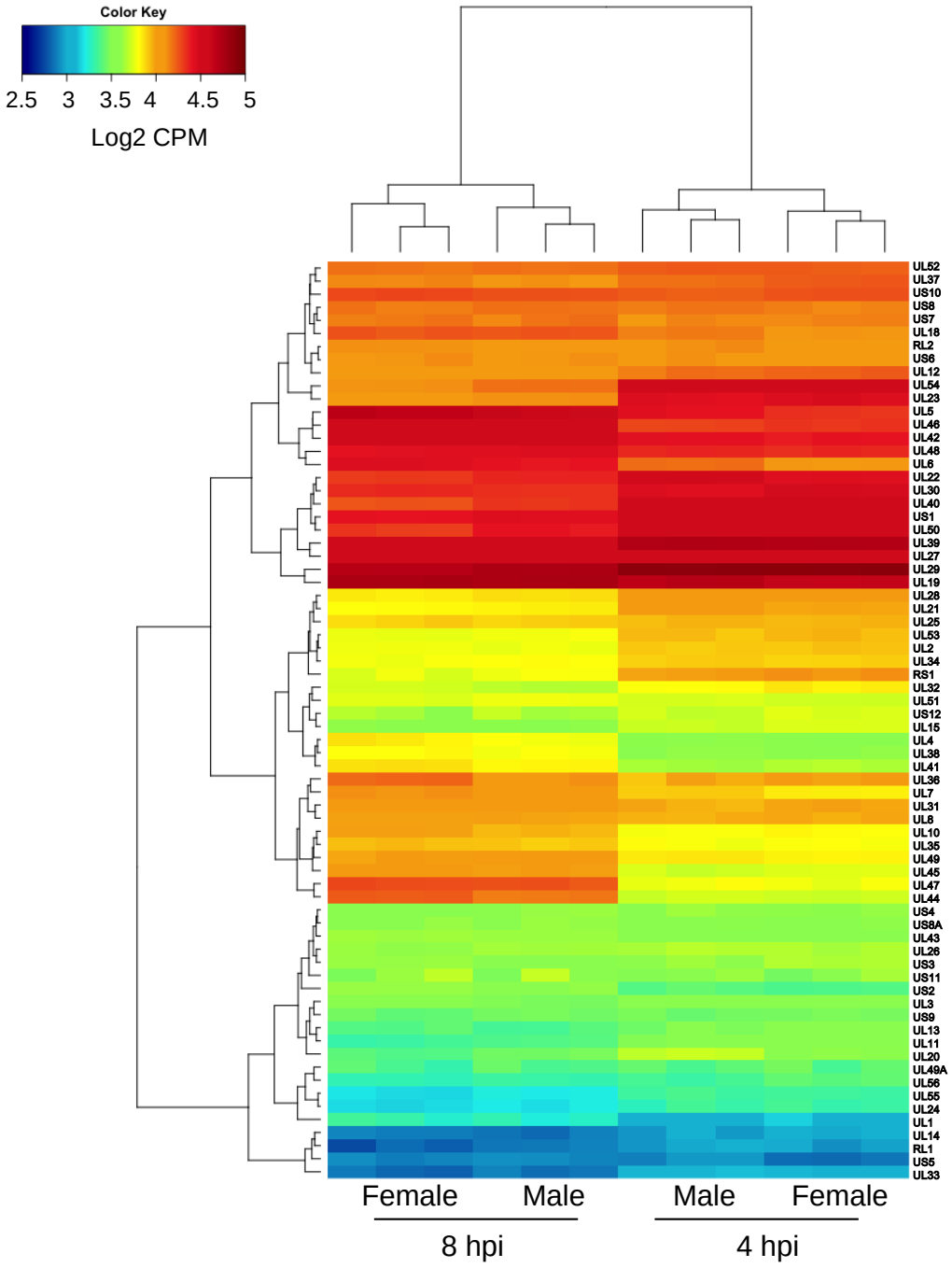

Figure 3-15. Expression of HSV-1 genes in male and female cells at 4 and 8 hpi. Reads that mapped to the HSV-1 genome were converted to counts per million (CPM) using the featureCounts package. Log_2 CPM of each HSV-1 gene at 4 and 8 hpi, in male and female cells from three individual mice, is plotted and grouped by hierarchical average linkage clustering and Euclidean distances. Density of individual samples are colour-coded: red=high density, blue=low density.

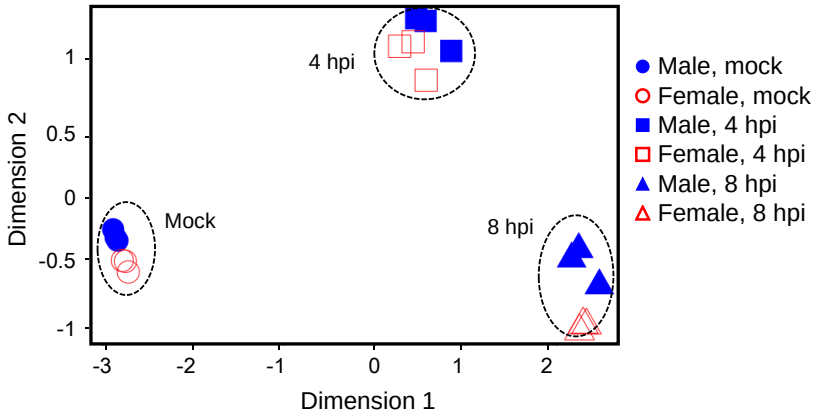

Figure 3-16. Principal coordinate analysis (PCA) of transcriptional expression in male and female cells during HSV-1 infection. PCA was performed based on the transcriptional levels in host genes (n=500) in mock (circle), and at 4 (square) or 8 (triangle) hpi, over dimensions 1 and 2, in male (blue) and female (red) cells from three individual mice.

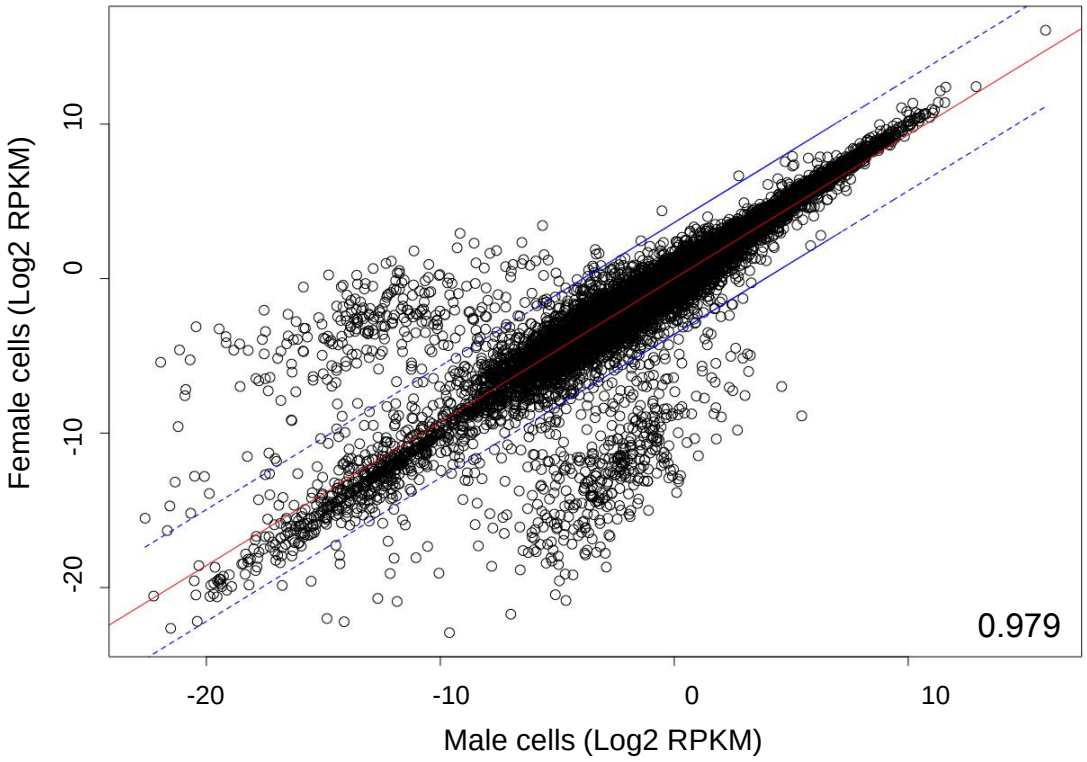

Figure 3-17. Baseline transcription levels in male and female cells. This scatterplot illustrates the relationship of baseline mRNA expression (mock) between male cells and female cells according to the $\log_2$ normalised reads per kilobase of transcript per million mapped reads (RPKM) (n=34,618). Pearson's correlation coefficient is indicated in the bottom right corner. Significantly differentially expressed transcripts are those with p-value <0.05 and FDR <0.05 (n=1890). A simple linear regression model was fitted (red line) and dashed lines are confidence intervals for thresholds calling differentially expressed transcripts between the two sexes.

3.2.5.5 GO and KEGG pathway analysis of up- and downregulated transcripts in male and female cells

In an attempt to identify molecular functions regulated by HSV-1 infection that differed between male and female cells, transcripts that were up- or downregulated at 4 or 8 hpi in male and female cells were compiled into lists for biological process enrichment classification in the GO database via the DAVID analysis tool (Harris et al., 2004; Huang et al., 2007; Huang da et al., 2009). Representative subsets of the GO terms in the upregulated or downregulated transcripts at 4 and 8 hpi were combined and displayed using REVIGO, a clustering algorithm that is dependent on semantic similarity measures, in order to remove redundant GO terms and visualise them in scatterplots (Supek et al., 2011) (Figure 3-21). Specifically, upregulated transcripts in male cells at 4 and/or 8 hpi were widely involved in regulation of binding [GO:0051098], protein folding [GO:0006457], positive regulation of organelle organisation [GO:0010638], RNA modification [GO:0009451] and interphase [GO:0051325] (Figure 3-21A). Male cells downregulated several cellular functions, such as flagellum organisation [GO:0043064], amino sugar metabolic process [GO:0006040] and tRNA processing [GO:0008033] (Figure 3-21B). In female cells, protein modification by small protein removal [GO:0070646], regulation of DNA repair [GO:0006282], biological regulation [GO:0065007] and vesicle docking [GO:0048278] were the classes upregulated at 4 and/or 8 hpi (Figure 3-21C). Furthermore, the downregulated subsets included endocytosis [GO:0006897], cellular amine metabolic process [GO:0044106], protein homooligomerisation [GO:0051260] and regulation of endothelial cell proliferation [GO:0001936] (Figure 3-21D). The biological meaning of these GO terms for HSV-1 infection was broad and not obvious so they were not pursued further.

In addition to the GO database, differentially regulated transcripts in male and female cells were analysed by KEGG pathways through the DAVID online tool to reveal differentially regulated pathways (Huang et al., 2007; Huang da et al., 2009). Male cells specifically upregulated one carbon pool by folate [mmu00670], alanine, aspartate and glutamate metabolism [mmu00250] and colorectal cancer pathways [mmu05210] at 4 hpi, and the dorso-ventral axis formation pathway [mmu04320] at both 4 and 8 hpi. For female cells, the small cell lung cancer pathway [mmu05222] was induced at 4 hpi and the non-small cell lung cancer [mmu05223] and cytosolic DNA-sensing pathways [mmu04623] were stimulated at 8 hpi. Details of differentially regulated pathways between male and female cells are shown in Table 3-3 and each pathway is also plotted

in a heatmap (Figure 3-22 and Figure 3-23). Collectively, male and female cells regulated several pathways differentially during HSV-1 infection including these associated with metabolism, cancer and of particular interest innate immune responses.

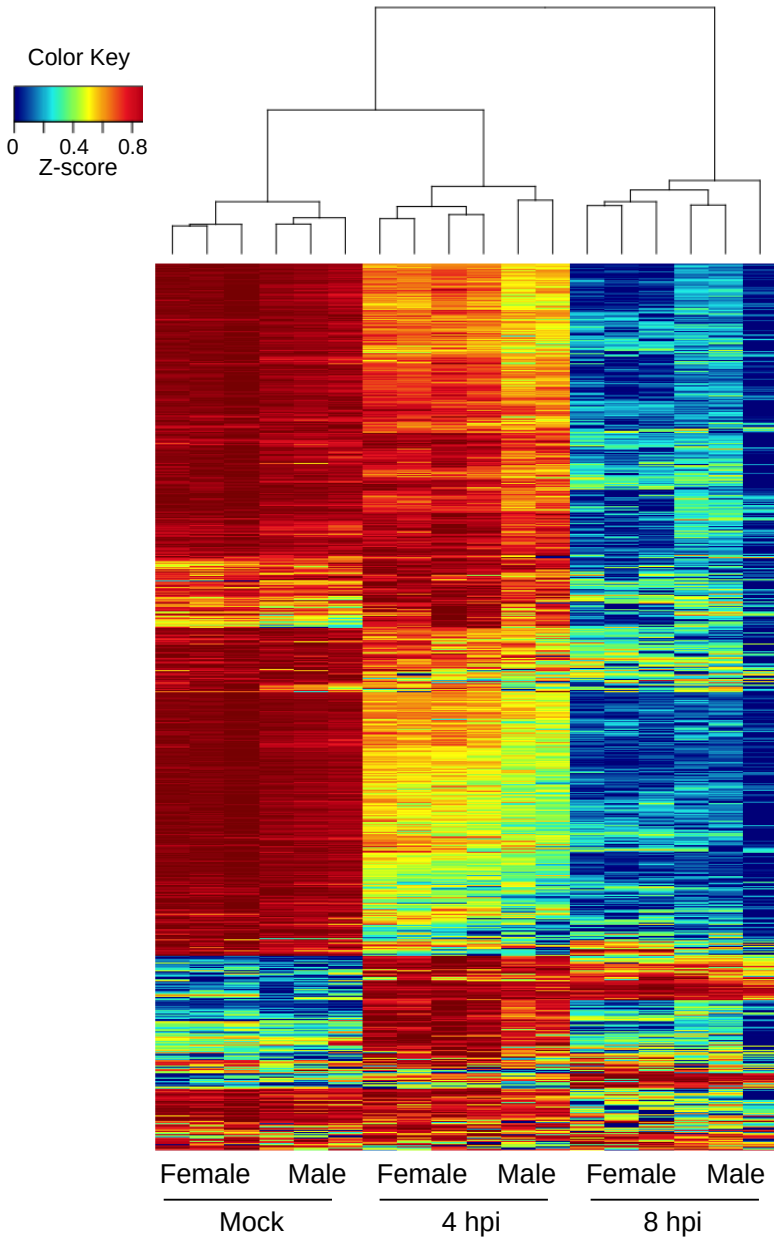

Figure 3-18. Comparison of host transcriptomes in male and female cells infected with HSV-1. A heatmap with hierarchical clustering of each transcript in male and female cells (n=34,618) at 4 hpi, 8 hpi and mock is depicted. The vertical dendrogram represents the clustering of infection condition and sex of cells based on the similarities in transcriptional expression. Reads per kilobase of transcript per million mapped reads (RPKM) were normalised to the maximum RPKM across all samples in each transcript, resulting in Z-scores (values between 0 and 1). Red indicates relatively high expression and blue refers to relatively low expression.

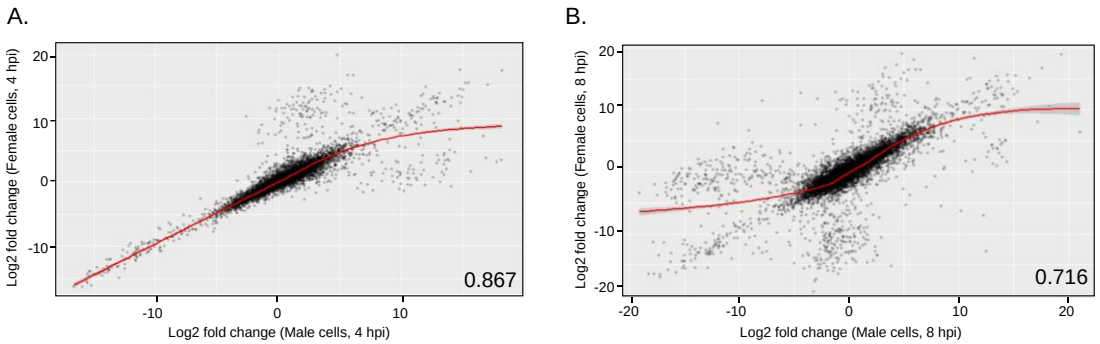

Figure 3-19. Relationships of transcriptional regulation by HSV-1 infection between male and female cells. Scatterplots show correlations between transcriptional changes due to HSV-1 infection in male and female cells at (A) 4 hpi (n=17150) and (B) 8 hpi (n=16068). Genes having fold changes equal to 0 were excluded. Pearson's correlation coefficients are shown in the bottom right corners. Simple linear regression models were fitted and are illustrated as red lines through each scatterplot.

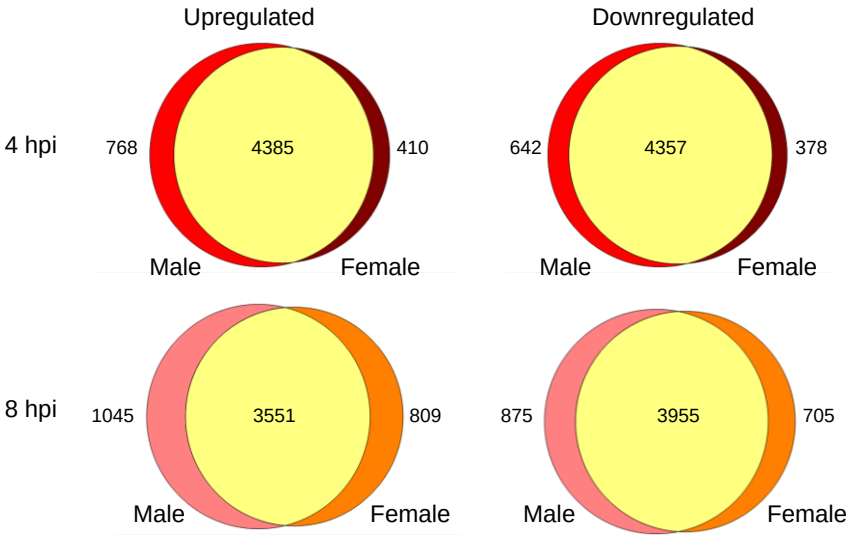

Figure 3-20. Transcripts differentially regulated by HSV-1 infection between male and female cells. Transcripts differentially regulated by HSV-1 infection at 4 and 8 hpi in male or female cells were determined as pairwise comparisons relative to mock infection. Two-way proportional Venn diagrams were drawn according to the number and overlap of significantly differentially regulated transcripts (p-value <0.05 and FDR <0.05).

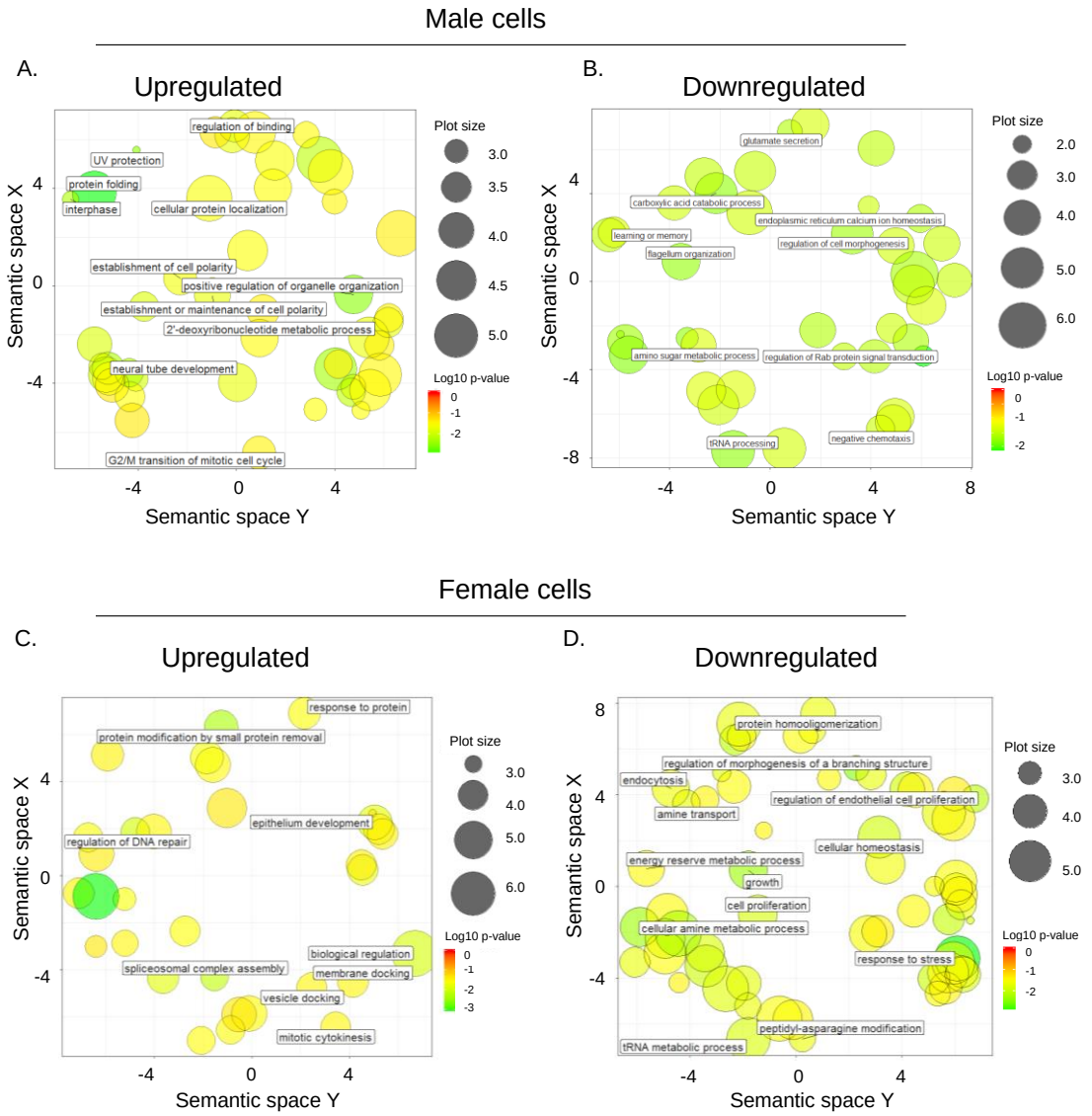

Figure 3-21. Gene ontology (GO) analysis of differentially regulated transcripts in male and female cells during HSV-1 infection. GO terms enriched in the upregulated or downregulated transcripts in male or female cells at 4 or 8 hpi were analysed. The results of up- or downregulated GO terms at 4 and 8 hpi were combined in (A-B) male and (C-D) female cells and further visualised by REVIGO, where GO terms that were identical and redundant were removed. The uncorrected log10 p-value for each parent GO term is represented by the circle colour. The size of the circle indicates the number of enriched child GO populations contributing to the parent term. Semantic space is the outcome of multi-dimensional scaling where similar GO populations cluster together.

Table 3-3. Differentially regulated KEGG pathways between male and female cells during HSV-1 infection.

Cell	KEGG pathway	p-value	Adjusted p-value	hpi	hpi
Female	**mmu04623 Cytosolic DNA-sensing pathway**	0.0046	0.042	8	upregulated
	mmu05222 Small cell lung cancer	0.01	0.049	4	upregulated
	mmu05223 Non-small cell lung cancer	0.001	0.0177	8	upregulated
Male	mmu00250 Alanine, aspartate and glutamate metabolism	0.0023	0.0263	8	upregulated
	mmu00670 One carbon pool by folate	1.88E-04	0.0043	8	upregulated
	mmu04320 Dorso-ventral axis formation	0.0026	0.0146	4	upregulated
	mmu04320 Dorso-ventral axis formation	0.0012	0.017	8	upregulated
	mmu05210 Colorectal cancer	0.0025	0.0271	8	upregulated

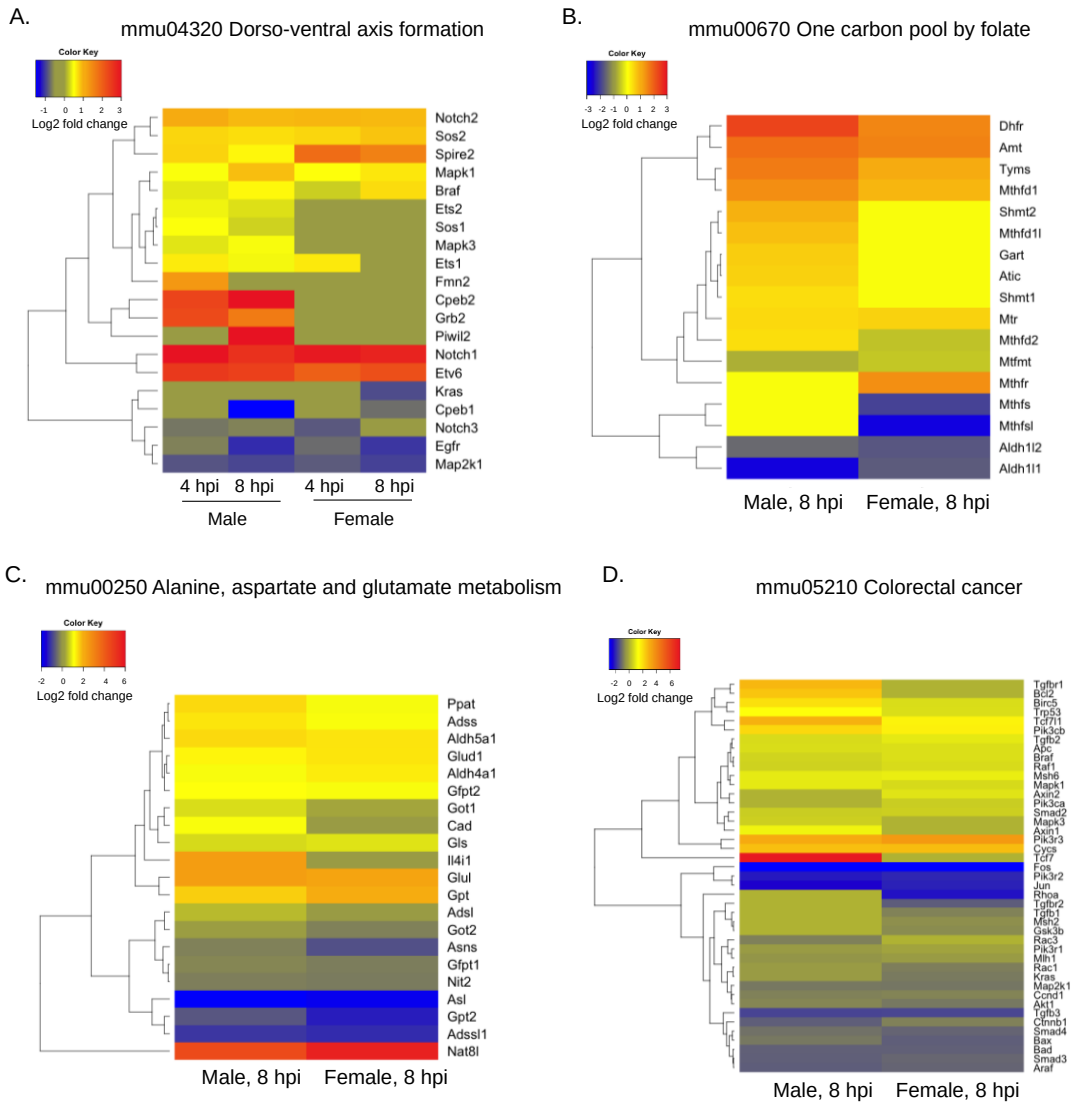

Figure 3-22. Differentially regulated pathways in male cells during HSV-1 infection. Upregulated genes at 4 or 8 hpi in male cells were subject to the KEGG pathway analysis. Pathways regulated by HSV-1 infection uniquely in male cells at 4 or 8 hpi are illustrated in heatmaps, including the (A) dorso-ventral axis formation pathway, (B) one carbon pool by folate pathway, (C) alanine, aspartate and glutamate metabolism pathway and (D) colorectal cancer pathway.

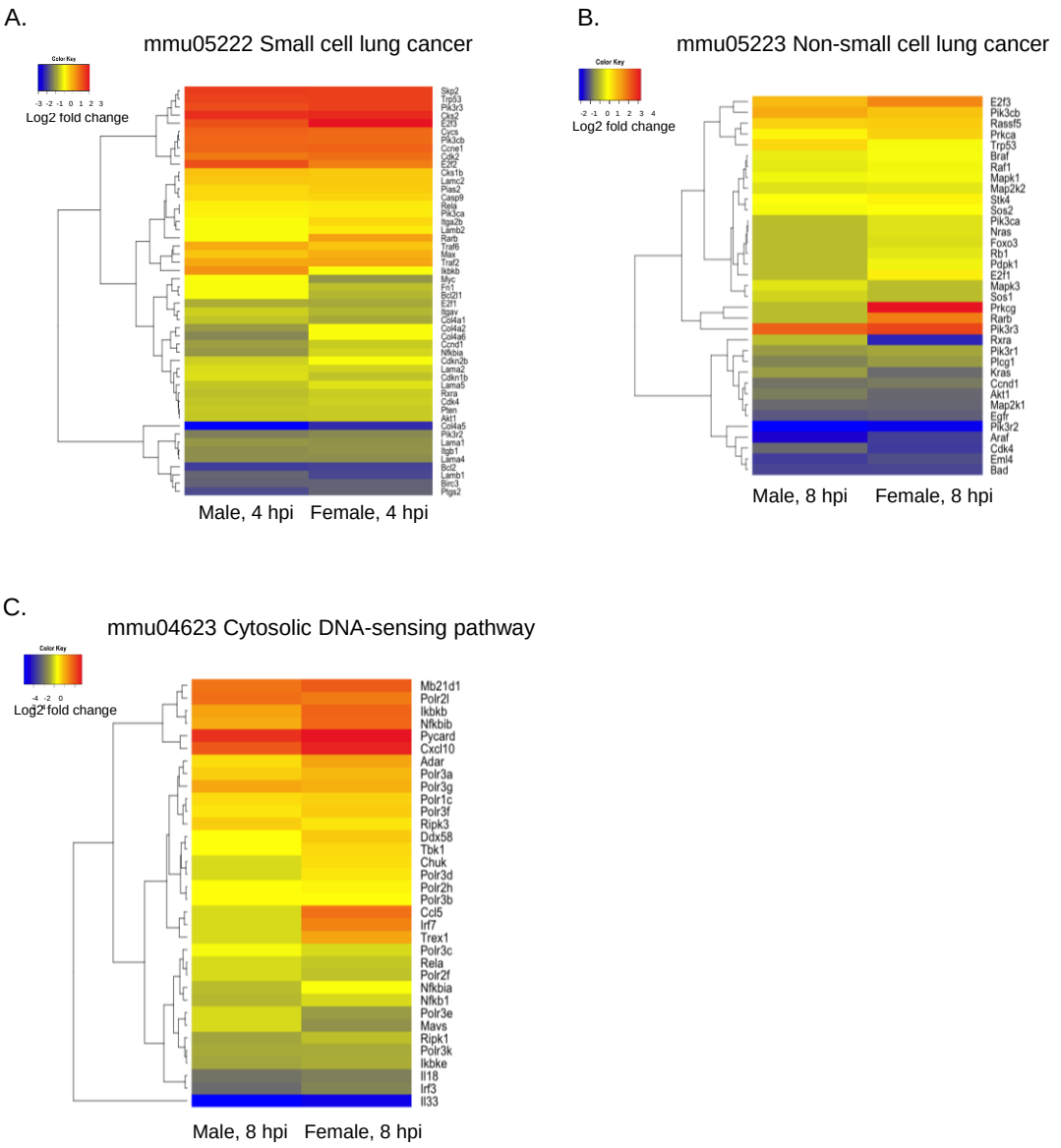

Figure 3-23. Differentially regulated pathways in female cells during HSV-1 infection. Upregulated genes at 4 or 8 hpi in female cells were analysed by the KEGG database. Pathways regulated by HSV-1 infection uniquely in female cells at 4 or 8 hpi are shown in heatmaps, including the (A) small cell lung cancer pathway, (B) non-small cell lung cancer pathway and (C) cytosolic DNA-sensing pathway.

3.2.5.6 Validation of RNA-seq data in the cytosolic DNA-sensing pathway by qPCR and Western Blotting

Previously in Section 3.2.5.5, several pathways differentially regulated by HSV-1 infection between male and female cells were identified. These included pathways involving cellular metabolism, cancer and strikingly, a cytosolic DNA-sensing pathway (Table 3-3). As the detection of intracellular nucleic acids has emerged to be an essential event in the innate immune response to viruses (Rathinam and Fitzgerald, 2011; Orzalli and Knipe, 2014), this pathway may be a potential mechanism to explain the different HSV-1 growth phenotypes between the two sexes (Figure 3-1). HSV-1 infection induced higher expression of many genes in the nucleic acid-sensing pathway in female cells than in male cells after infection with HSV-1, and this phenomenon was more obvious at 8 hpi (Figure 3-24). In order to validate the RNA-seq results, we used the same RNA sent for RNA-seq to confirm RNA regulation in HSV-1-infected male and female cells and to ensure that the changes were only happening in infected cells.. A subset of transcripts involved in this pathway, including *Mb21d1* (*cGAS*), *Ddx58* (*Rig-I*), *Ifih1* (*Mda5*), *Tbk1*, *Irf1* and *Irf7*, were chosen for quantitative real-time polymerase chain reaction (qPCR) analysis. In all cases, differential regulation by HSV-1 was confirmed between male and female cells at both times, except for *cGAS* at 4 hpi (Figure 3-25).

In addition to regulation of mRNA, protein expression was examined by WB. Male and female cells were infected with HSV-1 pICP47 recombinant virus at an MOI of 0.5 for four and eight hours. Protein samples were prepared and analysed by WB as described in Section 2.2.24. Each band was then quantitated by densitometry using ImageJ software (Version 1.50). There was no statistically significant difference in the levels of any proteins at 4 hpi between the sexes. However, at 8 hpi, amounts of protein were significantly higher in female cells than in male cells for all tested genes (Figure 3-25A and Figure 3-25B).

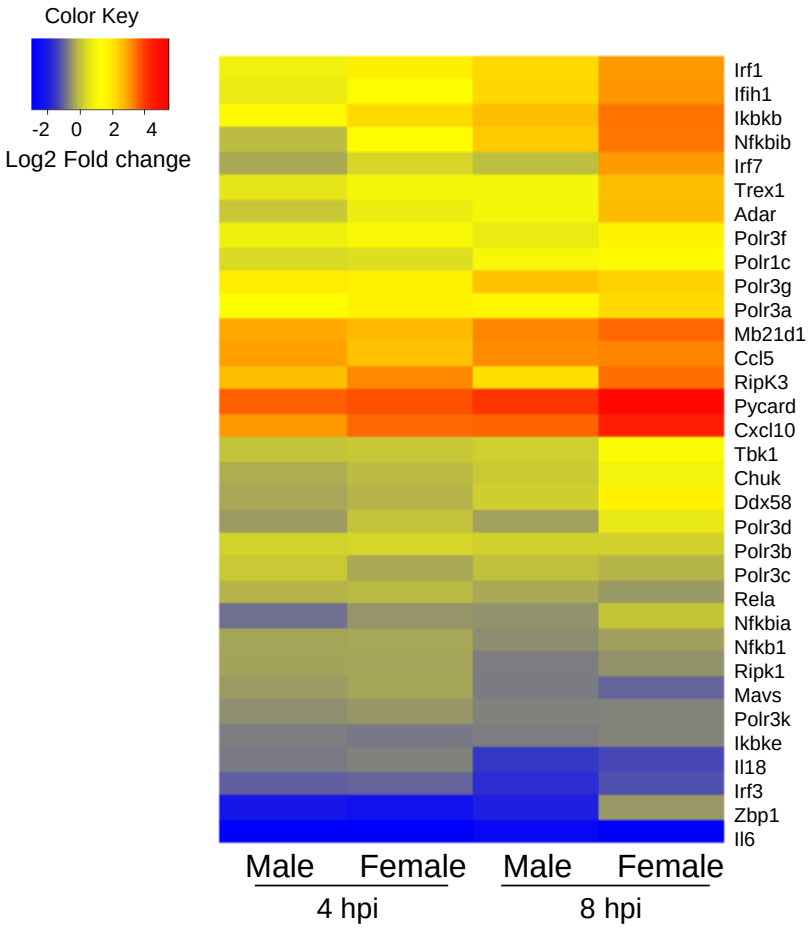

Figure 3-24. Cytosolic sensing pathway is upregulated to a greater extent in female cells. Regulation by HSV-1 infection of significantly regulated genes in the cytosolic DNA sensing pathway at 4 and 8 hpi illustrated as a heatmap. Blue represents lower regulation and red indicates higher regulation.

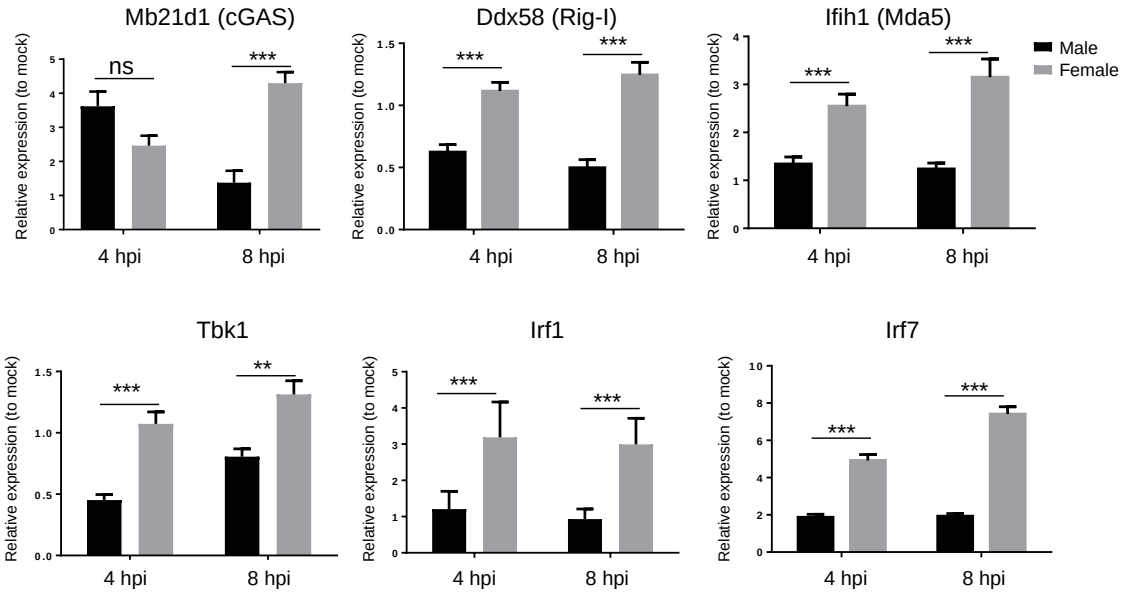

Figure 3-25. Validation of RNA-seq data for selected genes in the cytosolic sensing pathway by qPCR. Differential regulation was confirmed by qPCR for *Mb21d1* (*cGAS*), *Ddx58* (*Rig-I*), *Ifih1* (*Mda5*), *Tbk1*, *Irf1* and *Irf7* in HSV-1-infected male and female cells. Differential regulation was assessed by the $2^{-\Delta\Delta CT}$ method based on the expression relative to mock and normalised to 18S rRNA. The results are from at least six biological replicates and shown as mean ± SEM. One-way ANOVA with Tukey's post-tests was used to examine differences between means. ** and *** indicate p-value <0.01 and <0.001, respectively. ns, no significant difference.

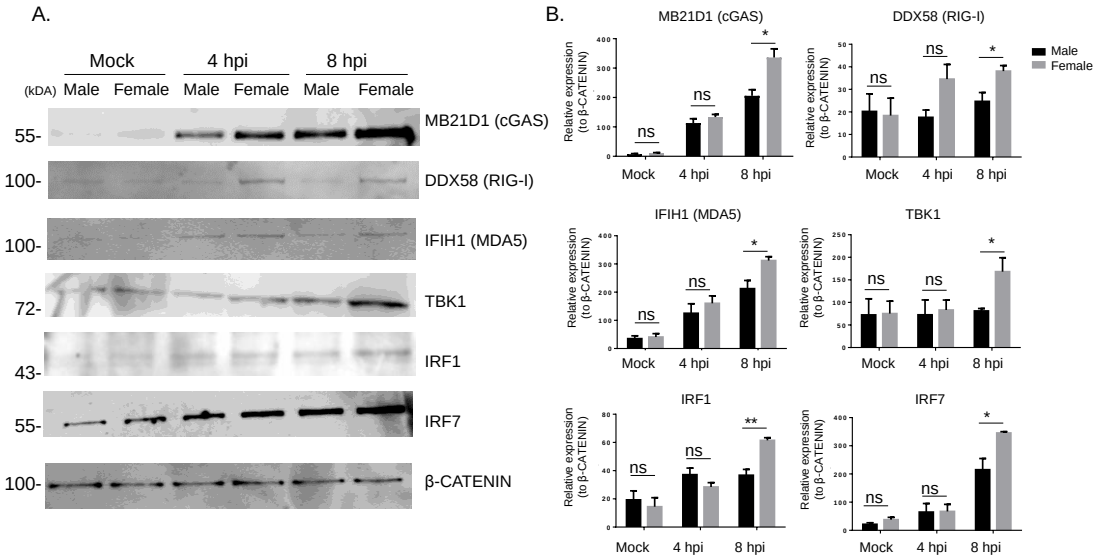

Figure 3-26. Protein expression of differentially regulated genes in the cytosolic sensing pathway. (A) Protein expression of genes of interest, including *Mb21d1* (*cGAS*), *Ddx58* (*Rig-I*), *Ifih1* (*Mda5*), *Tbk1*, *Irf1* and *Irf7*, was measured by Western blotting (WB). β-CATENIN was applied as the loading control. WB blots are representative of three independent experiments. The intensity of each band was quantified by ImageJ and the ratio of the individual protein to β-CATNEIN is shown as mean ± SEM in (B). A linear model was used to evaluate significant differences for each protein between the two sexes. A p-value less than 0.05 indicates a statistically significant difference. * and ** indicate p-value <0.05 and <0.01. ns, no significant difference.

3.3 Discussion

This chapter began with the investigation of the growth kinetics of HSV-1 in male and female cells at a series of MOIs. Primary skin fibroblasts were chosen as host cells given that skin is the major organ where HSV-1 initiates infection (Curry, 1980; Mindel et al., 1990). HSV-1 replicated more efficiently at low MOI (0.0003 and 0.0001) in male cells than female cells (Figure 3-1D and Figure 3-1E), indicating that distinct responses against HSV-1 infection can arise between the sexes and these differences can impact virus replication. Infections often begin with a very small number of initiating viral particles. Therefore, the outcome of an infection is likely to be influenced by the initial molecular interactions between the virus and host cells. Using low MOI also allows many rounds of replication in a single culture and this means that subtle differences can be seen. It has been reported that different MOIs induce distinct patterns of IFN subtypes and ISGs (Zaritsky et al., 2015). For example, JAK/STAT signalling via IFNAR occurs to a greater extent in human cells infected with lower virus concentrations, which mirrors both the classical model of the IFN pathway and natural infection (Devasthanam, 2014; Garcia-Sastre, 2017). Accordingly, a low MOI (<1) was applied for most of the experiments in the present study to avoid a biased disruption in specific signalling in the cultures infected with high amounts of virus and to prevent premature cell death which may mask any evidence of gene modulation by host cells.

As HSV-1 yields were different between male and female cells during low MOI exposure, we then asked whether the different selective pressure from each sex could drive distinct mutations in the HSV-1 genome. An experimental evolution modified from a protocol for VACV was performed to characterise the evolutionary pressures and adaptive ability of HSV-1 replication in primary mouse skin cells from each sex (Elde et al., 2012). HSV-1 was passaged 30 times starting at a low MOI in three biological replicates of male cells (male passage virus), female cells (female passage virus) or by alternating between male and female cells (cross passage virus) (Figure 3-4). The replication activity of these serial passage viruses in male or female cells was then evaluated by inoculating a new batch of male or female cells with each adapted virus at multiple passages (Figure 3-5). The viral titres in the male or female cells were then determined by plaque assays on Vero cells. Surprisingly, HSV-1 was found to adapt to each sex and gain replication fitness after as fewer as 10 rounds of serial passage. Specifically, male passage virus was found to replicate more efficiently in male cells and female passage virus produced more infectious particles in female cells (Figure 3-6). In addition, our data support a concept that HSV-1 is capable of adapting

to mouse skin cells as the viral yields in both male and female cells positively correlated with the serial passage number (Figure 3-6). The subsequent experiments both in Section 4.2 and 5.2 suggested that the effect we saw was cell-intrinsic, although we cannot not formally exclude a role for secreted factors that might act in a dominant fashion. Thus, performing an evaluation on a 50:50 mixture of male and female cells may be employed in the future to find whether there is another undiscovered mechanism from factors released into the medium. The specific adaptation of a virus to a given host, cell or other factors, such as antiviral drugs, usually results in fitness gains in the selective condition, but fitness declines in other host environments (Parrish et al., 2008; McWhite et al., 2016). The use of cell culture to produce adapted virus strains has been well documented for the alphaviruses and flaviviruses (Halstead and Marchette, 2003; Greene et al., 2005). For example, gains in fitness for Sindbis virus (SINV), a mosquito-borne alphavirus, were found after serial passage in mosquito cell culture and fitness declines were observed in baby hamster kidney cells (Greene et al., 2005). An increasing number of studies report that there is cell-specific adaptation when cell culture models are used to characterise viral adaptation (Weaver et al., 1999; Ciota et al., 2007a; Ciota et al., 2007b). Arboviruses, naturally maintained by transmission cycles between susceptible vertebrate hosts and arthropod vectors, increase their efficiency of infection for insect cells after only 10 selective passages, but the lineages adapted to growth in avian cells remain relatively non-infectious in avian cells (Cooper and Scott, 2001).

Compared to DNA viruses, RNA viruses are capable of rapid evolution owing to their high mutation rates, large population sizes and short replication times (Drake and Holland, 1999; Smith, 2017). Moreover, genome size appears to negatively correlate with mutation rate (Sanjuan and Domingo-Calap, 2016). Several studies have shown that some DNA viruses evolve at rates close to those of RNA viruses, including emerging canine parvovirus strains, human parvovirus B19, the circovirus SEN-V and the plant geminivirus (Shackelton et al., 2005; Shackelton and Holmes, 2006; Duffy and Holmes, 2008). These findings suggest that viral evolution may rely on multiple factors. In some cases, mutation rates for herpesviruses approach those observed in RNA viruses. A novel model of time-structured data demonstrated that high substitution rates can occur in the thymidine kinase gene of HSV-1 and the genome-wide evolution rate of HCMV is higher than previously thought for large dsDNA viruses (Firth et al., 2010; Renzette et al., 2015). Selection of HSV-1 variants by hosts that have evolved defensive mechanisms against virus infection have contributed to a greater substitution rate and more rapid adaptive evolution than previously believed (Drake and Hwang, 2005; Firth et al., 2010; Parsons et al., 2015; Renner and Szpara,

2018). Whole genome analysis of mutations in the sex-adapted viruses revealed that there were slightly more mutations in female passage viruses than their male counterparts (Figure 3-10A). These observations suggest that higher anti-HSV-1 responses may be produced by female cells and the mechanism behind this will be investigated in Chapter 5. Furthermore, single-sex passage series underwent more specific nucleotide and amino acid changes compared to viruses forced to replicate alternately in each sex (Figure 3-10B). This result is similar to what has been discovered in alphaviruses, such as SINV and equine encephalitis virus (EEEV), whereby single-host adaptation leads to more mutations than alternating cell passages (Weaver et al., 1999; Cooper and Scott, 2001; Greene et al., 2005).

Our SNP/INDEL analysis suggests that selective pressures from male and female cells induce mutations in the coding sequence of gH and gE, respectively. The envelope of herpesviruses contains at least five viral membrane proteins that have functions in viral entry. A gH/gL heterodimer binds integrins on the host cells as a regulator for fusion, and therefore, defines the tropism for the virus into epithelial and endothelial cells (Sinzger et al., 2008; Chesnokova et al., 2009). This heterodimeric complex is also a main target for HSV neutralising antibodies, which underscores its importance for virus infection (Peng et al., 1998; Macagno et al., 2010). Interestingly, mutation of gE gene was found as early as after 10 serial cultures and was maintained until passage 30 in female passage viruses (Table 3-1 and Table 3-2). HSV-1 gE is a key factor in cell-to-cell spread and virus-induced cell fusion. Mutations in the external domain of gE have been shown to block cell-to-cell spread (Wisner et al., 2000; Polcicova et al., 2005). Furthermore, gE is important for virus spread from epithelial cells to neurons and a coordinated complex of gE with tegument proteins, contributes to virus assembly and egress (Wang et al., 2010a; Han et al., 2011; Han et al., 2012). Perhaps there are differences in the cell membrane content between male and female cells, which could be further tested by electrospray ionisation and high-performance liquid chromatography mass spectrometry (Nealon et al., 2008; Russell et al., 2018). Lastly, based on our current data, we do not know whether these changes in glycoproteins, particularly the predicted frameshift in male passage viruses, may alter viral entry until we confirm these mutations by Sanger sequencing and then make recombinant viruses accordingly to investigate the importance of these mutations in virus replication.

In addition to glycoproteins, mutations in the UL48 gene (VP16) at different locations were separately identified in male and female passage viruses (Figure 3-11). VP16 is a multifunctional and conserved tegument protein in the herpesviruses (Liu et al., 1999). VP16 directly delivered by the infecting virions plays an essential role at the earliest

stage of infection and it induces IE gene expression via the recruitment of host transcription factors and RNA polymerase II to the IE promoters (Triezenberg et al., 1988a; Triezenberg et al., 1988b). Moreover, the interaction of VP16 with a number of virion tegument proteins and gH has been shown to promote viral assembly (Gross et al., 2003). Recent reports suggest that VP16 abrogates IFN signalling by various strategies, including suppressing the expression of immediate-early ISGs downstream of MAVS, inhibiting NF-κB activation and blocking the association between IRF3 and its coactivator (Xing et al., 2013; Zheng and Su, 2017). A single substitution in the VP16 sequence is lethal to HSV-1 due to blockage of virus assembly and virion maturation, suggesting that VP16 is important for these steps in HSV-1 replication (Ace et al., 1989; Weinheimer et al., 1992). Coincidently, the mutation site (amino acid residue 344) of VP16 identified in the female passage viruses (Table 3-2) has been found to be critical for binding to the virion host shutoff protein (vhs) and for productive infection (Knez et al., 2003). In the study published by Knez et al. (Knez et al., 2003), an L-to-F substitution at residue 344 of VP16 was found to act like wild-type VP16 and did not affect the interaction with host cell factor-1 (HCF-1). However, whether this circumstance is similar to our case requires further investigation to reveal the underlying molecular mechanisms.

Several regions in the HSV-1 genome were found to be prone to mutations that due to selective pressure from serial passage in mouse skin fibroblasts. For example, US3 is a multifunctional protein that mediates numerous cellular and viral functions. HSV-1 US3 has been reported to block apoptosis (Leopardi et al., 1997; Ogg et al., 2004), regulate intracellular transport and trafficking (Mou et al., 2009; Kato et al., 2011) and modulate host responses in innate and adaptive immune systems (Sloan et al., 2003; Wang et al., 2013b; Kalamvoki and Roizman, 2014). Mutation in the US3 gene was observed across male, female and cross passage viruses (Table 3-1 and Table 3-2), although it occurred at different locations. Notably, a G341R substitution in US3 was identified at passage 10 and maintained at passage 30 in female passage viruses, highlighting the importance of US3 in responding to the selective pressure from female cells. Insertions in two intergenic regions, UL25/UL26 and RL2/RL1, were also identified across male, female and cross passage viruses, suggesting that these mutations are acquired from the selective pressure of mouse skin fibroblasts. How these mutations might influence HSV-1 infection is unknown.

Given that different growth phenotypes were found between male and female cells during low MOI HSV-1 infection (Figure 3-1), and differential selective pressure in experimental evolution against HSV-1 was observed between the two sexes (Figure 3-

10 and Figure 3-11), we then employed RNA-seq to comprehensively investigate differences in the transcriptional program of these cells in responses to HSV-1. RNA-seq has been developed to reduce, and in some cases eliminate, the limitations associated with microarray-based analysis of a transcriptome, such as a limited dynamic range, high background noise and applicability only to detect known messages (Wang et al., 2009; Fang et al., 2012). In order to compare differential regulation by HSV-1 at the transcript level, the Tuxedo suite pipeline for RNA-seq data, a fragments per kilobase per million reads (FPKM)-based method, was performed as quantifying expression at the gene level may occasionally mask alterations if two or more isoforms have different expression patterns (Trapnell et al., 2012; Kim et al., 2013). In addition, we only focused on the HSV-1-infected cells by sorting the infected cell population. This method was chosen for several reasons. First, the difference in transcriptional modulation between the two sexes was expected to be very subtle. Inoculation of very low amounts of virus revealed a difference in HSV-1 replication between male and female cells (Figure 3-1), but a low MOI of HSV-1 infection may leave a large uninfected population that could mask genuine transcriptional regulation. Second, Schmidt et al. showed that HSV-1 triggers host DNA synthesis in uninfected cells via a virus-induced paracrine effector during infection. This was initiated by a single viral particle with progressive cell-cell transmission (Schmidt et al., 2015). This mechanism supports the notion that the inclusion of all cell populations in measurements may mask crucial properties of the signalling networks (Korobkova et al., 2004). Using an MOI of 0.5 lead to around 85-89% infection rate at 8 hpi (Figure 3-11), indicating most of the cells were infected and only a small proportion of cells left uninfected. This MOI and time point were always used in investigating RNA regulation between male and female cells to make it comparable with our RNA-seq experiments (MOI=0.5, 8 hpi). Whilst differences in HSV-1 replication were only observed at very low MOI (<0.0003), we were able to observe different host responses at a higher MOI (0.5). It is most likely that these antiviral effects were relatively subtle, but have a cumulative effect that is only seen after several rounds of infection.

Although our RNA-seq analysis revealed no significant difference in viral gene expression between the two sexes at both 4 and 8 hpi, cells still clustered by sex within each time point, indicating sex does play some roles during the infection. However, the host gene regulation by HSV-1 infection gradually diverged and this finding was supported by our PCA (Figure 3-16) and Pearson's correlations (Figure 3-18). In order to organise differentially expressed transcripts into a more meaningful framework, two well-established databases (GO and KEGG) were utilised to identify differentially regulated pathways between the two sexes. The results of the GO analysis (Figure 3-

21) revealed that most of the biological process terms were too broad and not obviously related to virus infection to obviously inform further investigation. According to the KEGG pathways analysis, various cellular functions were regulated differentially between male and female cells, including several cancer, metabolic and innate immune pathways. Cancer-related pathways are of interest in herpesvirus infections because at least two members in the human herpesviruses have been identified to be oncogenic viruses. Human herpesvirus 8 (HHV-8) is the oncogenic virus related to Kaposi's sarcoma and Epstein–Barr virus (EBV), the first virus found to cause cancer in humans, is associated with a wide spectrum of human cancers originating from epithelial cells, lymphocytes and mesenchymal cells (Sunil et al., 2010; Chen et al., 2015b; Naseem et al., 2018). There is less evidence that HSV-1 might be related to cancer. Two studies used serological analyses to investigate the relationship between HSV infections and primary central nervous system malignancy, showing a high percentage of seropositivity (76-86%) in glioblastoma, glioma and meningioma (Poltermann et al., 2006; Saddawi-Konefka and Crawford, 2010). There seems to be a trend towards a positive correlation of anti-HSV antibodies with glioma (Poltermann et al., 2006). However, the statistical analysis showed no significant difference between seroprevalences in brain tumor patients and the general population (Poltermann et al., 2006). Therefore, more clinical samples are required to support the hypothesis of an association of herpesviruses with the development of primary brain tumors. Vastag et al., found that HCMV and HSV-1 trigger different metabolic changes in their cellular hosts, such as human skin and lung fibroblats (Vastag et al., 2011). HCMV largely affects the production of substrates for lipid metabolism, whereas HSV-1 greatly impacts carbon metabolism toward the synthesis of pyrimidine nucleotides. Particularly, carbamoyl-aspartate levels are significantly induced both in HCMV and HSV-1 infections. In addition to the regulation of amino acids, a cohort of 50 patitents with recurrent HSV eye diseases showed that recurrence rate of herpetic keratitis was lower in patients with higher blood level of folic acid (Savic et al., 2019). The data suggest that folic acid might play an role in HSV keratitis reactivation. However, more experiments are needed to understand how these metabolic pathways might be involved in the sex-specific difference in our cultures. Lastly, there is no literature relevant to genes in developmental pathways, such as dorso-ventral axis formation in HSV infection, so the reason why this was found in the pathway analysis of genes upregualted by HSV-1 infection remains to be investigated.

Importantly, our results revealed that HSV-1 induced greater upregulation of multiple genes in a cytosolic DNA sensing pathway in female cells (Table 3-3), which was confirmed by qPCR and WB for selected genes (Figure 3-25 and Figure 3-26). As the

first line of host defence, the innate immune system has evolved a multi-faceted surveillance network to prevent virus infection (Bhat and Fitzgerald, 2014; Ma and He, 2014; Chow et al., 2018). Accumulating evidence suggests that cytosolic sensors recognise HSV-1 to induce IFN secretion and expression of ISGs. Herein, three nucleic acid sensors, including *cGAS*, *Rig-I* and *Mda5*, and three signalling transducers, *Tbk1*, *Irf1* and *Irf7*, were found to be upregulated to a higher degree in female cells than male cells. All of the genes mentioned above have been shown to play a role in the induction of antiviral immunity against HSV-1. *cGAS* deficiency renders mice susceptible to herpes simplex encephalitis and correlates with impaired type I IFN expression in microglia (Li et al., 2013; Reinert et al., 2016). Two other sensors, *Rig-I* and *Mda5*, primarily recognise virus-derived RNA and are responsible for HSV-induced cytokine and chemokine expression in early innate recognition (Melchjorsen et al., 2010; Xing et al., 2012b). Signalling transduced from recognition of foreign nucleic acids leads to a conformational change by STING, allowing recruitment of TBK1 and IRFs. This process then activates IRFs in a TBK1-dependent manner to regulate ISGs expression. An innate antiviral pathway can be activated in an IFN-independent manner, which is consistent with our observation that there were no IFNs detected in both male and female cells based on our RNA-seq analysis (data not shown) (Paladino et al., 2006; Tanaka and Chen, 2012; Iversen et al., 2016). Therefore, upregulation of these genes in the cytosolic sensing pathway in female cells may be a key factor that influences the difference in growth of HSV-1 between male and female cells (Figure 3-1).

While there were genes in the nucleic acid-sensing pathway upregulated in female cells and also some ISGs, there was a surprising absence of type I IFN. This gave rise to two questions:

1. In the absence of IFNs, what are the anti-viral effectors downstream of the nucleic acid-sensing pathway?

2. What is the mechanism that underlies the greater upregulation of genes in the nucleic acid-sensing pathway in response to HSV-1 in female cells?

For the first question, a potential anti-HSV-1 effector expressing in an IFN-independent manner will be discussed in Chapter 4. The regulation of nucleic acid-sensing pathway by HSV-1 infection will be further investigated and discussed at a mechanistic level in Chapter 5.

Chapter 4. Is viperin an anti-HSV-1 effector and an important factor for the sex-specific difference?

4.1 Introduction

Virus recognition by cellular sensors typically leads to production of an antiviral state, which is established by the activity of various ISGs (Schneider et al., 2014; Schoggins 2014). These downstream effectors have a range of functions, such as induction of programmed cell death, inhibition of virus replication and recruitment of immune cells to infected sites (Wang et al., 2017). As nucleic acid sensing pathways were upregulated by HSV-1 infection (Section 3.2.5.5), downstream antiviral proteins, many of which are also ISGs, are expected to be upregulated (Junt and Barchet, 2015; Ahlers and Goodman, 2016). Indeed, there were several potential antiviral ISGs upregulated in HSV-1-infected cultures, including the OAS family, the GBP family, viperin and *Cxcl10* (data not shown). Of these, we found that viperin was upregulated to a very high level and ranked at the top of lists of upregulated ISGs in male and female cells based on our RNA-seq analysis. However, viperin induction was higher in female compared with male cells after HSV-1 infection. This was intriguing because the only publication on viperin and HSV suggests that viperin is not induced by HSV infection, which contradicts our observations (Shen et al., 2014). Shen et al., have shown that HSV-1 was found to induce a trace amount of viperin in a female human cell line (HEK293 cells) and ectopically expressed viperin had no effect on the replication of HSV-1 (Shen et al., 2014). For this reason, we wanted to explore viperin further.

The first aim of this chapter is to investigate whether or not viperin can be upregulated by HSV-1 infection and play an antiviral role in a variety of cell types. In addition, which domain of viperin contributes to the antiviral function against HSV-1 was investigated. Lastly, we investigated whether viperin is an essential factor responsible for the increased resistance to HSV-1 in female cells.

4.2 Results

4.2.1 Validation of viperin upregulation during HSV-1 infection

4.2.1.1 Confirmation of viperin upregulation by qPCR and WB in male and female cells from mice

Our RNA-seq analysis (Section 3.2.5.3) indicated that viperin was upregulated at 4 and 8 hpi in both male and female cells during HSV-1 infection (Figure 4-1A). To confirm this, qPCR using primer sets specific for mouse viperin was performed to confirm

upregulation of viperin in male and female cells (Figure 4-1B). For normalisation, mouse 18S rRNA was used as an internal control since it cannot be degraded by HSV-1 vhs (Zenner et al., 2013). Consistent with the RNA-seq data, an increased amount of viperin was detected with approximately 3 and 9-fold induction at 4 hpi and 10 and 40-fold changes at 8 hpi, in male and female cells, respectively. This analysis also confirmed that female cells upregulated viperin expression more in response to HSV-1 infection as compared with male cells at 8 hpi (Figure 4-1B).

In addition to RNA level, expression of viperin protein during HSV-1 infection was determined. Male and female cells were infected with HSV-1 pICP47 recombinant virus at an MOI of 0.5 for four or eight hours. Cells were then harvested and subjected to WB analysis with antibodies against mouse viperin. In line with mRNA upregulation, viperin protein levels were higher in male and female cells four and eight hours post-infection (Figure 4-2A). Moreover, female cells produced a significantly greater amount of viperin protein than male cells at 8 hpi (Figure 4-2B).

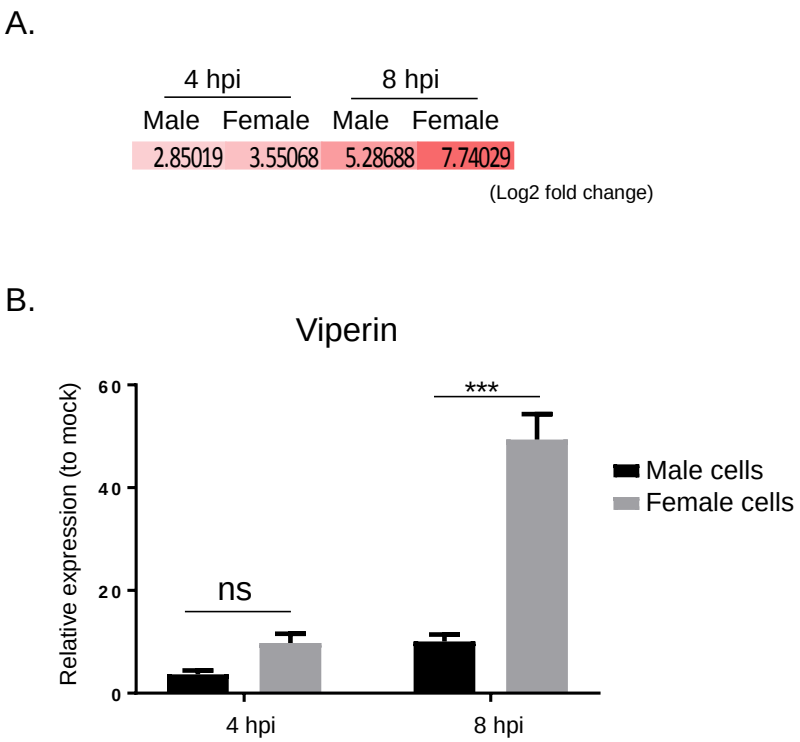

Figure 4-1. Regulation of viperin by HSV-1 infection in male and female cells from mice at 4 and 8 hpi. (A) Log_2 fold changes of viperin in male and female cells at 4 and 8 hpi, compared to mock from RNA-seq analysis. (B) Male and female cells from three individual mice were infected with HSV-1 pICP47 recombinant virus at an MOI of 0.5 for four and eight hours. Total RNA was then extracted, followed by cDNA synthesis and qPCR analysis for viperin expression. Differential regulation of viperin mRNA was assessed by the $2^{-\Delta\Delta CT}$ method based on expression relative to mock infected cells and normalised to 18S rRNA. The results are shown as mean ± SEM. One-way ANOVAs with Tukey's tests were used to examine differences between means. *, ** and *** indicate p-value <0.05, <0.01 and <0.001, respectively.

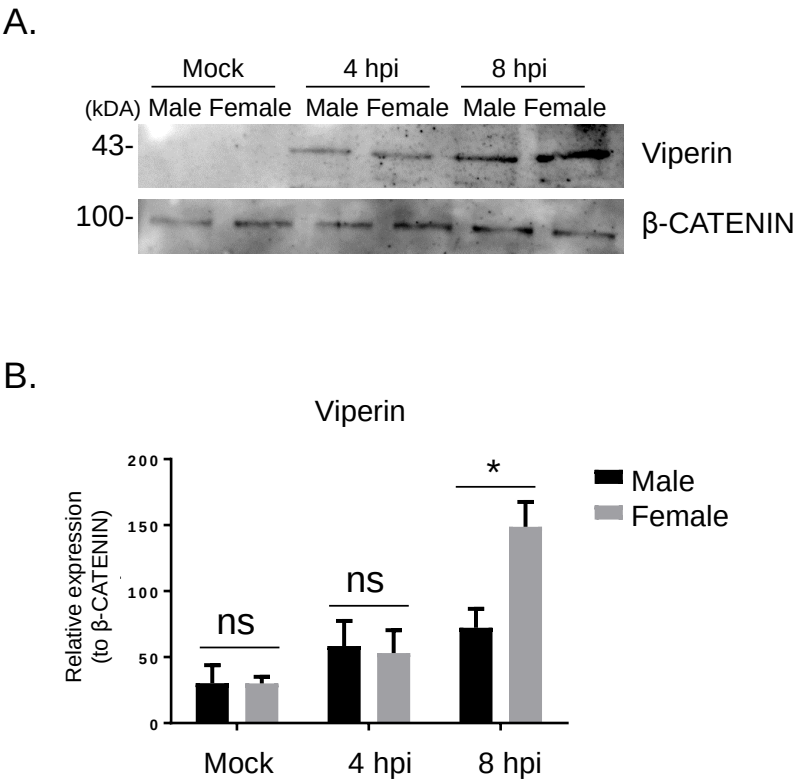

Figure 4-2. Protein expression of viperin in male and female cells at 4 and 8 hpi. Male and female cells from three individual mice were mock infected or infected with HSV-1 pICP47 recombinant virus at an MOI of 0.5 for four and eight hours. Cell lysates were harvested for Western blotting analysis (WB). β-CATENIN acted as the loading control. (A) Representative WB shown for one pair of male and female cultures. (B) Quantification of WBs by densitometry using ImageJ. The ratio of viperin to β-CATNEIN pooled from three replicates is shown. A linear model was used to evaluate significant differences between the two sexes. * indicates p-value <0.05. ns, no significant difference.

4.2.1.2 A time course study of viperin regulation by HSV-1 infection in RNA and protein levels

In order to understand the dynamics of viperin expression in mouse cells, a time course study of viperin levels in male and female cells during HSV-1 infection was performed using qPCR for absolute quantification. Male and female cells were infected with HSV-1 pICP47 recombinant virus at an MOI of 1 and then total RNA was isolated at indicated time points (4, 8, 12 and 24 hpi) for cDNA synthesis and qPCR reaction. To provide a copy number control, plasmid DNA containing the coding sequence of full-length mouse viperin was used. The concentration of this plasmid was determined by Nanodrop spectroscopy and 10-fold dilutions were prepared from 10^1 to 10^8 copies/µl to construct a standard curve. The standard curve had an R^2 value of 0.99 and the linear regression equation shown was used to calculate viperin copy number (Figure 4-3A). In male and female cells, viperin expression gradually increased from 4 to 12 hpi and was decreased at 24 hpi. The decrease at the latest time most likely represents the reduced viability of cells at this time. Furthermore, significant differences in viperin levels in male and female cells were found at 8, 12 and 24 hpi (Figure 4-3B).

Next, a time course of viperin protein expression during HSV-1 infection was investigated in female cells, as HEK293 cells used in the previous report were derived from female human embryonic kidney (Shen et al., 2014). Female mouse cells were infected with HSV-1 pICP47 recombinant virus at an MOI of 2 for 0, 4, 8, 12 and 24 hours. Following this, WB analysis was performed with antibodies detecting viperin. Quantification of individual bands was carried out by densitometry using ImageJ software (version 1.50). In female mouse cells, the protein level of viperin started to increase from 4 hpi, plateaued at 12 hpi and began to decrease after 24 hours of infection (Figure 4-3C and Figure 4-3D).

4.2.1.3 Regulation of viperin in a variety of human cell types by HSV-1 infection

Upregulation of viperin by HSV-1 infection has been found in mouse skin fibroblasts in the previous sections. However, Shen et al. showed that viperin is not induced during HSV-1 infection in a human cell line (HEK293). Therefore, we wanted to explore whether upregulation of viperin by infection is strictly species- and/or cell-type-specific. To further explore the role of viperin in other human cell types, four human cell types, two of each sex were included in the experiment: HFF (male), MRC5 (male), HEK293 (female) and HeLa (female). HEK293 cells were used to confirm Shen et al.'s

observation. In the four tested human cell types, except for HeLa cells at 8 hpi, viperin was not induced compared to mock infected cells at 4 and 8 hpi (Figure 4-4). Viperin was however significantly induced by infection in HeLa cells compared with other human cell types. This upregulation of viperin in HeLa cells was clear, but was around a tenth of what we observed with mouse cells being a five-fold increase, compared with a 50-fold increase in the mouse cultures (Figure 4-1).

In addition to regulation of viperin mRNA by HSV-1, we extended the analysis to the protein level. A time course of viperin protein expression during HSV-1 infection was investigated in two human cell types (HEK293 and HeLa cells). HEK293 cells were used for comparison with the data from Shen et al and HeLa cells were utilized as HSV-1 induced significantly more viperin mRNA in HeLa compared with other tested human cell types (Figure 4-4). There was no significant increase of viperin protein in HEK293 cells during HSV-1 infection (Figure 4-5A and Figure 4-5B), which is consistent with previous findings (Shen et al., 2014). In HeLa cells, viperin protein started to increase from 8 hpi and then decreased after 12 hours of infection (Figure 4-5C and Figure 4-5D) such that level and duration of viperin induction were lower and shorter compare with female mouse fibroblasts (Figure 4-3C). Taken together, regulation of viperin by HSV-1 infection is dependent on different species and cell types.

4.2.1.4 HSV-1 can stimulate viperin expression in an IFN-independent manner

According to the RNA-seq result in Section 3.2.5.3, there was no difference in IFN regulation by HSV-1 infection between male and female cells (data not shown), indicating that IFN may not be involved in the differential regulation of viperin between the sexes during early HSV-1 infection. There is a precedent for IFN-independent regulation of viperin transcripts (Fitzgerald, 2011; Duschene and Broderick, 2012), but it remained to be shown formally whether viperin upregulation in our culture was independent on type I IFN. To investigate this, two approaches were used to identify whether soluble factors and specifically IFNs, are important for induction of viperin in our cultures. First, conditioned medium was collected from the supernatant of male or female cells that had been infected with HSV-1 for eight hours at an MOI of 1. This was then centrifuged to remove virus particles and cell debris. The supernatant was then used to treat a fresh monolayer of male or female cells for 24 hours. Following this, RNA extraction, cDNA synthesis and qPCR analysis for viperin expression was performed. No induction of viperin was observed in either male or female cells, suggesting that soluble factors released by HSV-1-infected cells are not sufficient to stimulate viperin expression (Figure4-6).

Next, to rule out a role for type I IFNs in particular, viperin induction by HSV-1 infection was investigated using IFNAR knockout cells ($IFNAR^{-/-}$). Male and female cells derived from three-day-old WT or IFNAR knockout C57BL/6 mice (Section 2.1.10) were infected with HSV-1 KOS strain at an MOI of 0.5 for 24 hours. Total RNA was isolated and reverse transcribed into cDNA for further qPCR analysis. Both in WT and $IFNAR^{-/-}$ cells, female cells consistently induced higher viperin expression than male cells (Figure 4-7). Further, viperin levels were lower in the absence of IFNAR compared to WT cells, but the difference was not statistically significant. The data suggest that type I IFNs play a minor role in viperin induction after HSV-1 infection in primary mouse skin fibroblasts and do not contribute to the difference in viperin upregulation between cells from male and female mice.

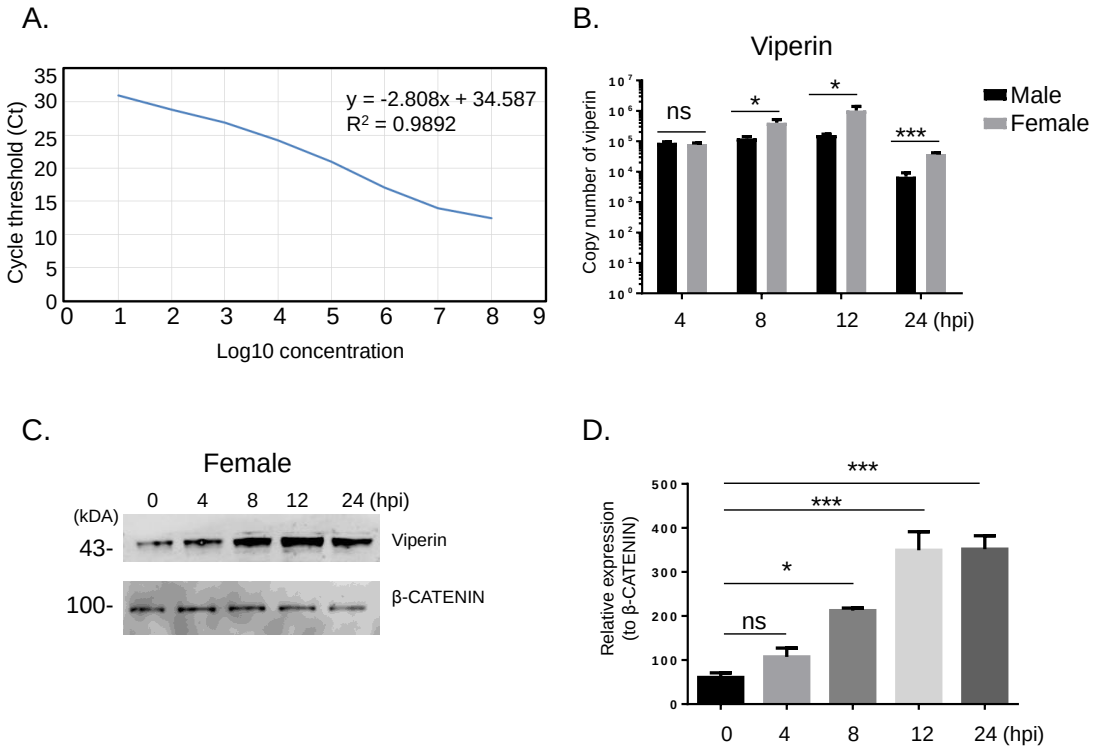

Figure 4-3. Absolute quantification of viperin expression during HSV-1 infection. (A) A standard curve was generated by plotting the mean cycle threshold (Ct) values versus the concentration of p3xFLAG-viperin plasmid from a dilution series (10^0 to 10^9 copies/µl). (B) Male and female cells were infected with HSV-1 pICP47 recombinant virus at an MOI of 0.5. Total RNA was isolated at indicated time points and then subjected to cDNA synthesis and qPCR for determining viperin expression. Ct values were changed into copy numbers by the equation shown in (A). The data were from three individual mice and shown as mean ± SEM. A linear model was used to evaluate significant differences between the two sexes in (B). Female mouse cells from three individual mice were infected with HSV-1 pICP47 recombinant virus at an MOI of 2. Cell lysates were collected at indicated time points and then protein levels of viperin were measured by Western blotting. (C) Representative blots of one culture of female cells. (D) Quantification of each band was performed using ImageJ and the ratio of viperin normalised to β-CATNEIN are shown as mean ± SEM. One-way ANOVA with Tukey's post-tests was used to examine differences between means. * and *** indicate p-value <0.05 and <0.001, respectively. ns, no -significant difference.

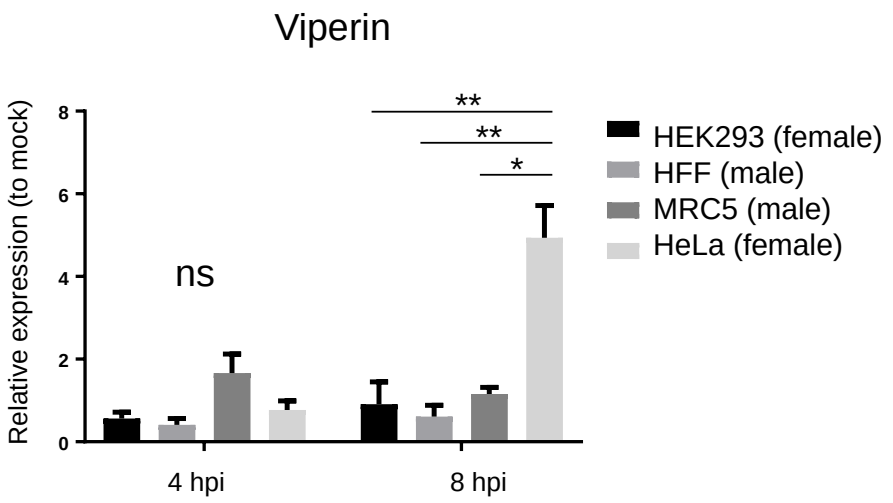

Figure 4-4. Regulation of viperin by HSV-1 infection in different human cell types. Triplicates of HEK293, HFF, MRC5 and HeLa cells were infected with HSV-1 pICP47 recombinant virus at an MOI of 0.5 for four and eight hours. Total RNA was isolated, followed by cDNA synthesis and qPCR analysis for viperin expression. Differential regulation of viperin mRNA was assessed by the $2^{-\Delta\Delta CT}$ method based on expression relative to mock infected cells and normalised to 18S rRNA. The results are shown as mean ± SEM. One-way ANOVA with Tukey's post-tests was used to examine differences between means. * and ** indicate p-value <0.05 and <0.01, respectively. ns, no -significant difference.

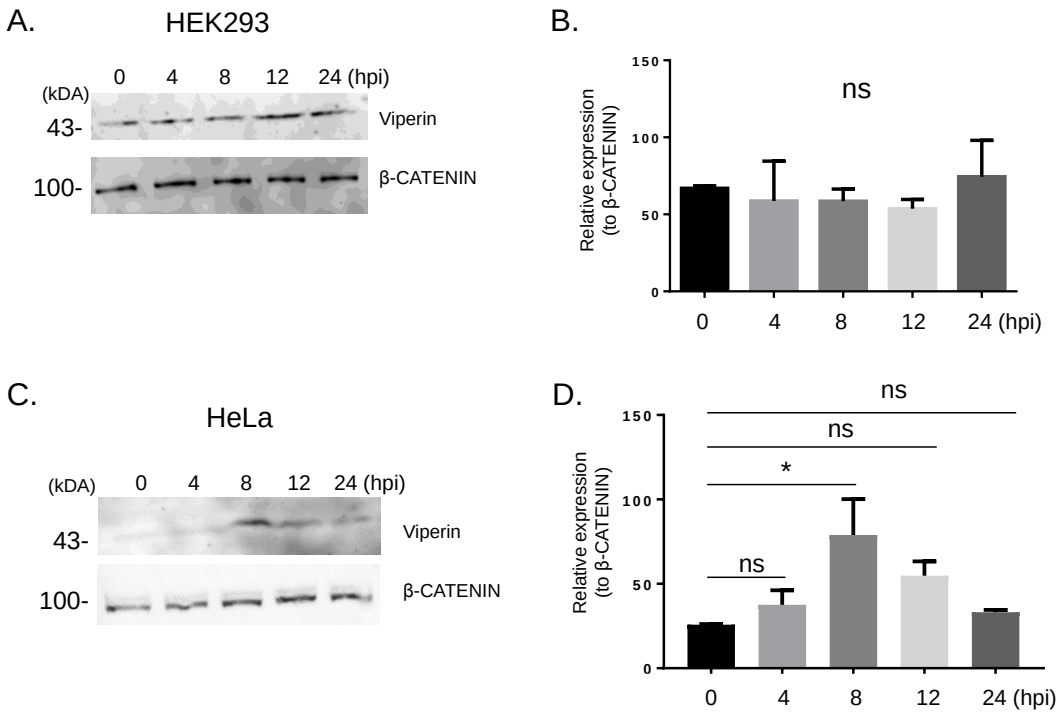

Figure 4-5. Viperin protein expression in HEK293 and HeLa cells during HSV-1 infection. Triplicates of (A-B) HEK293 and (C-D) HeLa cells were infected with HSV-1 pICP47 recombinant virus at an MOI of 2. (A, C) Cell lysates were collected at indicated time points and then protein levels of viperin were measured by Western blotting. (B, D) Quantification of each band was performed using ImageJ and the ratio of viperin normalised to β-CATNEIN are shown as mean ± SEM. One-way ANOVA with Tukey's post-tests was used to examine differences between means. * indicates p-value <0.05. ns, no -significant difference.

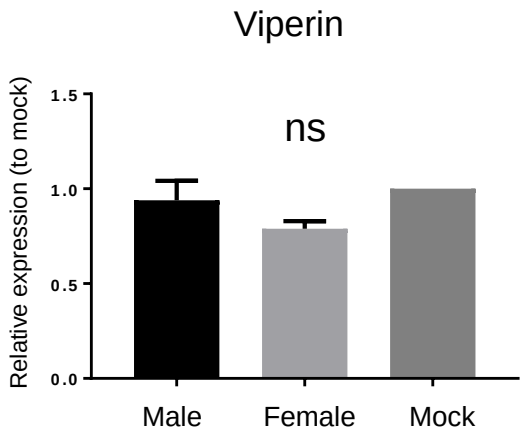

Figure 4-6. Soluble factors are not sufficient to induce viperin expression. Male and female cells from three individual mice were infected with HSV-1 for eight hours at an MOI of 1. Medium from infected cells was collected and centrifuged at 25,000 for 60 minutes. The supernatant of the conditioned medium was applied to treat new batches of male or female cells for 24 hours. Total RNA was extracted from the medium-treated cells and detection of viperin expression was performed using qPCR. Differential regulation was assessed by the $2^{-\Delta\Delta CT}$ method based on expression relative to mock and normalised to 18S rRNA. The results are expressed as mean ± SEM. One-way ANOVA was used to examine differences between means. ns, no significant difference.

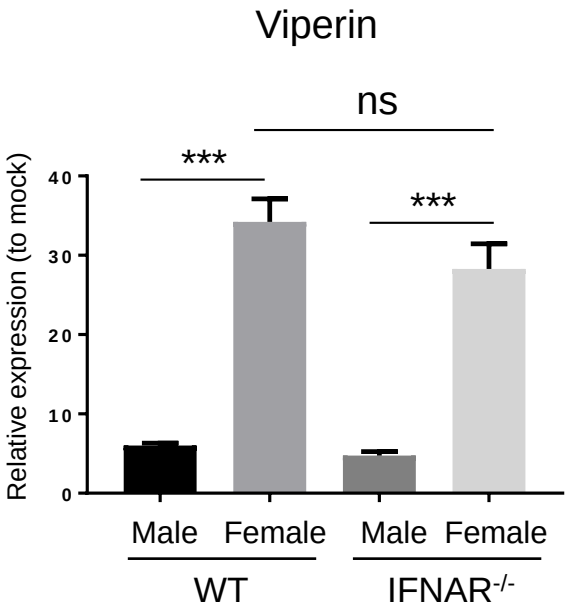

Figure 4-7. Viperin can be induced in an IFN-independent manner. Male or female cells from three individual mice were generated from three-day-old wild-type (WT) or IFNAR knockout (IFNAR$^{-/-}$) C57BL/6 mice. The cells were infected with HSV-1 strain KOS at an MOI of 0.5 for 24 hours. The cell lysate was harvested for qPCR analysis of viperin expression, which was normalised to 18S rRNA and compared with mock. The results are expressed as mean ± SEM. One-way ANOVA with Tukey's post-tests was used to evaluate differences between means. ***p-value <0.001.

4.2.2 Identification of viperin as an anti-HSV-1 protein

4.2.2.1 Ectopic expression of viperin suppresses the replication of HSV-1

The data in Section 4.2.1 showed that viperin is upregulated in male and female mouse cells. Next, we investigated whether viperin has an anti-HSV-1 function. Viperin has been identified to inhibit virus replication in a broad range of viruses, including influenza virus, flaviviruses and human cytomegalovirus (Chin and Cresswell, 2001; Tan et al., 2012; Helbig et al., 2013; Panayiotou et al., 2018). However, whether viperin can play a role to counter HSV-1 infection is not well- explored. First, ectopic expression of viperin was used to examine any inhibitory effect on HSV-1 replication. Male and female cells were transfected with a plasmid expressing full-length mouse viperin (wild-type viperin; WT viperin) for 24 hours. Following this, inoculation of HSV-1 strain KOS was performed at an MOI of 1. Cell lysates were harvested for titration to determine viral titres. Transient expression of WT viperin both in male and in female cells significantly inhibited HSV-1 replication (Figure 4-8A and Figure 4-8B). Figure 4-8C and Figure 4-8D show the transfection efficiency of WT viperin in male and female cells, respectively. To show this in another way, we examined the ability of viperin to reduce fluorescence in cells infected with HSV-1 pICP47 by microscopy. After transfection of male and female cells with WT viperin and infection with HSV-1 pICP47 virus, GFP expression was obviously reduced compared with control transfected cells (Figure 4-9 and Figure 4-9B).

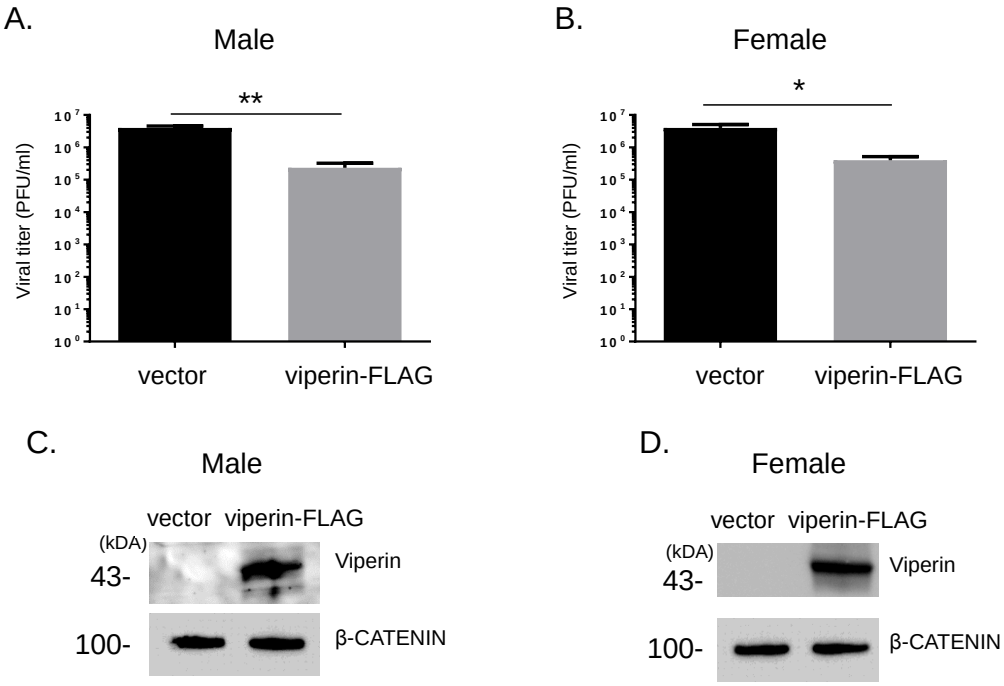

Figure 4-8. Ectopic expression of viperin inhibits HSV-1 replication in male and female cells. (A, C) Male and (B, D) female cells from three individual mice were transfected with 2 μg of p3xFLAG-viperin. After 24 hours, cells were (A-B) infected with HSV-1 strain KOS at an MOI of 1 and viral yields were then measured or (C-D) harvested for determination of transfection efficiency of p3xFLAG-viperin by Western blotting with representative blots shown. (A-B) The viral titres are presented as mean ± SEM and unpaired Student's t-tests were used to evaluate differences between means. * and ** indicate p-value <0.05 and <0.01, respectively.

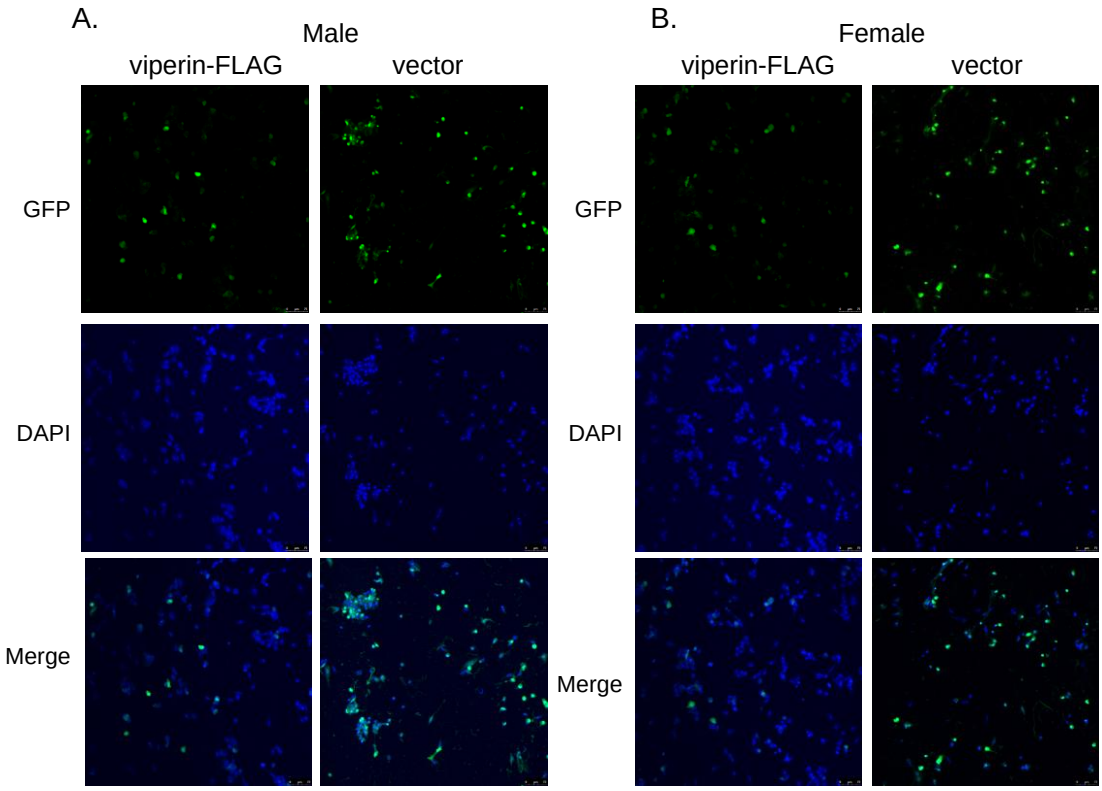

Figure 4-9. Overexpression of viperin suppresses HSV-1 replication in male and female cells. Male and female cells were transfected with 2 μg of p3xFLAG-viperin, followed by inoculation of HSV-1 pICP47 recombinant virus expressing GFP at an MOI of 1. After eight hours of infection, cells were then fixed, stained with DAPI to localise the nucleus and examined by confocal microscopy. The data are representative of three independent experiments.

4.2.2.2 A dose-dependent effect of viperin against HSV-1 infection and the region of viperin involved in the inhibitory effect

Our experiments so far showed that viperin can suppress HSV-1, but this may have been due to overexpression from the plasmid. For this reason, we examined a range of viperin levels. Male or female cells were transfected with 0, 0.5, 1, 2, 4 or 8 µg of WT viperin plasmid and were then infected with HSV-1 strain KOS for 24 hours. Quantitation of viral titres in cell lysates by plaque assays revealed a dose-dependent inhibition of HSV-1 infection in these cultures (Figure 4-10A and Figure 4-10B). A significant inhibitory effect was observed in cells transfected with 1 µg or more of WT viperin plasmid and the effect reached its peak level with transfection of 4 µg plasmid. Expression of the indicated concentration of WT viperin in both male and female cells was confirmed by WB analysis (Figure 4-10C and Figure 4-10D). Collectively, the results described above indicate the anti-HSV-1 activity of viperin is dose-dependent and can be observed when half the amount of plasmid is used than in our original experiments. We note that there will be endogenous viperin expressed and this might mask the effect of small amounts of additional viperin.

Different domains of viperin are responsible for different functions and this protein works in a virus-specific manner (Seo et al., 2011a; Helbig and Beard, 2014). Therefore, the residues or domains required for the antiviral ability against HSV-1 are of interest. To address this issue, a panel of viperin mutants, including deletions of the amphipathic helix domain (N-terminal domain; Δ9-42), the radical SAM domain (central domain; Δ71-182) and the C-terminal domain (Δ218-361), were constructed and transfected into male or female cells. Stability of the viperin variants was determined by WB (Figure 4-11A and Figure 4-11B). After transfection for 24 hours, cells were infected with HSV-1 strain KOS at an MOI of 1 for another 24 hours and viral titres in the cell lysate of each sample were then measured. Transient overexpression of WT viperin in both male and female cells significantly reduced HSV-1 replication by around 10-fold, which was comparable to the effect of Δ71-182 and Δ218-361 groups, indicating that the radical SAM domain and C-terminal domain of viperin are dispensable for the anti-HSV-1 activity (Figure 4-11C and Figure 4-11D). By contrast, removal of the N-terminal domain, which was the smallest deletion examined, abolished the anti-HSV-1 activity of viperin. These data emphasise the importance of the N-terminal domain of viperin in the antiviral activity against HSV-1.

4.2.2.3 Induction of viperin expression cannot fully explain the sex difference in HSV-1 replication between male and female cells

As viperin was upregulated more in female cells (Section 4.2.1) and was confirmed as an anti-HSV-1 effector (Section 4.2.2), we then investigated whether differential regulation of viperin by HSV-1 between the sexes is a key factor that explains the sex difference in HSV-1 replication in our cultures (Figure 3-1). First of all, the necessity of induction of viperin in restricting HSV-1 replication was assessed by transient expression of lentiCRISPR plasmid containing the coding sequence of Cas9 and a gRNA targeting the viperin gene (Sanjana et al., 2014). In brief, male and female cells were transfected with lentiCRISPRmCherry-Rsad2 (Viperin) (Table 2-5) for 24 hours, and then infected with HSV-1 at an MOI of 0.1. HSV-1 infection in the viperin knockout cells resulted in a significant, approximately 10-fold enhancement of infectious HSV-1 release at 24 hpi compared with control cells, in male and female cells (Figure 4-12A and Figure 4-12B). In addition to mouse skin fibroblasts, we also examined whether viperin is necessary for inhibiting HSV-1 replication in HeLa cells, a human cell line that has been found to upregulate viperin during HSV-1 infection (Section 4.2.1.3). HSV-1 yields in the viperin knockdown HeLa cells were significantly higher than in control cells (Figure 4-12C). Knockout efficiency of viperin in male, female and HeLa cells was evaluated by WB after 24 hours transfection and found to be similar (Figure 4-12D, Figure 4-12E and Figure 4-12F). Collectively, these data suggest that viperin was required to restrict HSV-1 replication in male and female mouse cells and in HeLa cells.

Next, male and female cells were transfected with siRNA specific for viperin for 24 hours and the cells were then infected with HSV-1 pICP47 recombinant virus at a very low level (0.0003 PFU/cell). These were the conditions used to reveal a difference in HSV-1 replication between male and female cells. Knockdown of viperin led to significant more replication of HSV-1 both in male and female cells (Figure 4-13A and Figure 4-13B). However, the knockdown had a significantly greater impact on female cells, increasing titres by around 15-fold, compared to approximately 3-fold in male cells (Figure 4-13C and Figure 4-13D). Likewise, the effect of viperin knockdown on spread of virus in cultures was also significantly greater in female than in male cells. Despite this, viral titres (Figure 4-13A) and infected cell populations (Figure 4-13B) remained significant higher in male cells compared with female cells irrespective of viperin knockdown cells. These data show that while the sex difference in HSV-1 infection is narrowed in viperin knockdown cells if is not eliminated. Thus, viperin alone cannot explain the sex difference in HSV-1 replication.

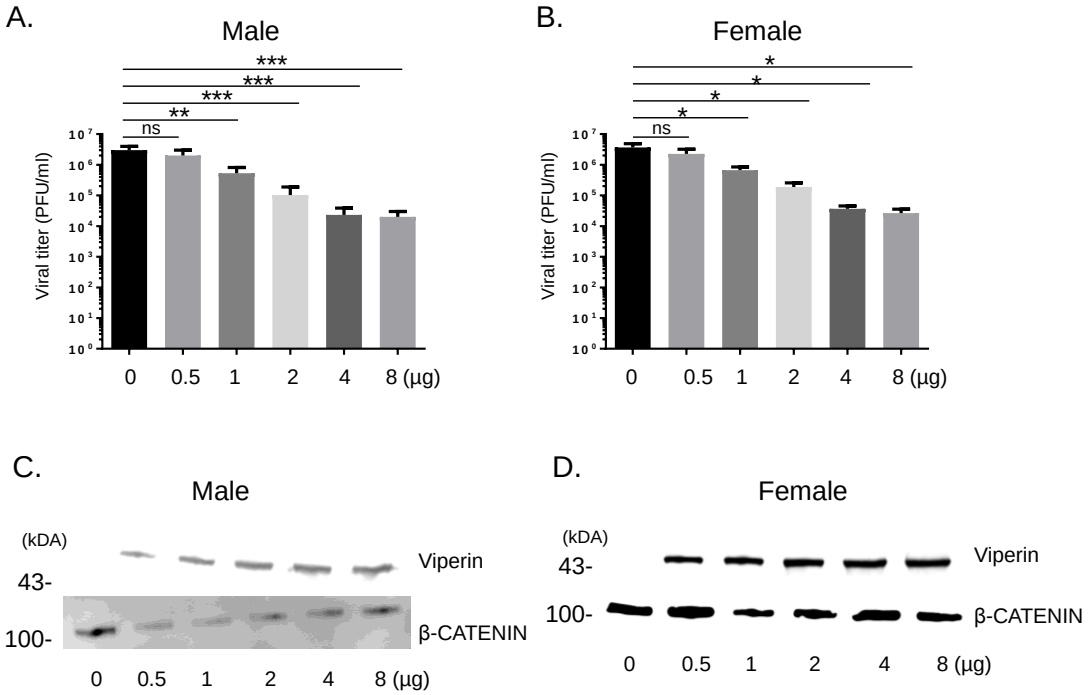

Figure 4-10. A dose-dependent effect of viperin against HSV-1. Male and female cells from three individual mice were transfected with p3xFLAG-viperin at indicated concentrations and were then infected with HSV-1 strain KOS at an MOI of 1. After 24 hours infection, viral titres in (A) male and (B) female cells were determined by plaque assays. Overexpression of viperin at various concentrations in (C) male and (D) female cells was measured by Western blotting. The data are shown as mean ± SEM. One-way ANOVA with Tukey's post-tests was used to evaluate differences between means. *, ** and *** indicate p-value <0.05, <0.01 and <0.001, respectively. ns, no significant difference.

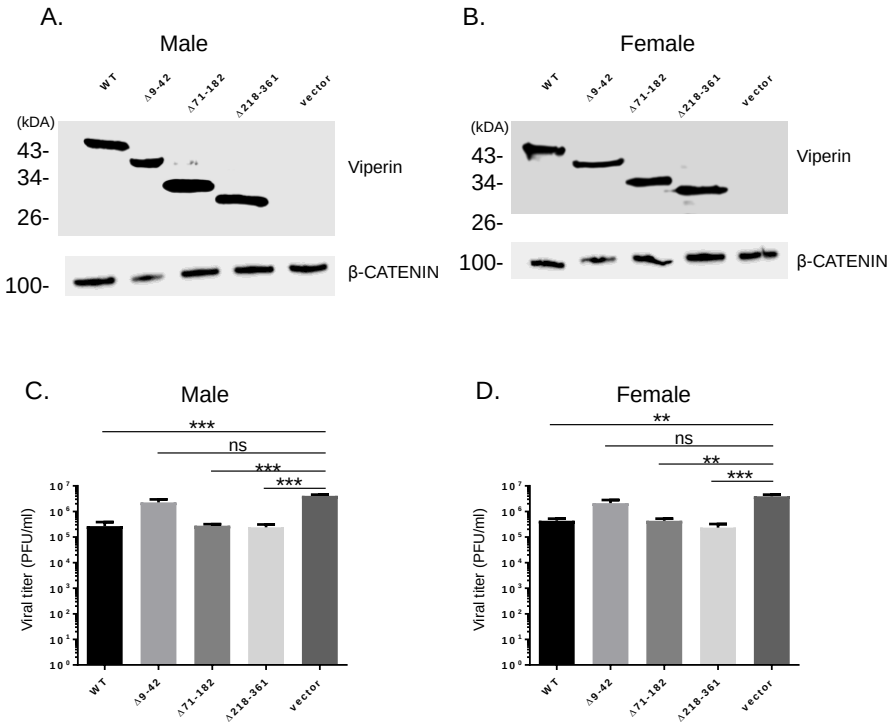

Figure 4-11. The N-terminal domain of viperin is required for the anti-HSV-1 activity of viperin. Plasmids expressing FLAG-tagged full-length viperin (WT) and Δ9-42, Δ71-182 and Δ218-361 mutants of viperin, or empty vectors (2 μg), were transfected into male or female cells from three individual mice. After 24 hours, cells were then (A-B) harvested for Western blotting analysis using anti-FLAG or anti-β-CATNEIN antibodies or (C-D) infected with HSV-1 strain KOS at an MOI of 1. HSV-1 titres in (C) male or (D) female cells were then measured by plaque assays. The results are shown as mean ± SEM and analysed using One-way ANOVA with Tukey's post-tests. ** and *** indicate p-value <0.01 and <0.001, respectively. ns, no significant difference.

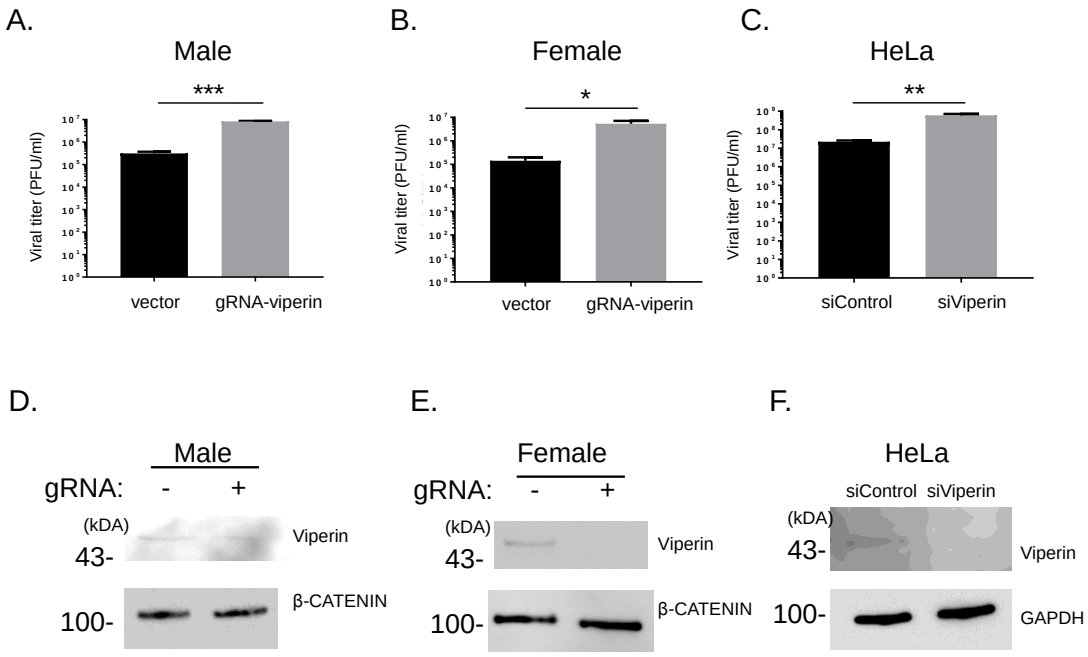

Figure 4-12. Viperin is required to restrict HSV-1 replication. (A-B, D-E) LentiCRISPR vectors (2 μg) or (C, F) 50 nM of siRNA targeting the viperin gene were transfected into male and female cells from three individual mice or HeLa cells. These cells were then infected with HSV-1 strain KOS at MOI of 0.1 for 24 hours. (A-C) Viral titres were determined by plaque assays. (D-F) Knockout or knockdown efficiency prior to infection was evaluated by Western blotting using an anti-viperin antibody. The results are shown as mean ± SEM. Unpaired Student's t-tests were used to test differences between means. * and *** indicate p-value <0.05 and <0.001, respectively.

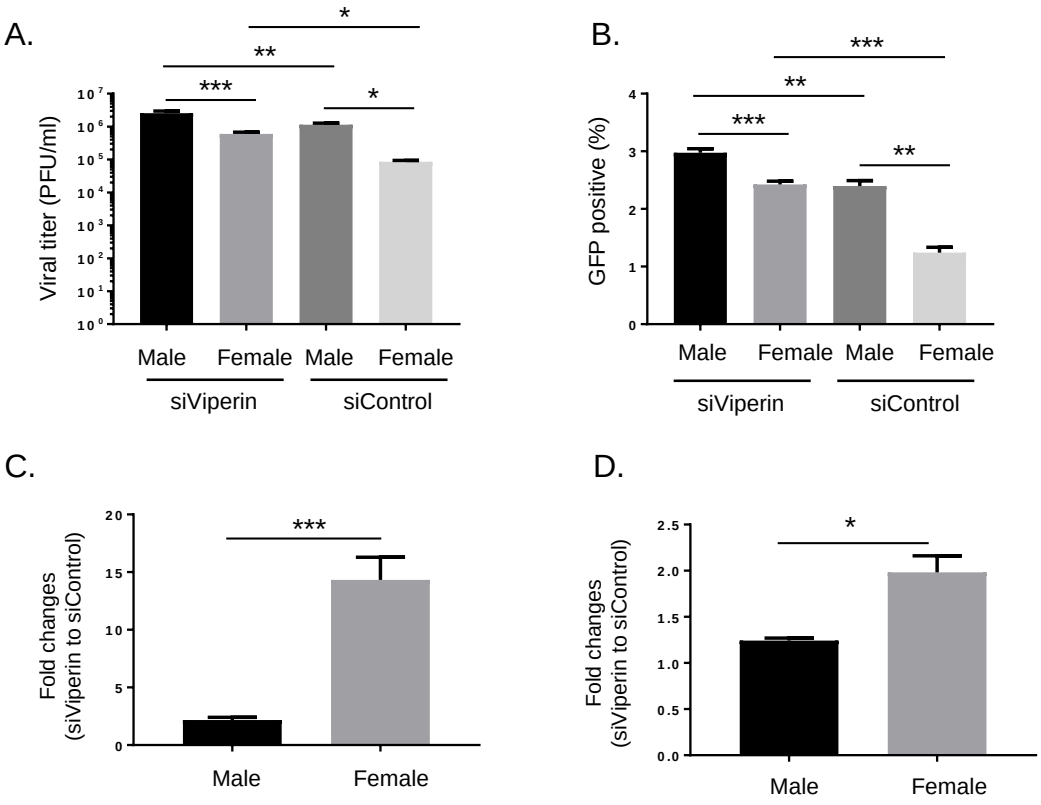

Figure 4-13. Viperin alone cannot explain the replication difference between male and female cells. Male or female cells were transfected with 50 nM of control siRNA (siControl) or siRNA specific for viperin for 24 hours and were then infected with HSV-1 pICP47 recombinant virus at an MOI of 0.0003. (A) Viral titres in the cell lysates from three individual mice were determined by plaque assays and (B) GFP percentage was measured at 72 hpi by flow cytometry. Fold changes of (C) viral titres or (D) GFP percentage between knockdown and control cells were calculated in male and female cells. The results are expressed as mean ± SEM. One-way ANOVA with Tukey's tests and unpaired Student's t-tests were used to test differences between means in (A-B) and (C-D), respectively. *p-value <0.05; **p-value <0.01; ***p-value <0.001.

4.3 Discussion

Viperin has a broad spectrum of antiviral functions and inhibits virus replication by various mechanisms (Duschene and Broderick, 2012; Helbig and Beard, 2014). However, most of the current literature is aimed at RNA viruses, and whether viperin functions efficiently against DNA viruses is controversial (Chin and Cresswell, 2001; Seo et al., 2011b; Shen et al., 2014). Taking HSV-1 as an example, although Shen et al. found that HSV-1 only induces a trace amount of viperin and overexpression of viperin cannot suppress HSV-1 replication, they did not mention which HSV-1 strain they used and the species origin of viperin was not specified (Shen et al., 2014). By contrast, Zheng and Su concluded that HSV-1 can trigger the MAVS-dependent induction of viperin using identical cells (HEK293) and a similar MOI (0.1-0.2). Therefore, the role of viperin against HSV-1 infection is not clear (Zheng and Su, 2017).

At the beginning of this chapter, we confirmed that viperin, a potential downstream effector of nucleic acid-sensing signalling, was upregulated in mouse skin fibroblasts during HSV-1 infection. Female cells induced greater expression of viperin than male cells, as determined by qPCR and WB (Figure 4-1 and Figure 4-2). Therefore, in our culture system we found strong evidence of viperin induction by HSV-1 infection and this varied between the sexes.

We then investigated whether the induction of viperin during HSV-1 requires type I IFNs or not. Viperin has been found to be induced in a variety of cell types by IFN, LPS, dsDNA, dsRNA analogue poly I:C and by infection with a diverse range of viruses. The IFN-dependent and IFN-independent signalling pathways are not mutually exclusive in the mediation of the upregulation of viperin. In IFN-dependent signalling, treatment with specific ligands, such as LPS, poly I:C and multiple RNA viruses, stimulates RLRs, TLR3 and TLR4, leading to activation of IRF3 and IRF7 to produce type I IFN. The interaction between IFN and IFNAR further facilitates a signalling cascade in the formation of ISGF3 to bind to the viperin promoter, and therefore, induce its expression (Severa et al., 2006; Xu et al., 2009). However, viperin can be induced in an IFN-independent manner by some viruses (Boudinot et al., 2000; Severa et al., 2006). The transcriptional factor IRF1 has been found to act as a critical mediator of viperin induction via the overexpression of RLRs. For example, RIG-I and MDA5 directly activate viperin promoter regulation via the TBK1/IRF3 axis through an IFN-independent pathway (Severa et al., 2006; Stirnweiss et al., 2010). Similarly, a recent study has revealed an innate antiviral pathway acting before the IFN pathway in HSV-

infected epithelial surfaces, which indicates that host cells can rapidly employ ISGs as the first line of defence against viruses in an IFN-independent manner at the beginning of virus infection (Iversen et al., 2016). HCMV can induce viperin expression by the binding of the gB component of the viral envelope to an unknown cell surface receptor in human fibroblasts independent of IFNs (Chin and Cresswell, 2001)(Rossini et al., 2012). Additionally, IFN-independent pathways of viperin regulation have been found to be directly regulated by IRF1 or IRF3 in VSV and JEV infection (Chan et al., 2008). Our data add to these host-virus models where upregulation of viperin can be detected during the initial infection in the absence of IFNs and other soluble factors (Figure 4-6 and Figure 4-7).

In addition to the upregulation of viperin in both male and female cells, ectopically expressed mouse viperin was found to inhibit HSV-1 infection and endogenous viperin was shown to restrict HSV-1 replication (Figure 4-8 and Figure 4-12). These findings demonstrate that in our cultures viperin is able to counteract HSV-1 infection unlike those reported by Shen et al (Shen et al., 2014). This allowed us to dissect the roles of the various domains of viperin with respect to their anti-HSV-1 function. Since viperin is composed of different functional domains, mutants with deletions of each individual domain, namely, N-terminal domain (Δ9-42), radical SAM domain (Δ71-182) and C-terminal domain (Δ218-361), were generated and tested for their anti-HSV-1 abilities. An *in vitro* study indicated that viperin inhibits the release of influenza particles from plasma membrane by disrupting the formation of the lipid raft where influenza virus buds (Wang et al., 2007). In addition, viperin also restricts human immunodeficiency virus (HIV) egress from the cell, which is dependent on the SAM domain of viperin (Nasr et al., 2012). Viperin uses different mechanisms to restrict flavivirus infections, including DENV and ZIKV. DENV infection was found to significantly induce viperin expression, thus inhibiting DENV RNA synthesis and infectious virus release (Helbig et al., 2013). This anti-DENV activity was mediated by residues within the C-terminal domain of viperin, but not the N-terminal helix domain and SAM motifs (Helbig et al., 2013). Viperin has been documented to control ZIKV infection by the C-terminal region and viperin knockout mouse embryonic fibroblasts were found to have increased ZIKV infection compared with wild-type cells (Van der Hoek et al., 2017). Furthermore, viperin can directly interact with the non-structural (NS) protein of ZIKV and further reduce the expression of NS3 by inducing proteasome-dependent degradation. ZIKV replication was rescued when NS3 was overexpressed in the presence of viperin, indicating that ZIKV NS3 is the specific target of viperin (Panayiotou et al., 2018). Our data in Figure 4-11 show that the N-terminal domain of viperin is essential for its anti-HSV-1 function. This domain has been found to be

crucial for the association between the endoplasmic reticulum and lipid droplets whereby viperin interacts with HCV non-structural protein 5A to inhibit virus replication (Hinson and Cresswell, 2009a; Hinson and Cresswell, 2009b; Helbig et al., 2011). Likewise, the amphipathic helix in the N terminus of viperin is necessary for its antiviral activity against the release of chikungunya virus (CHIKV) and equine infectious anaemia virus (EIAV) (Teng et al., 2012; Tang et al., 2014). Thus, viperin might use a similar strategy by residing in the endoplasmic reticulum to suppress HSV-1 release, although this hypothesis requires further investigation.

An obvious difference between our experiments and those published previously for HSV-1 was the use of mouse cells. Therefore, it was important to extend our study to human cells. We examined a variety of human cells and found that viperin was significantly induced in HeLa cells compared with other tested human cell types (Figure 4-4). Our conclusion about the role of viperin in HSV-1 infection is that it has cell-type-specific actions and may be important in mouse and human cells. In line with this, viperin levels induced by rabies virus (RABV) seems to be cell-type-specific. Replication of RABV was found to be restricted by both transient overexpression and stable expression of viperin through a TLR4- and IRF3-dependent pathway (Tang et al., 2016). Viperin was apparently upregulated in macrophage RAW264.7 cells, but there was only weak upregulation detected in NA, BHK-21 and BSR cells (Tang et al., 2016). In another cell-type-specific case, Szretter et al. (Szretter et al., 2011) showed that there was an increase in the viral load of West Nile virus (WNV) when primary viperin$^{-/-}$ macrophages and dendritic cells were infected with WNV. However, no significant differences were found in viperin deficient mouse embryonic cortical neurons and fibroblasts, compared with wild-type cells, during WNV infection (Szretter et al., 2011).

In summary, viperin can be an important antiviral function against HSV-1, although it only partially explained the sex difference in HSV-1 replication (Figure 4-13). Several other genes with antiviral functions were also upregulated more in female than in male cells and it is likely that these also play roles in the sex-related difference in HSV-1 replication. It is possible that many or all of these antiviral effectors are under the control of the same pathway, which our RNA-seq data suggests is linked to detection of viral DNA. So, the next obvious direction is to examine this upstream pathway. The upregulation of viperin in female cells provides an ideal marker to probe such a pathway for mechanistic leads. Therefore, viperin will be used as a readout in the next chapter (Chapter 5) to investigate the regulation of the cytosolic DNA-sensing pathway by HSV-1 infection in male and female cells.

Chapter 5. Regulation of the cytosolic sensing pathway by HSV-1 infection in male and female cells.

5.1 Introduction

The detection of viral components involves numerous PRRs, leading to signal transduction, and ultimately, the production of type I IFNs and/or antiviral proteins (Akira and Hemmi, 2003; Reikine et al., 2014). A broad variety of viral products can serve as triggers for the molecular recognition of HSV-1 infection, including viral genomic DNA, virion components and replication intermediates (Chew et al., 2009; Rathinam and Fitzgerald, 2011). The major stimuli for cellular recognition of viral infection are viral nucleic acids, because they can be identified at many cellular locations (Whittaker and Helenius, 1998; Chew et al., 2009). Nucleic acid sensors are classified into different categories based on the structure of the nucleic acid detected and the cellular localisation. These comprise the TLRs, the Nod-like receptors (NLRs), the RLRs and cytosolic DNA sensors such as DAIs and cGAS.

A number of these nucleic acid sensors have been shown to play an important role during HSV-1 infection (Sharma and Fitzgerald, 2011; Paludan and Bowie, 2013). In the endosomal compartment, the recognition of dsDNA containing CpG motifs by TLR9 is required for early type I IFN expression in response to HSV-1 infection through a cell-type-specific mechanism (Hochrein et al., 2004; Rasmussen et al., 2007). In addition, TLR3 exerts protective immunity to HSV-1 in the central nervous system and notably, HSV-1 replicates more efficiently in TLR3-deficient astrocytes and dendritic cells, which have impaired production of type I IFNs (Davey et al., 2010; Lafaille et al., 2012). In the cytoplasmic compartment, recognition of intracellular HSV-1 DNA by cytosolic DNA sensors leads to a TLR-independent mechanism that activates IRFs via TBK1 (Ishii et al., 2006). Among these sensors, DAI, cGAS and IFI16 induce innate antiviral signalling through the STING-TBK1 axis in response to HSV infection (Takaoka et al., 2007; Unterholzner et al., 2010; Sun et al., 2013). Moreover, RLRs such as RIG-I and MDA5 can sense viral dsRNA in the cytoplasm and then elicit antiviral responses (Dixit and Kagan, 2013; Chan and Gack, 2016). HSV-1 viral dsRNAs are detectable in infected cells, which may arise as a result of highly structured single-stranded RNA or from overlapping transcription. Thus, these serve as the ligands for RLRs (Weber et al., 2006). RLRs further transmit signals to the MAVS protein, leading to the activation of IRFs and NF-κB. This process results in upregulation of IFNs, inflammatory cytokines and ISGs (Loo and Gale, 2011; Reikine et al., 2014).

As multiple players in cytosolic nucleic acid-sensing pathways were differentially regulated between mouse cells of the two sexes in the initial stage of HSV-1 infection (Section 3.2.5.4), we focused next on dissecting the mechanism behind these differences. In Chapter 4, we found that viperin cannot fully explain the sex-difference in HSV-1 replication, although it has anti-HSV-1 activity. To understand upstream events that lead to the sex-specific difference, we relied on the use of CRISPR knockout and siRNA knockdown systems to reveal the crucial cellular sensors that regulate the sex difference using viperin as a readout. Lastly, differentially regulated transcription factors on the sex chromosomes were screened for their abilities to regulate the sex-specific differences. A potential candidate was then examined to determine whether it has a critical role in mediating the sex difference in the cytosolic sensing pathway, and the different growth phenotypes of HSV-1 in mouse male and female cells.

5.2 Results

5.2.1 Determining which components from nucleic acids-sensing pathways contribute to differential antiviral responses in male and female cells

5.2.1.1 *cGAS* and *Tbk1* are essential for the sex difference in antiviral responses

The results in Section 3.2.5.5 showed that female cells induced higher expression of several genes in the nucleic acid-sensing pathways than male cells. These genes included nucleic acid sensors such as *cGAS*, *Rig-I* and *Mda5*, and a signalling adaptor, *Tbk1*. In addition to the genes mentioned above, *Tlr3* and *Tlr4*, two key nucleic acid sensors that also signal via TBK1, leading to viperin upregulation, were also investigated (Figure 5-1). These were included as negative controls because we had no evidence for their involvement from our initial RNA-seq experiment.

The lentiCRISPR system was applied to knockout each indicated gene in male and female cells. An empty lentiCRISPR plasmid or one that contained guide a RNA targeting *cGAS*, *Rig-I*, *Mda5*, *Tbk1*, *Tlr3* or *Tlr4* (Table 2-5), was transfected into male and female cells. After 24 hours, cells were infected with HSV-1 strain KOS at an MOI of 0.5 for eight hours. Cell lysates were harvested for RNA isolation, cDNA synthesis and qPCR detection of viperin expression. When *Tlr3* and *Tlr4* were deficient, viperin upregulation due to infection was similar to the appropriate control both in male and in female cells. This suggests that as we expected *Tlr3* and *Tlr4* are not involved in the regulation of viperin due to HSV-1 infection (Figure 5-1). On the contrary, *cGAS*, *Rig-I*, *Mda5* and *Tbk1* were all required for full induction of viperin in male and female

cells. However, of these, *cGAS* and *Tbk1* were the only genes required to maintain the difference in viperin upregulation between male and female cells. When *cGAS* and *Tbk1* were knocked out, viperin upregulation was decreased such that it reached a comparable level in male and female cells (Figure 5-1). Importantly, similar knockout efficiency for each gene was found by comparing cells transfected with lentiCRISPR empty vectors to those having gene-specific guide RNA by using qPCR analysis (Figure 5-2). These data suggest that while *Rig-I* and *Mda5* may play some roles in viperin induction by HSV-1 in our cultures, only *cGAS* and *Tbk1* are necessary for the difference observed between male and female cells.

A.

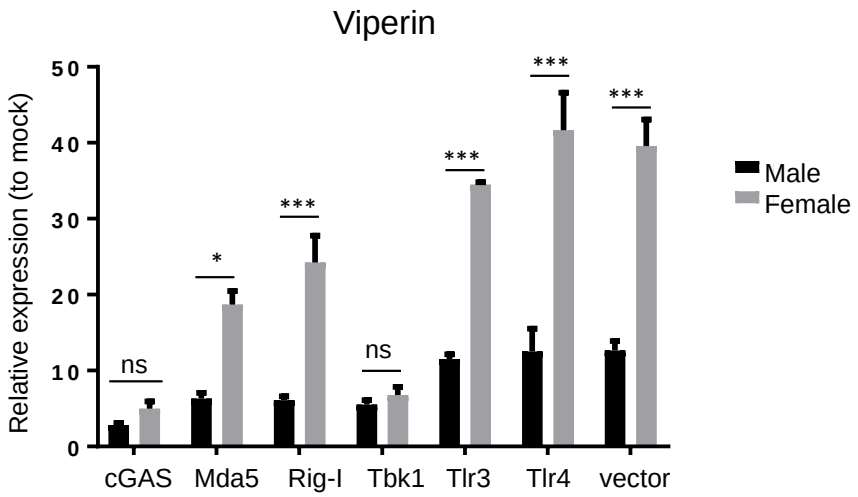

B.

Pairwise comparisons from (A)														
	cGAS	Mda5	Rig-I	Tbk1	Tlr3	Tlr4	vector	cGAS	Mda5	Rig-I	Tbk1	Tlr3	Tlr4	vector
cGAS		ns	ns	ns	**	**	**	ns	**	***	ns	***	***	***
Mda5			ns	ns	ns	ns	*	ns	*	***	ns	***	***	***
Rig-I				ns	ns	*	*	ns	*	***	ns	***	***	***
Tbk1					ns	*	*	ns	*	***	ns	***	***	***
Tlr3						ns	ns	ns	ns	*	ns	***	***	***
Tlr4							ns	ns	ns	*	ns	***	***	***
vector								ns	ns	*	ns	***	***	***
cGAS									**	***	ns	***	***	***
Mda5										ns	*	**	***	***
Rig-I											***	ns	***	**
Tbk1												***	***	***
Tlr3													ns	ns
Tlr4														ns
vector														

Figure 5-1. Nucleic acids sensors contributing to viperin regulation by HSV-1 infection. (A) Male or female cells from three individual mice were transfected with 2 µg of empty lentiCRISPR vectors or those containing gRNA specific for *cGAS*, *Mda5*, *Rig-I*, *Tbk1*, *Tlr3* or *Tlr4*. Cells were then infected with HSV-1 strain KOS at an MOI of 0.5. RNA level of viperin was measured at 8 hpi. Differential regulation was assessed by the $2^{-\Delta\Delta CT}$ method based on expression relative to mock infected cells and normalised to 18S rRNA. The data are expressed as mean ± SEM. (B) One-way ANOVA with Tukey's tests was used to evaluate differences between means. Blue and red indicate male and female cells respectively. *p-value <0.05; ***p-value <0.001. ns, no significant difference.

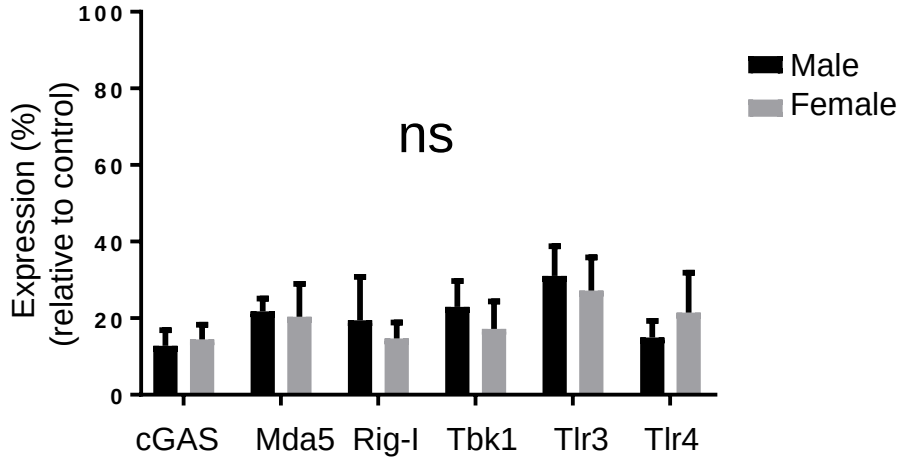

Figure 5-2. Knockout efficiency of lentiCRISPR targeting cGAS, Mda5, Rig-I, Tbk1, Tlr3 or Tlr4. RNA from the experiment in Figure 5-1, cell lysates were harvested for RNA isolation, cDNA synthesis and qPCR reaction using primers for the genes being knocked out. The results are expressed as mean ± SEM. No statistically significant differences (ns) were found by one-way ANOVA with Tukey's tests.

5.2.1.2 Involvement of *Irf1*, *Irf3* and *Irf7* in viperin induction during HSV-1 infection

A growing number of studies have shown that the initial entry of the enveloped virus into cells, especially epithelial cells and fibroblasts, can elicit an antiviral defence that is independent of IFNs and sometimes the most likely sensors like TLRs and RLRs. Nonetheless, this reaction requires the participation of IRFs (Paladino et al., 2006; Noyce et al., 2011). IRF3 is the most obvious transcription factor to examine as many papers have pointed out it is an important factor for regulation of ISGs during virus infection (Hiscott, 2007; Chen et al., 2016). We included IRF1 and IRF7 as well because they are associated with other pathogen sensing pathways (Kimura et al., 1994; Ning et al., 2005). In particular, the roles of IRF1 and IRF3 in viperin regulation were confirmed in an IFN-independent manner during VSV infection (Dixit et al., 2010), but whether HSV-1 triggers a similar mechanism is unknown. To address this issue, the siRNA knockdown method was employed. In brief, male or female cells were transfected with control siRNA (siControl) or siRNA targeting *Irf1*, *Irf3* or *Irf7*, respectively, for 24 hours, followed by inoculation of HSV-1 strain KOS and detection of viperin expression after eight hours infection.

In the absence of *Irf1*, *Irf3* or *Irf7*, the upregulation of viperin relative to mock was significantly reduced both in male and in female cells (Figure 5-3). When *Irf1* was knocked down, upregulation of viperin was almost nil for cells of both sex. This makes it difficult to be sure whether this is a critical determinant of the male and female difference, or simply required for any signalling through the relevant pathway. *Irf3* and *Irf7* also play roles in the viperin regulation by HSV-1. However, knockdown of these two genes did not completely eliminate the sex difference in viperin level (Figure 5-3). Moreover, knockdown of *Irf7* increased the difference in viperin upregulation by HSV-1 infection between male and female cells. Knockdown efficiency of each siRNA was demonstrated to be equal by qPCR and is shown in Figure 5-4. The results suggest that *Irf3* and *Irf7* are involved in this pathway, but *Irf1* was the most critical factor as knockdown of *Irf1* ablated all viperin expression.

5.2.1.3 *Irf1* transduces signals upstream of *cGAS*, but not *Tbk1*, *Irf3* and *Irf7*, during initial HSV-1 infection

As *Irf1* had such an important role in response to HSV-1 infection (Figure 5-3), we speculated that *Irf1* is required upstream of other sensors and IRFs at the beginning of

HSV-1 infection. To test this hypothesis and keep the focus on the canonical pathway, two candidates in the nucleic acids-sensing pathway, *cGAS* and *Tbk1*, which have been shown to participate in viperin regulation by HSV-1 infection and are required for the difference between male and female cells, and two IRFs, *Irf3* and *Irf7*, were examined in this experiment. Male and female cells were transfected with siRNA to knock down the expression of *Irf1*. After 24 hours, the cells were infected with HSV-1 at an MOI of 0.5 for eight hours. Gene expression of *cGAS*, *Tbk1*, *Irf3* and *Irf7* was then analysed by qPCR in *Irf1* knockdown and siControl cells.

When *Irf1* was reduced in male and in female cells, the upregulation of *Tbk1*, *Irf3* and *Irf7* did not differ statistically from siControl cells (Figure 5-5). However, *cGAS* upregulation was significantly decreased in the *Irf1* knockdown cells, regardless of sex. Moreover, the difference in the *cGAS* upregulation between the two sexes disappeared (Figure 5-5). These data suggest that *Irf1* is required for *cGAS* upregulation by HSV-1 infection and therefore, for the stronger response by female cells. This notion was further investigated by detecting protein expression of *cGAS* via WB in *Irf1*, *Irf3* or *Irf7* deficient cells. Male and female cells were transfected with siRNA to knockdown *Irf1*, *Irf3* and *Irf7* for 24 hours. Cells were then infected with HSV-1 strain KOS. The results indicated that the cGAS protein level was reduced to a comparable level between male and female cells when *Irf1* was knocked down (Figure 5-6). This is consistent with the regulation of mRNA shown in Figure 5-5. There was no significant decrease in cGAS protein in the *Irf3* or *Irf7* knockdown cells and the sex difference in cGAS expression remained in these cultures (Figure 5-6).

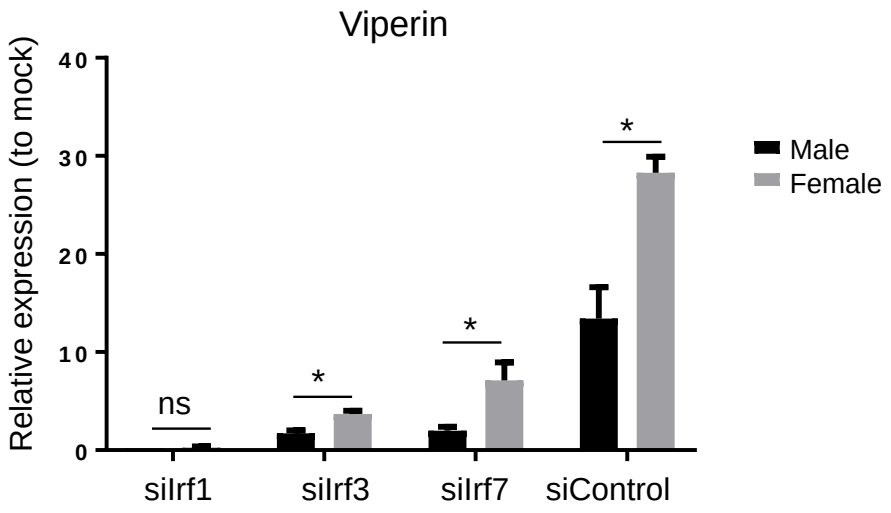

Figure 5-3. Involvement of IRFs in the regulation of viperin by HSV-1 infection. Male or female cells from three individual mice were transfected with 50 nM of control siRNA (siControl) or siRNA specific for *Irf1*, *Irf3* or *Irf7* for 24 hours. Cells were then infected with HSV-1 strain KOS at an MOI of 0.5. Total RNA was isolated at 8 hpi and then viperin expression was determined by qPCR. Differential regulation was assessed by the $2^{-\Delta\Delta CT}$ method based on expression relative to mock and normalised to 18S rRNA. The results are expressed as mean ± SEM. One-way ANOVA with Tukey's tests was used to evaluate differences between means. *p-value <0.05. ns, no significant difference.

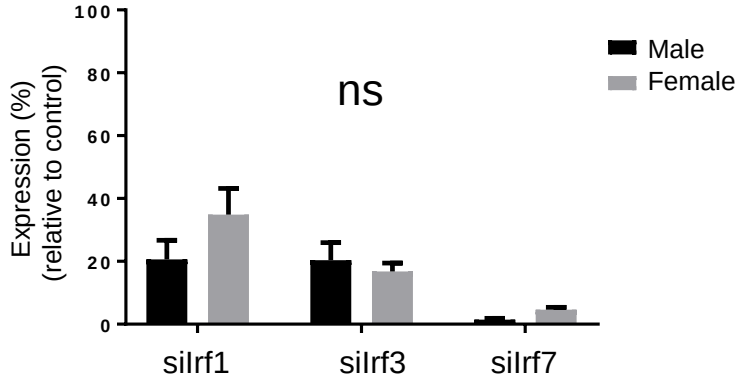

Figure 5-4. Knockdown efficiency of siRNA targeting Irf1, Irf3 and Irf7. RNA from the experiment in Figure 5-3 were used to determine the level of knockdown by siRNA, using qPCR with primers for the relevant genes. The results are shown relative to the control siRNA treatment and expressed as mean ± SEM. No significant difference (ns) were seen between any pair of male and female cells by one-way ANOVA with Tukey's tests.

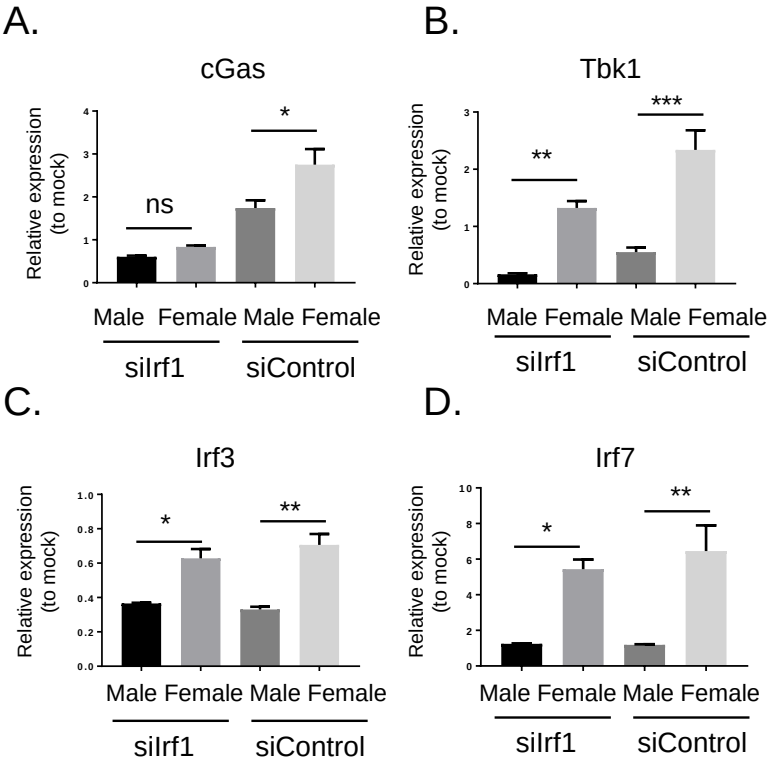

Figure 5-5. Irf1 regulates cGAS upregulation during HSV-1 infection. Male or female cells from three individual mice were transfected with 50 nM of siRNA specific for *Irf1* or control siRNA, and were then infected with HSV-1 strain KOS at an MOI of 0.5. RNA expression of (A) *cGAS*, (B) *Tbk1*, (C) *Irf3* and (D) *Irf7* was measured at 24 hpi. The data are normalised to 18S rRNA and are presented as the relative fold change over normalised RNA from mock. The data are expressed as mean ± SEM. One-way ANOVA with Tukey's tests was used to evaluate differences between means. Asterisks indicate values that are statistically significant (*p-value <0.05; **p-value <0.01; ***p-value <0.001). ns, no significant difference.

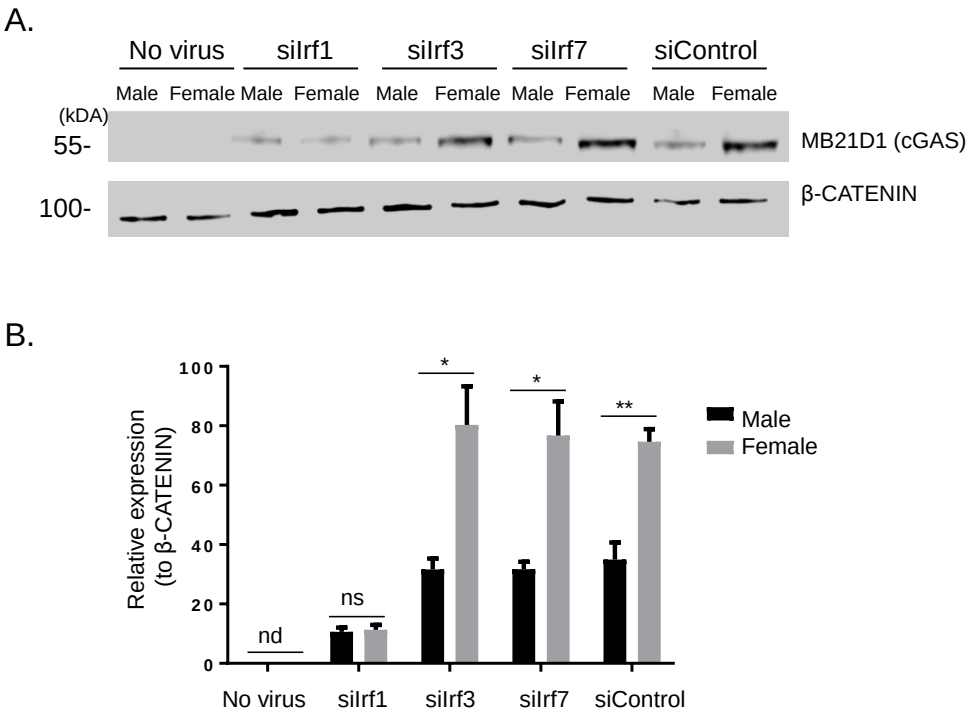

Figure 5-6. Irf1 is important for cGAS protein expression during HSV-1 infection. Male or female cells from three individual mice were transfected with 50 nM of control siRNA (siControl) or siRNA specific for *Irf1*, *Irf3* or *Irf7* and were then infected with HSV-1 strain KOS at an MOI of 0.5. Cell lysates were harvested at 24 hpi. Protein levels of cGAS were examined by Western blotting using an anti-cGAS antibody. (A) Representative WB images. (B) Each band was quantified by densitometry and normalised to β-CATENIN. The results are expressed as mean ± SEM. A linear model was employed to determine differences between the sexes. Asterisks indicate values that are statistically significant (*p-value <0.05; **p-value <0.01). ns, no statistically significant difference; nd, not detectable.

5.2.2 Regulation of viperin expression by transcription factors on the sex chromosomes

5.2.2.1 Potential transcription factors to mediate viperin expression on the sex chromosomes

Irf1 explains the cGAS difference in Section 5.2.1.3, but there is no obvious link from *Irf1* or any of the other genes of interest to the sex chromosomes or other possible explaination of the sex-specific difference. In order to understand the mechanism underlying the difference in the nucleic acid-sensing pathway between male and female cells, we turned our attention to transcription factors on the sex chromosomes. Differential expression of immune regulated genes on sex chromosomes have previously been suggested to lead to differences in immune responses between males and females, so we reasoned that this might extend to transcriptional regulators. Firstly, transcripts from the X or Y chromosome that were differentially regulated between mock and 4 or 8 hpi, in male or female cells, were collected. A further filtering parameter was set to acquire those predicted to have the ability to interact with enhancer binding sites in the differentially regulated genes in the cytosolic sensing pathway, such as *cGAS*, *Mda5*, *Rig-I*, *Tbk1*, *Irf1* or *Irf7*, based on the GeneCards® database (http://www.genecards.org/). Eight transcripts from seven genes, including *Taf1*, *Zbtb33*, *Phf8*, *Hdac8*, *Elk1* and *Hcfc1*, on the X chromosome met the filtering criteria (Figure 5-7), but none were found on the Y chromosome (data not shown). Fold changes between mock and 4 or 8 hpi of these transcripts in male and female cells, were plotted in a heatmap (Figure 5-7). Detailed description of these regulators is provided in Table 5-1, including gene symbol, full gene name and list of genes for which each one has binding sites upstream. Most of the genes were regulated similarly between male and female cells. For instance, *Taf1*, *Phf8* and *Hcfc1* were upregulated at both 4 and 8 hpi in male and female cells (Figure 5-7). *Hdac5* was downregulated at the two time points and *Elk1* was downregulated at 8 hpi. Interestingly, two different transcripts of *Zbtb33* were both decreased during HSV-1 infection in female cells, but were slightly increased at 4 hpi (NM_020256) or were unchanged (NM_007079513) in male cells (Figure 5-7).

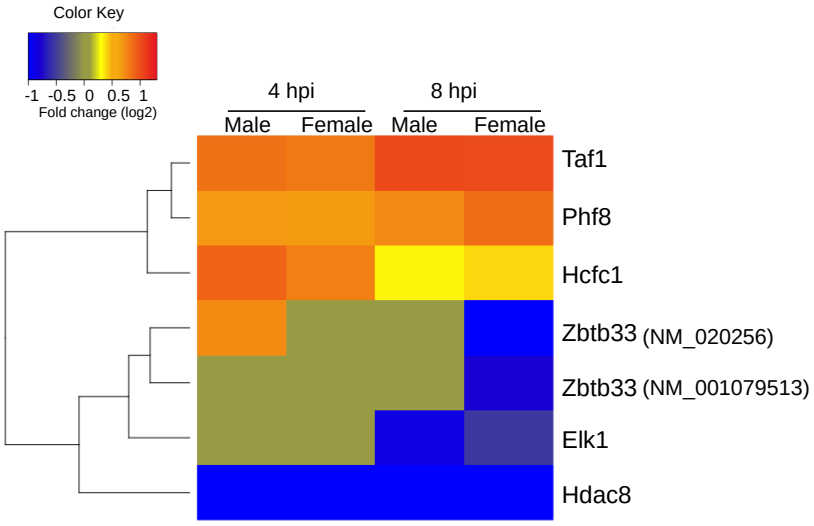

Figure 5-7. Transcription regulators on the X chromosome with binding sites upstream of genes of interest. (A) The heatmap shows $\log_2$ fold changes of transcription factors on the X chromosome that have a predicted ability to bind within the enhancer regions in *cGAS*, *Rig-I*, *Mda5*, *Tbk1*, *Irf1* or *Irf7* and that were also differentially regulated post HSV-1 infection.

Table 5-1. Details of the differential regulated transcriptional regulators on the X chromosome.

Gene symbol	Gene name	Enhancer binding sites
Taf1	TATA-box binding protein associated factor 1	*Ifih1* (*Mda5*), *Ddx58* (*Rigi*), *Irf1*, *Irf7*, *Mb21d1* (*cGAS*), *Tbk1*
Zbtb33	Zinc finger and BTB domain containing 33	*Ifih1* (*Mda5*), *Ddx58* (*Rigi*), *Tbk1*
Phf8	PHD finger protein 8	*Ddx58* (*Rigi*), *Irf1*, *Irf7*, *Tbk1*
Hdac8	Histone deacetylase 8	*Irf1*,*Irf7*, *Tbk1*
Elk1	Ets family of transcription factors	*Ddx58* (*Rigi*), *Irf1*,*Tbk1*
Hcfc1	Host cell factor C1	*Ddx58* (*Rigi*),*Tbk1*

5.2.2.2 Transcription factors on the X chromosome affect viperin regulation during HSV-1 infection

Next, we investigated whether these differentially regulated transcription factors on the X chromosome might regulate the cGAS pathway in HSV-1 infection. To do this, siRNA targeting *Taf1*, *Phf8*, *Hdac8*, *Elk1*, *Zbtb33* or *Hcfc1* were used to knock down gene expression in male and female cells. In brief, siRNA were transfected into male or female cells for 24 hours, followed by inoculation of the HSV-1 virus at an MOI of 0.5. Viperin expression was then detected from the total RNA in the infected cells by qPCR and the change in level compared to mock cells was determined.

When *Taf1*, *Hdac8* or *Elk1* was deficient in male and female cells, viperin regulation by HSV-1 infection did not differ greatly for male or female cells (Figure 5-8). Although viperin level was reduced in all cells with *Phf8* knocked down, the difference between the two sexes remained. On the contrary, viperin significantly increased both in male and in female cells when *Hcfc1* was depleted, as compared to siControl cells, but this increased the difference between the sexes (Figure 5-8). Most notably, viperin upregulation was detected in male and female cells deficient in *Zbtb33*, leading to a comparable upregulation of viperin between the sexes (Figure 5-8). The knockdown efficiency of each siRNA was evaluated by qPCR and is shown in Figure 5-9. Because two transcripts of *Zbtb33* were differentially regulated between the two sexes during HSV-1 infection (Figure 5-7), the lentiCRISPR technique described in Section 5.2.1.1 was done to knock out *Zbtb33* in male and female cells, followed by inoculation with HSV-1. When *Zbtb33* was knocked out, viperin regulation by HSV-1 infection was at a comparable level between male and female cells (Figure 5-10), consistent with the data in Figure 5-8A. Together, these results indicate that *Zbtb33* is a key gene that is required for the sex difference in viperin induction during HSV-1 infection.

5.2.2.3 *Zbtb33* negatively regulates the cytosolic sensing pathway via *Tbk1* in HSV-1 infection

Given that *Zbtb33* was negatively correlated with viperin upregulation and removed the sex difference in HSV-1 infection (Section 5.2.1.1), it is of interest to understand where *Zbtb33* intervenes in the cytosolic DNA-sensing pathway. The obvious targets are those have been shown to be required for the sex difference in viperin regulation by HSV-1, including, *cGAS*, *Tbk1* and *Irf1* (Section 5.2.1.1 and Section 5.2.1.2). To investigate this, *Zbtb33* knockout cells were prepared as described in Section 5.2.2.2 and were

infected with HSV-1 strain KOS for eight hours. The regulation by infection of candidate genes that may be modified by *Zbtb33*, including *cGAS, Tbk1*, *Irf1*, *Irf3* and *Irf7*, was determined by qPCR. When *Zbtb33* was knocked out, levels of regulation by infection of *cGAS, Irf1*, *Irf3* and *Irf7* were similar between knockout and control cells in both male and in female cells (Figure 5-11). Moreover, the sex difference in regulation of these genes was maintained. By contrast, *Tbk1* was induced to a greater degree in the *Zbtb33*-deficient cells than control cells and in these cells there was no difference between the sexes in *Tbk1* regulation by HSV-1 infection.

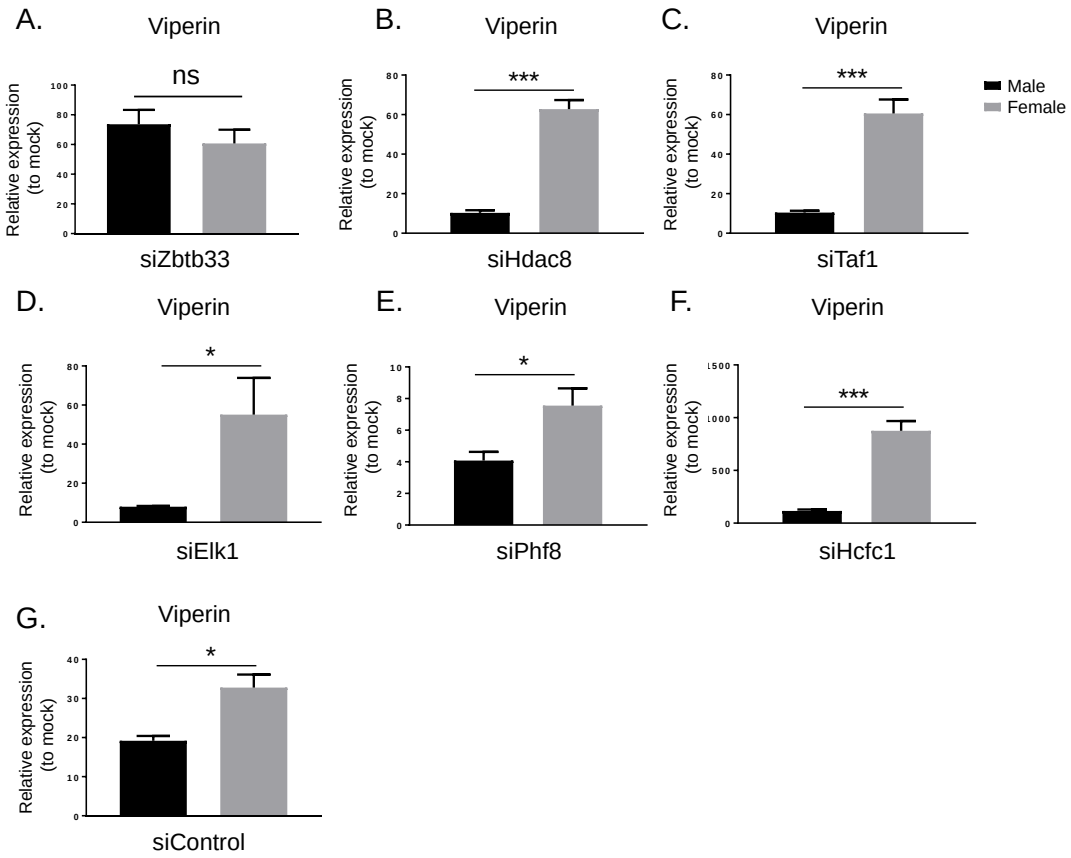

Figure 5-8. Effect of Zbtb33, Hdac8, Taf1, Elk1, Phf8, and Hcfc1 on viperin regulation in HSV-1 infection. Male or female cells from three individual mice were transfected with 50 nM of siRNA specific for (A) *Zbtb33*, (B) *Hdac8*, (C) *Taf1* (D) *Elk1*, (E) *Phf8*, (F) *Hcfc1*, or (G) control siRNA (siControl). Cells were then inoculated with HSV-1 strain KOS at an MOI of 0.5. After 24 hours of infection, total RNA was extracted and viperin expression was measured by qPCR. Differential regulation was assessed by the $2^{-\Delta\Delta CT}$ method based on expression relative mock and normalised to 18S rRNA. The data are presented as mean ± SEM. Unpaired Student's t-tests were applied to examine differences between means. Asterisks indicate values that are statistically significant (*p-value <0.05; ***p-value <0.001). ns, no statistically significant difference

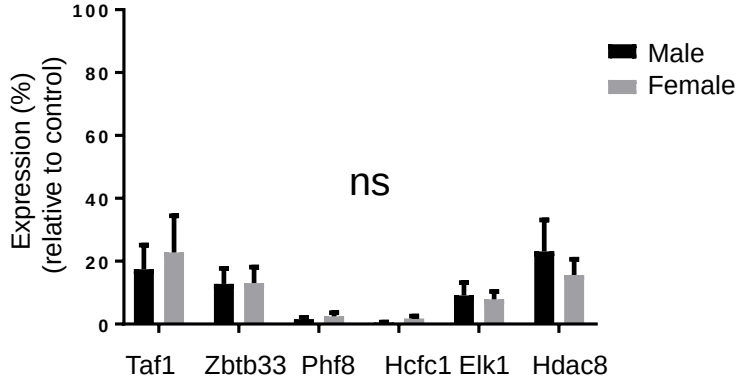

Figure 5-9. Knockdown efficiency of siRNA specific for *Taf1*, *Zbtb33*, *Phf8*, *Hcfc1*, *Elk1* or *Hdac8* in male and female cells. RNA from the experiment in Figure 5-8 were used to evaluate the level of knockdown by siRNA, using qPCR with primers for the relevant genes. The results are shown relative to the control siRNA treatment and expressed as mean ± SEM. No significant difference (ns) were seen between any pair of male and female cells by one-way ANOVA with Tukey's tests.

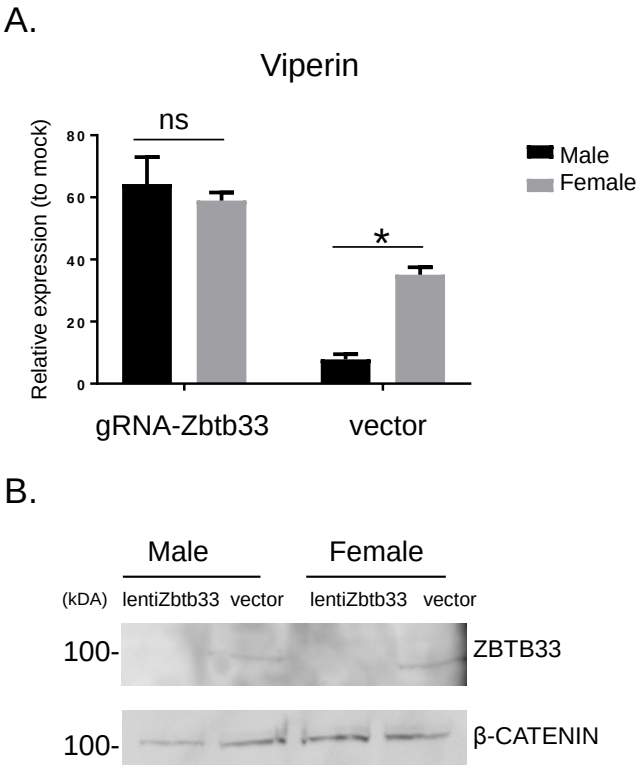

Figure 5-10. *Zbtb33* negatively regulates viperin expression during HSV-1 infection. (A) Male or female cells from three individual mice were transfected with 2 μg of empty lentiCRISPR vectors or those containing gRNA targeting *Zbtb33*. These cells were infected with HSV-1 strain KOS at an MOI of 0.5 or (B) were harvested for Western blotting analysis using indicated antibodies. Viperin expression was measured by qPCR at 8 hpi. Differential regulation was assessed by the $2^{-\Delta\Delta CT}$ method based on expression relative to mock and normalised to 18S rRNA. The data are presented as mean ± SEM. One-way ANOVA with Tukey's tests was used to evaluate differences between means. An asterisk indicates values that are statistically significant (*p-value <0.05). ns, no significant difference. Graphs are representative of three independent experiments.

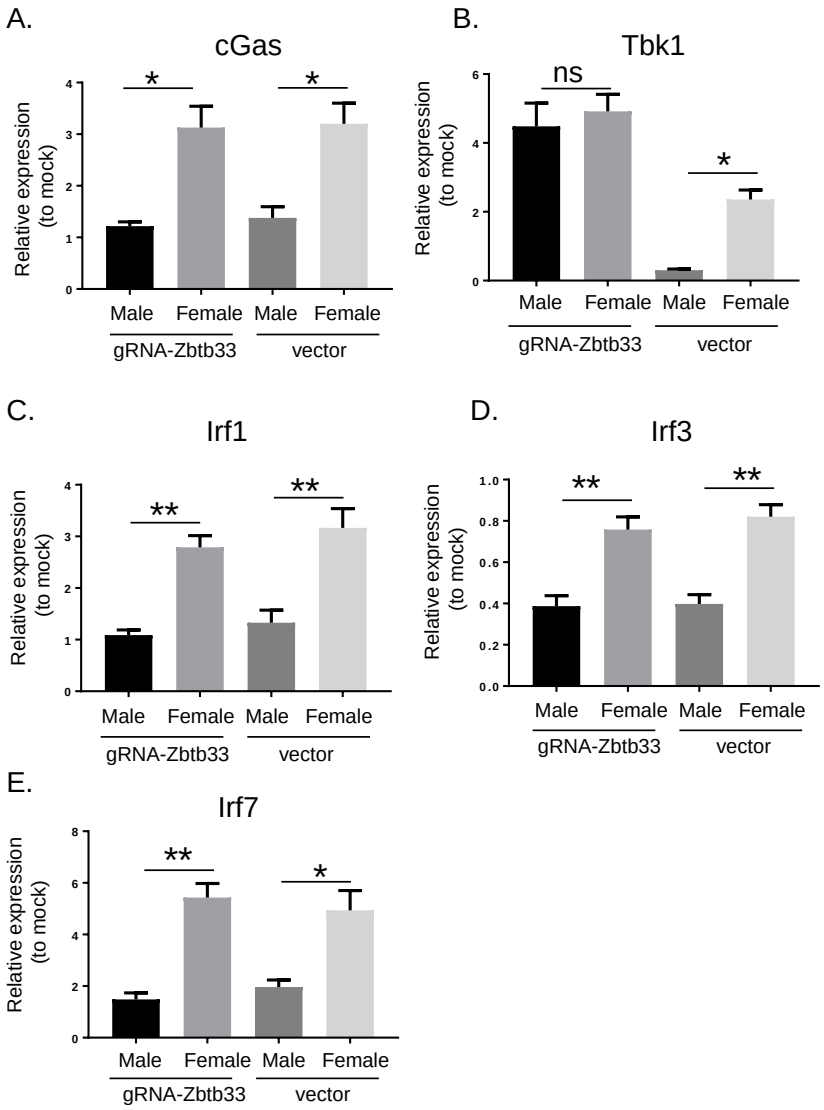

Figure 5-11. *Zbtb33* negatively regulates Tbk1 induction in HSV-1 infection. Male or female cells from three individual mice were transfected with 2 μg of empty lentiCRISPR vectors or those containing gRNA targeting *Zbtb33*, followed by inoculation of HSV-1 strain KOS at an MOI of 0.5. At 8 hpi, (A) *cGAS*, (B) *Tbk1*, (C) *Irf1*, (D) *Irf3* and (E) Irf7 regulation by infection was measured by qPCR. Differential regulation was assessed by the $2^{-\Delta\Delta CT}$ method based on expression relative to mock and normalised to 18S rRNA. The data are expressed as mean ± SEM. One-way ANOVA with Tukey's tests was used to examine differences between means. Asterisks indicate values that are statistically significant (*p-value <0.05 and ** p-value <0.01). ns, no significant difference.

In Section 3.2.5.6, we found that mRNA regulation by HSV-1 infection and protein levels of *Tbk1* were higher in female cells than in male cells. Further, *Zbtb33* seems likely to regulate viperin expression by inhibiting *Tbk1* expression (Section 5.2.2.3), highlighting the importance of *Tbk1* in the observed sex difference. However, a more accurate indication of TBK1 activity is its phosphorylation status. Therefore, the phosphorylated form of TBK1 was detected by WB analysis using anti-phosphorylated TBK1 antibody. In Figure 5-12A, more active TBK1 was produced in female cells compared to male cells, likely due to the higher TBK1 expression in female cells. When *Zbtb33* was knocked out, both the basal and active form of TBK1 were significantly elevated and reached a similar level in cells of both sex, which correlated with viperin protein expression (Figure 5-12). Quantification of each band was performed by densitometry and expression level of basal and activated TBK1 and viperin was normalised to β-Catenin (Figure 5-12B). Collectively, the data suggest that *Zbtb33* is a negative regulator of viperin through suppressing *Tbk1* expression, and therefore, also limiting amounts of active TBK1.

5.2.2.3 *Zbtb33* is a proviral factor during HSV-1 infection leading to male and female differences in replication

Lastly, we wanted to test whether the key role of *Zbtb33* shown above extended to control of HSV-1 replication. To do this the siRNA and lentiCRISPR technique was employed to knock down or knock out *Zbtb33* in male and female cells, which were then infected with HSV-1 at an MOI of 1 for 24 hours. HSV-1 titres were significantly lower in the *Zbtb33* knockdown and knockout cells than the control (Figure 5-13A and Figure 5-13B). This experiment was then repeated using a very low MOI in the *Zbtb33* knockout male and female cells (Figure 5-13C and Figure 5-13D). The difference in virus titre and fraction of infected cells seen between male and female cells in the control vector cultures was not found in the *Zbtb33* knockout cells. Further, in line with the experiment in Figure 5-13A, both measures of infection were reduced in the *Zbtb33* knockout cells. These data, along with those from the immediately previous sections, suggest that *Zbtb33* is an important negative regulator of *Tbk1* expression and thus, antiviral effectors, such as viperin. As a result, *Zbtb33* is an important factor in the sex-specific difference in HSV-1 replication we observed at the beginning of Chapter 3.

A.

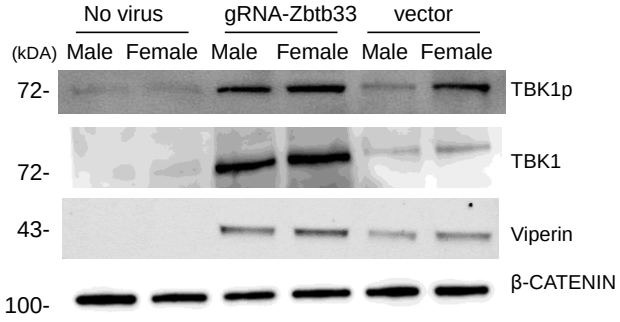

B.

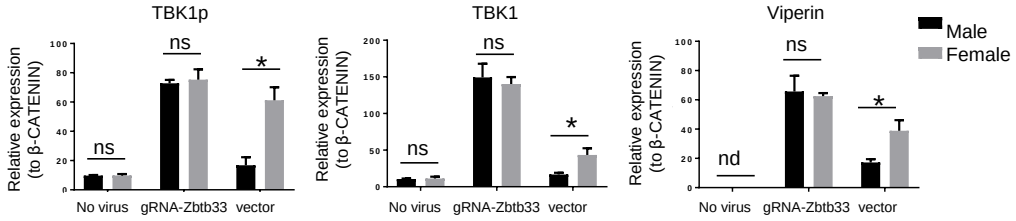

Figure 5-12. *Zbtb33* negatively regulates the cytosolic sensing pathway via Tbk1 in HSV-1 infection. Male or female cells from three individual mice were transfected with 2 μg of empty lentiCRISPR vectors or those containing gRNA targeting *Zbtb33*, followed by inoculation of HSV-1 strain KOS at an MOI of 1. At 8 hpi, cell lysates were collected for Western blotting analysis using anti-TBK1p, anti-TBK1, anti-viperin and anti-β-CATENIN antibodies. (A) Bolts shown are representative of three independent experiments. (B) Quantification of blots by densitometry using ImageJ. The intensity of bands was normalised to β-CATENIN. The results are expressed as mean ± SEM. A linear model was employed to determine the significance of differences between the two sexes. Asterisks indicate values that are statistically significant (*p-value <0.05). ns, not statistically significant; nd, not detectable.

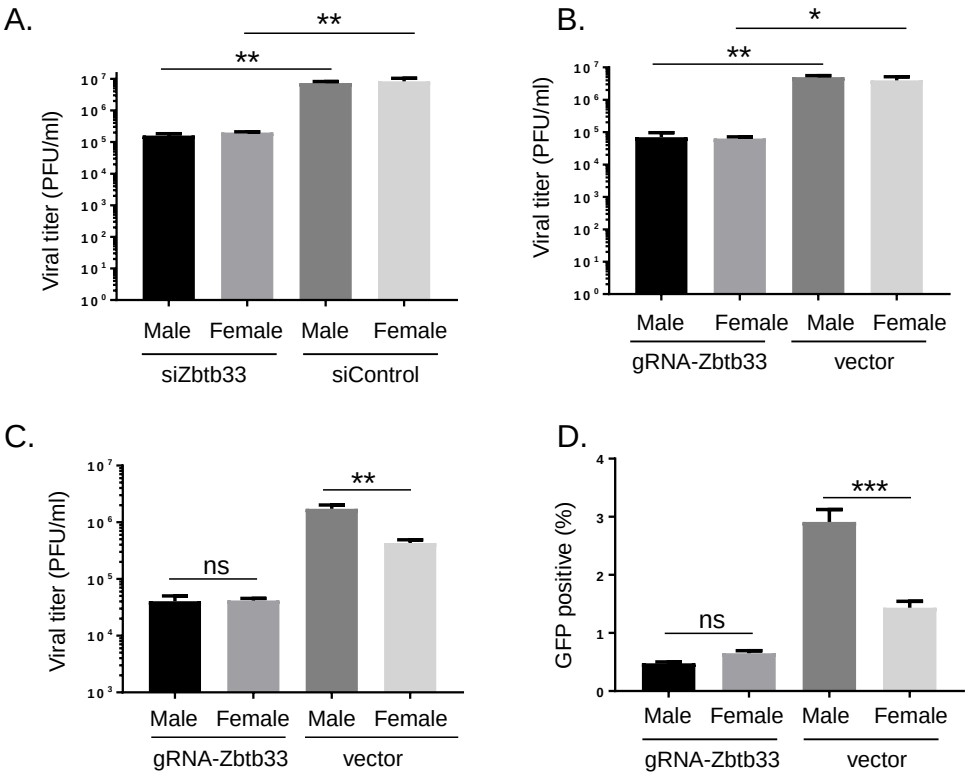

Figure 5-13. *Zbtb33* is a proviral factor in HSV-1 infection that leads to male and female differences in replication. Male or female cells from three individual mice were transfected with (A) 50 nM of control siRNA (siControl) or siRNA specific for *Zbtb33* or (B-C) 2 μg of empty lentiCRISPR vectors or those with gRNA targeting *Zbtb33*, followed by inoculation of (A-B) HSV-1 strain KOS at an MOI of 1 for 24 hours or (C-D) HSV-1 pICP47 at an MOI of 0.0001 for 72 hours. (A-C) Viral titres or (D) GFP percentage were then determined by plaque assays or flow cytometry respectively. The results are expressed as mean ± SEM. One-way ANOVAs with Tukey's post-tests was applied to examine differences between means. Asterisks indicate values that are statistically significant (*p-value <0.05 and **p-values <0.01). ns, not statistically significant.

5.2.3 Role of *Xist* in regulating an antiviral pathway and therefore HSV-1 replication in female cells

The results in Section 5.2.2 revealed that *Zbtb33*, a transcription factor on the X chromosome, is downregulated in female cells but not in male cells. It then regulates *Tbk1* expression and influences viperin regulation by HSV-1 infection. This section aims to identify a factor upstream of *Zbtb33* that only downregulates genes in females, not in males. We chose *Xist* as a reasonable candidate due to both its function and its upregulation during HSV-1 infection (Pasieka et al., 2006). One of the two X chromosomes in female mammals is transcriptionally silenced during embryogenesis to balance the dosage of gene expression between the two sexes. This is called X chromosome inactivation (Brockdorff and Duthie, 1998; Kay, 1998). *Xist*, a long non-coding RNA, is a main mediator of this process, inducing a series of events leading to stable silencing by accumulating repressive marks on the future inactive X chromosome (Leung and Panning, 2014; da Rocha and Heard, 2017). However, it has been observed that some X-linked genes are subject to regulation beyond dosage compensation by *Xist* (Disteche et al., 2002; Berletch et al., 2011). As noted above, *Xist* was found to be upregulated during HSV-1 infection in mouse embryonic fibroblasts in a previous microarray experiment (Pasieka et al., 2006). Further, our RNA-seq results found that *Xist* was induced at 4 and 8 hpi, but only in female cells. So we examined a set of X-linked genes that have been reported to be regulated by *Xist* beyond dosage compensation. These are illustrated in a heatmap, based on our RNA-seq analysis, in Figure 5-14 (Gayen et al., 2016; Lv et al., 2016; da Rocha and Heard, 2017). Many of these genes were downregulated by HSV-1 infection in female cells but not male cells at 8 hpi, consistent with the idea that increased *Xist* during HSV-1 infection is able to drive changes in gene expression.

5.2.3.1 *Xist* inhibits *Zbtb33* and therefore, regulates *Tbk1* and antiviral gene expression during HSV-1 infection

Firstly, the upregulation of *Xist* in HSV-1 infection was confirmed by qPCR. Male and female cells were infected with HSV-1 strain KOS at an MOI of 0.5 for four and eight hours. The expression of *Xist* was then analysed by qPCR using a specific primer set targeting mouse *Xist* (Table 2-7). Compared to the mock cells, *Xist* expression was around 10-fold higher at 4 hpi, increasing to 20-fold higher at 8 hpi in female cells (Figure 5-15A). However, this was not observed in male cells. Next, to identify whether *Xist* regulates *Zbtb33* and genes in the cytosolic DNA-sensing pathway during HSV-1

infection, siRNA was utilised to knockdown *Xist*, and the regulation by HSV-1 of *Zbtb33*, *Tbk1* and viperin were detected by qPCR. The knockdown efficiency of *Xist* in these cells was also determined by qPCR and were found that *Xist* expression was reduced by 80-90% in female cells. Conversely, there was no effect on the male cells (Figure 5-15B), which was expected because somatic cells in male mice generally do not express any *Xist* (Kay et al., 1993). Strikingly, when *Xist* was depleted in female cells before infection, *Zbtb33* regulation by infection was rescued to a similar level as that in male cells (Figure 5-15C), suggesting that HSV-1-induced *Xist* has the ability to reduce *Zbtb33* expression in female cells. Furthermore, both *Tbk1* (Figure 5-15D) and viperin (Figure 5-15E) upregulation by HSV-1 infection in female cells were reduced to levels comparable with male cells after *Xist* knockdown. These findings support the idea that upregulation of viperin and other antiviral effectors in female cells is due to the release of *Tbk1* expression from regulation by *Zbtb33*, via induction of *Xist* during HSV-1 infection.

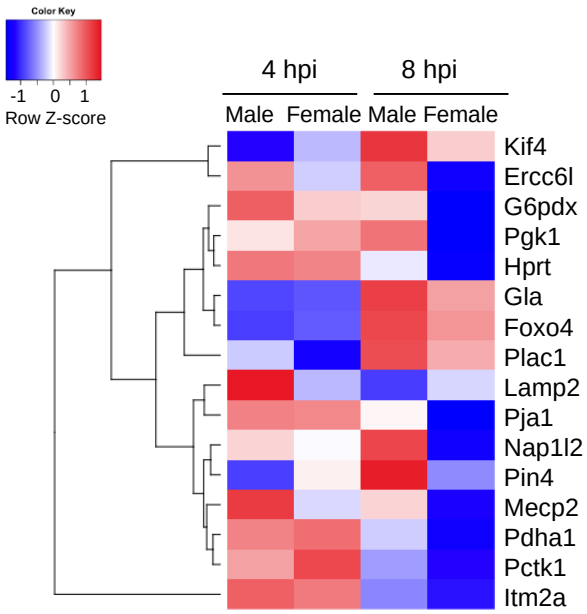

Figure 5-14. Changes in expression of genes known to be negatively regulated by Xist during HSV-1 infection. Using our data from RNA-seq experiment, $\log_2$ fold changes of published target genes of *Xist* at 4 and 8 hpi are shown in a heatmap. Red and blue indicate high and low regulation, respectively.

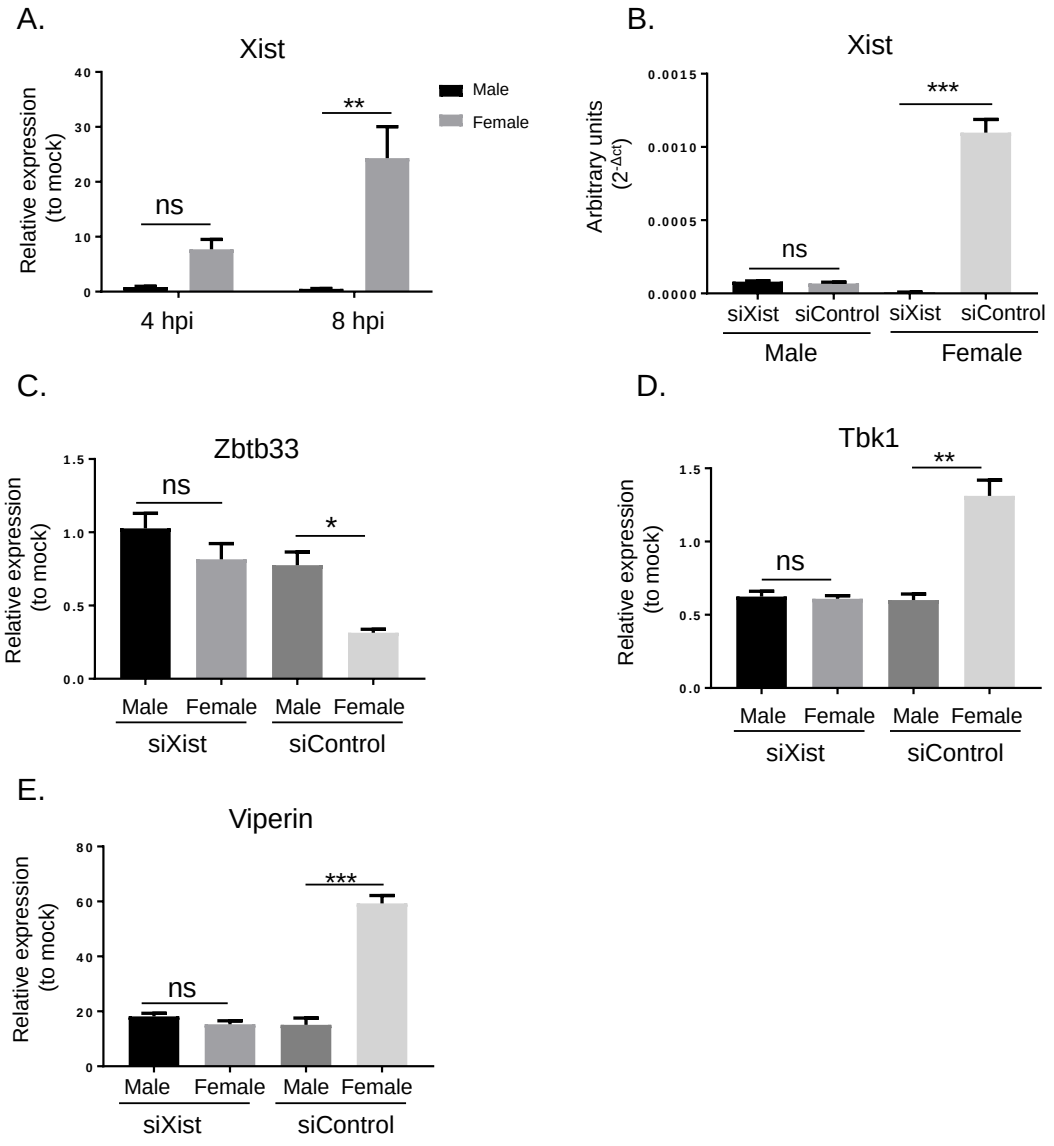

Figure 5-15. *Xist* is induced by HSV-1 in female cells and controls the regulation of *Zbtb33, Tbk1* and viperin. (A) *Xist* expression was measured by qPCR in male and female cells from three individual mice infected with HSV-1 pICP47 recombinant virus at an MOI of 0.5 for four and eight hours. (B-E) Male and female cells were transfected with 50 nM of control siRNA (siControl) or siRNA specific for *Xist* and then infected with HSV-1 at an MOI of 0.5 for eight hours. Following this, (B) *Xist*, (C) *Zbtb33*, (D) *Tbk1*, or (E) viperin mRNAs were measured by qPCR. The results are presented as mean ± SEM. One-way ANOVAs with Tukey's tests was applied to examine differences between means. Asterisks indicate values that are statistically significant (*p-value <0.05; **p-value <0.01; ***p-value <0.001). ns, not statistically significant.

5.2.3.2 Silencing *Xist* eliminates the difference in HSV-1 growth in male and female cells

While *Xist* is important for the sex difference in *Zbtb33* regulation by infection (Section 5.2.3.1), it remained to be shown whether it also altered HSV-1 replication. For this reason, we examined the growth phenotypes of HSV-1 in male and female cells lacking *Xist* expression. Cells depleted with *Xist* or control cells were infected with HSV-1 at an MOI of 0.0003, followed by titration using plaque assays at indicated time points. In male cells, there was no difference in HSV-1 replication between control and *Xist* knockdown cells (Figure 5-16A). By contrast, HSV-1 replicated significantly more efficiently in female cells lacking *Xist* than in the control female cells. In addition to viral titres, the infected cell populations at 72 hpi were measured and these results showed that *Xist* knockdown increased the spread of HSV-1 in female cultures (Figure 5-16B). These data indicate that induced *Xist* is required for the difference in HSV-1 replication between male and female cells.

5.2.3.3 *Xist* regulates sensing of DNA and HSV-1 replication in a human cell line.

Since HSV-1 is a human pathogen, we further examined whether the regulatory circuit described in Section 5.2.2 and Section 5.2.3 occurs in human female cells. To address this, we used HeLa cells, because they are commonly used for virology research and we found viperin upregulation in these cells after HSV-1 infection (Figure 4-4). HSV-1 induced *Xist* expression significantly above mock levels in HeLa cells (Figure 5-17A). The induction of *Xist* reduced *Zbtb33* expression (Figure 5-17B) and positively correlated with *Tbk1* and viperin regulation (Figure 5-17C and Figure 5-17D) as shown by an siRNA knockdown experiment. In the same manner observed in mouse cells, knockdown of *Zbtb33* demonstrated that this gene impacted *Tbk1* and viperin upregulation by HSV-1 infection in HeLa cells (Figure 5-17E and Figure 5-17F). Lastly, a knockdown of *Xist* in HeLa cells increased HSV-1 yields and the percentage of infected cells (Figure 5-17G and Figure 5-17H). Taken together, HeLa cells act similarly to female mouse cells during HSV-1 infection. That is, the upregulation of *Xist* reduces *Zbtb33* upregulation leading to increased *Tbk1* and antiviral effector expression, which inhibits HSV-1 replication.

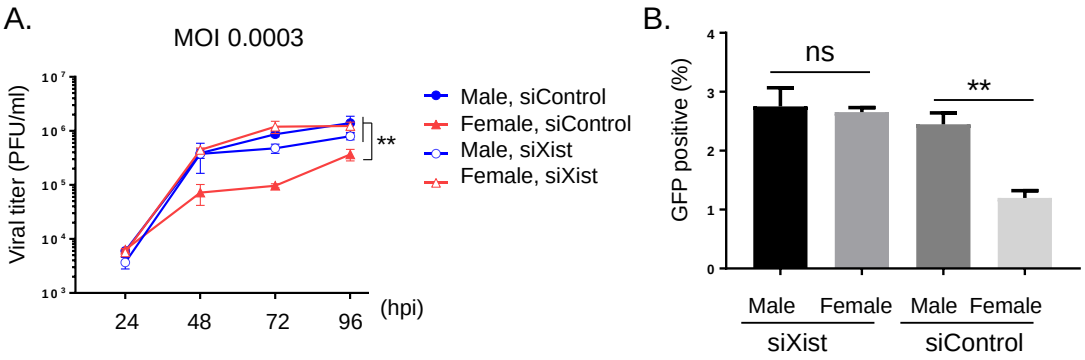

Figure 5-16. *Xist* is required for reduced HSV-1 replication in female cells compared with male cells. Male or female cells from three individual mice were transfected with 50 nM of siRNA specific for *Xist* (siXist) or control siRNA (siControl) and were then infected with HSV-1 pICP47 recombinant virus at an MOI of 0.0003. (A) Viral yields were evaluated at indicated time points by plaque assays and (B) GFP percentage was measured at 72 hpi. The results are presented as mean ± SEM. Two-way ANOVA and one-way ANOVA with Tukey's tests were applied to test differences between means in (A) and (B) respectively. Asterisks indicate values that are statistically significant (**p-value <0.01). ns, not statistically significant.

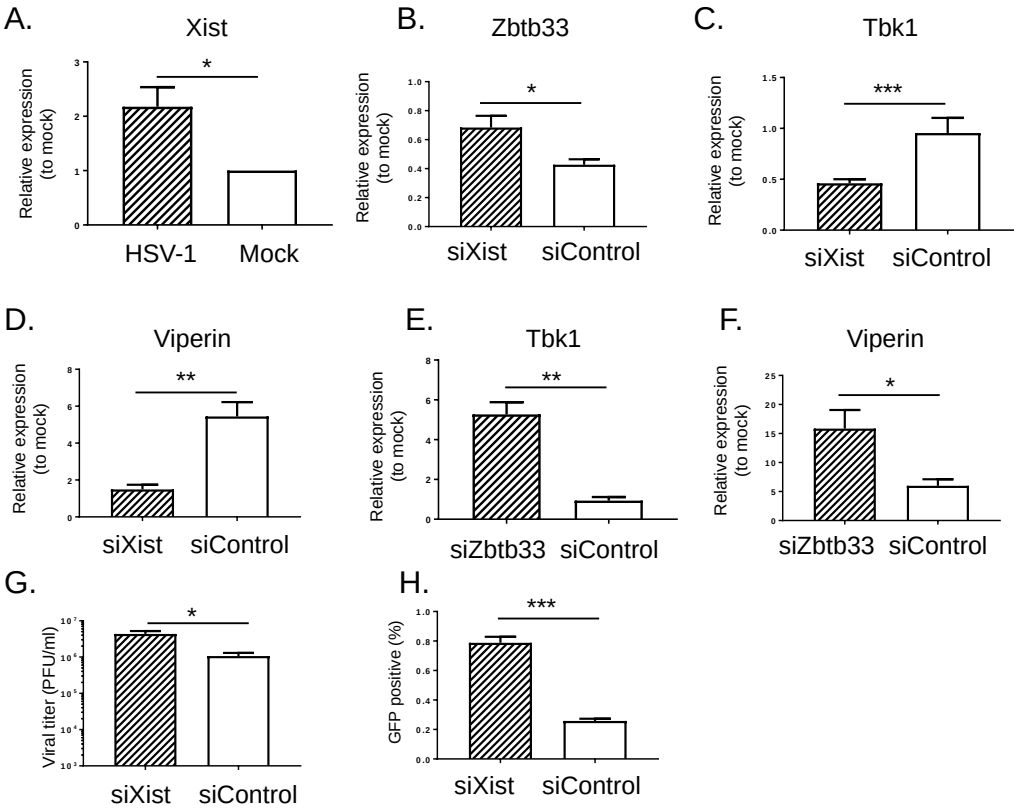

Figure 5-17. *Xist* is induced in HeLa cells and regulates HSV-1 infection. (A) HeLa cells were infected with HSV-1 pICP47 recombinant virus at an MOI of 1 and *Xist* expression was then determined by qPCR at 24 hpi relative to mock. (B-H) HeLa cells were transfected with 50nM of control siRNA (siControl) or siRNA specific for *Xist* (B-D and G-H) or *Zbtb33* (E-F), followed by inoculation of HSV-1 pICP47 recombinant virus at an MOI of 1. (B) *Zbtb33*, (C and E) *Tbk1*, and (D and F) viperin expression were then measured by qPCR at 24 hpi relative to mock. (G) Viral titres and (H) GFP percentage were determined by plaque assays and evaluated by flow cytometry, respectively, at 48 hpi. Unpaired Student's t-tests were performed to test differences between means. Asterisks indicate values that are statistically significant (*p-value <0.05; **p-value <0.01; ***p-value <0.001).

5.2.4 HSV-1 genes involved in the upregulation of *Xist*

Based on the results in Section 5.2.3, we found that *Xist* is required for the sex-specific difference in HSV-1 replication. However, how HSV-1 might induce *Xist* expression was not clear. To address this, we first narrowed down the range of possible viral functions that might be involved by treating cells with cycloheximide during infection to inhibit protein synthesis. In the absence of protein synthesis, *Xist* upregulation was still detected in female cells (Figure 5-18). These data indicate that *de novo* protein expression was not required for *Xist* upregulation. This also ruled out non-specific effects of virus infection on cells. Instead, it suggests that HSV-1 proteins carried into cells by the virion may play a role in regulation of *Xist*. Apart from structural components, herpesvirus virions have a store of proteins that are carried into cells to carry out functions that prepare the cell for virus replication or that act as transcription factors for viral IE genes. These proteins are in the tegument of the virion so that we examined the list of HSV-1 tegumant proteins for likely candidates for *Xist* regulation. The first one was VP16, a viral transcription factor that recognizes an octamer motif, of which we found two copies upstream of *Xist* in the promoter region (Figure 5-19). The other one was ICP34.5, which is a neurovirulence factor and a regulator of TBK1/IRF3 signalling (Wilcox and Longnecker, 2016; Manivanh et al., 2017). Further, we found that a HSV-1 lacking this gene is unable to upregulate *Xist* in a published microarray data set (Pasieka et al., 2006). These genes were cloned into expression vectors and transfected into male and female cells to see if either or both together might induce *Xist* expression. When we overexpressed VP16 alone, it did not significantly increase *Xist* regulation in female cells compared with male cells (Figure 5-20). Expression of ICP34.5 had a modest effect on *Xist* RNA level, but co-expression of these two genes led to substantial *Xist* upregulation. Collectively, these data show that VP16 and ICP34.5, which are carried into cells by the HSV-1 virion, can co-operate to induce *Xist* expression.

5.2.5 Sex differences between male and female cells in other DNA viruses

The mechanism established above suggests that the difference in virus replication between male and female cells discovered in this study may be an HSV-1-specific phenomemnon. To explore this possibility, given that we discovered sex-related differences in a DNA sensing pathway during HSV-1 infection, we selected another three large DNA viruses to look for differences in replication between male and female cells. These included another herpesvirus, mouse cytomegalovirus (MCMV) and two poxviruses, VACV and cowpox virus (CPXV). CPXV, but not MCMV and VACV,

showed a significant difference in replication in male and female cells inoculated with very low doses of virus (Figure 5-21). Next, we asked whether *Xist* might be involved in the reduced replication of CPXV using the same siRNA knockdown approach used with HSV-1. When *Xist* was knocked down, this did not alter the difference in CPVX replication between male and female cells (Figure 5-22). The results suggest that effect of *Xist* on virus replication may be HSV-1-specific, but implies that there are multiple mechanisms that can result in sex-related differences in virus replication in cell cultures.

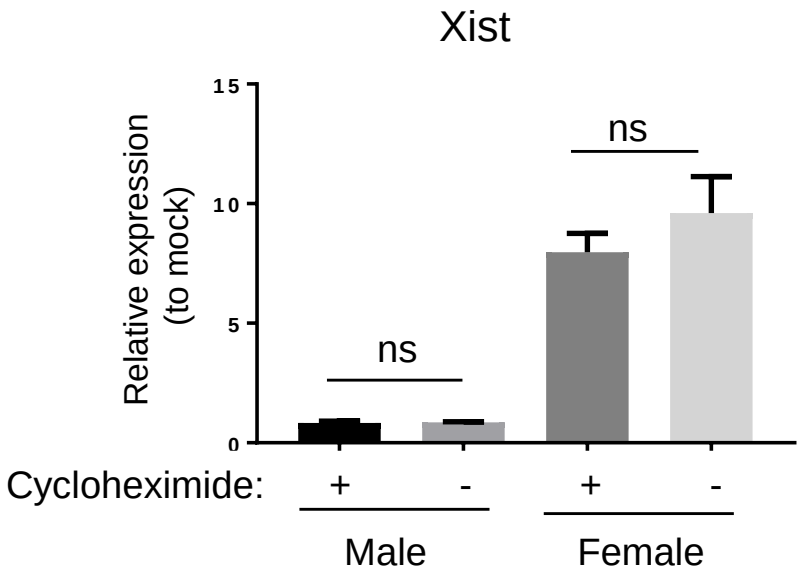

Figure 5-18. *Xist* regulation by HSV-1 infection in male and female cells treated with cycloheximide. Male and female cells from three individual mice were pretreated with 100 µg/ml cycloheximide for one hour, followed by inoculation of HSV-1 pICP47 recombinant virus at an MOI of 0.5 in the media containing 100 µg/ml cycloheximide. *Xist* expression was then measured by qPCR at 8 hpi. Differential regulation was assessed by the $2^{-\Delta\Delta CT}$ method based on expression relative to mock and normalised to 18S rRNA. The results are expressed as mean ± SEM. One-way ANOVAs with Tukey's tests was applied to test differences between means. ns, not statistically significant.

-301~-400 tctcctcatc tgaggtcgcc aactaatgca gaagaacttc tagtgtccaa gacgcggagc gatacatggt ttgtccaagt agaagatata ttgaaatttt
-201~-300 gcatagacag gtgtgtgacc taatgtacat tatttaatgt ttatgtggaa gttctacata aacgttttta gctgtaaaat aggataatcc ttcattatcg
-101~-200 cgcaaaataa tgaaattcac gcgtcatgtc actgagctta cgtacctcca tctttattca ttttaatttt tttataatat agttagacct aaaggtccaa
-1~-100 taagatgtca gaattgcaat ctttgtggcc actcctcttc tggtctctcc gccttcagcg ccgcggatca gttaaaggcg tgcaacggct tgctccagcc
+1~+100 atgtttgctc gtttcccgtg gatgtgcggt tcttccgtgg tttctctcca tctaaggagc tttgggggaa catttttagt tcccctacca ccaagcctta

Figure 5-19. A schematic diagram of sequence near the start codon of *Xist* (-400~+100). The sequence started from -400 to +100 of *Xist* is shown. Red highlights the start codon of *Xist*. Yellow shows two predicted octamer motifs for VP16 binding with the consensus sequence "TAATGARAT". Note that the first one is a relatively poor match and exists on the opposite strand.

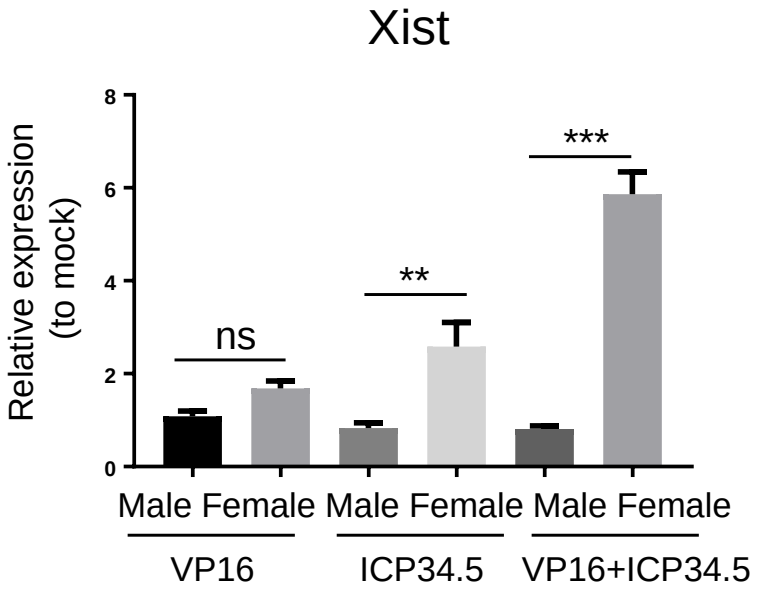

Figure 5-20. Effects of overexpression of VP16 and/or ICP34.5 on *Xist* regulation. Male and female cells from three individual mice were transfected with 2 µg of plasmids expressing VP16 or ICP34.5 or were co-transfected with 1 µg of each of these plasmids. *Xist* expression was then determined by qPCR at 24 post transfection. Differential regulation was assessed by the $2^{-\Delta\Delta CT}$ method based on expression relative to control transfectants and normalised to 18S rRNA. The results are shown as mean ± SEM. One-way ANOVAs with Tukey's tests was applied to test differences between means. Asterisks indicate values that are statistically significant (**p-value <0.01 and ***p-values <0.001). ns, not statistically significant.

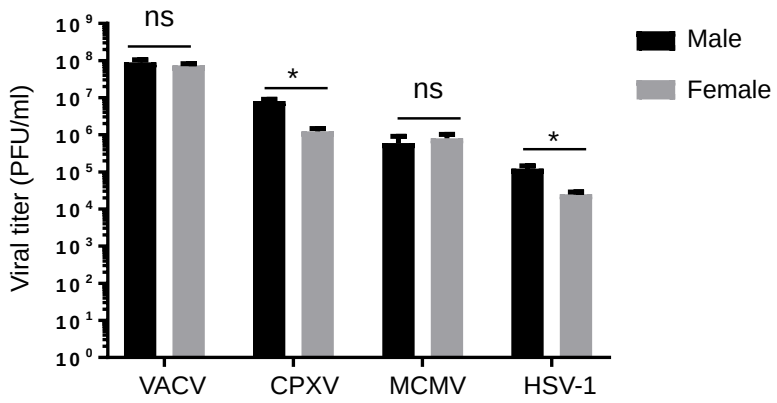

Figure 5-21. VACV, CPXV, MCMV and HSV-1 replication in male and female cells. Male and female cells from three individual mice were infected with VAVC (MOI 0.0001), CPVX (MOI 0.00001), MCMV (MOI 0.00001) and HSV-1 (MOI 0.0001). Viral titres were then measured by plaque assays at 72 hpi. The results are expressed as mean ± SEM. One-way ANOVAs with Tukey's tests was applied to test differences between means. Asterisks indicate values that are statistically significant (*p-value <0.05). ns, not statistically significant.

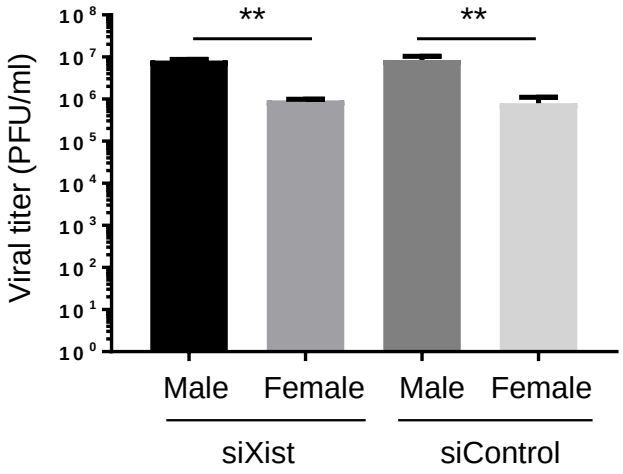

Figure 5-22. Replication of CPXV in *Xist*-kockdown cells. Male and female cells from three individual mice were transfected with 50 nM of control siRNA (siControl) or siRNA specific for *Xist* for 24 hr, followed by inoculation of CPXV at an MOI of 0.00001. Viral titres were measured by plaque assays at 72 hpi. The results are shown as mean ± SEM. One-way ANOVAs with Tukey's tests was applied to test differences between means. Asterisks indicate values that are statistically significant (**p-value <0.05).

5.3 Discussion

In this chapter, a mechanism that regulates the sex-specific difference in HSV-1 infection via nucleic acid sensors was dissected. We found that *cGAS* and *Tbk1* in the cytosolic sensing pathway are two key players in a nucleic acid-sensing pathway required for differential upregulation of viperin between male and female cells (Figure 5-1). Higher upregulation of *Irf1* in female cells led to higher *cGAS* expression (Figure 5-6), although current data do not identify a ligand that stimulates *Irf1* upregulation. Furthermore, we then linked our observations to sex chromosomes by showing that an X-linked transcription factor (*Zbtb33*) is important for regulating *Tbk1* and therefore downstream antiviral effectors between the sexes (Figure 5-12). Next, a sex-specific gene (*Xist*) was shown to explain the difference in *Zbtb33* expression and HSV-1 replication (Figure 5-16). Finally, two HSV-1 tegument proteins, namely VP16 and ICP34.5 were shown to be able to induce *Xist* expression in female cells. A schematic diagram of this mechanism is presented in Figure 5-23.

Mossman's lab has used many approaches to find support for a model whereby the first line of innate antiviral defence in response to enveloped viruses, including HSV-1 and HCMV, occurs before virus replication (Mossman et al., 2001; Collins et al., 2004; Paladino et al., 2006). This mechanism is characterised by the induction of a subset of ISGs independent of TLRs and NF-κB in response to cytoplasmic DNA, following the activation of the TBK1/IRFs pathway, during a low MOI infection in fibroblasts and epithelial cells (Lin et al., 2004; Paladino et al., 2010; Noyce et al., 2011). Similarly, we found that IRFs such as IRF1, IRF3 and IRF7 are essential for viperin induction in mouse skin fibroblasts during low MOI infection with HSV-1 (Figure 5-3). Previous findings suggesting that IRF1 also controls IFN-independent signalling via peroxisomal MAVS for rapid ISG upregulation in a conventional manner at the bottom of a nucleic acid-sensing pathway (Dixit et al., 2010). However, we show evidence here for a novel mechanism whereby *Irf1* acts upstream of nucleic acid sensing by regulating *cGAS* expression and thereby, potentiates an innate immune response in HSV-1 infection (Figure 5-6). Presumably, this is the result of sensing some other aspect of infection, but this remains unknown. Binding of viral particles to the cell surface is not sufficient to elicit IFN-mediated pathways. Therefore, if the signalling cascades upstream of IRFs are independent of nucleic acids and viral structural components (Nicholl et al., 2000; Mossman et al., 2001; Paladino et al., 2006; Tsitoura et al., 2009), the most reasonable explanation may be that membrane fusion triggered by enveloped viruses, such as HSV-1 and HCMV, results in activation of IRFs through ion transport (Hare et al., 2015).

We speculated that this may be the case in our model, where neither RIG-I family members, the sensor upstream of MAVS, nor *Tlr3* or *Tlr4* had as strong an impact on virperin expression as *cGAS* and *Irf1*.

In addition to *cGAS*, *Tbk1* is another factor that is required for the sex difference in viperin regulation by infection (Figure 5-1). As *Tbk1* was not regulated by *Irf1* in our experiments (Figure 5-5), we further searched transcription factors on the sex chromosomes that may function upstream of the cytosolic sensing pathway during HSV-1 infection. Approximately 1,000 genes are expressed on the X chromosome, most of which are distinct from the fewer than 100 genes that are encoded by the Y chromosome (Fish, 2008; Klein and Flanagan, 2016; Roved et al., 2017). This biological character may contribute to the lack of potential candidates on the Y chromosome for transcriptional regulation of *cGAS*, *Mda5*, *Rig-I*, *Tbk1*, *Irf1* or *Irf7*. Therefore, it was considered more likely that a potential candidate would be on the X chromosome. Several transcription regulators on the X chromosome were predicted to modify expression of the genes mentioned above, and so whether they could affect an antiviral pathway in male and female cells was further examined (Figure 5-7 and Figure 5-8). Of these genes, only the knockdown of *Zbtb33* reduced the difference in viperin induction and virus replication between male and female cells after infection with HSV-1. *Zbtb33*, also known as Kaiso, is a 95-kDa Zinc finger transcription factor that has been implicated in regulation of the cell cycle and tumour cell invasion (Pozner et al., 2016; Wang et al., 2016a; Bassey-Archibong et al., 2017). *Zbtb33* is recruited into the nucleus where it suppresses gene expression by binding to methylated CpG motifs in response to extracellular signals and then forms the repressor complex with the histone deacetylase-nuclear receptor (Yoon et al., 2003; Buck-Koehntop et al., 2012).

To date, there is no literature that has found a role for *Zbtb33* in the innate immune response. However, Zhenilo et al. (Zhenilo et al., 2018) found that ZBTB33 is a transcriptional repressor for *Trim25* during hyperosmotic stress. TRIM25 is an E3 ubiquitin ligase enzyme with multiple functions, including regulation of the innate immune response against viruses (Gack et al., 2007; Castanier et al., 2012; Martin-Vicente et al., 2017). TRIM25 has been well-characterised for its role in the regulation of RIG-I signalling and therefore, IFN-β production in response to viral infection in mouse embryonic fibroblasts (Sanchez et al., 2016; Martin-Vicente et al., 2017). Herein, our RNA-seq data found that *Trim25* regulation by HSV-1 was inversely related to *Zbtb33* and was stimulated to a higher degree in female cells (data not shown). This pathway should be investigated to determine if it contributes to the effect of *Zbtb33* regulation by HSV-1 infection in female cells.

In our model, *Zbtb33* was found to negatively regulate *Tbk1* expression, and hence, levels of activated TBK1. *Tbk1* is an essential transducer which receives signals from different pathogen-associated molecular patterns, TLRs and cytosolic receptors post-recognition of foreign pathogens (Weidberg and Elazar, 2011). As TBK1 signalling plays a pivotal role in signal transduction, HSV-1 deploys at least two proteins, the IE protein ICP27 and the tegument protein UL46 to target this signalling pathway. The action of these proteins prevents phosphorylation of IRF3 to evade cellular sensing in human macrophages and epithelial cells (Christensen et al., 2016; Deschamps and Kalamvoki, 2017). We did not explore the role of these proteins in our model, but they add to the complexity of HSV-host interaction and so this should be examined.

Another key finding of this chapter is that *Xist* is induced by HSV-1 infection in female cells. This process increases antiviral responses through restricting *Zbtb33* induction (Figure 5-15). This also explains the different growth phenotypes whereby HSV-1 was found to replicate more efficiently in male cells than female cells after inoculation with very low doses of virus (Figure 5-16). This complete pathway starting with *Xist* upregulation and ending in reduced HSV-1 replication was also found in the human female cell, HeLa. However, the extent of differences in the regulation of target genes and virus replication seen when *Xist* was knocked down was modest compared with female mouse cells. This may be a species difference, or something particular to HeLa cells. For example, it has been noted that these cells have high level of *Xist* expression (Sun et al., 2018), but it is unclear what this might mean for our model.

Xist is a non-coding RNA expressed from the X chromosome and it is involved in X-linked gene silencing by recruiting a protein complex to the future inactive X chromosome in female mammals during early embryonic development (Brockdorff and Duthie, 1998; Kay, 1998). X-inactivation serves as a compensation mechanism to achieve dosage equivalence for X-linked genes between males and females. Currently, most studies focus on the relationship between *Xist* and cancer since *Xist* is crucial for the regulation of different types of cancers (Lopes et al., 2008; Dai et al., 2010; Yildirim et al., 2013; Yu et al., 2017). For example, X reactivation leads to genome-wide changes driving induction of an aggressive and lethal blood cancer specific to females (Yildirim et al., 2013). However, this study is the first to link levels of *Xist* to control of an immune process. X-inactivation does not achieve perfect dosage compensation as described for more and more genes (Berletch et al., 2011; Mugford et al., 2014; Disteche and Berletch, 2015). While over-expression of X-linked genes in females has been examined as a reason for sexually dimorphic immune responses, under-

expression, such as we described for *Zbtb33*, has not been suggested previously, neither has the role of *Xist* in this context. However, *Xist* plays crucial roles in various multigenetic human diseases, including cancers, neurological diseases and autoimmune diseases (Agrelo and Wutz, 2010; Seton-Rogers, 2013). Moreover, recent studies have reported that differentiation of B cells has correlation with *Xist* expression and the inactive X chromosome is predisposed to become partially reactivated particularly in female lymphocytes (Wang et al., 2016b; Syrett et al., 2017).

Two HSV-1 genes were found to cooperatively induce *Xist* expression. VP16 is a transcriptional activation of viral immediate early genes and there are two octamer binding motifs of VP16 in the promoter region of *Xist* (Figure 5-19). This background supported VP16 as a potential candidate for understanding *Xist* regulation. However, surprisingly, overexpression of VP16 alone did not lead to upregulation of *Xist* (Figure 5-20). We then found a published microarray data set showing HSV-1 ICP34.5, but not an ICP34.5 deletion mutant of HSV-1, induces *Xist* expression, though *Xist* was not mentioned in the paper (Pasieka et al., 2006). We found upregulation of *Xist* in female cells expressing ICP34.5 and this became more pronounced if VP16 was co-expressed (Figure 5-20). VP16 and ICP34.5 serve multiple functions and both have been shown to interfere with TBK1/IRF3 signalling. Of relevance here, while some direct interaction have been reported, there are also some indirect effects (Xing et al., 2013; Manivanh et al., 2017). However, the relative effects of any direct effect of these proteins and the indirect effect we show here via *Xist* in female cells remains unknown. This point reinforces the importance of taking the sex of cells into account when dissecting the roles of viral genes.

Finally, we investigated whether the sex-specific difference in virus replication found for HSV-1 might occur for other large DNA viruses. We found that in addition to HSV-1, CPXV replicated more efficiently in male cells than in female cells, but no difference was noted for VACV or MCMV (Figure 5-21). We note that for MCMV in particular, primary skin fibroblasts are not an especially relevant host cells. So perhaps a sex difference might be found in other cell types. In addition, there remains many viruses and cell types where sex may play a role. Coming back to CPXV, the difference in viral titres was not changed by knockdown of *Xist* (Figure 5-22). Overall, these data suggest that there are multiple mechanisms leading to sex-related differences in virus replication in cells. Further, the effect of knocking down *Xist* on virus replication appears to be HSV-1-specific and not a pan-viral effect, or a derangement of these cells such that they no longer support virus replication.

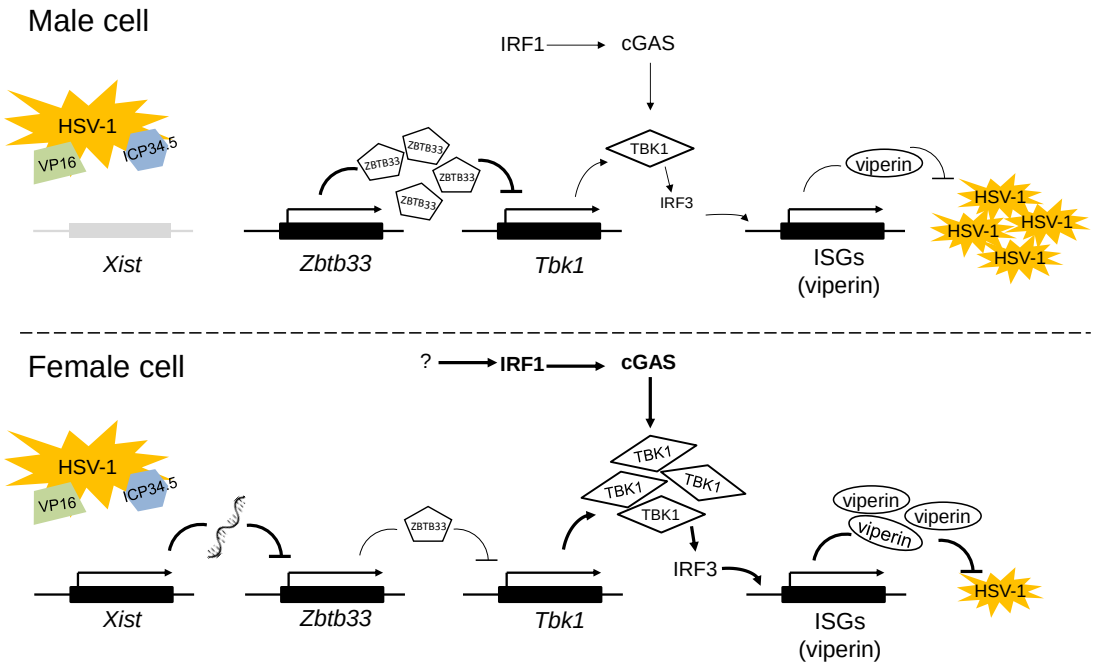

Figure 5-23. A schematic diagram of HSV-1-triggered cytosolic sensing pathway in male and female cells. During HSV-1 infection, female cells induce higher IRF1 which acts upstream of cGAS to drive viperin upregulation. In addition, upregulation of *Xist* in female cells leads to inhibition of *Zbtb33*, and therefore, enhancement of *Tbk1* regulation and function, which finally contributes to greater antiviral activity against HSV-1 infection in female cells.

Chapter 6. Different responses between human and mouse cells during HSV-1 infection.

6.1 Introduction

Humans are the only natural host for HSV-1, but investigating infections in humans is difficult for several reasons, including the fact that primary infections are frequently asymptomatic (Klysik et al., 2018). Likewise, HSV-1 establishes latency in sensory neurons, such as trigeminal ganglia or dorsal root ganglia, which makes investigation of the immune mechanism that controls the reactivation of latent infection in humans more complicated (Jones, 1998; Preston and Efstathiou, 2007; Grinde, 2013). This is because the only access to collect human nervous samples are from post-mortem samples (Schmutzhard, 2001; Steiner, 2011). Therefore, animal models have been developed to achieve a better understanding of HSV-1 pathogenesis. Mouse models are frequently used to study HSV diseases (Mester and Rouse, 1991; Brandt et al., 1992; Parr et al., 1994). Different routes of HSV-1 infection, including flank skin, corneal epithelium and footpads, have been used to examine various stages and types of HSV infection (Kollias et al., 2015). Even though there are many HSV-1 models, the translation of murine experimental results to human diseases remains challenging, not least because of species-specific differences that may exist in the host responses to the virus.

Several lines of evidence have shown that host cells respond in species-specific ways to HSV-1 infection. For example, both caspase-8-mediated apoptosis and RIP3-induced necroptosis are suppressed in human cells by the large subunit of the HSV-1 ribonucleotide reductase (Langelier et al., 2002; Yu et al., 2015). By contrast, after sensing HSV-1, mouse cells directly induce necroptosis which inhibits virus replication (Guo et al., 2015a; Guo et al., 2015b). In another case, ICP47, an IE protein of HSV-1, efficiently blocks MHC class I antigen presentation to $CD8^+$ T cells via inhibition of the human transporter associated with antigen presentation (TAP) (York et al., 1994; Fruh et al., 1995). However, mouse TAP is relatively resistant to inhibition by the HSV-1 ICP47 protein, and therefore, mouse fibroblasts infected with HSV-1 are effectively lysed by anti-HSV $CD8^+$ cytotoxic T lymphocytes (CTL), as compared to human cells (Ahn et al., 1996; Jugovic et al., 1998). Our data also show human-mouse differences against HSV-1 replication whereby viperin is upregulated in mouse skin fibroblasts but not significantly in human cells such as HFF, MRC5 and HEK293 cells and relatively poorly in HeLa cells (Section 4.2.1.3). However, to date, there is no global understanding and investigation of human-mouse differences in HSV-1 infection. Hence, the aim of this chapter was to investigate overall differences between human and mouse cells in the regulation of transcription during HSV-1 infection.

6.2 Results

Two human cell lines and one mouse cell type were used in this chapter, including primary human foreskin fibroblasts (HFF), an immortalised human cell line, MRC5 and primary male mouse skin fibroblasts. Both HFF and MRC5 are from males. In order to avoid the sex difference, mouse skin fibroblasts (MF) and IFNAR$^{-/-}$ cells were only collected from male mice in this chapter. Data from HFF and MRC5 are from replicate infections, but for the mouse cells, we generated and infected cultures from individual mice, as in the previous chapters.

6.2.1 Different HSV-1 growth phenotypes between human and mouse cells

To investigate whether HSV-1 replication differs between human and mouse cells in our fibroblast culture model, single and multi-step growth experiments were done in two human cell lines (HFF and MRC5) and in primary male mouse fibroblasts (MF). HSV-1 yields were comparable in the three tested cell types in a single round infection, indicating all cultures support basic HSV-1 replication (Figure 6-1A). The pattern of the multi-step growth curves of HSV-1 in HFF and MRC5 were similar, but differed markedly from that generated using mouse cells (Figure 6-1B). The data indicated that there was significantly more HSV-1 replication in the human primary and immortalised cells than in primary mouse cells. Taken together, these results suggest that human and mouse cells may respond differently to HSV-1 *in vitro* with mouse cells being able to limit virus replication compared with human cells.

6.2.2 Infection rate of HSV-1 pICP47 recombinant virus in HFF, MRC5 and MF

In order to set up a suitable MOI and suitable infection time points for investigation of transcriptional differences, we then infected human and mouse cells with HSV-1 pICP47 that expresses GFP to allow infection to be monitored by flow cytometry. About 70% of cells were GFP-positive when HFF, MRC5 and MF were infected with HSV-1 pICP47 recombinant virus at an MOI of 0.5 for four hours. After eight hours of infection, infection rates increased to around 85% among these three cells (Figure 6-2). However, there was no significant difference in infection rate across the four cell types at either time.

6.2.2.1 Transcriptional analysis by RNA-seq for HSV-1-infected HFF, MRC5 and MF

The transcriptional analysis presented here was an extension of the RNA-seq experiment described in Chapter 3 (Section 3.2.5.2). Given that HFF and MRC5 are male human cells, RNA-seq data from male mouse cells (Section 3.2.5) were incorporated for downstream analysis. The male mouse cell cultures used here were the same that we used for comparison with female mouse cells.

HFF and MRC5 cells were infected at the same time with the same conditions (See Section 2.2.15). To reduce any confounding data from uninfected cells, as mentioned in Section 3.2.5.1, sorting was employed to collect infected cell populations based on the GFP signals in the triplicates of HHF and MRC5 post HSV-1 pICP47 virus infection. Total RNA was isolated from sorted cells for library preparation and then subjected to RNA-seq using the Illumina platform as described in Section 2.2.15. A customised pipeline for cross-species analysis were used to identify comprehensive differences between human and mouse cells during HSV-1 infection.

6.2.3 Expression of HSV-1 genes in HFF, MRC5 and MF

The resulting reads from the HFF and MRC5 samples were aligned to the human genome and those from MF were mapped against the mouse genome, as described in Section 3.2.5.2. The unmapped reads were then aligned to the sequence of the HSV-1 KOS strain that had been modified to remove repeat regions in the genome. More detail on the analysis of HSV-1 transcripts is given in Section 2.2.31.4. Expression of individual HSV-1 genes is plotted in a heatmap (Figure 6-3). Each replicate of HFF, MRC5 and MF clustered together, indicating that there was no significant difference between each replicate. Samples clustered first by infection time. At 4 hpi they clustered according to species, but at 8 hpi the two primary cell types (HFF and MF) were clustered together and the immortalized MRC5 was the outlier. Despite the fact that replicate infections were used for the human cell lines and independently derived cells were used for mouse cultures, in each case the clustering by cell type was similarly close.

To observe the dynamic change in HSV-1 gene expression between the two time points, gene abundance of HSV-1 between the mouse and two human cell types at 4 and 8 hpi was plotted in genome coverage figures (Figure 6-4). Changes in the expression of individual viral genes between 4 and 8 hpi were observed and these data generally reflected the established viral gene expression patterns for HSV-1 infection. Although some regions were appeared to be regulated slightly differently across these three cell types, such as UL4 in HFF at 8 hpi, there were no statistically significant differences

for any HSV-1 gene between human and mouse cells at either time based on the selection criteria: p-value <0.05 and $\log_2$ fold change >1.

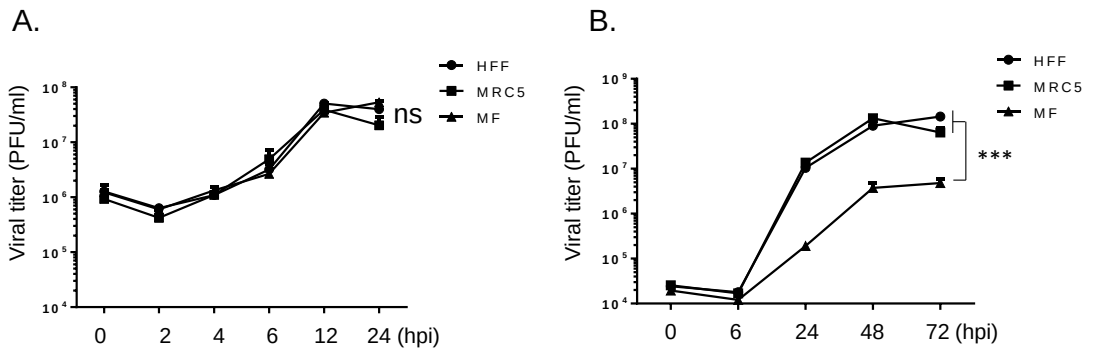

Figure 6-1. Growth kinetics of HSV-1 in human and mouse cells. (A) Triplicate cultures of HFF and MRC5 or MF from three individual mice were infected with HSV-1 pICP47 recombinant virus at an MOI of (A) 10 or (B) 0.001 and then cell lysates were collected at the indicated time points. Plaque assays were performed to measure viral titres. The results are expressed as mean ± SEM. Two-way ANOVA with Tukey's post-tests was used to test differences between means across the growth curves. ***p <0.001. ns, no significant difference.

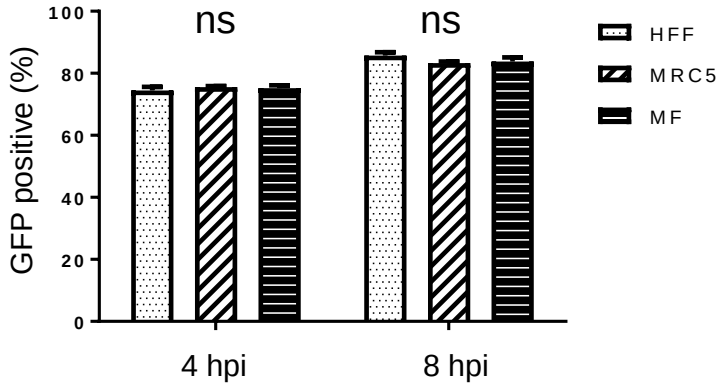

Figure 6-2. Infection rate of HSV-1 in HFF, MRC5 and MF. Triplicate cultures of HFF and MRC5 or MF from three individual mice were infected with HSV-1 pICP47 recombinant virus at an MOI of 0.5 for four or eight hours and then analysed by flow cytometry. The percentages of cells that were GFP positive are presented in a bar chart and expressed as mean ± SEM. One-way ANOVAs with Tukey's tests was applied to analyse differences between means. ns, no significant difference.

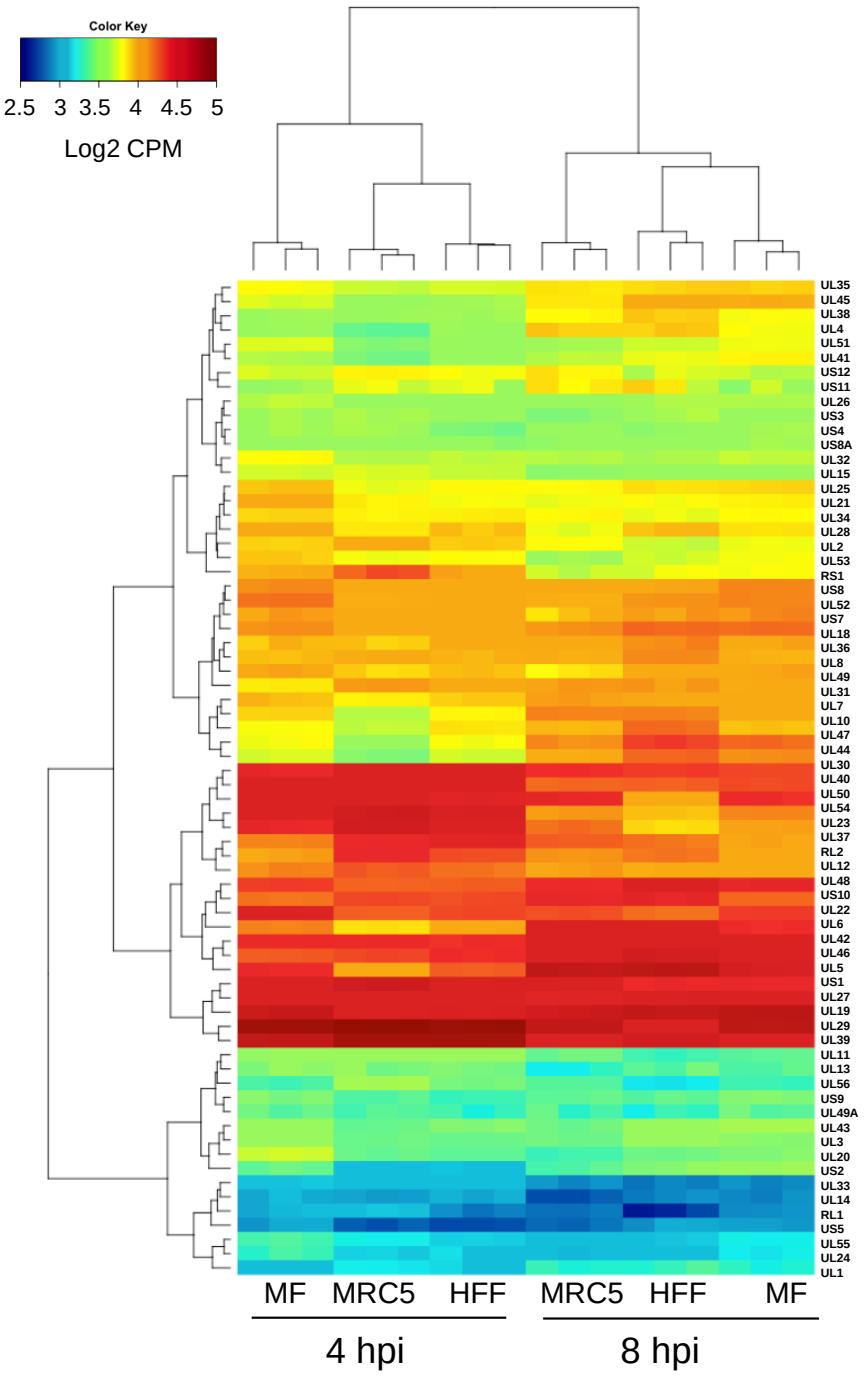

Figure 6-3. Expression of HSV-1 genes in HFF, MRC5 and MF at 4 and 8 hpi. Reads that mapped to the HSV-1 genome were converted into counts per million (CPM) using the featureCounts package. The $\log_2$ CPM of each HSV-1 gene at 4 and 8 hpi, in three replicates of HFF and MRC5 and MF from three mice were clustered by hierarchical average linkage clustering and Euclidean distances. The density of reads mapping to each gene is colour-coded according to the color key above (red=high density, blue=low density).

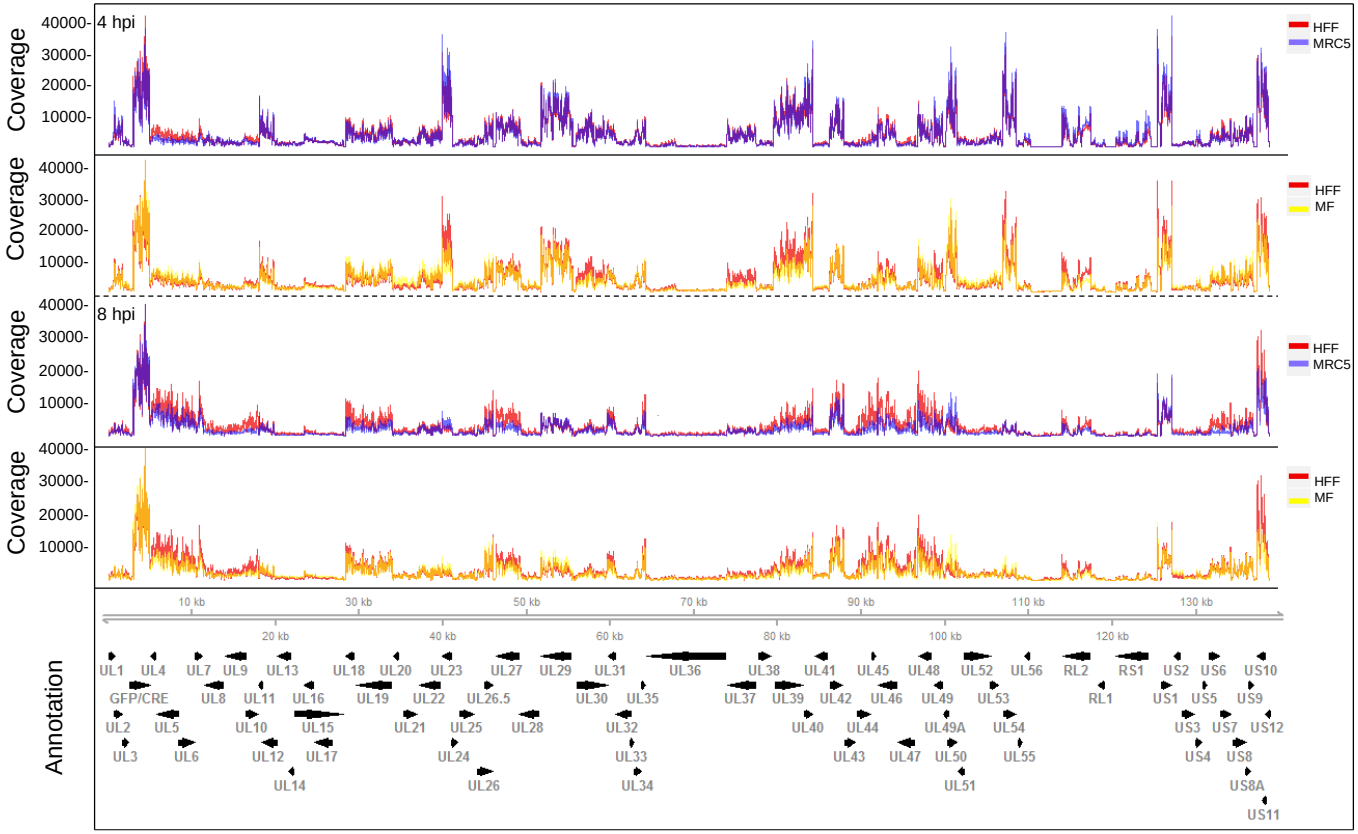

Figure 6-4. Location and relative coverage of mapped reads across the HSV-1 genome. The position of reads at 4 and 8 hpi between HFF and MRC5 or MF are marked relative to a map of HSV-1 genes. In order to compare gene abundance between the different cell types, the scales of the plots were normalised to the total reads. The modified genome is shown without the long and short terminal repeats in the HSV-1 genome and sequences in these two regions are represented in the internal repeats.

6.2.4 Distinct gene regulation by HSV-1 infection between human and mouse cells

Reads that mapped to the human genome in HFF and MRC5 or those mapped to the mouse genome in MF were calculated by the featureCounts package and were then transferred into CPM (Liao et al., 2014). The trimmed mean of the log expression ratios (trimmed mean of M values) was used to normalise each library using edgeR (Robinson et al., 2010). Ensembl IDs were then converted into gene symbols and shared gene symbols between humans and mice were used for an analysis of differentially regulated genes using the limma package (Law et al., 2014; Ritchie et al., 2015). A detailed description of the analysis of the cross-species data is provided in Section 2.2.31.3.

Expression of the top 500 genes was analysed by multidimensional scaling (MDS) to visualise the similarity between individual samples (Figure 6-5). Each replicate clustered together, but all different infection times were separated in human and mouse samples. In addition, mouse cell samples were located a substantial distance from the two human cell types on a plot of the first two dimensions (Figure 6-5), suggesting substantial differences in gene expression between the species at all times.

Next, hierarchical clustering of all host transcript levels in each RNA-seq sample was arranged as a heat map. This figure further confirms the high reproducibility of the transcriptional signature within each infection condition with replicates clustering together. It also shows that human and mouse cells were transcriptionally distinct before and during HSV-1 infection, as all mouse samples were clustered together and away from the two human samples (Figure 6-6).

Next fold changes in host gene expression at 4 and 8 hpi were calculated by comparison with mock infected samples, HFF and MRC5 shared high similarity in RNA regulation by HSV-1 infection, with Pearson's correlations of 0.76 and 0.81 at 4 and 8 hpi (Figure 6-7A and Figure 6-7C). However, the correlation of regulation of orthologous genes between primary human (HFF) and primary mouse cells (MF) was extremely low at both times (Figure 6-7B and Figure 6-7D). Taken together, the data show that human and mouse cells are transcriptionally distinct and respond to HSV-1 infection with different transcriptional changes.

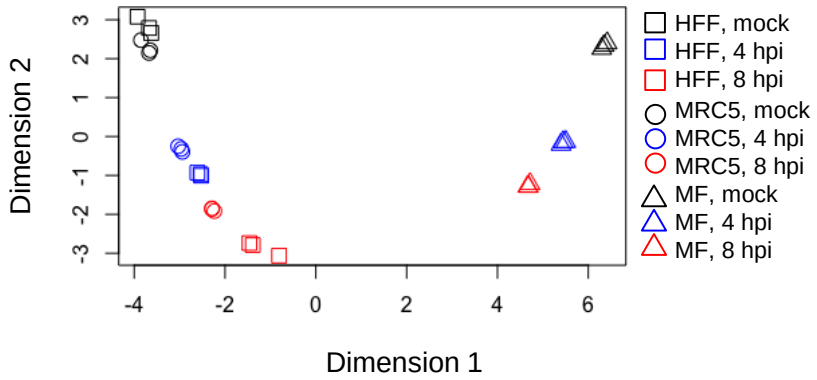

Figure 6-5. Multidimensional scaling analysis of transcriptome data from human and mouse cell samples during HSV-1 infection. Multidimensional scaling analysis was conducted based on the expression of the top 500 genes from the mock, 4 or 8 hpi samples of each cell type and their position over dimensions 1 and 2 are shown. Mock, 4 hpi and 8 hpi samples are presented in black, blue and red with three replicates. □, HFF; ○, MRC5; Δ, MF.

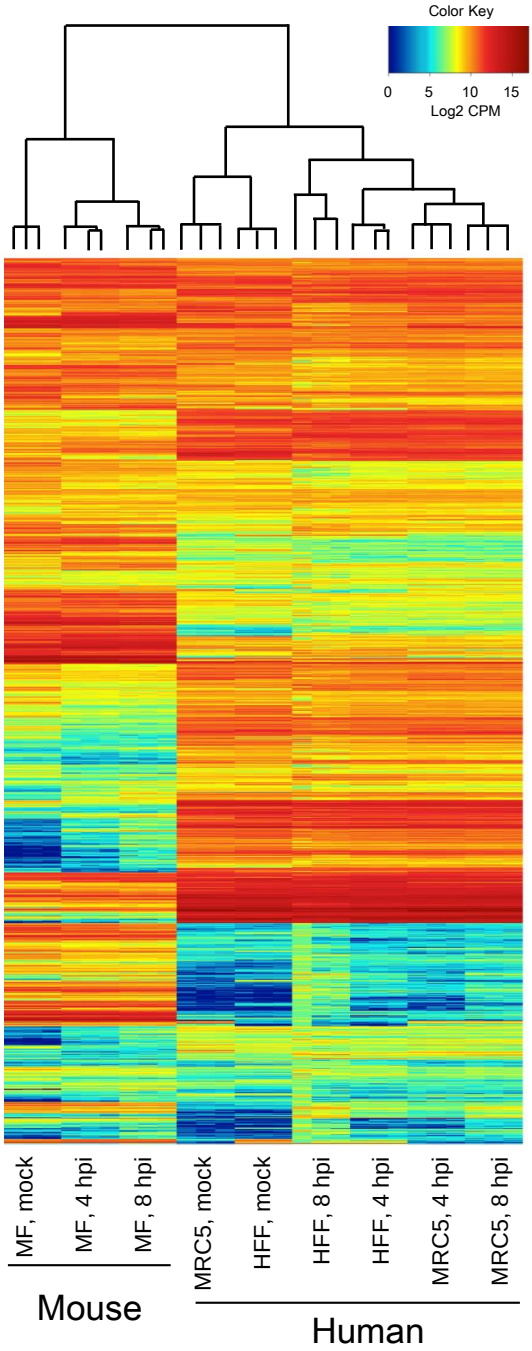

Figure 6-6. Distinct transcriptional profiles between human and mouse cells before and during HSV-1 infection. Hierarchical clustering of expression level of each orthologous gene in HFF, MRC5 and MF at 4 hpi, 8hpi and mock is shown. The vertical dendrogram shows the clustering of each sample and its infection condition according to similarities in transcript expression. Red refers to relatively high expression and blue refers to relatively low expression. The expression value for each gene is given based on $\log_2$ CPM.

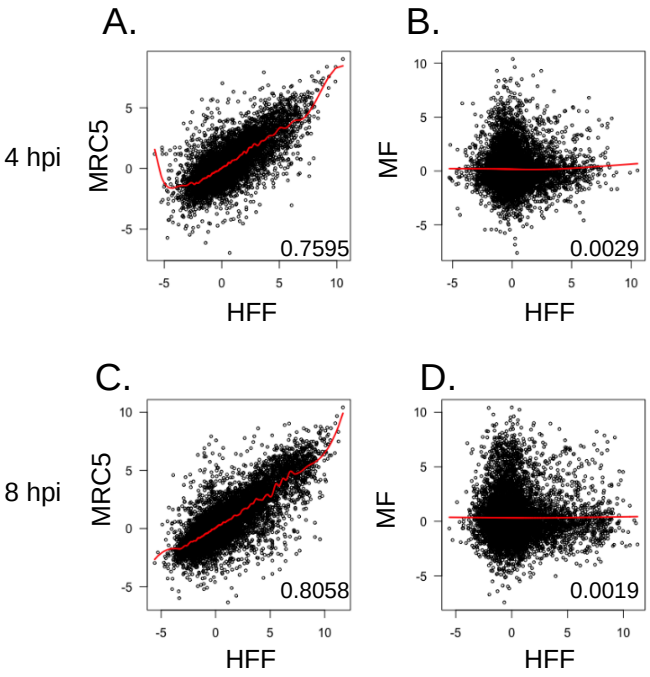

Figure 6-7. Correlation of fold changes of differentially regulated genes during HSV-1 infection between human and mouse cells. Scatterplots of the correlations in $\log_2$ fold changes in transcripts due to infection between HFF and MRC5 or MF at (A-B) 4 and (C-D) 8 hpi relative to mock are shown. Pearson's correlation coefficients are given at the bottom right. Linear regression models were fitted and are illustrated as a red line in each scatterplot.

6.2.5 Differentially regulated cellular functions and pathways between human and mouse cells in HSV-1 infection

In order to acquire a functional profile of differentially regulated genes between human and mouse cells, GO analysis was performed on the combined list of genes that were differentially up- or downregulated by infection, between HFF and MRC5 or MF. When investigating the difference between HFF and MRC5, no significant GO terms were detected, indicating that gene regulation by infection is very similar in these two human cell types. On the contrary, a broad range of GO enrichment results were revealed between human and mouse cells. Specifically regulation was observed with regard to signal transduction [GO:0009966], the apoptotic process [GO:0006915], ion transport [GO:0006811] and protein phosphorylation [GO:0006468] (Figure 6-8). These data show that multiple cellular functions are regulated differently between the two species in response to HSV-1 infection.

Next, to organise the information from gene lists into pathways, ROAST was applied to identify differentially regulated pathways between human and mouse cells by utilising a commonly used pathway database, namely REACTOME (Wu et al., 2010). When comparing 4 or 8 hpi to mock, about 500 differentially regulated REACTOME pathways were discovered across the three tested cell types (Figure 6-9). To compare these data for the three cell types, the number of pathways regulated by infection for each are shown in three-circle Venn diagrams (Figure 6-9). If the direction of regulation by infection for a modified pathway was the same in the comparison of two cell types, it was placed into the intersection. Other situations, such as different directions of regulation or regulation by only one of the cell types, were considered to be cell-type-specific. More uniquely regulated pathways were detected in the cross-species comparison and these accounted for 60-70% of all differentially regulated pathways (Figure 6-9). A relatively smaller number of uniquely regulated pathways were identified when comparing the two human cell types. This observation occurred at both times after infection. The top 20 pathways upregulated in MF but downregulated in both human cell types at 8 hpi are listed in Table 6-1 and ranked by number of genes. In summary, by these two analysis methods, the two human cell types were found to respond similarly to HSV-1 infection, while mouse cells had a distinct transcriptional response.

6.2.5.1 Mouse cells upregulate an antiviral pathway characterized by ISG expression, but human cell types downregulate this pathway during HSV-1 infection

According to Section 6.2.5, there were many differentially regulated pathways between human and mouse cells, however, we chose to focus on just one for a deeper analysis. The results of the ROAST analysis in the REACTOME database in Section 6.2.5 found that the pathway called "Antiviral mechanism by IFN stimulated genes" (hereafter referred to as the antiviral/ISG pathway) was upregulated in mouse cells but downregulated both in HFF and in MRC5. We chose this pathway for further analysis, because ISGs have diverse antiviral functions. Therefore, different regulation of this pathway between the two species may be a potential mechanism that explains the restricted growth in MF compared to the human cell types (Figure 6-1). The expression of each gene in the antiviral/ISG pathway was collected and combined into a boxplot (Figure 6-10). A significantly upregulated pattern was observed in MF at both times after infection. On the contrary, genes in this pathway were both significantly downregulated by HSV-1 infection at 8 hpi in the human cells (Figure 6-10).

In addition to viewing the data at the pathway level, genes that were significantly differentially regulated by HSV-1 infection at 4 and/or 8 hpi in HFF, MRC5 and MF within the antiviral/ISG pathway were extracted and then presented in a heatmap (Figure 6-11). As expected, HFF and MRC5 clustered together, while MF diverged from the human cells. This phenomenon was observed both at 4 and at 8 hpi. In particular, several signalling transducers and downstream effectors were found to be highly upregulated in MF at 8 hpi, including *Jak1*, *Stat2*, *Mapk1*, *Eif2ak2*, *Mx1* and *Mx2* (Figure 6-11B).

In order to validate this cross-species RNA-seq analysis, regulation of these genes by HSV-1 infection was further confirmed by qPCR (Figure 6-12). We included the kinase JAK1 and the transcription factor STAT2, because they act apically in type I IFN signalling pathways. In addition to classical JAK-STAT pathway, MAPK pathways are also activated by type I IFNs to induce ISG expression. Therefore, expression of MAPK1, a signalling component receiving signals from JAK1, was also tested to explore possible cross-talk between components in the antiviral/ISG pathway. We chose MX proteins and EIF2AK2, as downstream antiviral effectors, to understand the differences at the end of the antiviral/ISG pathway. In particular, MX genes were included as a control, because of that they have been found by others to be upregulated

in mouse embryonic fibroblasts (MEFs), but downregulated in human primary fibroblasts during HSV-1 infection (Pasieka et al., 2006; Peng et al., 2008).

The transcription of genes mentioned above was examined by qPCR and the regulation of each by HSV-1 infection showed a significant difference when comparing MF to HFF and to MRC5 at 8 hpi. Furthermore, some genes, such as *Stat2* and *Mx1*, were significantly upregulated by HSV-1 infection in MF compared with the two human cell types at 4 hpi. In summary, the data suggest that HSV-1 infection induces expression of genes in the antiviral/ISG pathway in mouse cells but not human cells.

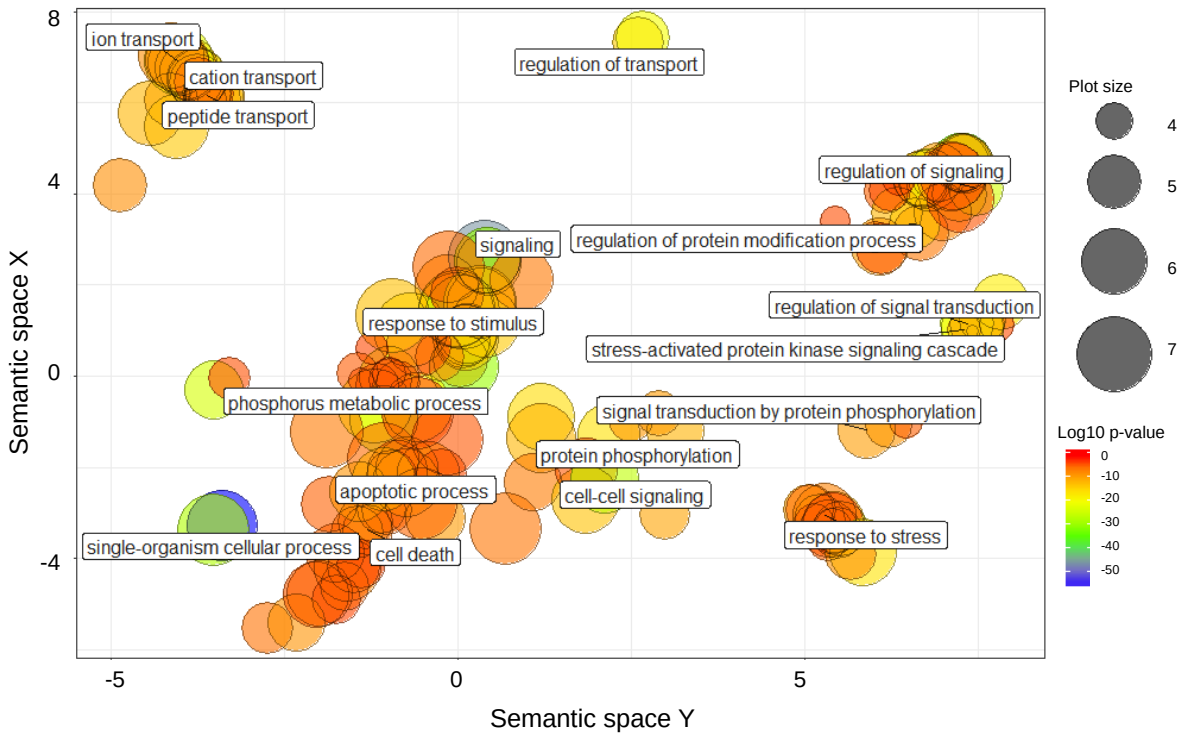

Figure 6-8. Gene ontology (GO) analysis visualised by REVIGO. GO terms enriched in the transcriptomes defined by differential regulation by HSV-1 infection between HFF and MF at 8 hpi were analysed. The results were visualised by REVIGO, where same and redundant GO terms were removed. The log10 p-value for each parent GO term is represented by the circle colour. The size of the circle indicates the number of enriched child GO populations contributing to the parent term. Semantic space was the outcome of multi-dimensional scaling, where similar GO populations clustered together.

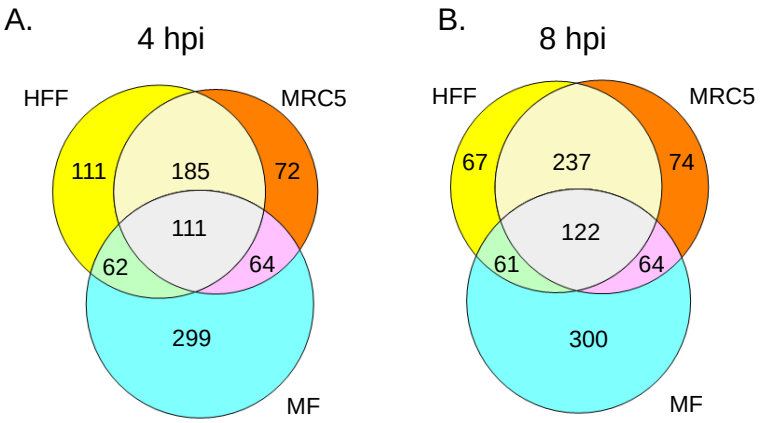

Figure 6-9. Pathways differentially regulated by HSV-1 between human and mouse cells. Pathways differentially regulated by HSV-1 infection were defined based on the pairwise comparison between mock and (A) 4 or (B) 8 hpi in HFF, MRC5 and MF with both p-value and FDR <0.05. Analyses were performed by the ROAST method using the REACTOME database.

Table 6-1. Pathways regulated by HSV-1 infection differentially between human and mouse cells.

Pathway name	Number of genes	p-value	FDR
REACTOME_RESPONSE_TO_ELEVATED_PLATELET_CYTOSOLIC_CA2_	109	0.001	0.001
REACTOME_ANTIVIRAL_MECHANISM_BY_IFN_STIMULATED_GENES	64	0.001	0.001
REACTOME_SIGNALING_BY_WNT	54	0.001	0.001
REACTOME_SPHINGOLIPID_METABOLISM	47	0.001	0.001
REACTOME_CHEMOKINE_RECEPTORS_BIND_CHEMOKINES	44	0.001	0.001
REACTOME_AQUAPORIN_MEDIATED_TRANSPORT	37	0.001	0.001
REACTOME_METABOLISM_OF_STEROID_HORMONES_AND_VITAMINS_A_AND_D	35	0.001	0.001
REACTOME_REGULATION_OF_WATER_BALANCE_BY_RENAL_AQUAPORINS	33	0.001	0.001
REACTOME_MYOGENESIS	31	0.001	0.001
REACTOME_PREFOLDIN_MEDIATED_TRANSFER_OF_SUBSTRATE_TO_CCT_TRIC	27	0.001	0.001
REACTOME_PERK_REGULATED_GENE_EXPRESSION	26	0.001	0.001
REACTOME_DNA_STRAND_ELONGATION	25	0.001	0.001
REACTOME_CA_DEPENDENT_EVENTS	24	0.001	0.001
REACTOME_SULFUR_AMINO_ACID_METABOLISM	22	0.001	0.001
REACTOME_HDL_MEDIATED_LIPID_TRANSPORT	21	0.001	0.001
REACTOME_SIGNALING_BY_BMP	20	0.001	0.001
REACTOME_OTHER_SEMAPHORIN_INTERACTIONS	20	0.001	0.001
REACTOME_GLYCOLYSIS	20	0.001	0.001
REACTOME_NEPHRIN_INTERACTIONS	20	0.001	0.001
REACTOME_HYALURONAN_METABOLISM	18	0.001	0.001

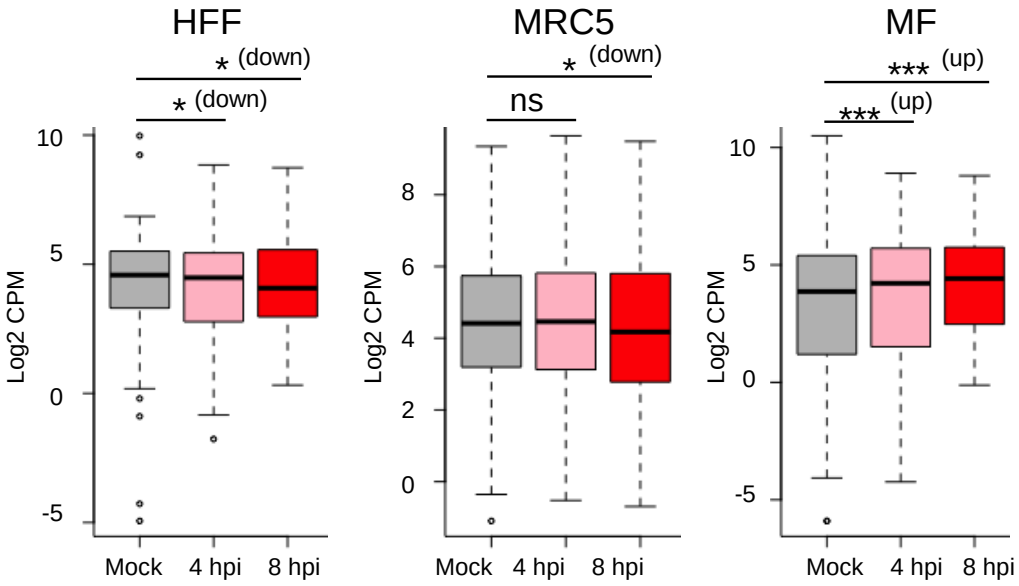

Figure 6-10. Regulation of gene expression in the antiviral/ISG pathway in HSV-1-infected HFF, MRC5 and MF. Log_2 CPM values of individual genes in the antiviral/ISG pathway at each condition were collected and plotted in boxplots. Grey, pink and red represent mock, 4 hpi and 8 hpi, respectively. *FDR <0.05, ***FDR <0.001 and ns, no significant difference.

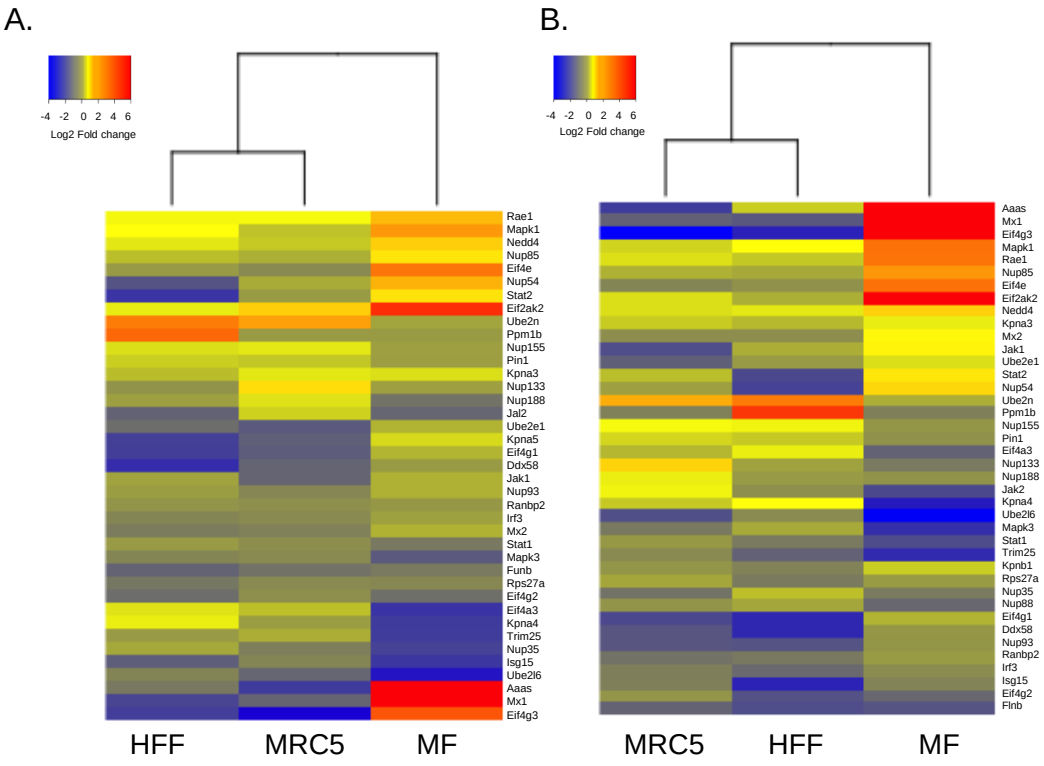

Figure 6-11. Profile of regulation of genes in the antiviral/ISG pathway by HSV-1 infection. Genes significantly up- or downregulated regulated by HSV-1 infection at (A) 4 and (B) 8 hpi in each cell type are illustrated in heat maps. The log_2 fold change of each gene relative to mock infected cells is shown. Blue represents lower regulation and red indicates higher regulation.

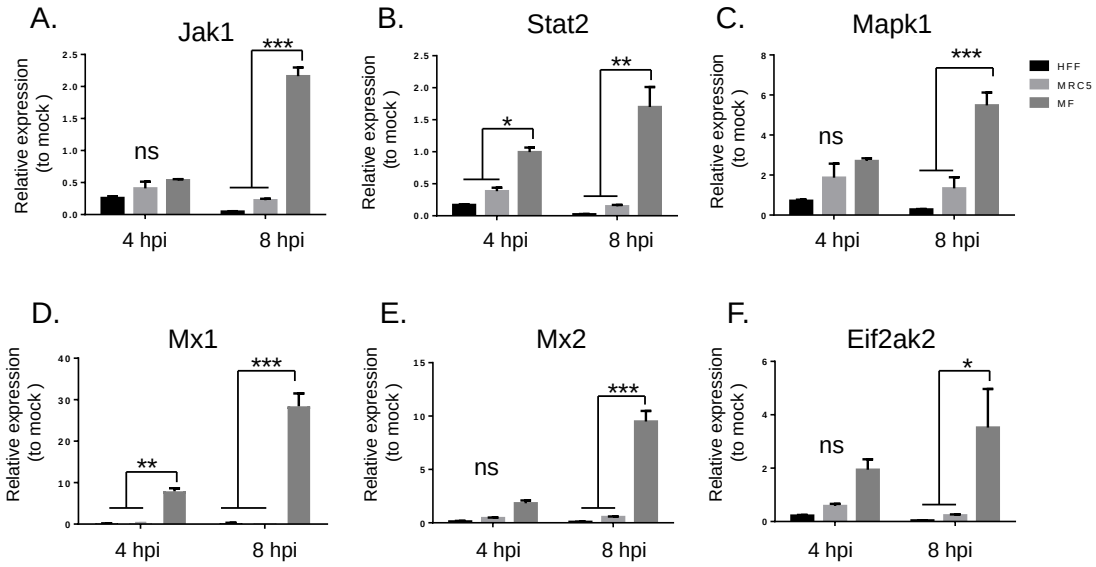

Figure 6-12. Validation of the cross-species RNA-seq analysis by qPCR. Selected genes from the antiviral/ISG pathway regulated by HSV-1 infection in mouse and human cells (n=3) were confirmed by qPCR, including (A) *Jak1*, (B) *Stat2*, (C) *Mapk1*, (D) *Mx1*, (E) *Mx2* and (F) *Eif2ak2*. Differential regulation was determined by the $2^{-\Delta\Delta CT}$ method based on relative expression between mock and infected samples, followed by normalisation to 18S rRNA. One-way ANOVA with Tukey's tests was applied to evaluate differences between cell types. The results are expressed as mean ± SEM. *p <0.05, **p <0.01, ***p <0.001 and ns, no significant difference.

6.2.6 Regulation and importance of *Jak1* in human and mouse cells in HSV-1 infection

6.2.6.1 *Jak1* is essential for generating the human-mouse difference in HSV-1 replication

We then directly investigated whether *Jak1* plays a role during HSV-1 infection in human and mouse cells, because this protein acts furthest upstream in the IFN signalling pathway. HFF, MRC5, C57BL/6 MF and BALB/c MF were transfected with empty plasmids or indicated lentiCRISPR vectors with gRNA targeting the human or mouse *Jak1* gene. Knockout efficiency was evaluated by qPCR and WB (Figure 6-13A and Figure 6-13B). Knockout efficiency was at least 80% in each culture based on the qPCR analysis (Figure 6-13A) and JAK1 protein was not detected in human and mouse *Jak1* knockout cells (Figure 6-13B). When *Jak1* was depleted in the cells, HSV-1 replicated equally well among HFF, MRC5 and MF (Figure 6-14A). This observation was then extended to MF derived from BALB/c mice, which gave consistent results with those observed with C57BL/6 MF cells (Figure 6-14B).

To further confirm the importance of JAK1, we examined whether JAK1 activation influences the replication of HSV-1 in human and mouse cells. HFF, MRC5, C57BL/6 MF and BALB/c MF were treated with Ruxolitinib (100 nM), a selective JAK1/2 inhibitor and infected with HSV-1 for 24 hours. Treatment with Ruxolitinib led to HSV-1 replication that was equivalent among the tested cell types (Figure 6-15). However, treatment with vehicle did not alter the usual pattern of reduced HSV-1 replication in mouse cells compared with human cells. Collectively, the data indicate that upregulation and activation of JAK1 are essential factors contributing to the human-mouse difference in HSV-1 replication.

A.

B.

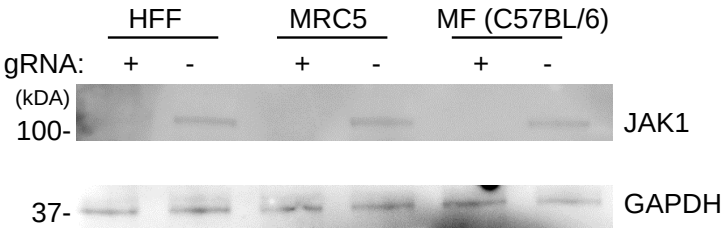

Figure 6-13. Knockout efficiency of lentiCRISPR targeting *Jak1*. Triplicates of HFF and MRC5 or MF from three individual mice were transfected with empty lentiCRISPR vectors or lentiCRISPR vectors designed to knockout *Jak1* gene. Each transfected cell type was harvested for investigation of knockout efficiency by (A) qPCR in *Jak1* or (B) Western blotting (WB) for JAK1 protein level. One-way ANOVA with Tukey's tests was applied to determine differences between means. The results are expressed as mean ± SEM. Graphs of WB are representative of three independent experiments. ns, no significant difference.

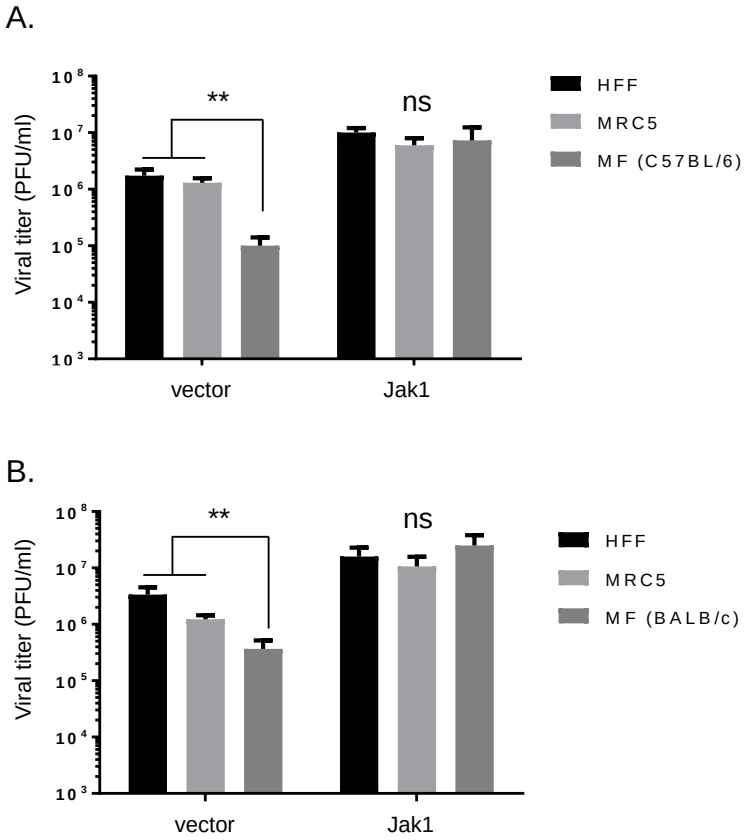

Figure 6-14. Importance of JAK1 in the human-mouse difference during HSV-1 replication. Triplicates of HFF and MRC5, or (A) C57BL/6 MF and (B) BALB/c MF cells from three individual mice were transfected with empty lentiCRISPR vectors or lentiCRISPR vectors targeting *Jak1*, followed by inoculation of HSV-1 pICP47 recombinant virus at an MOI of 0.5 for 24 hours. Infected cell lysates were then collected and prepared for determination of viral titres by plaque assays. One-way ANOVA with Tukey's tests was applied to test differences between means (**p <0.01). The results are expressed as mean ± SEM. ns, no significant difference.

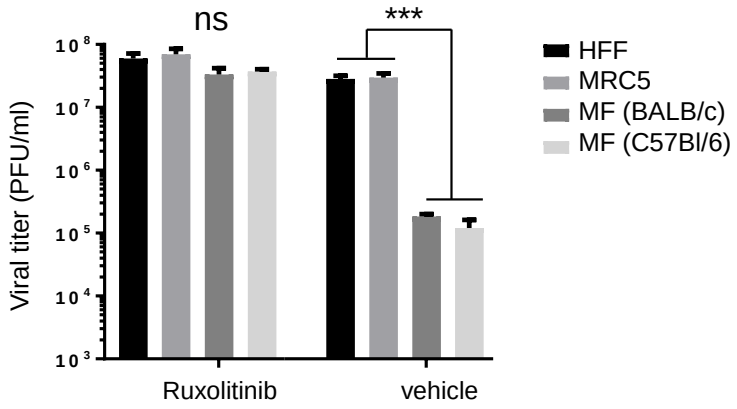

Figure 6-15. Effect of JAK1 inhibitor on HSV-1 infection. Triplicates of HFF and MRC5 or C57BL/6 MF and BALB/c MF from three individual mice were infected with wild-type HSV-1 at an MOI of 0.01 for 24 hours in the presence of 100 nM Ruxolitinib or DMSO vehicle control. Following this, viral titres were measured using plaque assays. One-way ANOVA with Tukey's tests was used to evaluate differences between means. The results are expressed as mean ± SEM. ***p <0.001 and ns, no significant difference.

6.2.7 HSV-1 virion host shutoff protein vhs, but not ICP27, is an important viral gene regulating the human-mouse difference

Host species differences in virus infection can occur if a viral immune evasion strategy functions more effectively in one species than another. This can occur if one species is the natural host and the other species does not faithfully model an interaction that is the result of a co-evolved host response and viral counter-response. HSV-1 has several strategies to inhibit the IFN signalling pathway at multiple sites. Of particular interest, HSV-1 vhs has been shown to be responsible for the reduction of JAK1 and STAT2 protein expression (Chee and Roizman, 2004). Further, HSV-1 IE protein ICP27 may cooperate with vhs to regulate mRNA stability, but also decreases the phosphorylation of STAT1 and inhibits the accumulation of STAT1 in the nucleus (Yokota et al., 2001; Johnson et al., 2008). Therefore, we explored whether these viral genes might regulate Jak1 differently in human and mouse cells.

6.2.7.1 HSV-1 vhs and ICP27 decrease *Jak1* upregulation, but only vhs is required for the species-specific difference in *Jak1* upregulation

To directly test whether vhs and/or ICP27 might impact *Jak1* expression in response to HSV-1 differently across species, we used virus strains with these genes ablated. The viruses were a truncation mutant of vhs (ΔSma) and a deletion mutant of ICP27 (5dl1.2) (McCarthy et al., 1989; Read et al., 1993). Both of these HSV-1 mutants were generated from HSV-1 strain KOS (Corcoran et al., 2006). HFF, MRC5 and MF were infected with wild-type HSV-1 strain KOS, ΔSma or 5dl1.2 and *Jak1* upregulation was determined by qPCR.

In the ICP27 deletion mutant, *Jak1* upregulation was observed in all cell types, but was still significantly higher in MF than in the human cells, suggesting that ICP27 limits *Jak1* expression during HSV-1 infection, but does so similarly in human and mouse cells (Figure 6-16). Conversely, during vhs mutant virus infection, *Jak1* upregulation was increased in all cell types and strikingly was induced to a comparable degree irrespective of host species (Figure 6-16). These data suggest that ICP27 and vhs act to limit *Jak1* expression in response to HSV-1, but vhs has the stronger effect. More importantly here, vhs is necessary for the differential upregulation of *Jak1* in mouse compared with human cells.

6.2.7.2 HSV-1 vhs regulates the protein expression and the activation of JAK1 during HSV-1 infection

We extended this finding to investigate the protein level and activation of JAK1 during HSV-1 infection. HFF, MRC5 and MF derived from C57BL/6 and BALB/c were infected with wild-type HSV-1 and the vhs mutant virus and JAK1 protein level and phosphorylation status were analysed by WB using anti-JAK1 and anti-phosphorylated JAK1 antibodies (Figure 6-17A and Figure 6-17B). Quantification of each band was performed by densitometry and levels of basal and activated JAK1 was normalised to GAPDH (Figure 6-17C and Figure 6-17D). Wild-type HSV-1 induced significantly higher levels of basal and activated JAK1 in MF compared with HFF and MRC5. Further, this observation was found consistently in MF collected from C57BL/6 and BALB/c strains. By contrast, in the absence of vhs, protein expression and phosphorylation of JAK1 was similar among the tested cell types. These data confirm the qPCR results above, supporting the conclusion that vhs is required for the species-specific difference in JAK1 expression and function observed during HSV-1 infection.

6.2.7.3 Growth kinetics of HSV-1 ICP27 and vhs mutants in human and mouse cells

Finally, to investigate whether the differential effect of vhs in human and mouse cells extends to HSV-1 replication, a multi-step growth analysis was performed using the two recombinant HSV-1 viruses. In HHF, MRC5 and MF, attenuated yields were detected when HSV-1 was defective for ICP27 (Figure 6-18A). Consistent with published results for Vero and 3-3 cells (McCarthy et al., 1989). However, even with ICP27 deletion, HSV-1 still replicated more efficiently in human cells than in mouse cells from 72 hpi (Figure 6-18A). By contrast, the growth kinetics of the HSV-1 vhs mutant virus were the same irrespective of species. The ΔSma viral titres were reduced about 1000-fold and 10-fold compared to the wild-type virus in human and mouse cells, respectively (Figure 6-18B). Taken together, the data indicate that vhs is required for the difference in HSV-1 replication seen between human and mouse cells. This is consistent with a model in which vhs antagonises *Jak1* expression and/or function more effectively in human versus mouse cells.

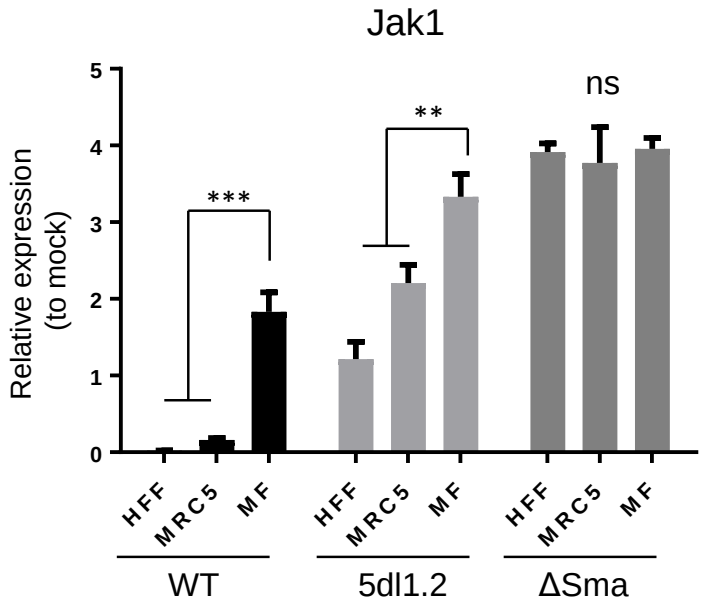

Figure 6-16. Regulation of Jak1 by HSV-1 vhs and ICP27. Triplicates of HFF and MRC5 or MF cells from three individual mice were infected with wild-type, ICP27 deletion mutant (5dl1.2) or vhs mutant virus (ΔSma) at an MOI of 0.5 for eight hours. Cell lysates were subjected to RNA extraction, cDNA synthesis and qPCR analysis for *Jak1* RNA levels, which were shown relative to mock infected cells. One-way ANOVA with Tukey's tests was used to examine differences between means. The results are expressed as mean ± SEM. **p <0.01, ***p <0.001 and ns, no significant difference.

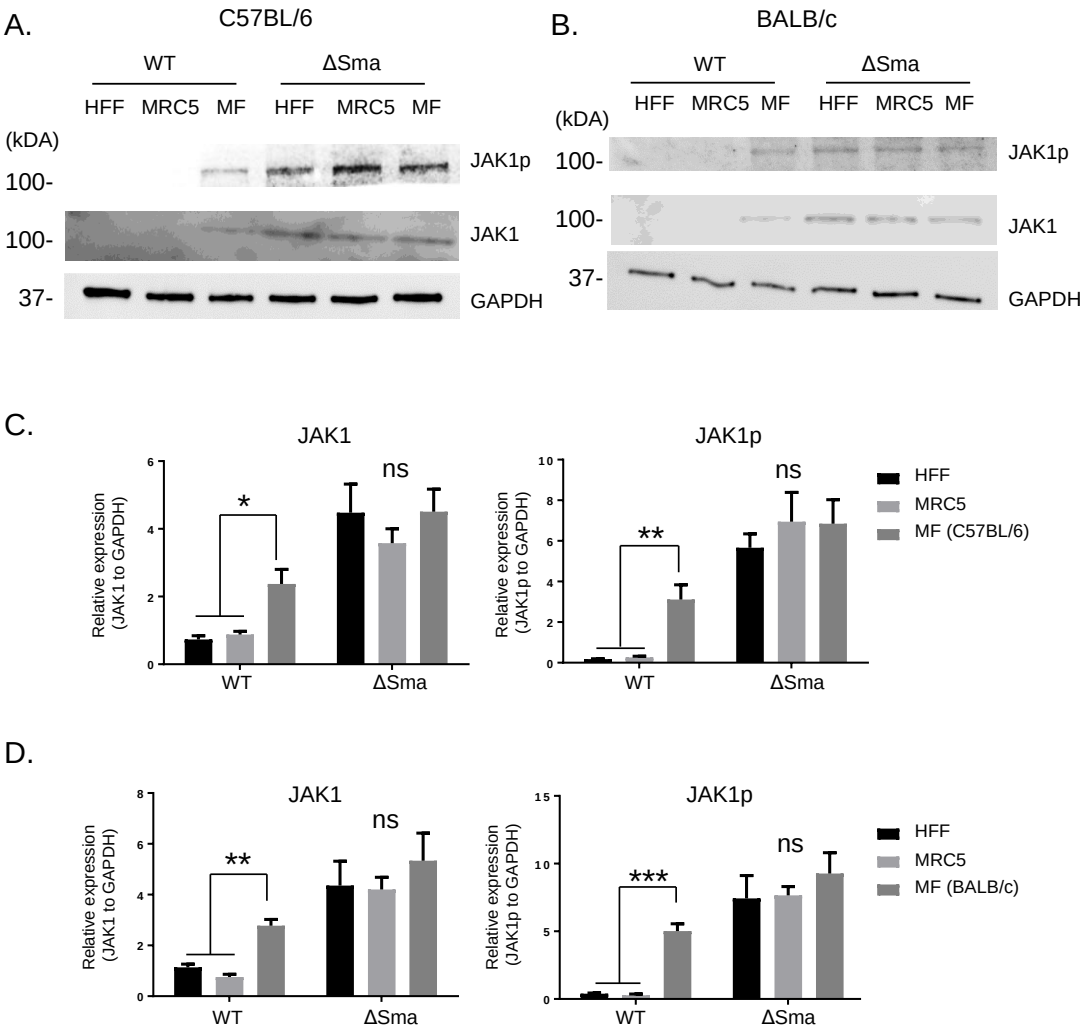

Figure 6-17. Activation of JAK1 in human and mouse cells during HSV-1 infection. Triplicates of HFF and MRC5 or MF from three individual mice prepared from (A, C) C57BL/6 or (B, D) BALB/c strains were infected with wild-type (WT) or vhs mutant (ΔSma) at an MOI of 0.5 for eight hours. Following this, Western blotting analysis (WB) for JAK1 protein expression (JAK1) and activation (JAK1p) was performed. Images of WB are representative of three independent experiments. Quantification of JAK1, JAK1p and GAPDH in each band from three replicates was conducted by densitometry using ImageJ. A linear model was used to evaluate differences between human and mouse cells. The results are expressed as mean ± SEM. *p <0.05, **p <0.01 and ns, no significant difference.

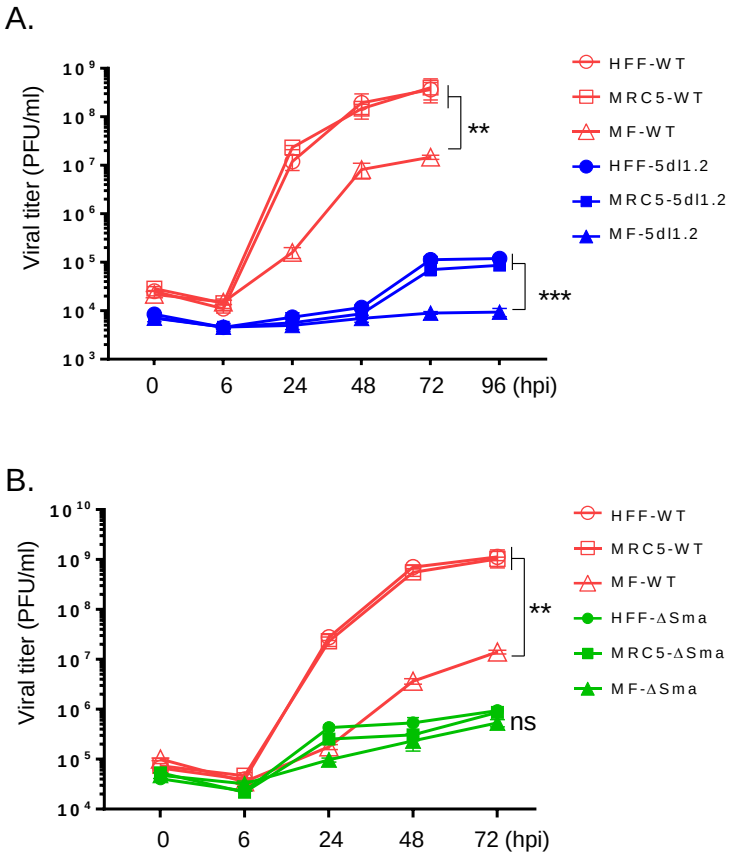

Figure 6-18. HSV-1 vhs is required for different growth of HSV-1 in human and mouse cells. Triplicates of HFF and MRC5 or MF cells from three individual mice were infected with wild-type (WT) HSV-1, (A) ICP27 deletion mutant (5dl1.2) or (B) vhs mutant (ΔSma) at an MOI of 0.01 and were harvested at indicated time points. Viral titres were then measured by plaque assays. Two-way ANOVA with Tukey's tests was employed to test differences between means in growth curves. The results are expressed as mean ± SEM. **p <0.01, ***p <0.001 and ns, no significant difference.

6.3 Discussion

For HSV-1, several antiviral reactions, such as programmed cell death and antigen presentation, have been found to be differentially regulated between human and mouse cells (Jugovic et al., 1998; Guo et al., 2015b; Huang et al., 2015; Yu and He, 2016). Furthermore, microarray data from two different studies have separately showed that HSV-1 regulates ISGs expression in opposing directions, including *Mda5*, *Mx* and *Gbp* family members in primary mouse embryonic cells and human fibroblasts (Pasieka et al., 2006; Peng et al., 2008). In this chapter, the human-mouse difference during HSV-1 infection was comprehensively investigated by RNA-seq and analysed by using a computational pipeline for cross-species analysis. Raw RNA-seq data from primary male mouse skin fibroblasts were extracted from Section 3.2.5 and compared to primary male human skin cells (HFF) in this chapter. Moreover, we included another commonly used cell line for propagation and study of HSV-1, namely MRC5, an immortalised male human cell line (Earnshaw et al., 1992; Harkness et al., 2014). Therefore, the baseline of the difference between the two human cell types could be set as a standard and control to more fairly evaluate the extent of differences between primary human and mouse cells. At the beginning of this chapter, our data showed greater viral yields in human cells than in mouse cells (Figure 6-1), which further encouraged us to thoroughly understand the molecular mechanism regulating the human-mouse difference in HSV-1 infection. RNA-seq analysis based on the shared orthologues between humans and mice consistently showed that the cross-species difference was larger than the difference between the two human cell types (Figure 6-5 and Figure 6-6). Importantly, this customised pipeline found previously reported human-mouse differences in the apoptotic process [GO:0006915] and cell death pathways [GO:0008219] (Guo et al., 2015b; Huang et al., 2015), indicating fair sensitivity and specificity of our tailored analysis of the cross-species data.

The pathway that took our immediate interest was the antiviral/ISG pathway, which was upregulated in mouse cells but downregulated in the two human cell types (Figure 6-10). We then selected *Jak1* as our candidate gene as JAK1 receives convergent signals at one of the most upstream positions of the IFN signalling pathway (Schindler et al., 2007; Babon et al., 2014). Initially, JAK1 was generally thought to be activated due to the interaction of cytokines and IFNs with their specific receptors, resulting in cellular signalling to recruit and subsequently activate JAKs by auto- or trans-phosphorylation (Miyazaki et al., 1994; Bellucci et al., 2015). However, our preliminary data indicate that knockout of IFNAR and secreted soluble proteins in the

supernatant of HSV-1-infected cells were not sufficient to eliminate the difference in *Jak1* upregulation between human and mouse cells (data not shown). These results suggest that the human-mouse difference in *Jak1* expression is IFN-independent and could be due to intrinsic stimulation. In addition to cytokines, previous reports have revealed a binary regulation of JAK-STAT signalling by cytokine- and calcium-dependent pathways (Sengupta et al., 1996; Wang et al., 2008a). Coincidently, HSV infection can trigger calcium-signalling pathways and the phosphorylation of cellular proteins may occur in conjunction with calcium signalling (Cheshenko et al., 2003; Cheshenko et al., 2013; Cheshenko et al., 2014). However, to date, there is no clear evidence showing whether JAK1 activation is regulated by calcium transport during HSV-1 infection. According to the results of our GO analysis in Figure 6-8, human and mouse cells react differently in ion transport [GO:0006811], cation transport [GO:0006812] and protein phosphorylation [GO:0006468]. The above findings suggest that we can further investigate the link between JAK1 phosphorylation and calcium signalling in primary human and mouse skin fibroblasts. For example, by treating cells with a cell-permeant calcium chelator to block calcium transport, we may understand whether calcium plays a role in the induction of phosphorylated JAK1 during HSV-1 infection.

When *Jak1* was deficient, HSV-1 replicated equally well in human and mouse cells (Figure 6-14), indicating that *Jak1* is essential for regulating the human-mouse difference in HSV-1 replication. Previous data from HSV-1 mutants showed that the decrease in JAK1 is regulated by vhs during early infection (Chee and Roizman, 2004). As ICP27 collectively regulates mRNA stability with vhs during HSV-1 infection, it is likely that ICP27 affects *Jak1* upregulation as well (Brown et al., 1995; Chee and Roizman, 2004; Taddeo et al., 2010). Herein, our results revealed that both ICP27 and vhs are important for restriction of *Jak1* upregulation, but only vhs can restore *Jak1* in mouse cells to a similar level as those in the two human cell types (Figure 6-16). This finding correlates with the growth phenotypes of vhs mutant virus among HFF, MRC5 and MF (Figure 6-18), indicating that vhs is a key viral gene in the human-mouse difference. Several mechanisms can be used to interpret the different efficiency of vhs in the degradation of *Jak1* between human and mouse cells, although detailed experiments are required to provide further support for these mechanisms. Previous studies have suggested that the rate of vhs-mediated mRNA degradation is dependent on the cell type (Saffran et al., 2010; Dauber et al., 2011). A difference in vhs activity can be identified between cells in two close species, or even in the same species (Dauber et al., 2011). It has been shown that the growth defect of HSV-1 vhs mutants is dependent on differences in the translation machinery in the respective cell (Saffran et

al., 2010; Eaton et al., 2014). In addition, the efficiency of the interaction of vhs with cellular translation factors, including eukaryotic initiation factors (eIFs), might differ between human and mouse cells. This may also influence the capacity of vhs to degrade mRNA, as the association between vhs and eIFs guides vhs to the preferred cleavage sites (Feng et al., 2005; Page and Read, 2010).

In addition to *Herpesviridae*, accumulating evidence has shown that there are human-mouse differences in the regulation of innate immune responses by other viruses (Zschaler et al., 2014). Species-specific activity of antiviral genes has also been well-documented in HIV, a virus adapted to replicate in human cells (Sawyer et al., 2004; Sawyer et al., 2005; McNatt et al., 2009). For instance, there is a resistance of non-human tetherin proteins to antagonise HIV infection such that magnitude of the reduction in HIV yield varies depending on what species of the tetherin protein is overexpressed (McNatt et al., 2009). Likewise, IFN antagonism of ZIKV seems to be species dependent (Aliota et al., 2016; Rossi et al., 2016). In support of this, ZIKV infection results in the degradation of STAT2 in primary human fibroblasts, but STAT2 protein expression is not affected in MEFs (Hamel et al., 2015). Moreover, no detectable virus production was found in wild-type MEFs infected with ZIKV, but INFAR-deficient MEFs supported ZIKV replication. These data indicate that both STAT2 and IFNAR are essential for maintaining intact IFN signalling during ZIKV infection and species-specific IFN countermeasures may further contribute to the control of ZIKV replication (Morrison and Diamond, 2017; Dong and Liang, 2018). In another case, the NS1 protein of influenza B virus counteracts host antiviral responses via binding to ISG15. NS1 also exhibits species-specific binding and it interacts with human and non-human primate ISG15, but not mouse and canine counterparts. Sridharan et al. (Sridharan et al., 2010) identified that the small 5-amino acid hinge between the two ubiquitin-like domains of ISG15 is critical for the species-specific binding with Influenza B virus NS1 protein. Furthermore, a recent study found that ISG15 plays a role in antiviral immunity in mice, but displays more complicated functions in humans (Speer et al., 2016). ISG15-deficient individuals exhibit a persistent elevation in ISG expression and resist viral infection from various virus families, in contrast to what has been observed in ISG15-deficient mice. The difference in viral susceptibility between ISG15-deficient humans and mice was further explained by a species-specific interaction of ISG15 with ubiquitin specific peptidase 18, a negative regulator of IFN-α/β signalling which downregulates the IFN-α/β reactions in humans, but not in mice (Zhang et al., 2015; Speer et al., 2016).

In summary, here we performed a comprehensive analysis of differentially regulated pathways between human and mouse cells during HSV-1 infection. Our customised pipeline for cross-species analysis of RNA-seq data showed many differences between the two species, including some that were already known and a previously unexplored difference in the IFN signalling pathway and ISGs. Furthermore, we found that HSV-1 vhs has a species-specific immune evasion role via more effective suppression of *Jak1* in human cells than in mouse cells. These data provide new leads for further investigation of the differences in responses of human and mouse cell to HSV-1 infection. They also suggest that the role of IFN and ISGs differ in significant ways between these species and this needs to be taken into account in interpreting mouse models of HSV-1 diseases.

Chapter 7. Final discussion

The work in this thesis began by considering some of the assumptions that are commonly made in the virology literature. The first one was that the sex of cells in culture is not important and the second is that species differences can be ignored, even if they are more often acknowledged. We present the first comprehensive analysis of these two factors for HSV-1. Herpesviruses are distributed worldwide and the global burden from HSV-1 diseases is huge (Looker et al., 2015a; Looker et al., 2015b). However, there are various aspects of HSV-1 infection that remain unclear. The outcome of infection with many pathogens differs between males and females, but the basis of this in HSV-1 is not well-explored. To date, most studies *in vivo* indicate that sex hormones influence the immune system and may play the role in the control of viral infections (Klein and Flanagan, 2016; Ghosh and Klein, 2017). These sex-determined differences can operate at the level of individual cells. Yet, sex is rarely considered as a variable in studies that aim to reveal the molecular mechanisms of viral disease *in vitro*. Therefore, we investigated the ways in which chromosomal, rather than hormonal, differences influence the outcome of HSV-1 infection in culture. In addition, given that many primary infections by HSV-1 can be asymptomatic and the neurotropic properties of HSV-1 make it hard to obtain information from infected humans, researchers extensively use mouse models to study HSV-1 diseases. However, mice are not a natural host for this virus and more and more papers show cross-species differences in response to viral infection. Therefore, it is important to have comprehensive knowledge of cross-species differences between mice and humans in HSV-1 infection.

At the time we began our study (July, 2015), there were only two research articles using RNA-seq to study HSV-1. The first paper utilised this method to measure the viral gene expression of wild-type HSV-1 and IE gene mutant viruses simulating latent infection in immortalised human embryonic lung cells (MRC5) and primary mouse trigeminal neurons (Harkness et al., 2014). This study revealed that MRC5 cells have more restricted viral transcription than trigeminal neurons. There were also divergences in the cascade expression of early genes in lytic infection. Moreover, genes adjacent to LAT were especially actively transcribed during the latent period in neurons (Harkness et al., 2014). The other paper used RNA-seq to exploit ribosome profiling and 4-thiouridine (4sU)-tagging of freshly made RNA to measure global changes in RNA processing and transcription during HSV-1 lytic infection in human foreskin fibroblasts (Rutkowski et al., 2015). The results showed that lytic infection by HSV-1 can specifically interrupt transcription termination of cellular genes, rather than viral ones, and abnormal splicing events were induced by HSV-1 infection independent of vhs or

ICP27 proteins (Rutkowski et al., 2015). In this thesis, we exploited RNA-seq to acquire whole transcriptomic changes at deeper resolution as sex-specific and/or human-mouse differences might be subtle during HSV-1 infection in cultures.

Using a model system in which HSV-1 was used to infect primary mouse skin fibroblasts, we uncovered several findings that were due to cell-intrinsic differences between the two sexes. During low MOIs of infection (MOI=0.0001 and 0.0003), HSV-1 was found to replicate better in male cells, suggesting that the two sexes have different responses to HSV-1 infection, and female cells may induce stronger antiviral responses. Further, serial passage of HSV-1 on male cells produced a strain of virus that replicated more efficiently on male than on female cells, and vice versa was also true for HSV-1 serial passaged on female cells. The data showed that HSV-1 is able to adapt to grow more efficiently in cells of one sex, in as few as around 10 serial passes. This was surprising because HSV-1 as a dsDNA virus with a high fidelity polymerase, has been considered in the past to have a slow rate of evolution (McGeoch, 1987; Umene and Sakaoka, 1999). However, several studies now suggest that the original estimates of HSV-1 evolutionary rate may be too low because continuous positive selection was not considered and the data were not measured independently from the hypothesis of codivergence (Drake and Hwang, 2005; Firth et al., 2010; Hughes et al., 2010).

Much less is known about the adaptive strategies of large DNA viruses as compared to RNA viruses. In order to counteract host immune responses, RNA viruses have high mutation rates and short generation time, leading to rapid adaptation and expansion of tropism in various animal species (Vignuzzi et al., 2006; Fitzsimmons et al., 2018). However, DNA viruses evolve more slowly than RNA viruses, but they generate highly competent lineages (Drake and Holland, 1999; Lynch, 2010). Historically, a key measure of the evolutionary rate of herpesviruses was from the analysis of 242 HSV-1 samples from six different countries (Sakaoka et al., 1994; Firth et al., 2010). A substitution rate of 3.5×10^{-8} substitution/site/year was estimated (Sakaoka et al., 1994). In addition to nucleotide substitution, Elde et al. revealed that DNA viruses can adapt to a new host environment through intermediates of transient gene expansion (Elde et al., 2012), which explains a variety of observations in the gene expansion of myxoma virus, herpesviruses and chemically induced gene amplification in vaccinia (Slabaugh et al., 1989; Searles et al., 1999; Kerr et al., 2010). Although we did not find any evidence that the experimental evolution strategy in male and female cells induced gene expansion in the genome of herpesvirus, specific substitutions were identified due to selection pressure driven by sex. For example, sex pressure in mouse skin fibroblasts targeted HSV-1 glycoproteins, such as gH (T132H) in male and gE (S477L) in female

passage viruses .Mutations in the gE and gH have been shown to affect HSV entry and cell fusion (Dingwell et al., 1994; Fan et al., 2015). Interestingly, gH(T132H) in male passage viruses was predicted to be a frameshift mutation, which may lead to a conformational functional change of gH. More experiments are required to investigate this issue, although insertion mutations of HSV-1 gH is relatively tolerant and allow normal processing and transport of glycoproteins complex to the cell surface (Jackson et al., 2010). Furthermore, both male (D67N) and female (L344F) passage viruses have nucleotide changes in UL48 (VP16) as compared to the parent virus that was used for infection. VP16 is a transcription factor of HSV-1 that is involved in the activation of the viral IE genes (Triezenberg et al., 1988a; Triezenberg et al., 1988b). Based on recent studies, VP16 plays a role in regulation of host innate immune responses, such as blocking the production of type I IFNs by inhibiting NF-κB activation and interfering with IRF3 translocation (Xing et al., 2013; Zheng and Su, 2017). Additionally, we found that VP16 worked cooperatively with ICP34.5 to upregulate *Xist* during HSV-1 infection. Thus, it is tempting to speculate that the mutations in female passage viruses may eliminate the antiviral functions of VP16. Female passage viruses received a point mutation in US3 (G341R) after 10 serial passages and this mutation was maintained in passage 30. US3 has been shown to dampen NF-κB activation, modulate virion packaging via VP11/12 phosphorylation and regulate phosphatidylinositol 3-Kinase/Akt signalling activity (Eaton et al., 2014; Wang et al., 2014). However, these mutations need to be confirmed by Sanger sequencing in the future. Further, more experiments are required to assess whether these mentioned mutations are necessary in the sex-adapted HSV-1 viruses by reverting nucleotide changes back to the parent sequence and examining the growth on male and female cells. To investigate whether a mutation is sufficient for the adaptation, HSV-1 pICP47 recombinant virus should be modified to match the mutation found in the sex-adapted HSV-1 viruses, and growth on male and female cells should be tested.

Given that evolution pressure from a specific sex leads to different mutations in the HSV-1 genome, and HSV-1 replicates more efficiently in male than in female cells, RNA-seq was utilised to identify mechanisms that may explain these observations. Pathway analysis revealed that the two sexes respond to HSV-1 infection distinctively in various ways, including cancer, metabolism and immunity. In particular, female cells induced cytosolic DNA-sensing pathway to a higher degree than male cells, which could be a potential explanation for the different growth phenotypes between the two sexes. We confirmed that one DNA sensor (cGAS), two RNA sensors (RIG-I and MDA5) and two IRFs (IRF1 and IRF7) and one signalling adaptor (TBK1) were upregulated to a greater degree in female cells, at both RNA and protein levels. Previous

reports have shown that HSV can be recognised by cytosolic DNA and RNA receptors (Chew et al., 2009). cGAS is a multifunctional protein that mediates various biological process, including cytosolic sensing, cellular senescence and cancer formation (Xiao and Fitzgerald, 2013; Schoggins et al., 2014; Gluck et al., 2017). For instance, HSV-1 triggers cGAS production and subsequent activation of IRFs in both murine and human cell lines (Wu et al., 2013). Depletion of cGAS decreases IRF3 activation during HSV-1 infection, and thereby, cGAS acts as a cytosolic DNA sensor that recognises HSV-1 in infected cells. Likewise, evidence indicates that another DNA sensor, IFI16, is involved in multiple mechanisms to sense HSV-1 in a cell-type-dependent manner (Unterholzner et al., 2010; Horan et al., 2013). IFI16 can recognise viral DNA in both the cytoplasm and nucleus to induce type I IFN production and inflammatory cytokines, indicating that IFI16 is a restricting factor for HSV-1 replication (Unterholzner et al., 2010; Conrady et al., 2012). In our RNA-seq data, IFI16 was downregulated in male cells but not in female cells in response to HSV-1 infection (data not shown). This observation in some way also supports the finding that female cells induce higher cytosolic sensing at the beginning of HSV-1 infection. Likewise, the connection between HSV-1 and RIG-I-like receptors is supported by data showing that HSV-1 replicates more efficiently in human cells lacking a functional RIG-I (Cheng et al., 2007). MDA5 has been reported to recognise HSV-1 and play an essential role in HSV-1-induced type I IFNs and cytokine production (Melchjorsen et al., 2010; Xing et al., 2012b). In this thesis, we found that both RIG-I and MDA5 were important in the upregulation of viperin in mouse skin fibroblasts, although neither of them were required for the sex difference in HSV-1 replication. Although cytosolic DNA and RNA sensors have specificities for different ligands, they both induce a signalling pathway that triggers the production of type I IFNs and ISGs (Wu and Chen, 2014; Radoshevich and Dussurget, 2016). Multiple cellular recognition events lead to signal transduction which eventually converges on TBK1 or NFκB signalling (Akira et al., 2006; Paludan et al., 2011). The induction of these kinases results in the activation of IRFs leading to the production of type I IFNs and ISGs, whose ultimate role is to restrain virus replication and spread through the initial establishment of an antiviral state (Ma and He, 2014).

The general understanding is that IFN expression can act in both autocrine and paracrine manners to amplify ISG expression (Schoggins and Rice, 2011; Wang et al., 2017), but ISGs can be induced directly upon viral infection in the absence of IFN signalling (Collins et al., 2004; Noyce et al., 2011). For example, Paladino et al. proposed a model for an IFN-independent response to entry of virus when a low multiplicity inoculation is used in primary fibroblasts. In this model, the entry of the

enveloped virus particles is sufficient to induce a subset of ISGs in an IFN-independent manner, indicating that innate antiviral pathways can act before or in the absence of type I IFNs in epithelial cells (Paladino et al., 2006; Iversen et al., 2016). This hypothesis is correlated with our findings where viperin, an ISG that has well-documented antiviral activity against a broad spectrum of viruses (Helbig and Beard, 2014), was induced in IFNAR knockout fibroblasts after a low multiplicity infection with HSV-1. In addition, we found that IRFs, including IRF1, IRF3 and IRF7, were all important for viperin regulation at the initial stage of HSV-1 infection in mouse skin fibroblasts. This confirms the existence of unidentified receptors and ligands that are able to activate an IRF and ISGs (Collins et al., 2004; Noyce et al., 2011). IRF1 may control IFN-independent signalling events leading to ISG upregulation and antiviral immunity given that when *Irf1* was depleted in mouse fibroblasts, viperin level was abolished during HSV-1 infection. As cytosolic sensors themselves act substantially in cooperation with IRFs to upregulate ISG expression in an IFN-independent manner (Fitzgerald, 2011; Seo et al., 2011a; Duschene and Broderick, 2012), we then further investigated this hypothesis and found that IRF1 acts upstream of cytosolic sensing via mediation of *cGAS* transcription, thereby affecting viperin upregulation. This adds another layer of complexity in the role of cGAS in innate immunity.

TBK1 is a key factor mediating the sex difference in antiviral responses to HSV-1. TBK1 functions as an adaptor kinase that receives upstream inputs and modulates downstream outputs to transduce signals in various signalling pathways, including innate immunity and cell proliferation (Li et al., 2011; Ou et al., 2011). Due to the importance of TBK1 in antiviral immunity, HSV-1 has evolved several proteins to inhibit TBK1-mediated pathways. Ma et al. reported that ICP34.5 inhibits TBK1 through its N-terminus, which facilitates virus replication and neuroinvasion *in vitro* and *in vivo* (Ma et al., 2012). Moreover, HSV-1 US11 precludes the access of TBK1 to the IFN promoter, and therefore, suppresses expression of type I IFNs and ISGs in human cells overexpressed with US11 (Liu et al., 2018). In order to identify an upstream regulator of TBK1 leading to the sex difference in HSV-1 infection, we screened differentially regulated transcription factors on the sex chromosomes and identified that ZBTB33 negatively mediates *Tbk1* expression, and thus, antiviral responses are maintained at a higher level in female cells. However, *Zbtb33* seems to have no direct impact on the expression of *Irf*s, including *Irf1*, *Irf3* and *Irf7*. This outcome arises an issue that whether downregulation of *Tbk1* by *Zbtb33* influences the activation of IRFs instead and further regulates antiviral activities (Stirnweiss et al., 2010; Fitzgerald, 2011). To address this question in the future, we would like to understand the cytoplasm-to-nucleus translocation proportion of IRFs in the *Zbtb33*-

deficient cells after HSV-1 infection. ZBTB33 is a methyl-DNA-binding protein and a zinc finger transcription factor that can interact with methylated DNA, resulting in the repression of transcription (Filion et al., 2006). In general, it is involved in the methyl-dependent repression of gene transcription by recruiting corepressors, such as the nuclear receptor corepressor and silencing-mediator for retinoid/thyroid hormone receptors (Yoon et al., 2003; Raghav et al., 2012). In addition to interacting with methylated DNA, ZBTB33 can target CTGCNA sequences, but not hydroxymethylated DNA (Daniel et al., 2002; Qin et al., 2015). Thus, ZBTB33 has been implicated in the regulation of diverse biological functions, such as control of the cell cycle, inflammation and tumour cell invasion (Chaudhary et al., 2013; Pozner et al., 2016; Kwiecien et al., 2017). Furthermore, recent reports have also indicated its role in modifying immunological processes (Mino et al., 2018; Zhenilo et al., 2018). For example, Mino et al. showed that ZBTB33 is required for the modulation of chemokine-induced T cell migration via mediation of actin cytoskeleton structure and adhesion (Mino et al., 2018). In another case, rapid ZBTB33 deSUMOylation was found to occur under hyperosmotic stress, which reduced the expression of proinflammatory cytokines, including TGFb1, CD40 and IL26 (Zhenilo et al., 2018).

The X chromosome has a greater density of immunity-related genes compared to the Y chromosome (Bianchi et al., 2012). Based on this observation, several studies have suggested that females, having two X chromosomes and overexpression of some X-linked genes, have an immunological advantage over males (Ross et al., 2005; Spolarics, 2007). For instance, clinical data indicate that females produce more antibodies in some circumstances and males are more susceptible to bacterial and viral infections (Fischer et al., 2015; Klein and Flanagan, 2016; Ghosh and Klein, 2017). However, these strong female-specific immune responses are not always beneficial and can sometimes cause severe immunopathology and autoimmune diseases (Fish, 2008; Klein, 2012). In order to equalise the expression of X-linked genes between the two sexes during mammalian female embryogenesis, females selectively silence transcription of one X chromosome in a chromosome-wide manner. This is called X chromosome inactivation (Pinheiro and Heard, 2017). In this process, the long non-coding RNA *Xist* is required for the transcriptional silencing of one X chromosome in each cell (Brockdorff and Duthie, 1998; da Rocha and Heard, 2017). According to recent studies, long non-coding RNAs are essential regulators of gene expression via interactions with DNA, RNA or proteins (Zhang and Jeang, 2013; Diamantopoulos et al., 2018). Through interactions with transcription factors or chromatin-modifying complexes in the nucleus, long non-coding RNAs can alter the transcription of target genes or can control the stability of target mRNAs in the cytosol (Rinn and Chang,

2012). Besides regulation of the differentiation of immune cells, long non-coding RNAs also act as regulators of antimicrobial functions via mediation of proinflammatory signalling and regulation of ISGs (Rapicavoli et al., 2013; Ouyang et al., 2014). However, prior to this study, there was no indication that *Xist* might play a role in antiviral pathways. Here, we found that *Xist* is upregulated during HSV-1 infection both in human and in mouse female cells (HeLa cells and female mouse skin fibroblasts). The induction of *Xist* led to downregulation of several X-linked genes that have been previously reported, including *Hprt*, *Pgk1* and *Mecp2* (Gayen et al., 2016; Lv et al., 2016; Wang et al., 2016b). Importantly, HSV-1-stimulated *Xist* expression was related to suppression of *Zbtb33*, and hence, it led to higher levels of TBK1 and antiviral responses in female cells. Finally, upregulation of *Xist* explains the difference between male and female cells in HSV-1 replication, indicating that *Xist* is a key factor in the maintenance of greater innate immune responses in female cells through repression of *Zbtb33*. We have searched for human female cell lines that can match the primary human male cells we used in this thesis, but in vain. This is because available female cells are either immortalized (cancer cell lines) or not from skin. We can pursue this in the future by collecting clinical skin samples from males and females with similar ages.

In order to investigate how *Xist* was upregulated by HSV-1, we first ruled out the requirement of *de novo* protein expression, suggesting that viral proteins in the HSV-1 tegument might activate for *Xist* upregulation after viral entry. Our initial hypothesis was that the strong viral transactivator VP16 might bind to the promoter region of *Xist* and therefore drives the expression of *Xist*. VP16 has been shown to target the TAATGARATTC consensus sequence found in IE promoters through interactions with the host factors Oct1 and HCF (Preston et al., 1984; Gaffney et al., 1985; Ace et al., 1989; Wysocka and Herr, 2003). Indeed, our bioinformatic analysis indicated that there are two potential VP16-binding sites within the promoter region of *Xist*. However, expression of VP16 alone did not induce *Xist* level. We then examined another potential candidate, ICP34.5, based on a set of microarray data showing ICP34.5 is essential for induction of *Xist* (Pasieka et al., 2006). Our results showed that overexpression of ICP34.5 upregulated *Xist*. Although ICP34.5 has multiple roles during HSV-1 infection, there is no evidence showing that it can act as a transcriptional factor (Wilcox and Longnecker, 2016; Manivanh et al., 2017). Hence, more detailed experiments investigating whether ICP34.5 plays a role in direct regulation of gene expression are needed to delineate this issue. Furthermore, our data indicated that the sex-related difference in virus replication is a virus-dependent phenomenon. While CPXV was found to replicate better in male cells, knockdown of *Xist* did not eliminate the sex-

related difference in CPXV replication. This suggests that there are multiple mechanisms driving the sex-related differences in virus replication and the effect of *Xist* is specific for HSV-1.

To date, there are limited publications focusing on whether viperin plays a role during HSV-1 infection and the results are not always comparable between these studies (Shen et al., 2014; Zheng and Su, 2017). Shen et al. showed that protein expression of viperin was abrogated during HSV-1 infection, but another study indicated that HSV-1 infection induces a MAVS-dependent early production of viperin under similar infection conditions, such as MOI, infection time and cell line (Zheng and Su, 2017). In this thesis, we identified that viperin is highly upregulated by HSV-1 infection in mouse skin fibroblasts, but not in several human cell lines (HFF, MRC5 and HEK293), suggesting that the induction and function of viperin is cell- and species-specific. Besides differences in cell types and species, HEK293 cells might not be a particularly good cell line for study innate immune responses, because they have been found to express a very low level of TLR3 and lack functional O-linked glycosylation (de Bouteiller et al., 2005; Pohar et al., 2014; Termini et al., 2017). Our results suggest that murine viperin is antiviral against HSV-1, anti-HSV-1 activity requires N-terminal regions of the protein and induction of viperin is needed to restrict virus replication. The N-terminal amphipathic helix has been found to be required for its localisation to the cytosolic surface of the endoplasmic reticulum and lipid droplets (Hinson and Cresswell, 2009a; Hinson and Cresswell, 2009b; Seo et al., 2011a). This domain was also shown to be essential for antiviral activity against HCV and CHIKV via its association with different viral non-structural proteins, although the mechanism remains elusive (Helbig et al., 2011; Teng et al., 2012). In addition to the regulation by the ribonuclease function of HSV-1 vhs, we do not know yet whether there is another viral protein counteracting the antiviral activity of viperin by different mechanisms. The other caveat is that different MOIs were used for various purposes in this thesis and there may be an MOI-dependent manner in some cases, although they were within a reasonable range (0.5-2) and not too high to overwhelm cells.

Humans and mice respond distinctively against virus infection (Sawyer and Elde, 2012; Zschaler et al., 2014). However, there is not a systemic study to identify differences between these two species during HSV-1 infection. In this thesis, we showed that HSV-1 replicates more efficiently in cells of its natural host than in mouse cells. A computational pipeline was developed to analyse the cross-species RNA-seq data and we found that mouse cells upregulated more genes in the antiviral pathway driven by ISG. To antagonise the infection, many mammalian cells respond by launching an

intracellular signal transduction cascade leading to the synthesis and secretion of type I IFNs (Randall and Goodbourn, 2008). The binding of IFNs to IFNARs induces the phosphorylation and subsequent activation of JAKs, including JAK1 and TYK2, leading to the consequent phosphorylation of STAT1 and STAT 2. Activated STAT1, STAT2 and IRF9 further form the ISGF3 complex. This complex translocates to the nucleus and mediates transcriptional activation by interacting with interferon-stimulated regulatory elements within promoters of ISGs. Mouse cells specifically upregulate several antiviral effectors that are downstream of IFN signalling, including *Mx1*, *Mx2* and *Eif2ak2*, indicating that HSV-1 has evolved to counteract the innate immune responses in human cells, but not mouse cells. MX1 and MX2 proteins are well-documented antiviral proteins with broad antiviral activity to inhibit both DNA and RNA virus replication, including African swine fever virus and influenza virus (Pavlovic et al., 1990; Netherton et al., 2009). MX proteins belong to a family of large GTPases and the GTP binding domain is important for the antiviral activity of these proteins (Pitossi et al., 1993). EIF2AK2, also known as dsRNA-activated protein kinase (PKR), is another molecule induced by IFN that plays a critical role in antiviral responses (Garcia et al., 2006). PKR is constitutively expressed in mammalian cells and activated PKR can phosphorylate the alpha subunit of eIF2α. Phosphorylated eIF2α results in the inhibition of translation initiation, leading to a block of translation that impairs efficient viral reproduction and spread (Dauber and Wolff, 2009). HSV-1 US11 protein binds to PKR, interfering with the activation of PKR and thus, inhibiting PKR-mediated phosphorylation of eIF2α in an RNA-dependent manner (Cassady and Gross, 2002). In a similar way, KSHV vIRFs interact with PKR, blocking PKR activation and phosphorylation of eIF2 α (Burysek and Pitha, 2001). HCMV prevents phosphorylation of PKR by utilising its dsRNA binding proteins IRS1 and TRS1. Overexpression of TRS1 causes a redistribution of PKR from the cytoplasm to the nucleus, and thus, restrains the interaction of activated PKR with cytoplasmic eIF2α, limiting the initial activation of PKR by dsRNA in the cytoplasm (Hakki et al., 2006).

To identify the key component that influences the cross-species difference in HSV-1 replication, we used the CRISPR knockout method and identified that JAK1 is essential for generating the human-mouse difference. HSV-1 has evolved various viral proteins to inhibit IFN-induced defence mechanisms in hosts, which ultimately establishes successful infection. Two well-studied viral proteins, ICP27 and vhs, can suppress antiviral reactions through inhibiting the JAK/STAT signalling pathway (Chee and Roizman, 2004; Johnson et al., 2008). ICP27 has been found to decrease cellular mRNA stability and inhibit host splicing machinery by interacting with spliceosome-associated proteins. In addition, ICP27 helps HSV-1 evade type I IFN signalling by

downregulating STAT1 activation and preventing the accumulation of STAT1 in the nucleus (Johnson et al., 2008). At the same time, HSV-1 particles contain vhs proteins which can trigger rapid cleavages of both cellular and viral mRNAs upon viral entry into the cell (Kwong and Frenkel, 1987). HSV-1 vhs causes a significant decrease in the accumulation of STAT2 during infection and inhibits STAT1 activation by reducing the expression of *Jak1* (Chee and Roizman, 2004). Other herpesviruses also target the IFN signalling pathway. The product of open reading frame 10 of KSHV counteracts IFN signalling by associating with JAK1 and STAT2 (Bisson et al., 2009). As a result of these interactions, activation of JAK1, STAT1 and STAT2 is impaired, and therefore, the accumulation of ISGF3 in the nucleus is decreased. In another instance, HCMV reduces the basal levels of both JAK1 and IRF9, leading to interruption of phosphorylation of STAT1 and STAT2 (Miller et al., 1998; Miller et al., 1999).

Our data also suggest that HSV-1 ICP27 and vhs are critical for inhibiting IFN signalling via a reduction of *Jak1* expression. However, only vhs can eliminate the human-mouse difference in JAK1 expression both at RNA and at protein levels in infected HFF, MRC5 and MF cells. This also correlates with the comparable viral yields of vhs mutant virus between human and mouse cells. In general, the interaction of cytokine with its specific receptor can result in a series of signalling events which then activate JAKs by auto- or trans-phosphorylation (Babon et al., 2014). However, JAK-STAT signalling can be induced through specific calcium-dependent protein kinases (Sengupta et al., 1996; Wang et al., 2008a). A previous study showed that the calcium signalling pathways plays an essential role in facilitating early entry of HSV-1 (Cheshenko et al., 2003; Cheshenko et al., 2007). This process requires the full complement of key glycoproteins, including gB, gD and gH, to induce the calcium response and trigger focal adhesion kinase phosphorylation (Cheshenko et al., 2007). Indeed, we found mutations in HSV-1 glycoproteins in our experimental evolution of HSV-1 in mouse cells. Hare et al. discovered that both calcium signalling and recognition of viral genomes contribute to IRF3 activation in the absence of IFNs and this then enhances induction of certain ISGs upon low-levels of enveloped virus particle entry (Liu et al., 2012; Hare et al., 2015). These data suggest that calcium signalling can act as a danger signal prior to virus replication and the prototypic recognition response, priming the reaction to viral infection. We have preliminary results that show that HSV-1 infection induces JAK1 activation both in wild-type and $IFNAR^{-/-}$ mouse cells, but phosphorylation levels are significantly reduced while treating these cells with a cell-permeant calcium chelator (data not shown). This indicates that activation of JAK1 requires calcium transport in mouse cells during the initial infection prior to IFN stimulation. In human cells, JAK1 activation was barely detected during wild-type

HSV-1 infection. This may be explained by more efficient blockage of basal JAK1 protein expression by HSV-1 in human cells compared with mouse cells, which subsequently leads to less JAK1 that can be induced to active forms. However, mechanisms driving calcium transport by HSV-1 infection, resulting in phosphorylation of JAK1 are still unknown and human-mouse differences in this pathway require more investigation.

To summarise, this thesis investigated two broad but sometimes overlooked questions, namely, whether sex or species affect transcriptional changes in cells during HSV-1 infection. Our findings emphasise the importance of understanding basic differences in each cell type used for research. The results of this study indicate that HSV-1 has evolved to restrain innate immune responses in its natural host via JAK signalling, but this does not occur in mouse cells which are commonly used to study HSV-1 pathogenesis. In addition to the human-mouse difference, the chromosomal differences between the two sexes can by themselves generate different intensities of reactions against HSV-1, particularly in cytosolic DNA-sensing pathways. These findings define a sex-specific intrinsic program in the innate immune response, independent of sex hormones, at the initial stage of HSV-1 infection. Given that most of our observations were made in cell culture, further research is required, particularly with respect to *in vivo* study, to fully interpret both the human-mouse and sex differences during HSV-1 infection. This will provide a more in depth understanding of interactions between HSV-1 and its host cells.

References

Ablasser, A., F. Bauernfeind, G. Hartmann, E. Latz, K. A. Fitzgerald and V. Hornung (2009). "RIG-I-dependent sensing of poly(dA:dT) through the induction of an RNA polymerase III-transcribed RNA intermediate." Nat Immunol **10**(10): 1065-1072.

Ablasser, A., M. Goldeck, T. Cavlar, T. Deimling, G. Witte, I. Rohl, K. P. Hopfner, J. Ludwig and V. Hornung (2013). "cGAS produces a 2'-5'-linked cyclic dinucleotide second messenger that activates STING." Nature **498**(7454): 380-384.

Ace, C. I., M. A. Dalrymple, F. H. Ramsay, V. G. Preston and C. M. Preston (1988). "Mutational analysis of the herpes simplex virus type 1 trans-inducing factor Vmw65." J Gen Virol **69 (Pt 10)**: 2595-2605.

Ace, C. I., T. A. McKee, J. M. Ryan, J. M. Cameron and C. M. Preston (1989). "Construction and characterization of a herpes simplex virus type 1 mutant unable to transinduce immediate-early gene expression." J Virol **63**(5): 2260-2269.

Agrelo, R. and A. Wutz (2010). "ConteXt of change--X inactivation and disease." EMBO Mol Med **2**(1): 6-15.

Ahlers, L. R. and A. G. Goodman (2016). "Nucleic acid sensing and innate immunity: signaling pathways controlling viral pathogenesis and autoimmunity." Curr Clin Microbiol Rep **3**(3): 132-141.

Ahmed, C. M. and H. M. Johnson (2006). "IFN-gamma and its receptor subunit IFNGR1 are recruited to the IFN-gamma-activated sequence element at the promoter site of IFN-gamma-activated genes: evidence of transactivational activity in IFNGR1." J Immunol **177**(1): 315-321.

Ahn, K., T. H. Meyer, S. Uebel, P. Sempe, H. Djaballah, Y. Yang, P. A. Peterson, K. Fruh and R. Tampe (1996). "Molecular mechanism and species specificity of TAP inhibition by herpes simplex virus ICP47." EMBO J **15**(13): 3247-3255.

Akira, S. and H. Hemmi (2003). "Recognition of pathogen-associated molecular patterns by TLR family." Immunol Lett **85**(2): 85-95.

Akira, S. and K. Takeda (2004). "Toll-like receptor signalling." Nat Rev Immunol **4**(7): 499-511.

Akira, S., K. Takeda and T. Kaisho (2001). "Toll-like receptors: critical proteins linking innate and acquired immunity." Nat Immunol **2**(8): 675-680.

Akira, S., S. Uematsu and O. Takeuchi (2006). "Pathogen recognition and innate immunity." Cell **124**(4): 783-801.

Al-Dujaili, L. J., P. P. Clerkin, C. Clement, H. E. McFerrin, P. S. Bhattacharjee, E. D. Varnell, H. E. Kaufman and J. M. Hill (2011). "Ocular herpes simplex virus: how are latency,

reactivation, recurrent disease and therapy interrelated?" Future Microbiol **6**(8): 877-907.

Aliota, M. T., E. A. Caine, E. C. Walker, K. E. Larkin, E. Camacho and J. E. Osorio (2016). "Characterization of Lethal Zika Virus Infection in AG129 Mice." PLoS Negl Trop Dis **10**(4): e0004682.

Alzhanova, D., E. Hammarlund, J. Reed, E. Meermeier, S. Rawlings, et al. (2014). "T cell inactivation by poxviral B22 family proteins increases viral virulence." PLoS Pathog **10**(5): e1004123.

An, H., Y. Yu, M. Zhang, H. Xu, R. Qi, et al. (2002). "Involvement of ERK, p38 and NF-kappaB signal transduction in regulation of TLR2, TLR4 and TLR9 gene expression induced by lipopolysaccharide in mouse dendritic cells." Immunology **106**(1): 38-45.

Aravalli, R. N., S. Hu, T. N. Rowen, J. M. Palmquist and J. R. Lokensgard (2005). "Cutting edge: TLR2-mediated proinflammatory cytokine and chemokine production by microglial cells in response to herpes simplex virus." J Immunol **175**(7): 4189-4193.

Arnosti, D. N., C. M. Preston, M. Hagmann, W. Schaffner, R. G. Hope, G. Laughlan and B. F. Luisi (1993). "Specific transcriptional activation in vitro by the herpes simplex virus protein VP16." Nucleic Acids Res **21**(24): 5570-5576.

Babon, J. J., I. S. Lucet, J. M. Murphy, N. A. Nicola and L. N. Varghese (2014). "The molecular regulation of Janus kinase (JAK) activation." Biochem J **462**(1): 1-13.

Baines, J. D. (2011). "Herpes simplex virus capsid assembly and DNA packaging: a present and future antiviral drug target." Trends Microbiol **19**(12): 606-613.

Barber, G. N. (2014). "STING-dependent cytosolic DNA sensing pathways." Trends Immunol **35**(2): 88-93.

Bassey-Archibong, B. I., L. G. Rayner, S. M. Hercules, C. W. Aarts, A. Dvorkin-Gheva, J. L. Bramson, J. A. Hassell and J. M. Daniel (2017). "Kaiso depletion attenuates the growth and survival of triple negative breast cancer cells." Cell Death Dis **8**(3): e2689.

Baucke, R. B. and P. G. Spear (1979). "Membrane proteins specified by herpes simplex viruses. V. Identification of an Fc-binding glycoprotein." J Virol **32**(3): 779-789.

Bauer, S., C. J. Kirschning, H. Hacker, V. Redecke, S. Hausmann, S. Akira, H. Wagner and G. B. Lipford (2001). "Human TLR9 confers responsiveness to bacterial DNA via species-specific CpG motif recognition." Proc Natl Acad Sci U S A **98**(16): 9237-9242.

Beard, P. M., N. S. Taus and J. D. Baines (2002). "DNA cleavage and packaging proteins encoded by genes U(L)28, U(L)15, and U(L)33 of herpes simplex virus type 1 form a complex in infected cells." J Virol **76**(10): 4785-4791.

Beck, T. W. and R. L. Millette (1982). "Regulation of herpes simplex virus gene transcription in vitro." J Cell Biochem **19**(4): 333-347.

Bellucci, R., A. Martin, D. Bommarito, K. Wang, S. H. Hansen, G. J. Freeman and J. Ritz (2015). "Interferon-gamma-induced activation of JAK1 and JAK2 suppresses tumor cell susceptibility to NK cells through upregulation of PD-L1 expression." Oncoimmunology **4**(6): e1008824.

Ben-Zeev, A. and Y. Asher Y'Becker (1976). "Synthesis of herpes simplex virus-specified RNA by an RNA polymerase II in isolated nuclei in vitro." Virology **71**(1): 302-311.

Berletch, J. B., F. Yang, J. Xu, L. Carrel and C. M. Disteche (2011). "Genes that escape from X inactivation." Hum Genet **130**(2): 237-245.

Beutler, B. A. (2009). "TLRs and innate immunity." Blood **113**(7): 1399-1407.

Bhat, N. and K. A. Fitzgerald (2014). "Recognition of cytosolic DNA by cGAS and other STING-dependent sensors." Eur J Immunol **44**(3): 634-640.

Bianchi, I., A. Lleo, M. E. Gershwin and P. Invernizzi (2012). "The X chromosome and immune associated genes." J Autoimmun **38**(2-3): J187-192.

Bisson, S. A., A. L. Page and D. Ganem (2009). "A Kaposi's sarcoma-associated herpesvirus protein that forms inhibitory complexes with type I interferon receptor subunits, Jak and STAT proteins, and blocks interferon-mediated signal transduction." J Virol **83**(10): 5056-5066.

Bloom, D. C., N. V. Giordani and D. L. Kwiatkowski (2010). "Epigenetic regulation of latent HSV-1 gene expression." Biochim Biophys Acta **1799**(3-4): 246-256.

Boehme, K. W., J. Singh, S. T. Perry and T. Compton (2004). "Human cytomegalovirus elicits a coordinated cellular antiviral response via envelope glycoprotein B." J Virol **78**(3): 1202-1211.

Boehmer, P. E. and A. V. Nimonkar (2003). "Herpes virus replication." IUBMB Life **55**(1): 13-22.

Boetzer, M., C. V. Henkel, H. J. Jansen, D. Butler and W. Pirovano (2011). "Scaffolding pre-assembled contigs using SSPACE." Bioinformatics **27**(4): 578-579.

Boetzer, M. and W. Pirovano (2014). "SSPACE-LongRead: scaffolding bacterial draft genomes using long read sequence information." BMC Bioinformatics **15**: 211.

Boivin, N., R. Menasria, J. Piret and G. Boivin (2012). "Modulation of TLR9 response in a mouse model of herpes simplex virus encephalitis." Antiviral Res **96**(3): 414-421.

Boivin, N., Y. Sergerie, S. Rivest and G. Boivin (2008). "Effect of pretreatment with toll-like receptor agonists in a mouse model of herpes simplex virus type 1 encephalitis." J Infect Dis **198**(5): 664-672.

Bolger, A. M., M. Lohse and B. Usadel (2014). "Trimmomatic: a flexible trimmer for Illumina sequence data." Bioinformatics **30**(15): 2114-2120.

Booy, F. P., W. W. Newcomb, B. L. Trus, J. C. Brown, T. S. Baker and A. C. Steven (1991). "Liquid-crystalline, phage-like packing of encapsidated DNA in herpes simplex virus." Cell **64**(5): 1007-1015.

Boudinot, P., S. Riffault, S. Salhi, C. Carrat, C. Sedlik, N. Mahmoudi, B. Charley and A. Benmansour (2000). "Vesicular stomatitis virus and pseudorabies virus induce a vig1/cig5 homologue in mouse dendritic cells via different pathways." J Gen Virol **81**(Pt 11): 2675-2682.

Brandt, C. R., L. M. Coakley and D. R. Grau (1992). "A murine model of herpes simplex virus-induced ocular disease for antiviral drug testing." J Virol Methods **36**(3): 209-222.

Brockdorff, N. and S. M. Duthie (1998). "X chromosome inactivation and the Xist gene." Cell Mol Life Sci **54**(1): 104-112.

Brown, A. S., J. M. Davis, E. A. Murphy, M. D. Carmichael, A. Ghaffar and E. P. Mayer (2004). "Gender differences in viral infection after repeated exercise stress." Med Sci Sports Exerc **36**(8): 1290-1295.

Brown, C. J., A. Ballabio, J. L. Rupert, R. G. Lafreniere, M. Grompe, R. Tonlorenzi and H. F. Willard (1991). "A gene from the region of the human X inactivation centre is expressed exclusively from the inactive X chromosome." Nature **349**(6304): 38-44.

Brown, C. R., M. S. Nakamura, J. D. Mosca, G. S. Hayward, S. E. Straus and L. P. Perera (1995). "Herpes simplex virus trans-regulatory protein ICP27 stabilizes and binds to 3' ends of labile mRNA." J Virol **69**(11): 7187-7195.

Brown, J. C. (2007). "High G+C Content of Herpes Simplex Virus DNA: Proposed Role in Protection Against Retrotransposon Insertion." Open Biochem J **1**: 33-42.

Bryant-Hudson, K. M., A. J. Chucair-Elliott, C. D. Conrady, A. Cohen, M. Zheng and D. J. Carr (2013). "HSV-1 targets lymphatic vessels in the eye and draining lymph node of mice leading to edema in the absence of a functional type I interferon response." Am J Pathol **183**(4): 1233-1242.

Bryant, C. E. and T. P. Monie (2012). "Mice, men and the relatives: cross-species studies underpin innate immunity." Open Biol **2**(4): 120015.

Buck-Koehntop, B. A., M. A. Martinez-Yamout, H. J. Dyson and P. E. Wright (2012). "Kaiso uses all three zinc fingers and adjacent sequence motifs for high affinity binding to sequence-specific and methyl-CpG DNA targets." FEBS Lett **586**(6): 734-739.

Burcea, M., A. Gheorghe and M. Pop (2015). "Incidence of Herpes Simplex Virus Keratitis in HIV/AIDS patients compared with the general population." J Med Life **8**(1): 62-63.

Burgio, G. (2018). "Redefining mouse transgenesis with CRISPR/Cas9 genome editing technology." Genome Biol **19**(1): 27.

Burysek, L. and P. M. Pitha (2001). "Latently expressed human herpesvirus 8-encoded interferon regulatory factor 2 inhibits double-stranded RNA-activated protein kinase." J Virol **75**(5): 2345-2352.

Bustamante, C. I. and J. C. Wade (1991). "Herpes simplex virus infection in the immunocompromised cancer patient." J Clin Oncol **9**(10): 1903-1915.

Cai, W. and P. A. Schaffer (1992). "Herpes simplex virus type 1 ICP0 regulates expression of immediate-early, early, and late genes in productively infected cells." J Virol **66**(5): 2904-2915.

Cartier, A., T. Komai and M. G. Masucci (2003). "The Us3 protein kinase of herpes simplex virus 1 blocks apoptosis and induces phosporylation of the Bcl-2 family member Bad." Exp Cell Res **291**(1): 242-250.

Casellas, J. (2011). "Inbred mouse strains and genetic stability: a review." Animal **5**(1): 1-7.

Cassady, K. A. and M. Gross (2002). "The herpes simplex virus type 1 U(S)11 protein interacts with protein kinase R in infected cells and requires a 30-amino-acid sequence adjacent to a kinase substrate domain." J Virol **76**(5): 2029-2035.

Castanier, C., N. Zemirli, A. Portier, D. Garcin, N. Bidere, A. Vazquez and D. Arnoult (2012). "MAVS ubiquitination by the E3 ligase TRIM25 and degradation by the proteasome is involved in type I interferon production after activation of the antiviral RIG-I-like receptors." BMC Biol **10**: 44.

Challberg, M. D. (1986). "A method for identifying the viral genes required for herpesvirus DNA replication." Proc Natl Acad Sci U S A **83**(23): 9094-9098.

Chan, Y. K. and M. U. Gack (2016). "Viral evasion of intracellular DNA and RNA sensing." Nat Rev Microbiol **14**(6): 360-373.

Chan, Y. L., T. H. Chang, C. L. Liao and Y. L. Lin (2008). "The cellular antiviral protein viperin is attenuated by proteasome-mediated protein degradation in Japanese encephalitis virus-infected cells." J Virol **82**(21): 10455-10464.

Chaudhary, R., C. C. Pierre, K. Nanan, D. Wojtal, S. Morone, C. Pinelli, G. A. Wood, S. Robine and J. M. Daniel (2013). "The POZ-ZF transcription factor Kaiso (ZBTB33) induces inflammation and progenitor cell differentiation in the murine intestine." PLoS One **8**(9): e74160.

Chee, A. V., P. Lopez, P. P. Pandolfi and B. Roizman (2003). "Promyelocytic leukemia protein mediates interferon-based anti-herpes simplex virus 1 effects." J Virol **77**(12): 7101-7105.

Chee, A. V. and B. Roizman (2004). "Herpes simplex virus 1 gene products occlude the interferon signaling pathway at multiple sites." J Virol **78**(8): 4185-4196.

Chen, Q., L. Sun and Z. J. Chen (2016). "Regulation and function of the cGAS-STING pathway of cytosolic DNA sensing." Nat Immunol **17**(10): 1142-1149.

Chen, W. Q., Y. W. Hu, P. F. Zou, S. S. Ren, P. Nie and M. X. Chang (2015a). "MAVS splicing variants contribute to the induction of interferon and interferon-stimulated genes mediated by RIG-I-like receptors." Dev Comp Immunol **49**(1): 19-30.

Chen, X. Z., H. Chen, F. A. Castro, J. K. Hu and H. Brenner (2015b). "Epstein-Barr virus infection and gastric cancer: a systematic review." Medicine (Baltimore) **94**(20): e792.

Chen, Y. M. and D. M. Knipe (1996). "A dominant mutant form of the herpes simplex virus ICP8 protein decreases viral late gene transcription." Virology **221**(2): 281-290.

Cheng, G., J. Zhong, J. Chung and F. V. Chisari (2007). "Double-stranded DNA and double-stranded RNA induce a common antiviral signaling pathway in human cells." Proc Natl Acad Sci U S A **104**(21): 9035-9040.

Cheng, Y., Z. Ma, B. H. Kim, W. Wu, P. Cayting, et al. (2014). "Principles of regulatory information conservation between mouse and human." Nature **515**(7527): 371-375.

Chernakova, G. M., G. Arzhimatova, E. A. Kleshcheva and T. B. Semenova (2014). "[Herpesviruses in ophthalmology]." Vestn Oftalmol **130**(4): 127-131.

Cheshenko, N., B. Del Rosario, C. Woda, D. Marcellino, L. M. Satlin and B. C. Herold (2003). "Herpes simplex virus triggers activation of calcium-signaling pathways." J Cell Biol **163**(2): 283-293.

Cheshenko, N., W. Liu, L. M. Satlin and B. C. Herold (2007). "Multiple receptor interactions trigger release of membrane and intracellular calcium stores critical for herpes simplex virus entry." Mol Biol Cell **18**(8): 3119-3130.

Cheshenko, N., J. B. Trepanier, P. A. Gonzalez, E. A. Eugenin, W. R. Jacobs, Jr. and B. C. Herold (2014). "Herpes simplex virus type 2 glycoprotein H interacts with integrin alphavbeta3 to facilitate viral entry and calcium signaling in human genital tract epithelial cells." J Virol **88**(17): 10026-10038.

Cheshenko, N., J. B. Trepanier, M. Stefanidou, N. Buckley, P. Gonzalez, W. Jacobs and B. C. Herold (2013). "HSV activates Akt to trigger calcium release and promote viral entry: novel candidate target for treatment and suppression." FASEB J **27**(7): 2584-2599.

Chesnokova, L. S., S. L. Nishimura and L. M. Hutt-Fletcher (2009). "Fusion of epithelial cells by Epstein-Barr virus proteins is triggered by binding of viral glycoproteins gHgL to integrins alphavbeta6 or alphavbeta8." Proc Natl Acad Sci U S A **106**(48): 20464-20469.

Chew, T., K. E. Taylor and K. L. Mossman (2009). "Innate and adaptive immune responses to herpes simplex virus." Viruses **1**(3): 979-1002.

Chin, K. C. and P. Cresswell (2001). "Viperin (cig5), an IFN-inducible antiviral protein directly induced by human cytomegalovirus." Proc Natl Acad Sci U S A **98**(26): 15125-15130.

Chiu, Y. H., J. B. Macmillan and Z. J. Chen (2009). "RNA polymerase III detects cytosolic DNA and induces type I interferons through the RIG-I pathway." Cell **138**(3): 576-591.

Cho, Y. S., S. Challa, D. Moquin, R. Genga, T. D. Ray, M. Guildford and F. K. Chan (2009). "Phosphorylation-driven assembly of the RIP1-RIP3 complex regulates programmed necrosis and virus-induced inflammation." Cell **137**(6): 1112-1123.

Chockalingam, A., J. C. Brooks, J. L. Cameron, L. K. Blum and C. A. Leifer (2009). "TLR9 traffics through the Golgi complex to localize to endolysosomes and respond to CpG DNA." Immunol Cell Biol **87**(3): 209-217.

Choi, M. K., Z. Wang, T. Ban, H. Yanai, Y. Lu, et al. (2009). "A selective contribution of the RIG-I-like receptor pathway to type I interferon responses activated by cytosolic DNA." Proc Natl Acad Sci U S A **106**(42): 17870-17875.

Chow, K. T., M. Gale, Jr. and Y. M. Loo (2018). "RIG-I and Other RNA Sensors in Antiviral Immunity." Annu Rev Immunol **36**: 667-694.

Christensen, M. H., S. B. Jensen, J. J. Miettinen, S. Luecke, T. Prabakaran, et al. (2016). "HSV-1 ICP27 targets the TBK1-activated STING signalsome to inhibit virus-induced type I IFN expression." EMBO J **35**(13): 1385-1399.

Christensen, M. H. and S. R. Paludan (2017). "Viral evasion of DNA-stimulated innate immune responses." Cell Mol Immunol **14**(1): 4-13.

Ciota, A. T., A. O. Lovelace, S. A. Jones, A. Payne and L. D. Kramer (2007a). "Adaptation of two flaviviruses results in differences in genetic heterogeneity and virus adaptability." J Gen Virol **88**(Pt 9): 2398-2406.

Ciota, A. T., A. O. Lovelace, K. A. Ngo, A. N. Le, J. G. Maffei, et al. (2007b). "Cell-specific adaptation of two flaviviruses following serial passage in mosquito cell culture." Virology **357**(2): 165-174.

Cliffe, A. R. and A. C. Wilson (2017). "Restarting Lytic Gene Transcription at the Onset of Herpes Simplex Virus Reactivation." J Virol **91**(2).

Collins, S. E., R. S. Noyce and K. L. Mossman (2004). "Innate cellular response to virus particle entry requires IRF3 but not virus replication." J Virol **78**(4): 1706-1717.

Conrady, C. D., M. Zheng, K. A. Fitzgerald, C. Liu and D. J. Carr (2012). "Resistance to HSV-1 infection in the epithelium resides with the novel innate sensor, IFI-16." Mucosal Immunol **5**(2): 173-183.

Cooper, L. A. and T. W. Scott (2001). "Differential evolution of eastern equine encephalitis virus populations in response to host cell type." Genetics **157**(4): 1403-1412.

Corcoran, J. A., W. L. Hsu and J. R. Smiley (2006). "Herpes simplex virus ICP27 is required for virus-induced stabilization of the ARE-containing IEX-1 mRNA encoded by the human IER3 gene." J Virol **80**(19): 9720-9729.

Corey, L. and A. Wald (2009). "Maternal and neonatal herpes simplex virus infections." N Engl J Med **361**(14): 1376-1385.

Cotter, C. R., M. L. Nguyen, J. S. Yount, C. B. Lopez, J. A. Blaho and T. M. Moran (2010). "The virion host shut-off (vhs) protein blocks a TLR-independent pathway of herpes simplex virus type 1 recognition in human and mouse dendritic cells." PLoS One **5**(2): e8684.

Cui, C., A. Griffiths, G. Li, L. M. Silva, M. F. Kramer, T. Gaasterland, X. J. Wang and D. M. Coen (2006). "Prediction and identification of herpes simplex virus 1-encoded microRNAs." J Virol **80**(11): 5499-5508.

Cunningham, A. L., R. Taylor, J. Taylor, C. Marks, J. Shaw and A. Mindel (2006). "Prevalence of infection with herpes simplex virus types 1 and 2 in Australia: a nationwide population based survey." Sex Transm Infect **82**(2): 164-168.

Curry, S. S. (1980). "Cutaneous herpes simplex infections and their treatment." Cutis **26**(1): 41-58.

da Rocha, S. T. and E. Heard (2017). "Novel players in X inactivation: insights into Xist-mediated gene silencing and chromosome conformation." Nat Struct Mol Biol **24**(3): 197-204.

Dai, S. D., Y. Wang, G. Y. Jiang, P. X. Zhang, X. J. Dong, et al. (2010). "Kaiso is expressed in lung cancer: its expression and localization is affected by p120ctn." Lung Cancer **67**(2): 205-215.

Daniel, J. M., C. M. Spring, H. C. Crawford, A. B. Reynolds and A. Baig (2002). "The p120(ctn)-binding partner Kaiso is a bi-modal DNA-binding protein that recognizes both a sequence-specific consensus and methylated CpG dinucleotides." Nucleic Acids Res **30**(13): 2911-2919.

Dauber, B., J. Pelletier and J. R. Smiley (2011). "The herpes simplex virus 1 vhs protein enhances translation of viral true late mRNAs and virus production in a cell type-dependent manner." J Virol **85**(11): 5363-5373.

Dauber, B. and T. Wolff (2009). "Activation of the Antiviral Kinase PKR and Viral Countermeasures." Viruses **1**(3): 523-544.

Daubeuf, S., D. Singh, Y. Tan, H. Liu, H. J. Federoff, W. J. Bowers and K. Tolba (2009). "HSV ICP0 recruits USP7 to modulate TLR-mediated innate response." Blood **113**(14): 3264-3275.

Davey, G. M., M. Wojtasiak, A. I. Proietto, F. R. Carbone, W. R. Heath and S. Bedoui (2010). "Cutting edge: priming of CD8 T cell immunity to herpes simplex virus type 1 requires cognate TLR3 expression in vivo." J Immunol **184**(5): 2243-2246.

Davison, A. J. (2002). "Evolution of the herpesviruses." Vet Microbiol **86**(1-2): 69-88.

Davison, A. J., R. Eberle, B. Ehlers, G. S. Hayward, D. J. McGeoch, et al. (2009). "The order Herpesvirales." Arch Virol **154**(1): 171-177.

de Bouteiller, O., E. Merck, U. A. Hasan, S. Hubac, B. Benguigui, G. Trinchieri, E. E. Bates and C. Caux (2005). "Recognition of double-stranded RNA by human toll-like receptor 3 and downstream receptor signaling requires multimerization and an acidic pH." J Biol Chem **280**(46): 38133-38145.

de Jong, M. D., C. P. Simmons, T. T. Thanh, V. M. Hien, G. J. Smith, et al. (2006). "Fatal outcome of human influenza A (H5N1) is associated with high viral load and hypercytokinemia." Nat Med **12**(10): 1203-1207.

De Leon-Nava, M. A., K. Nava, G. Soldevila, L. Lopez-Griego, J. R. Chavez-Rios, J. A. Vargas-Villavicencio and J. Morales-Montor (2009). "Immune sexual dimorphism: effect of gonadal steroids on the expression of cytokines, sex steroid receptors, and lymphocyte proliferation." J Steroid Biochem Mol Biol **113**(1-2): 57-64.

Deane, J. A., P. Pisitkun, R. S. Barrett, L. Feigenbaum, T. Town, J. M. Ward, R. A. Flavell and S. Bolland (2007). "Control of toll-like receptor 7 expression is essential to restrict autoimmunity and dendritic cell proliferation." Immunity **27**(5): 801-810.

DeFilippis, V. R., B. Robinson, T. M. Keck, S. G. Hansen, J. A. Nelson and K. J. Fruh (2006). "Interferon regulatory factor 3 is necessary for induction of antiviral genes during human cytomegalovirus infection." J Virol **80**(2): 1032-1037.

Del Prete, G., M. De Carli, F. Almerigogna, M. G. Giudizi, R. Biagiotti and S. Romagnani (1993). "Human IL-10 is produced by both type 1 helper (Th1) and type 2 helper (Th2) T cell clones and inhibits their antigen-specific proliferation and cytokine production." J Immunol **150**(2): 353-360.

Delcher, A. L., S. L. Salzberg and A. M. Phillippy (2003). "Using MUMmer to identify similar regions in large sequence sets." Curr Protoc Bioinformatics **Chapter 10**: Unit 10 13.

Deschamps, T. and M. Kalamvoki (2017). "Evasion of the STING DNA-Sensing Pathway by VP11/12 of Herpes Simplex Virus 1." J Virol **91**(16).

Devasthanam, A. S. (2014). "Mechanisms underlying the inhibition of interferon signaling by viruses." Virulence **5**(2): 270-277.

Diamantopoulos, M. A., P. Tsiakanikas and A. Scorilas (2018). "Non-coding RNAs: the riddle of the transcriptome and their perspectives in cancer." Ann Transl Med **6**(12): 241.

Diner, B. A., K. K. Lum, A. Javitt and I. M. Cristea (2015). "Interactions of the Antiviral Factor Interferon Gamma-Inducible Protein 16 (IFI16) Mediate Immune Signaling and Herpes Simplex Virus-1 Immunosuppression." Mol Cell Proteomics **14**(9): 2341-2356.

Dingwell, K. S., C. R. Brunetti, R. L. Hendricks, Q. Tang, M. Tang, A. J. Rainbow and D. C. Johnson (1994). "Herpes simplex virus glycoproteins E and I facilitate cell-to-cell spread in vivo and across junctions of cultured cells." J Virol **68**(2): 834-845.

Disteche, C. M. and J. B. Berletch (2015). "X-chromosome inactivation and escape." J Genet **94**(4): 591-599.

Disteche, C. M., G. N. Filippova and K. D. Tsuchiya (2002). "Escape from X inactivation." Cytogenet Genome Res **99**(1-4): 36-43.

Dixit, E., S. Boulant, Y. Zhang, A. S. Lee, C. Odendall, et al. (2010). "Peroxisomes are signaling platforms for antiviral innate immunity." Cell **141**(4): 668-681.

Dixit, E. and J. C. Kagan (2013). "Intracellular pathogen detection by RIG-I-like receptors." Adv Immunol **117**: 99-125.

Dobson, B. M., D. J. Procter, N. A. Hollett, I. E. Flesch, T. P. Newsome and D. C. Tscharke (2014). "Vaccinia virus F5 is required for normal plaque morphology in multiple cell lines but not replication in culture or virulence in mice." Virology **456-457**: 145-156.

Dohner, K., A. Wolfstein, U. Prank, C. Echeverri, D. Dujardin, R. Vallee and B. Sodeik (2002). "Function of dynein and dynactin in herpes simplex virus capsid transport." Mol Biol Cell **13**(8): 2795-2809.

Dong, S. and Q. Liang (2018). "Recent Advances in Animal Models of Zika Virus Infection." Virol Sin **33**(2): 125-130.

Doyle, S., S. Vaidya, R. O'Connell, H. Dadgostar, P. Dempsey, et al. (2002). "IRF3 mediates a TLR3/TLR4-specific antiviral gene program." Immunity **17**(3): 251-263.

Drake, J. W. and J. J. Holland (1999). "Mutation rates among RNA viruses." Proc Natl Acad Sci U S A **96**(24): 13910-13913.

Drake, J. W. and C. B. Hwang (2005). "On the mutation rate of herpes simplex virus type 1." Genetics **170**(2): 969-970.

Du, Q., J. Xie, H. J. Kim and X. Ma (2013). "Type I interferon: the mediator of bacterial infection-induced necroptosis." Cell Mol Immunol **10**(1): 4-6.

Du, T., G. Zhou and B. Roizman (2011). "HSV-1 gene expression from reactivated ganglia is disordered and concurrent with suppression of latency-associated transcript and miRNAs." Proc Natl Acad Sci U S A **108**(46): 18820-18824.

Duerst, R. J. and L. A. Morrison (2004). "Herpes simplex virus 2 virion host shutoff protein interferes with type I interferon production and responsiveness." Virology **322**(1): 158-167.

Duffy, S. and E. C. Holmes (2008). "Phylogenetic evidence for rapid rates of molecular evolution in the single-stranded DNA begomovirus tomato yellow leaf curl virus." J Virol **82**(2): 957-965.

Dufour, F., L. Bertrand, A. Pearson, N. Grandvaux and Y. Langelier (2011a). "The ribonucleotide reductase R1 subunits of herpes simplex virus 1 and 2 protect cells against poly(I . C)-induced apoptosis." J Virol **85**(17): 8689-8701.

Dufour, F., A. M. Sasseville, S. Chabaud, B. Massie, R. M. Siegel and Y. Langelier (2011b). "The ribonucleotide reductase R1 subunits of herpes simplex virus types 1 and 2 protect cells against TNFalpha- and FasL-induced apoptosis by interacting with caspase-8." Apoptosis **16**(3): 256-271.

Duschene, K. S. and J. B. Broderick (2012). "Viperin: a radical response to viral infection." Biomol Concepts **3**(3): 255-266.

Earnshaw, D. L., T. H. Bacon, S. J. Darlison, K. Edmonds, R. M. Perkins and R. A. Vere Hodge (1992). "Mode of antiviral action of penciclovir in MRC-5 cells infected with herpes simplex virus type 1 (HSV-1), HSV-2, and varicella-zoster virus." Antimicrob Agents Chemother **36**(12): 2747-2757.

Eaton, H. E., H. A. Saffran, F. W. Wu, K. Quach and J. R. Smiley (2014). "Herpes simplex virus protein kinases US3 and UL13 modulate VP11/12 phosphorylation, virion packaging, and phosphatidylinositol 3-kinase/Akt signaling activity." J Virol **88**(13): 7379-7388.

Elde, N. C., S. J. Child, M. T. Eickbush, J. O. Kitzman, K. S. Rogers, J. Shendure, A. P. Geballe and H. S. Malik (2012). "Poxviruses deploy genomic accordions to adapt rapidly against host antiviral defenses." Cell **150**(4): 831-841.

Embil, J. A., F. R. Manuel and E. S. McFarlane (1981). "Concurrent oral and genital infection with an identical strain of herpes simplex virus type 1. Restriction endonuclease analysis." Sex Transm Dis **8**(2): 70-72.

Emes, R. D., L. Goodstadt, E. E. Winter and C. P. Ponting (2003). "Comparison of the genomes of human and mouse lays the foundation of genome zoology." Hum Mol Genet **12**(7): 701-709.

Everett, R. D., S. Rechter, P. Papior, N. Tavalai, T. Stamminger and A. Orr (2006). "PML contributes to a cellular mechanism of repression of herpes simplex virus type 1 infection that is inactivated by ICP0." J Virol **80**(16): 7995-8005.

Fan, Q., R. Longnecker and S. A. Connolly (2015). "A Functional Interaction between Herpes Simplex Virus 1 Glycoprotein gH/gL Domains I and II and gD Is Defined by Using Alphaherpesvirus gH and gL Chimeras." J Virol **89**(14): 7159-7169.

Fang, Z., J. Martin and Z. Wang (2012). "Statistical methods for identifying differentially expressed genes in RNA-Seq experiments." Cell Biosci **2**(1): 26.

Farrar, J. D., J. D. Smith, T. L. Murphy, S. Leung, G. R. Stark and K. M. Murphy (2000). "Selective loss of type I interferon-induced STAT4 activation caused by a minisatellite insertion in mouse Stat2." Nat Immunol **1**(1): 65-69.

Fatahzadeh, M. and R. A. Schwartz (2007). "Human herpes simplex labialis." Clin Exp Dermatol **32**(6): 625-630.

Feldman, L. T., A. R. Ellison, C. C. Voytek, L. Yang, P. Krause and T. P. Margolis (2002). "Spontaneous molecular reactivation of herpes simplex virus type 1 latency in mice." Proc Natl Acad Sci U S A **99**(2): 978-983.

Feng, P., D. N. Everly, Jr. and G. S. Read (2005). "mRNA decay during herpes simplex virus (HSV) infections: protein-protein interactions involving the HSV virion host shutoff protein and translation factors eIF4H and eIF4A." J Virol **79**(15): 9651-9664.

Filion, G. J., S. Zhenilo, S. Salozhin, D. Yamada, E. Prokhortchouk and P. A. Defossez (2006). "A family of human zinc finger proteins that bind methylated DNA and repress transcription." Mol Cell Biol **26**(1): 169-181.

Finberg, R. W., D. M. Knipe and E. A. Kurt-Jones (2005). "Herpes simplex virus and toll-like receptors." Viral Immunol **18**(3): 457-465.

Firth, C., A. Kitchen, B. Shapiro, M. A. Suchard, E. C. Holmes and A. Rambaut (2010). "Using time-structured data to estimate evolutionary rates of double-stranded DNA viruses." Mol Biol Evol **27**(9): 2038-2051.

Fischer, J., N. Jung, N. Robinson and C. Lehmann (2015). "Sex differences in immune responses to infectious diseases." Infection **43**(4): 399-403.

Fish, E. N. (2008). "The X-files in immunity: sex-based differences predispose immune responses." Nat Rev Immunol **8**(9): 737-744.

Fitzgerald, K. A. (2011). "The interferon inducible gene: Viperin." J Interferon Cytokine Res **31**(1): 131-135.

Fitzsimmons, W. J., R. J. Woods, J. T. McCrone, A. Woodman, J. J. Arnold, M. Yennawar, R. Evans, C. E. Cameron and A. S. Lauring (2018). "A speed-fidelity trade-off determines the mutation rate and virulence of an RNA virus." PLoS Biol **16**(6): e2006459.

Fraser, N. W. and T. Valyi-Nagy (1993). "Viral, neuronal and immune factors which may influence herpes simplex virus (HSV) latency and reactivation." Microb Pathog **15**(2): 83-91.

Friedman, H. M. (2003). "Immune evasion by herpes simplex virus type 1, strategies for virus survival." Trans Am Clin Climatol Assoc **114**: 103-112.

Fruh, K., K. Ahn, H. Djaballah, P. Sempe, P. M. van Endert, R. Tampe, P. A. Peterson and Y. Yang (1995). "A viral inhibitor of peptide transporters for antigen presentation." Nature **375**(6530): 415-418.

Furr, S. R., V. S. Chauhan, M. J. Moerdyk-Schauwecker and I. Marriott (2011). "A role for DNA-dependent activator of interferon regulatory factor in the recognition of herpes simplex virus type 1 by glial cells." J Neuroinflammation **8**: 99.

Gack, M. U., Y. C. Shin, C. H. Joo, T. Urano, C. Liang, et al. (2007). "TRIM25 RING-finger E3 ubiquitin ligase is essential for RIG-I-mediated antiviral activity." Nature **446**(7138): 916-920.

Gaffney, D. F., J. McLauchlan, J. L. Whitton and J. B. Clements (1985). "A modular system for the assay of transcription regulatory signals: the sequence TAATGARAT is required for herpes simplex virus immediate early gene activation." Nucleic Acids Res **13**(21): 7847-7863.

Galluzzi, L., O. Kepp, F. K. Chan and G. Kroemer (2017). "Necroptosis: Mechanisms and Relevance to Disease." Annu Rev Pathol **12**: 103-130.

Gao, M. and D. M. Knipe (1991). "Potential role for herpes simplex virus ICP8 DNA replication protein in stimulation of late gene expression." J Virol **65**(5): 2666-2675.

Garber, M., M. G. Grabherr, M. Guttman and C. Trapnell (2011). "Computational methods for transcriptome annotation and quantification using RNA-seq." Nat Methods **8**(6): 469-477.

Garcia-Sastre, A. (2017). "Ten Strategies of Interferon Evasion by Viruses." Cell Host Microbe **22**(2): 176-184.

Garcia, M. A., J. Gil, I. Ventoso, S. Guerra, E. Domingo, C. Rivas and M. Esteban (2006). "Impact of protein kinase PKR in cell biology: from antiviral to antiproliferative action." Microbiol Mol Biol Rev **70**(4): 1032-1060.

Gaudreault, E., S. Fiola, M. Olivier and J. Gosselin (2007). "Epstein-Barr virus induces MCP-1 secretion by human monocytes via TLR2." J Virol **81**(15): 8016-8024.

Gayen, S., E. Maclary, M. Hinten and S. Kalantry (2016). "Sex-specific silencing of X-linked genes by Xist RNA." Proc Natl Acad Sci U S A **113**(3): E309-318.

Geurs, T. L., E. B. Hill, D. M. Lippold and A. R. French (2012). "Sex differences in murine susceptibility to systemic viral infections." J Autoimmun **38**(2-3): J245-253.

Ghosh, S. and R. S. Klein (2017). "Sex Drives Dimorphic Immune Responses to Viral Infections." J Immunol **198**(5): 1782-1790.

Gianni, T., V. Leoni and G. Campadelli-Fiume (2013). "Type I interferon and NF-kappaB activation elicited by herpes simplex virus gH/gL via alphavbeta3 integrin in epithelial and neuronal cell lines." J Virol **87**(24): 13911-13916.

Gluck, S., B. Guey, M. F. Gulen, K. Wolter, T. W. Kang, et al. (2017). "Innate immune sensing of cytosolic chromatin fragments through cGAS promotes senescence." Nat Cell Biol **19**(9): 1061-1070.

Greene, I. P., E. Wang, E. R. Deardorff, R. Milleron, E. Domingo and S. C. Weaver (2005). "Effect of alternating passage on adaptation of sindbis virus to vertebrate and invertebrate cells." J Virol **79**(22): 14253-14260.

Grinde, B. (2013). "Herpesviruses: latency and reactivation - viral strategies and host response." J Oral Microbiol **5**.

Grondin, B. and N. DeLuca (2000). "Herpes simplex virus type 1 ICP4 promotes transcription preinitiation complex formation by enhancing the binding of TFIID to DNA." J Virol **74**(24): 11504-11510.

Gross, S. T., C. A. Harley and D. W. Wilson (2003). "The cytoplasmic tail of Herpes simplex virus glycoprotein H binds to the tegument protein VP16 in vitro and in vivo." Virology **317**(1): 1-12.

Gruffat, H., R. Marchione and E. Manet (2016). "Herpesvirus Late Gene Expression: A Viral-Specific Pre-initiation Complex Is Key." Front Microbiol **7**: 869.

Grunewald, K., P. Desai, D. C. Winkler, J. B. Heymann, D. M. Belnap, W. Baumeister and A. C. Steven (2003). "Three-dimensional structure of herpes simplex virus from cryo-electron tomography." Science **302**(5649): 1396-1398.

Guerra-Silveira, F. and F. Abad-Franch (2013). "Sex bias in infectious disease epidemiology: patterns and processes." PLoS One **8**(4): e62390.

Guigo, R., E. T. Dermitzakis, P. Agarwal, C. P. Ponting, G. Parra, et al. (2003). "Comparison of mouse and human genomes followed by experimental verification yields an estimated 1,019 additional genes." Proc Natl Acad Sci U S A **100**(3): 1140-1145.

Guo, H., R. P. Gilley, A. Fisher, R. Lane, V. J. Landsteiner, et al. (2018). "Species-independent contribution of ZBP1/DAI/DLM-1-triggered necroptosis in host defense against HSV1." Cell Death Dis **9**(8): 816.

Guo, H., W. J. Kaiser and E. S. Mocarski (2015a). "Manipulation of apoptosis and necroptosis signaling by herpesviruses." Med Microbiol Immunol **204**(3): 439-448.

Guo, H., S. Omoto, P. A. Harris, J. N. Finger, J. Bertin, P. J. Gough, W. J. Kaiser and E. S. Mocarski (2015b). "Herpes simplex virus suppresses necroptosis in human cells." Cell Host Microbe **17**(2): 243-251.

Guo, Y., M. Audry, M. Ciancanelli, L. Alsina, J. Azevedo, et al. (2011). "Herpes simplex virus encephalitis in a patient with complete TLR3 deficiency: TLR3 is otherwise redundant in protective immunity." J Exp Med **208**(10): 2083-2098.

Gupta, A., J. J. Gartner, P. Sethupathy, A. G. Hatzigeorgiou and N. W. Fraser (2006). "Anti-apoptotic function of a microRNA encoded by the HSV-1 latency-associated transcript." Nature **442**(7098): 82-85.

Gutierrez, K. M. (2007). "Rethinking herpes simplex virus infections in children and adolescents." J Pediatr **151**(4): 336-338.

Guzowski, J. F. and E. K. Wagner (1993). "Mutational analysis of the herpes simplex virus type 1 strict late UL38 promoter/leader reveals two regions critical in transcriptional regulation." J Virol **67**(9): 5098-5108.

Haehnel, V., L. Schwarzfischer, M. J. Fenton and M. Rehli (2002). "Transcriptional regulation of the human toll-like receptor 2 gene in monocytes and macrophages." J Immunol **168**(11): 5629-5637.

Hahne, F. and R. Ivanek (2016). "Visualizing Genomic Data Using Gviz and Bioconductor." Methods Mol Biol **1418**: 335-351.

Hakki, M., E. E. Marshall, K. L. De Niro and A. P. Geballe (2006). "Binding and nuclear relocalization of protein kinase R by human cytomegalovirus TRS1." J Virol **80**(23): 11817-11826.

Haley, P. J. (2003). "Species differences in the structure and function of the immune system." Toxicology **188**(1): 49-71.

Halford, W. P., L. A. Veress, B. M. Gebhardt and D. J. Carr (1997). "Innate and acquired immunity to herpes simplex virus type 1." Virology **236**(2): 328-337.

Halstead, S. B. and N. J. Marchette (2003). "Biologic properties of dengue viruses following serial passage in primary dog kidney cells: studies at the University of Hawaii." Am J Trop Med Hyg **69**(6 Suppl): 5-11.

Hamel, R., O. Dejarnac, S. Wichit, P. Ekchariyawat, A. Neyret, et al. (2015). "Biology of Zika Virus Infection in Human Skin Cells." J Virol **89**(17): 8880-8896.

Han, J., P. Chadha, D. G. Meckes, Jr., N. L. Baird and J. W. Wills (2011). "Interaction and interdependent packaging of tegument protein UL11 and glycoprotein e of herpes simplex virus." J Virol **85**(18): 9437-9446.

Han, J., P. Chadha, J. L. Starkey and J. W. Wills (2012). "Function of glycoprotein E of herpes simplex virus requires coordinated assembly of three tegument proteins on its cytoplasmic tail." Proc Natl Acad Sci U S A **109**(48): 19798-19803.

Han, X., P. Lundberg, B. Tanamachi, H. Openshaw, J. Longmate and E. Cantin (2001). "Gender influences herpes simplex virus type 1 infection in normal and gamma interferon-mutant mice." J Virol **75**(6): 3048-3052.

Hansen, K., T. Prabakaran, A. Laustsen, S. E. Jorgensen, S. H. Rahbaek, et al. (2014). "Listeria monocytogenes induces IFNbeta expression through an IFI16-, cGAS- and STING-dependent pathway." EMBO J **33**(15): 1654-1666.

Hardwicke, M. A. and R. M. Sandri-Goldin (1994). "The herpes simplex virus regulatory protein ICP27 contributes to the decrease in cellular mRNA levels during infection." J Virol **68**(8): 4797-4810.

Hare, D. N., S. E. Collins, S. Mukherjee, Y. M. Loo, M. Gale, Jr., L. J. Janssen and K. L. Mossman (2015). "Membrane Perturbation-Associated Ca2+ Signaling and Incoming Genome Sensing Are Required for the Host Response to Low-Level Enveloped Virus Particle Entry." J Virol **90**(6): 3018-3027.

Harkness, J. M., M. Kader and N. A. DeLuca (2014). "Transcription of the herpes simplex virus 1 genome during productive and quiescent infection of neuronal and nonneuronal cells." J Virol **88**(12): 6847-6861.

Harris, M. A., J. Clark, A. Ireland, J. Lomax, M. Ashburner, et al. (2004). "The Gene Ontology (GO) database and informatics resource." Nucleic Acids Res **32**(Database issue): D258-261.

Hayashi, K., L. C. Hooper, M. S. Chin, C. N. Nagineni, B. Detrick and J. J. Hooks (2006). "Herpes simplex virus 1 (HSV-1) DNA and immune complex (HSV-1-human IgG) elicit vigorous interleukin 6 release from infected corneal cells via Toll-like receptors." J Gen Virol **87**(Pt 8): 2161-2169.

He, B., M. Gross and B. Roizman (1997). "The gamma(1)34.5 protein of herpes simplex virus 1 complexes with protein phosphatase 1alpha to dephosphorylate the alpha subunit of the eukaryotic translation initiation factor 2 and preclude the shutoff of protein synthesis by double-stranded RNA-activated protein kinase." Proc Natl Acad Sci U S A **94**(3): 843-848.

He, X., Z. Jing and G. Cheng (2014). "MicroRNAs: new regulators of Toll-like receptor signalling pathways." Biomed Res Int **2014**: 945169.

Heckman, K. L. and L. R. Pease (2007). "Gene splicing and mutagenesis by PCR-driven overlap extension." Nat Protoc **2**(4): 924-932.

Helbig, K. J. and M. R. Beard (2014). "The role of viperin in the innate antiviral response." J Mol Biol **426**(6): 1210-1219.

Helbig, K. J., J. M. Carr, J. K. Calvert, S. Wati, J. N. Clarke, et al. (2013). "Viperin is induced following dengue virus type-2 (DENV-2) infection and has anti-viral actions requiring the C-terminal end of viperin." PLoS Negl Trop Dis **7**(4): e2178.

Helbig, K. J., N. S. Eyre, E. Yip, S. Narayana, K. Li, et al. (2011). "The antiviral protein viperin inhibits hepatitis C virus replication via interaction with nonstructural protein 5A." Hepatology **54**(5): 1506-1517.

Hewagama, A., D. Patel, S. Yarlagadda, F. M. Strickland and B. C. Richardson (2009). "Stronger inflammatory/cytotoxic T-cell response in women identified by microarray analysis." Genes Immun **10**(5): 509-516.

Hill, J. M., B. M. Gebhardt, R. Wen, A. M. Bouterie, H. W. Thompson, R. J. O'Callaghan, W. P. Halford and H. E. Kaufman (1996). "Quantitation of herpes simplex virus type 1 DNA and latency-associated transcripts in rabbit trigeminal ganglia demonstrates a stable reservoir of viral nucleic acids during latency." J Virol **70**(5): 3137-3141.

Hinson, E. R. and P. Cresswell (2009a). "The antiviral protein, viperin, localizes to lipid droplets via its N-terminal amphipathic alpha-helix." Proc Natl Acad Sci U S A **106**(48): 20452-20457.

Hinson, E. R. and P. Cresswell (2009b). "The N-terminal amphipathic alpha-helix of viperin mediates localization to the cytosolic face of the endoplasmic reticulum and inhibits protein secretion." J Biol Chem **284**(7): 4705-4712.

Hinson, E. R., N. S. Joshi, J. H. Chen, C. Rahner, Y. W. Jung, X. Wang, S. M. Kaech and P. Cresswell (2010). "Viperin is highly induced in neutrophils and macrophages during acute and chronic lymphocytic choriomeningitis virus infection." J Immunol **184**(10): 5723-5731.

Hiscott, J. (2007). "Triggering the innate antiviral response through IRF-3 activation." J Biol Chem **282**(21): 15325-15329.

Hochrein, H., B. Schlatter, M. O'Keeffe, C. Wagner, F. Schmitz, M. Schiemann, S. Bauer, M. Suter and H. Wagner (2004). "Herpes simplex virus type-1 induces IFN-alpha production via Toll-like receptor 9-dependent and -independent pathways." Proc Natl Acad Sci U S A **101**(31): 11416-11421.

Holler, N., R. Zaru, O. Micheau, M. Thome, A. Attinger, et al. (2000). "Fas triggers an alternative, caspase-8-independent cell death pathway using the kinase RIP as effector molecule." Nat Immunol **1**(6): 489-495.

Homa, F. L. and J. C. Brown (1997). "Capsid assembly and DNA packaging in herpes simplex virus." Rev Med Virol **7**(2): 107-122.

Honess, R. W. and B. Roizman (1974). "Regulation of herpesvirus macromolecular synthesis. I. Cascade regulation of the synthesis of three groups of viral proteins." J Virol **14**(1): 8-19.

Horan, K. A., K. Hansen, M. R. Jakobsen, C. K. Holm, S. Soby, et al. (2013). "Proteasomal degradation of herpes simplex virus capsids in macrophages releases DNA to the cytosol for recognition by DNA sensors." J Immunol **190**(5): 2311-2319.

Howard, M., J. W. Sellors, D. Jang, N. J. Robinson, M. Fearon, J. Kaczorowski and M. Chernesky (2003). "Regional distribution of antibodies to herpes simplex virus type 1 (HSV-1) and HSV-2 in men and women in Ontario, Canada." J Clin Microbiol **41**(1): 84-89.

Huang da, W., B. T. Sherman and R. A. Lempicki (2009). "Systematic and integrative analysis of large gene lists using DAVID bioinformatics resources." Nat Protoc **4**(1): 44-57.

Huang, D. W., B. T. Sherman, Q. Tan, J. Kir, D. Liu, et al. (2007). "DAVID Bioinformatics Resources: expanded annotation database and novel algorithms to better extract biology from large gene lists." Nucleic Acids Res **35**(Web Server issue): W169-175.

Huang, Z., S. Q. Wu, Y. Liang, X. Zhou, W. Chen, et al. (2015). "RIP1/RIP3 binding to HSV-1 ICP6 initiates necroptosis to restrict virus propagation in mice." Cell Host Microbe **17**(2): 229-242.

Hughes, A. L., S. Irausquin and R. Friedman (2010). "The evolutionary biology of poxviruses." Infect Genet Evol **10**(1): 50-59.

Hunter, K. W. (2012). "Mouse models of cancer: does the strain matter?" Nat Rev Cancer **12**(2): 144-149.

Into, T., M. Inomata, E. Takayama and T. Takigawa (2012). "Autophagy in regulation of Toll-like receptor signaling." Cell Signal **24**(6): 1150-1162.

Ishii, K. J., C. Coban, H. Kato, K. Takahashi, Y. Torii, et al. (2006). "A Toll-like receptor-independent antiviral response induced by double-stranded B-form DNA." Nat Immunol **7**(1): 40-48.

Ishikawa, H. and G. N. Barber (2011). "The STING pathway and regulation of innate immune signaling in response to DNA pathogens." Cell Mol Life Sci **68**(7): 1157-1165.

Ishikawa, H., Z. Ma and G. N. Barber (2009). "STING regulates intracellular DNA-mediated, type I interferon-dependent innate immunity." Nature **461**(7265): 788-792.

Iversen, M. B., L. S. Reinert, M. K. Thomsen, I. Bagdonaite, R. Nandakumar, et al. (2016). "An innate antiviral pathway acting before interferons at epithelial surfaces." Nat Immunol **17**(2): 150-158.

Jackson, J. O., E. Lin, P. G. Spear and R. Longnecker (2010). "Insertion mutations in herpes simplex virus 1 glycoprotein H reduce cell surface expression, slow the rate of cell fusion, or abrogate functions in cell fusion and viral entry." J Virol **84**(4): 2038-2046.

Jacquemont, B. and B. Roizman (1975). "RNA synthesis in cells infected with herpes simplex virus. X. Properties of viral symmetric transcripts and of double-stranded RNA prepared from them." J Virol **15**(4): 707-713.

Javier, R. T., J. G. Stevens, V. B. Dissette and E. K. Wagner (1988). "A herpes simplex virus transcript abundant in latently infected neurons is dispensable for establishment of the latent state." Virology **166**(1): 254-257.

Jean, S., K. M. LeVan, B. Song, M. Levine and D. M. Knipe (2001). "Herpes simplex virus 1 ICP27 is required for transcription of two viral late (gamma 2) genes in infected cells." Virology **283**(2): 273-284.

Jensen, S. and A. R. Thomsen (2012). "Sensing of RNA viruses: a review of innate immune receptors involved in recognizing RNA virus invasion." J Virol **86**(6): 2900-2910.

Jiang, D., H. Guo, C. Xu, J. Chang, B. Gu, L. Wang, T. M. Block and J. T. Guo (2008). "Identification of three interferon-inducible cellular enzymes that inhibit the replication of hepatitis C virus." J Virol **82**(4): 1665-1678.

Jin, H., Z. Yan, Y. Ma, Y. Cao and B. He (2011). "A herpesvirus virulence factor inhibits dendritic cell maturation through protein phosphatase 1 and Ikappa B kinase." J Virol **85**(7): 3397-3407.

Jin, H. K., K. Yoshimatsu, A. Takada, M. Ogino, A. Asano, J. Arikawa and T. Watanabe (2001). "Mouse Mx2 protein inhibits hantavirus but not influenza virus replication." Arch Virol **146**(1): 41-49.

Johnson, K. E., B. Song and D. M. Knipe (2008). "Role for herpes simplex virus 1 ICP27 in the inhibition of type I interferon signaling." Virology **374**(2): 487-494.

Johnston, C. and L. Corey (2016). "Current Concepts for Genital Herpes Simplex Virus Infection: Diagnostics and Pathogenesis of Genital Tract Shedding." Clin Microbiol Rev **29**(1): 149-161.

Jones, C. (1998). "Alphaherpesvirus latency: its role in disease and survival of the virus in nature." Adv Virus Res **51**: 81-133.

Jugovic, P., A. M. Hill, R. Tomazin, H. Ploegh and D. C. Johnson (1998). "Inhibition of major histocompatibility complex class I antigen presentation in pig and primate cells by herpes simplex virus type 1 and 2 ICP47." J Virol **72**(6): 5076-5084.

Junt, T. and W. Barchet (2015). "Translating nucleic acid-sensing pathways into therapies." Nat Rev Immunol **15**(9): 529-544.

Jurak, I., M. F. Kramer, J. C. Mellor, A. L. van Lint, F. P. Roth, D. M. Knipe and D. M. Coen (2010). "Numerous conserved and divergent microRNAs expressed by herpes simplex viruses 1 and 2." J Virol **84**(9): 4659-4672.

Kadowaki, N., S. Ho, S. Antonenko, R. W. Malefyt, R. A. Kastelein, F. Bazan and Y. J. Liu (2001). "Subsets of human dendritic cell precursors express different toll-like receptors and respond to different microbial antigens." J Exp Med **194**(6): 863-869.

Kalamvoki, M. and B. Roizman (2014). "HSV-1 degrades, stabilizes, requires, or is stung by STING depending on ICP0, the US3 protein kinase, and cell derivation." Proc Natl Acad Sci U S A **111**(5): E611-617.

Kastrukoff, L. F., A. S. Lau and E. E. Thomas (2012). "The effect of mouse strain on herpes simplex virus type 1 (HSV-1) infection of the central nervous system (CNS)." Herpesviridae **3**: 4.

Kato, A., Z. Liu, A. Minowa, T. Imai, M. Tanaka, K. Sugimoto, Y. Nishiyama, J. Arii and Y. Kawaguchi (2011). "Herpes simplex virus 1 protein kinase Us3 and major tegument protein UL47 reciprocally regulate their subcellular localization in infected cells." J Virol **85**(18): 9599-9613.

Kawaguchi, Y. (2013). "Us3, a multifunctional protein kinase encoded by herpes simplex virus 1: how does it function in vivo?" Cornea **32 Suppl 1**: S22-27.

Kawai, T. and S. Akira (2011). "Toll-like receptors and their crosstalk with other innate receptors in infection and immunity." Immunity **34**(5): 637-650.

Kawai, T., O. Takeuchi, T. Fujita, J. Inoue, P. F. Muhlradt, S. Sato, K. Hoshino and S. Akira (2001). "Lipopolysaccharide stimulates the MyD88-independent pathway and results in activation of IFN-regulatory factor 3 and the expression of a subset of lipopolysaccharide-inducible genes." J Immunol **167**(10): 5887-5894.

Kay, G. F. (1998). "Xist and X chromosome inactivation." Mol Cell Endocrinol **140**(1-2): 71-76.

Kay, G. F., G. D. Penny, D. Patel, A. Ashworth, N. Brockdorff and S. Rastan (1993). "Expression of Xist during mouse development suggests a role in the initiation of X chromosome inactivation." Cell **72**(2): 171-182.

Kerr, P. J., J. Hone, L. Perrin, N. French and C. K. Williams (2010). "Molecular and serological analysis of the epidemiology of myxoma virus in rabbits." Vet Microbiol **143**(2-4): 167-178.

Khoo, D., C. Perez and I. Mohr (2002). "Characterization of RNA determinants recognized by the arginine- and proline-rich region of Us11, a herpes simplex virus type 1-encoded double-stranded RNA binding protein that prevents PKR activation." J Virol **76**(23): 11971-11981.

Kieleczawa, J. and E. Mazaika (2010). "Optimization of protocol for sequencing of difficult templates." J Biomol Tech **21**(2): 97-102.

Kim, D., G. Pertea, C. Trapnell, H. Pimentel, R. Kelley and S. L. Salzberg (2013). "TopHat2: accurate alignment of transcriptomes in the presence of insertions, deletions and gene fusions." Genome Biol **14**(4): R36.

Kimura, T., K. Nakayama, J. Penninger, M. Kitagawa, H. Harada, et al. (1994). "Involvement of the IRF-1 transcription factor in antiviral responses to interferons." Science **264**(5167): 1921-1924.

Klein, S. L. (2012). "Sex influences immune responses to viruses, and efficacy of prophylaxis and treatments for viral diseases." Bioessays **34**(12): 1050-1059.

Klein, S. L. and K. L. Flanagan (2016). "Sex differences in immune responses." Nat Rev Immunol **16**(10): 626-638.

Klein, S. L., I. Marriott and E. N. Fish (2015). "Sex-based differences in immune function and responses to vaccination." Trans R Soc Trop Med Hyg **109**(1): 9-15.

Klysik, K., A. Pietraszek, A. Karewicz and M. Nowakowska (2018). "Acyclovir in the Treatment of Herpes Viruses - a Review." Curr Med Chem.

Knez, J., P. T. Bilan and J. P. Capone (2003). "A single amino acid substitution in herpes simplex virus type 1 VP16 inhibits binding to the virion host shutoff protein and is incompatible with virus growth." J Virol **77**(5): 2892-2902.

Knoblich, A., J. Gortz, V. Harle-Grupp and D. Falke (1983). "Kinetics and genetics of herpes simplex virus-induced antibody formation in mice." Infect Immun **39**(1): 15-23.

Koelle, D. M. and L. Corey (2008). "Herpes simplex: insights on pathogenesis and possible vaccines." Annu Rev Med **59**: 381-395.

Kollias, C. M., R. B. Huneke, B. Wigdahl and S. R. Jennings (2015). "Animal models of herpes simplex virus immunity and pathogenesis." J Neurovirol **21**(1): 8-23.

Korobkova, E., T. Emonet, J. M. Vilar, T. S. Shimizu and P. Cluzel (2004). "From molecular noise to behavioural variability in a single bacterium." Nature **428**(6982): 574-578.

Kracker, S. and A. Radbruch (2004). "Immunoglobulin class switching: in vitro induction and analysis." Methods Mol Biol **271**: 149-159.

Kramer, M. F. and D. M. Coen (1995). "Quantification of transcripts from the ICP4 and thymidine kinase genes in mouse ganglia latently infected with herpes simplex virus." J Virol **69**(3): 1389-1399.

Krishnan, K., R. Pine and J. J. Krolewski (1997). "Kinase-deficient forms of Jak1 and Tyk2 inhibit interferon alpha signaling in a dominant manner." Eur J Biochem **247**(1): 298-305.

Ku, C. C., X. B. Che, M. Reichelt, J. Rajamani, A. Schaap-Nutt, et al. (2011). "Herpes simplex virus-1 induces expression of a novel MxA isoform that enhances viral replication." Immunol Cell Biol **89**(2): 173-182.

Kuroda, H. (2015). "[Update on Herpes Simplex Encephalitis]." Brain Nerve **67**(7): 931-939.

Kurt-Jones, E. A., J. Belko, C. Yu, P. E. Newburger, J. Wang, M. Chan, D. M. Knipe and R. W. Finberg (2005). "The role of toll-like receptors in herpes simplex infection in neonates." J Infect Dis **191**(5): 746-748.

Kurt-Jones, E. A., M. Chan, S. Zhou, J. Wang, G. Reed, R. Bronson, M. M. Arnold, D. M. Knipe and R. W. Finberg (2004). "Herpes simplex virus 1 interaction with Toll-like receptor 2 contributes to lethal encephalitis." Proc Natl Acad Sci U S A **101**(5): 1315-1320.

Kurtz, S., A. Phillippy, A. L. Delcher, M. Smoot, M. Shumway, C. Antonescu and S. L. Salzberg (2004). "Versatile and open software for comparing large genomes." Genome Biol **5**(2): R12.

Kwiecien, J. M., B. I. Bassey-Archibong, W. Dabrowski, L. G. Rayner, A. R. Lucas and J. M. Daniel (2017). "Loss of Kaiso expression in breast cancer cells prevents intra-vascular invasion in the lung and secondary metastasis." PLoS One **12**(9): e0183883.

Kwong, A. D. and N. Frenkel (1987). "Herpes simplex virus-infected cells contain a function(s) that destabilizes both host and viral mRNAs." Proc Natl Acad Sci U S A **84**(7): 1926-1930.

Lachmann, R. (2003). "Herpes simplex virus latency." Expert Rev Mol Med **5**(29): 1-14.

Lafaille, F. G., I. M. Pessach, S. Y. Zhang, M. J. Ciancanelli, M. Herman, et al. (2012). "Impaired intrinsic immunity to HSV-1 in human iPSC-derived TLR3-deficient CNS cells." Nature **491**(7426): 769-773.

Lanfranca, M. P., H. H. Mostafa and D. J. Davido (2014). "HSV-1 ICP0: An E3 Ubiquitin Ligase That Counteracts Host Intrinsic and Innate Immunity." Cells **3**(2): 438-454.

Langelier, Y., S. Bergeron, S. Chabaud, J. Lippens, C. Guilbault, A. M. Sasseville, S. Denis, D. D. Mosser and B. Massie (2002). "The R1 subunit of herpes simplex virus ribonucleotide reductase protects cells against apoptosis at, or upstream of, caspase-8 activation." J Gen Virol **83**(Pt 11): 2779-2789.

Law, C. W., M. Alhamdoosh, S. Su, G. K. Smyth and M. E. Ritchie (2016). "RNA-seq analysis is easy as 1-2-3 with limma, Glimma and edgeR." F1000Res **5**: 1408.

Law, C. W., Y. Chen, W. Shi and G. K. Smyth (2014). "voom: Precision weights unlock linear model analysis tools for RNA-seq read counts." Genome Biol **15**(2): R29.

Lee, K., A. W. Kolb, Y. Sverchkov, J. A. Cuellar, M. Craven and C. R. Brandt (2015). "Recombination Analysis of Herpes Simplex Virus 1 Reveals a Bias toward GC Content and the Inverted Repeat Regions." J Virol **89**(14): 7214-7223.

Lehman, I. R. and P. E. Boehmer (1999). "Replication of herpes simplex virus DNA." J Biol Chem **274**(40): 28059-28062.

Leib, D. A., T. E. Harrison, K. M. Laslo, M. A. Machalek, N. J. Moorman and H. W. Virgin (1999). "Interferons regulate the phenotype of wild-type and mutant herpes simplex viruses in vivo." J Exp Med **189**(4): 663-672.

Lenschow, D. J., C. Lai, N. Frias-Staheli, N. V. Giannakopoulos, A. Lutz, et al. (2007). "IFN-stimulated gene 15 functions as a critical antiviral molecule against influenza, herpes, and Sindbis viruses." Proc Natl Acad Sci U S A **104**(4): 1371-1376.

Leopardi, R., C. Van Sant and B. Roizman (1997). "The herpes simplex virus 1 protein kinase US3 is required for protection from apoptosis induced by the virus." Proc Natl Acad Sci U S A **94**(15): 7891-7896.

Leung, K. N. and B. Panning (2014). "X-inactivation: Xist RNA uses chromosome contacts to coat the X." Curr Biol **24**(2): R80-82.

Levitz, R. E. (1998). "Herpes simplex encephalitis: a review." Heart Lung **27**(3): 209-212.

Levy, D. E., D. S. Kessler, R. Pine and J. E. Darnell, Jr. (1989). "Cytoplasmic activation of ISGF3, the positive regulator of interferon-alpha-stimulated transcription, reconstituted in vitro." Genes Dev **3**(9): 1362-1371.

Li, H. and R. Durbin (2009). "Fast and accurate short read alignment with Burrows-Wheeler transform." Bioinformatics **25**(14): 1754-1760.

Li, H., J. Zhang, A. Kumar, M. Zheng, S. S. Atherton and F. S. Yu (2006). "Herpes simplex virus 1 infection induces the expression of proinflammatory cytokines, interferons and TLR7 in human corneal epithelial cells." Immunology **117**(2): 167-176.

Li, S., L. Wang, M. Berman, Y. Y. Kong and M. E. Dorf (2011). "Mapping a dynamic innate immunity protein interaction network regulating type I interferon production." Immunity **35**(3): 426-440.

Li, T., B. A. Diner, J. Chen and I. M. Cristea (2012). "Acetylation modulates cellular distribution and DNA sensing ability of interferon-inducible protein IFI16." Proc Natl Acad Sci U S A **109**(26): 10558-10563.

Li, X. D., J. Wu, D. Gao, H. Wang, L. Sun and Z. J. Chen (2013). "Pivotal roles of cGAS-cGAMP signaling in antiviral defense and immune adjuvant effects." Science **341**(6152): 1390-1394.

Liao, Y., G. K. Smyth and W. Shi (2014). "featureCounts: an efficient general purpose program for assigning sequence reads to genomic features." Bioinformatics **30**(7): 923-930.

Libert, C., L. Dejager and I. Pinheiro (2010). "The X chromosome in immune functions: when a chromosome makes the difference." Nat Rev Immunol **10**(8): 594-604.

Lim, W. H., S. Kireta, G. R. Russ and P. T. Coates (2007). "Human plasmacytoid dendritic cells regulate immune responses to Epstein-Barr virus (EBV) infection and delay EBV-related mortality in humanized NOD-SCID mice." Blood **109**(3): 1043-1050.

Lima, G. K., G. P. Zolini, D. S. Mansur, B. H. Freire Lima, U. Wischhoff, et al. (2010). "Toll-like receptor (TLR) 2 and TLR9 expressed in trigeminal ganglia are critical to viral control during herpes simplex virus 1 infection." Am J Pathol **177**(5): 2433-2445.

Lin, R., R. S. Noyce, S. E. Collins, R. D. Everett and K. L. Mossman (2004). "The herpes simplex virus ICP0 RING finger domain inhibits IRF3- and IRF7-mediated activation of interferon-stimulated genes." J Virol **78**(4): 1675-1684.

Liu, T., K. M. Khanna, B. N. Carriere and R. L. Hendricks (2001). "Gamma interferon can prevent herpes simplex virus type 1 reactivation from latency in sensory neurons." J Virol **75**(22): 11178-11184.

Liu, X., D. Main, Y. Ma and B. He (2018). "Herpes Simplex Virus 1 Inhibits TANK-Binding Kinase 1 through Formation of the Us11-Hsp90 Complex." J Virol **92**(14).

Liu, Y., W. Gong, C. C. Huang, W. Herr and X. Cheng (1999). "Crystal structure of the conserved core of the herpes simplex virus transcriptional regulatory protein VP16." Genes Dev **13**(13): 1692-1703.

Liu, Y. P., L. Zeng, A. Tian, A. Bomkamp, D. Rivera, D. Gutman, G. N. Barber, J. K. Olson and J. A. Smith (2012). "Endoplasmic reticulum stress regulates the innate immunity critical transcription factor IRF3." J Immunol **189**(9): 4630-4639.

Loo, Y. M. and M. Gale, Jr. (2011). "Immune signaling by RIG-I-like receptors." Immunity **34**(5): 680-692.

Looker, K. J., A. S. Magaret, M. T. May, K. M. Turner, P. Vickerman, S. L. Gottlieb and L. M. Newman (2015a). "Global and Regional Estimates of Prevalent and Incident Herpes Simplex Virus Type 1 Infections in 2012." PLoS One **10**(10): e0140765.

Looker, K. J., A. S. Magaret, K. M. Turner, P. Vickerman, S. L. Gottlieb and L. M. Newman (2015b). "Global estimates of prevalent and incident herpes simplex virus type 2 infections in 2012." PLoS One **10**(1): e114989.

Lopes, E. C., E. Valls, M. E. Figueroa, A. Mazur, F. G. Meng, et al. (2008). "Kaiso contributes to DNA methylation-dependent silencing of tumor suppressor genes in colon cancer cell lines." Cancer Res **68**(18): 7258-7263.

Luker, G. D., J. L. Prior, J. Song, C. M. Pica and D. A. Leib (2003). "Bioluminescence imaging reveals systemic dissemination of herpes simplex virus type 1 in the absence of interferon receptors." J Virol **77**(20): 11082-11093.

Lund, J., A. Sato, S. Akira, R. Medzhitov and A. Iwasaki (2003). "Toll-like receptor 9-mediated recognition of Herpes simplex virus-2 by plasmacytoid dendritic cells." J Exp Med **198**(3): 513-520.

Lundberg, P., P. Welander, H. Openshaw, C. Nalbandian, C. Edwards, L. Moldawer and E. Cantin (2003). "A locus on mouse chromosome 6 that determines resistance to herpes simplex virus also influences reactivation, while an unlinked locus augments resistance of female mice." J Virol **77**(21): 11661-11673.

Lussignol, M., C. Queval, M. F. Bernet-Camard, J. Cotte-Laffitte, I. Beau, P. Codogno and A. Esclatine (2013). "The herpes simplex virus 1 Us11 protein inhibits autophagy through its interaction with the protein kinase PKR." J Virol **87**(2): 859-871.

Lv, Q., L. Yuan, Y. Song, T. Sui, Z. Li and L. Lai (2016). "D-repeat in the XIST gene is required for X chromosome inactivation." RNA Biol **13**(2): 172-176.

Lynch, M. (2010). "Evolution of the mutation rate." Trends Genet **26**(8): 345-352.

Ma, J. Z., T. A. Russell, T. Spelman, F. R. Carbone and D. C. Tscharke (2014). "Lytic gene expression is frequent in HSV-1 latent infection and correlates with the engagement of a cell-intrinsic transcriptional response." PLoS Pathog **10**(7): e1004237.

Ma, Y. and B. He (2014). "Recognition of herpes simplex viruses: toll-like receptors and beyond." J Mol Biol **426**(6): 1133-1147.

Ma, Y., H. Jin, T. Valyi-Nagy, Y. Cao, Z. Yan and B. He (2012). "Inhibition of TANK binding kinase 1 by herpes simplex virus 1 facilitates productive infection." J Virol **86**(4): 2188-2196.

Macagno, A., N. L. Bernasconi, F. Vanzetta, E. Dander, A. Sarasini, M. G. Revello, G. Gerna, F. Sallusto and A. Lanzavecchia (2010). "Isolation of human monoclonal antibodies that potently neutralize human cytomegalovirus infection by targeting different epitopes on the gH/gL/UL128-131A complex." J Virol **84**(2): 1005-1013.

MacMicking, J. D. (2012). "Interferon-inducible effector mechanisms in cell-autonomous immunity." Nat Rev Immunol **12**(5): 367-382.

Malmgaard, L., J. Melchjorsen, A. G. Bowie, S. C. Mogensen and S. R. Paludan (2004). "Viral activation of macrophages through TLR-dependent and -independent pathways." J Immunol **173**(11): 6890-6898.

Man, S. M., R. Karki, R. K. Malireddi, G. Neale, P. Vogel, M. Yamamoto, M. Lamkanfi and T. D. Kanneganti (2015). "The transcription factor IRF1 and guanylate-binding proteins target activation of the AIM2 inflammasome by Francisella infection." Nat Immunol **16**(5): 467-475.

Man, S. M., R. Karki, M. Sasai, D. E. Place, S. Kesavardhana, et al. (2016). "IRGB10 Liberates Bacterial Ligands for Sensing by the AIM2 and Caspase-11-NLRP3 Inflammasomes." Cell **167**(2): 382-396 e317.

Manivanh, R., J. Mehrbach, D. M. Knipe and D. A. Leib (2017). "Role of Herpes Simplex Virus 1 gamma34.5 in the Regulation of IRF3 Signaling." J Virol **91**(23).

Marcais, G., A. L. Delcher, A. M. Phillippy, R. Coston, S. L. Salzberg and A. Zimin (2018). "MUMmer4: A fast and versatile genome alignment system." PLoS Comput Biol **14**(1): e1005944.

Martin-Vicente, M., L. M. Medrano, S. Resino, A. Garcia-Sastre and I. Martinez (2017). "TRIM25 in the Regulation of the Antiviral Innate Immunity." Front Immunol **8**: 1187.

Matsuguchi, T., K. Takagi, T. Musikacharoen and Y. Yoshikai (2000). "Gene expressions of lipopolysaccharide receptors, toll-like receptors 2 and 4, are differently regulated in mouse T lymphocytes." Blood **95**(4): 1378-1385.

McCarthy, A. M., L. McMahan and P. A. Schaffer (1989). "Herpes simplex virus type 1 ICP27 deletion mutants exhibit altered patterns of transcription and are DNA deficient." J Virol **63**(1): 18-27.

McGeoch, D. J. (1987). "The genome of herpes simplex virus: structure, replication and evolution." J Cell Sci Suppl **7**: 67-94.

McGeoch, D. J., M. A. Dalrymple, A. J. Davison, A. Dolan, M. C. Frame, D. McNab, L. J. Perry, J. E. Scott and P. Taylor (1988). "The complete DNA sequence of the long unique region in the genome of herpes simplex virus type 1." J Gen Virol **69 (Pt 7)**: 1531-1574.

McGeoch, D. J., F. J. Rixon and A. J. Davison (2006). "Topics in herpesvirus genomics and evolution." Virus Res **117**(1): 90-104.

McNatt, M. W., T. Zang, T. Hatziioannou, M. Bartlett, I. B. Fofana, W. E. Johnson, S. J. Neil and P. D. Bieniasz (2009). "Species-specific activity of HIV-1 Vpu and positive selection of tetherin transmembrane domain variants." PLoS Pathog **5**(2): e1000300.

McWhite, C. D., A. G. Meyer and C. O. Wilke (2016). "Sequence amplification via cell passaging creates spurious signals of positive adaptation in influenza virus H3N2 hemagglutinin." Virus Evol **2**(2).

Medzhitov, R., P. Preston-Hurlburt and C. A. Janeway, Jr. (1997). "A human homologue of the Drosophila Toll protein signals activation of adaptive immunity." Nature **388**(6640): 394-397.

Melchjorsen, J., S. Matikainen and S. R. Paludan (2009). "Activation and evasion of innate antiviral immunity by herpes simplex virus." Viruses **1**(3): 737-759.

Melchjorsen, J., J. Rintahaka, S. Soby, K. A. Horan, A. Poltajainen, L. Ostergaard, S. R. Paludan and S. Matikainen (2010). "Early innate recognition of herpes simplex virus in human primary macrophages is mediated via the MDA5/MAVS-dependent and MDA5/MAVS/RNA polymerase III-independent pathways." J Virol **84**(21): 11350-11358.

Melchjorsen, J., J. Siren, I. Julkunen, S. R. Paludan and S. Matikainen (2006). "Induction of cytokine expression by herpes simplex virus in human monocyte-derived macrophages and dendritic cells is dependent on virus replication and is counteracted by ICP27 targeting NF-kappaB and IRF-3." J Gen Virol **87**(Pt 5): 1099-1108.

Melroe, G. T., L. Silva, P. A. Schaffer and D. M. Knipe (2007). "Recruitment of activated IRF-3 and CBP/p300 to herpes simplex virus ICP0 nuclear foci: Potential role in blocking IFN-beta induction." Virology **360**(2): 305-321.

Mester, J. C. and B. T. Rouse (1991). "The mouse model and understanding immunity to herpes simplex virus." Rev Infect Dis **13 Suppl 11**: S935-945.

Mettenleiter, T. C. (2002). "Herpesvirus assembly and egress." J Virol **76**(4): 1537-1547.

Migeon, B. R. (2007). "Why females are mosaics, X-chromosome inactivation, and sex differences in disease." Gend Med **4**(2): 97-105.

Miller, D. M., B. M. Rahill, J. M. Boss, M. D. Lairmore, J. E. Durbin, J. W. Waldman and D. D. Sedmak (1998). "Human cytomegalovirus inhibits major histocompatibility complex class II expression by disruption of the Jak/Stat pathway." J Exp Med **187**(5): 675-683.

Miller, D. M., Y. Zhang, B. M. Rahill, W. J. Waldman and D. D. Sedmak (1999). "Human cytomegalovirus inhibits IFN-alpha-stimulated antiviral and immunoregulatory responses by blocking multiple levels of IFN-alpha signal transduction." J Immunol **162**(10): 6107-6113.

Mindel, A., O. Carney and P. Williams (1990). "Cutaneous herpes simplex infections." Genitourin Med **66**(1): 14-15.

Mino, A., A. Troeger, C. Brendel, A. Cantor, C. Harris, M. F. Ciuculescu and D. A. Williams (2018). "RhoH participates in a multi-protein complex with the zinc finger protein kaiso that regulates both cytoskeletal structures and chemokine-induced T cells." Small GTPases **9**(3): 260-273.

Miyazaki, T., A. Kawahara, H. Fujii, Y. Nakagawa, Y. Minami, et al. (1994). "Functional activation of Jak1 and Jak3 by selective association with IL-2 receptor subunits." Science **266**(5187): 1045-1047.

Montville, R., R. Froissart, S. K. Remold, O. Tenaillon and P. E. Turner (2005). "Evolution of mutational robustness in an RNA virus." PLoS Biol **3**(11): e381.

Morrison, T. E. and M. S. Diamond (2017). "Animal Models of Zika Virus Infection, Pathogenesis, and Immunity." J Virol **91**(8).

Mossman, K. L. (2002). "Activation and inhibition of virus and interferon: the herpesvirus story." Viral Immunol **15**(1): 3-15.

Mossman, K. L., P. F. Macgregor, J. J. Rozmus, A. B. Goryachev, A. M. Edwards and J. R. Smiley (2001). "Herpes simplex virus triggers and then disarms a host antiviral response." J Virol **75**(2): 750-758.

Mou, F., E. Wills and J. D. Baines (2009). "Phosphorylation of the U(L)31 protein of herpes simplex virus 1 by the U(S)3-encoded kinase regulates localization of the nuclear envelopment complex and egress of nucleocapsids." J Virol **83**(10): 5181-5191.

Mugford, J. W., J. Starmer, R. L. Williams, Jr., J. M. Calabrese, P. Mieczkowski, D. Yee and T. Magnuson (2014). "Evidence for local regulatory control of escape from imprinted X chromosome inactivation." Genetics **197**(2): 715-723.

Murphy, J. A., R. J. Duerst, T. J. Smith and L. A. Morrison (2003). "Herpes simplex virus type 2 virion host shutoff protein regulates alpha/beta interferon but not adaptive immune responses during primary infection in vivo." J Virol **77**(17): 9337-9345.

Musikacharoen, T., T. Matsuguchi, T. Kikuchi and Y. Yoshikai (2001). "NF-kappa B and STAT5 play important roles in the regulation of mouse Toll-like receptor 2 gene expression." J Immunol **166**(7): 4516-4524.

Nailwal, H. and F. K. Chan (2019). "Necroptosis in anti-viral inflammation." Cell Death Differ **26**(1): 4-13.

Naseem, M., A. Barzi, C. Brezden-Masley, A. Puccini, M. D. Berger, et al. (2018). "Outlooks on Epstein-Barr virus associated gastric cancer." Cancer Treat Rev **66**: 15-22.

Nasr, N., S. Maddocks, S. G. Turville, A. N. Harman, N. Woolger, et al. (2012). "HIV-1 infection of human macrophages directly induces viperin which inhibits viral production." Blood **120**(4): 778-788.

Nealon, J. R., S. J. Blanksby, T. W. Mitchell and P. L. Else (2008). "Systematic differences in membrane acyl composition associated with varying body mass in mammals occur in all phospholipid classes: an analysis of kidney and brain." J Exp Biol **211**(Pt 19): 3195-3204.

Netherton, C. L., J. Simpson, O. Haller, T. E. Wileman, H. H. Takamatsu, P. Monaghan and G. Taylor (2009). "Inhibition of a large double-stranded DNA virus by MxA protein." J Virol **83**(5): 2310-2320.

Newcomb, W. W., F. L. Homa and J. C. Brown (2006). "Herpes simplex virus capsid structure: DNA packaging protein UL25 is located on the external surface of the capsid near the vertices." J Virol **80**(13): 6286-6294.

Nhamoyebonde, S. and A. Leslie (2014). "Biological differences between the sexes and susceptibility to tuberculosis." J Infect Dis **209 Suppl 3**: S100-106.

Nicholl, M. J., L. H. Robinson and C. M. Preston (2000). "Activation of cellular interferon-responsive genes after infection of human cells with herpes simplex virus type 1." J Gen Virol **81**(Pt 9): 2215-2218.

Nicoll, M. P., W. Hann, M. Shivkumar, L. E. Harman, V. Connor, H. M. Coleman, J. T. Proenca and S. Efstathiou (2016). "The HSV-1 Latency-Associated Transcript Functions to Repress Latent Phase Lytic Gene Expression and Suppress Virus Reactivation from Latently Infected Neurons." PLoS Pathog **12**(4): e1005539.

Nicoll, M. P., J. T. Proenca and S. Efstathiou (2012). "The molecular basis of herpes simplex virus latency." FEMS Microbiol Rev **36**(3): 684-705.

Ning, S., L. E. Huye and J. S. Pagano (2005). "Regulation of the transcriptional activity of the IRF7 promoter by a pathway independent of interferon signaling." J Biol Chem **280**(13): 12262-12270.

Nogusa, S., R. J. Thapa, C. P. Dillon, S. Liedmann, T. H. Oguin, 3rd, et al. (2016). "RIPK3 Activates Parallel Pathways of MLKL-Driven Necroptosis and FADD-Mediated Apoptosis to Protect against Influenza A Virus." Cell Host Microbe **20**(1): 13-24.

Noyce, R. S., K. Taylor, M. Ciechonska, S. E. Collins, R. Duncan and K. L. Mossman (2011). "Membrane perturbation elicits an IRF3-dependent, interferon-independent antiviral response." J Virol **85**(20): 10926-10931.

O'Neill, L. A., F. J. Sheedy and C. E. McCoy (2011). "MicroRNAs: the fine-tuners of Toll-like receptor signalling." Nat Rev Immunol **11**(3): 163-175.

Ogg, P. D., P. J. McDonell, B. J. Ryckman, C. M. Knudson and R. J. Roller (2004). "The HSV-1 Us3 protein kinase is sufficient to block apoptosis induced by overexpression of a variety of Bcl-2 family members." Virology **319**(2): 212-224.

Ojala, P. M., B. Sodeik, M. W. Ebersold, U. Kutay and A. Helenius (2000). "Herpes simplex virus type 1 entry into host cells: reconstitution of capsid binding and uncoating at the nuclear pore complex in vitro." Mol Cell Biol **20**(13): 4922-4931.

Orvedahl, A., D. Alexander, Z. Talloczy, Q. Sun, Y. Wei, W. Zhang, D. Burns, D. A. Leib and B. Levine (2007). "HSV-1 ICP34.5 confers neurovirulence by targeting the Beclin 1 autophagy protein." Cell Host Microbe **1**(1): 23-35.

Orzalli, M. H., N. M. Broekema, B. A. Diner, D. C. Hancks, N. C. Elde, I. M. Cristea and D. M. Knipe (2015). "cGAS-mediated stabilization of IFI16 promotes innate signaling during herpes simplex virus infection." Proc Natl Acad Sci U S A **112**(14): E1773-1781.

Orzalli, M. H., N. A. DeLuca and D. M. Knipe (2012). "Nuclear IFI16 induction of IRF-3 signaling during herpesviral infection and degradation of IFI16 by the viral ICP0 protein." Proc Natl Acad Sci U S A **109**(44): E3008-3017.

Orzalli, M. H. and J. C. Kagan (2017). "Apoptosis and Necroptosis as Host Defense Strategies to Prevent Viral Infection." Trends Cell Biol **27**(11): 800-809.

Orzalli, M. H. and D. M. Knipe (2014). "Cellular sensing of viral DNA and viral evasion mechanisms." Annu Rev Microbiol **68**: 477-492.

Ou, Y. H., M. Torres, R. Ram, E. Formstecher, C. Roland, et al. (2011). "TBK1 directly engages Akt/PKB survival signaling to support oncogenic transformation." Mol Cell **41**(4): 458-470.

Ouyang, J., X. Zhu, Y. Chen, H. Wei, Q. Chen, et al. (2014). "NRAV, a long noncoding RNA, modulates antiviral responses through suppression of interferon-stimulated gene transcription." Cell Host Microbe **16**(5): 616-626.

Ouyang, Q., X. Zhao, H. Feng, Y. Tian, D. Li, M. Li and Z. Tan (2012). "High GC content of simple sequence repeats in Herpes simplex virus type 1 genome." Gene **499**(1): 37-40.

Page, H. G. and G. S. Read (2010). "The virion host shutoff endonuclease (UL41) of herpes simplex virus interacts with the cellular cap-binding complex eIF4F." J Virol **84**(13): 6886-6890.

Paladino, P., S. E. Collins and K. L. Mossman (2010). "Cellular localization of the herpes simplex virus ICP0 protein dictates its ability to block IRF3-mediated innate immune responses." PLoS One **5**(4): e10428.

Paladino, P., D. T. Cummings, R. S. Noyce and K. L. Mossman (2006). "The IFN-independent response to virus particle entry provides a first line of antiviral defense that is independent of TLRs and retinoic acid-inducible gene I." J Immunol **177**(11): 8008-8016.

Paludan, S. R. and A. G. Bowie (2013). "Immune sensing of DNA." Immunity **38**(5): 870-880.

Paludan, S. R., A. G. Bowie, K. A. Horan and K. A. Fitzgerald (2011). "Recognition of herpesviruses by the innate immune system." Nat Rev Immunol **11**(2): 143-154.

Panayiotou, C., R. Lindqvist, C. Kurhade, K. Vonderstein, J. Pasto, K. Edlund, A. S. Upadhyay and A. K. Overby (2018). "Viperin restricts Zika virus and tick-borne encephalitis virus replication by targeting NS3 for proteasomal degradation." J Virol.

Park, D., J. Lalli, L. Sedlackova-Slavikova and S. A. Rice (2015). "Functional comparison of herpes simplex virus 1 (HSV-1) and HSV-2 ICP27 homologs reveals a role for ICP27 in virion release." J Virol **89**(5): 2892-2905.

Parker, R. F., L. H. Bronson and R. H. Green (1941). "Further Studies of the Infectious Unit of Vaccinia." J Exp Med **74**(3): 263-281.

Parr, M. B., L. Kepple, M. R. McDermott, M. D. Drew, J. J. Bozzola and E. L. Parr (1994). "A mouse model for studies of mucosal immunity to vaginal infection by herpes simplex virus type 2." Lab Invest **70**(3): 369-380.

Parrish, C. R., E. C. Holmes, D. M. Morens, E. C. Park, D. S. Burke, C. H. Calisher, C. A. Laughlin, L. J. Saif and P. Daszak (2008). "Cross-species virus transmission and the emergence of new epidemic diseases." Microbiol Mol Biol Rev **72**(3): 457-470.

Parsons, L. R., Y. R. Tafuri, J. T. Shreve, C. D. Bowen, M. M. Shipley, L. W. Enquist and M. L. Szpara (2015). "Rapid genome assembly and comparison decode intrastrain variation in human alphaherpesviruses." MBio **6**(2).

Pasieka, T. J., T. Baas, V. S. Carter, S. C. Proll, M. G. Katze and D. A. Leib (2006). "Functional genomic analysis of herpes simplex virus type 1 counteraction of the host innate response." J Virol **80**(15): 7600-7612.

Pasieka, T. J., B. Lu, S. D. Crosby, K. M. Wylie, L. A. Morrison, D. E. Alexander, V. D. Menachery and D. A. Leib (2008). "Herpes simplex virus virion host shutoff attenuates establishment of the antiviral state." J Virol **82**(11): 5527-5535.

Pavlovic, J., O. Haller and P. Staeheli (1992). "Human and mouse Mx proteins inhibit different steps of the influenza virus multiplication cycle." J Virol **66**(4): 2564-2569.

Pavlovic, J., T. Zurcher, O. Haller and P. Staeheli (1990). "Resistance to influenza virus and vesicular stomatitis virus conferred by expression of human MxA protein." J Virol **64**(7): 3370-3375.

Pedersen, I. M., G. Cheng, S. Wieland, S. Volinia, C. M. Croce, F. V. Chisari and M. David (2007). "Interferon modulation of cellular microRNAs as an antiviral mechanism." Nature **449**(7164): 919-922.

Peng, T., M. Ponce-de-Leon, H. Jiang, G. Dubin, J. M. Lubinski, R. J. Eisenberg and G. H. Cohen (1998). "The gH-gL complex of herpes simplex virus (HSV) stimulates neutralizing antibody and protects mice against HSV type 1 challenge." J Virol **72**(1): 65-72.

Peng, T., J. Zhu, Y. Hwangbo, L. Corey and R. E. Bumgarner (2008). "Independent and cooperative antiviral actions of beta interferon and gamma interferon against herpes simplex virus replication in primary human fibroblasts." J Virol **82**(4): 1934-1945.

Perales-Linares, R. and S. Navas-Martin (2013). "Toll-like receptor 3 in viral pathogenesis: friend or foe?" Immunology **140**(2): 153-167.

Peri, P., R. K. Mattila, H. Kantola, E. Broberg, H. S. Karttunen, M. Waris, T. Vuorinen and V. Hukkanen (2008). "Herpes simplex virus type 1 Us3 gene deletion influences toll-like receptor responses in cultured monocytic cells." Virol J **5**: 140.

Perng, G. C. and C. Jones (2010). "Towards an understanding of the herpes simplex virus type 1 latency-reactivation cycle." Interdiscip Perspect Infect Dis **2010**: 262415.

Perng, G. C., S. M. Slanina, H. Ghiasi, A. B. Nesburn and S. L. Wechsler (2001). "The effect of latency-associated transcript on the herpes simplex virus type 1 latency-reactivation phenotype is mouse strain-dependent." J Gen Virol **82**(Pt 5): 1117-1122.

Persson, R. H., S. Bacchetti and J. R. Smiley (1985). "Cells that constitutively express the herpes simplex virus immediate-early protein ICP4 allow efficient activation of viral delayed-early genes in trans." J Virol **54**(2): 414-421.

Peschon, J. J., P. J. Morrissey, K. H. Grabstein, F. J. Ramsdell, E. Maraskovsky, et al. (1994). "Early lymphocyte expansion is severely impaired in interleukin 7 receptor-deficient mice." J Exp Med **180**(5): 1955-1960.

Pham, T. H., K. M. Kwon, Y. E. Kim, K. K. Kim and J. H. Ahn (2013). "DNA sensing-independent inhibition of herpes simplex virus 1 replication by DAI/ZBP1." J Virol **87**(6): 3076-3086.

Pinheiro, I., L. Dejager and C. Libert (2011). "X-chromosome-located microRNAs in immunity: might they explain male/female differences? The X chromosome-genomic context may affect X-located miRNAs and downstream signaling, thereby contributing to the enhanced immune response of females." Bioessays **33**(11): 791-802.

Pinheiro, I. and E. Heard (2017). "X chromosome inactivation: new players in the initiation of gene silencing." F1000Res **6**.

Pinninti, S. G. and D. W. Kimberlin (2014). "Preventing Herpes Simplex Virus in the Newborn." Clinics in Perinatology **41**(4): 945-+.

Piras, V. and K. Selvarajoo (2014). "Beyond MyD88 and TRIF Pathways in Toll-Like Receptor Signaling." Front Immunol **5**: 70.

Piroozmand, A., A. H. Koyama, Y. Shimada, M. Fujita, T. Arakawa and A. Adachi (2004). "Role of Us3 gene of herpes simplex virus type 1 for resistance to interferon." Int J Mol Med **14**(4): 641-645.

Pitossi, F., A. Blank, A. Schroder, A. Schwarz, P. Hussi, M. Schwemmle, J. Pavlovic and P. Staeheli (1993). "A functional GTP-binding motif is necessary for antiviral activity of Mx proteins." J Virol **67**(11): 6726-6732.

Pizer, L. I., D. G. Tedder, J. L. Betz, K. W. Wilcox and P. Beard (1986). "Regulation of transcription in vitro from herpes simplex virus genes." J Virol **60**(3): 950-959.

Pohar, J., N. Pirher, M. Bencina, M. Mancek-Keber and R. Jerala (2014). "The ectodomain of TLR3 receptor is required for its plasma membrane translocation." PLoS One **9**(3): e92391.

Polcicova, K., K. Goldsmith, B. L. Rainish, T. W. Wisner and D. C. Johnson (2005). "The extracellular domain of herpes simplex virus gE is indispensable for efficient cell-to-cell spread: evidence for gE/gI receptors." J Virol **79**(18): 11990-12001.

Poltermann, S., B. Schlehofer, K. Steindorf, P. Schnitzler, K. Geletneky and J. R. Schlehofer (2006). "Lack of association of herpesviruses with brain tumors." J Neurovirol **12**(2): 90-99.

Pontier, D. B. and J. Gribnau (2011). "Xist regulation and function explored." Hum Genet **130**(2): 223-236.

Poppers, J., M. Mulvey, D. Khoo and I. Mohr (2000). "Inhibition of PKR activation by the proline-rich RNA binding domain of the herpes simplex virus type 1 Us11 protein." J Virol **74**(23): 11215-11221.

Pozner, A., T. W. Terooatea and B. A. Buck-Koehntop (2016). "Cell-specific Kaiso (ZBTB33) Regulation of Cell Cycle through Cyclin D1 and Cyclin E1." J Biol Chem **291**(47): 24538-24550.

Preston, C. M., M. G. Cordingley and N. D. Stow (1984). "Analysis of DNA sequences which regulate the transcription of a herpes simplex virus immediate early gene." J Virol **50**(3): 708-716.

Preston, C. M. and S. Efstathiou (2007). Molecular basis of HSV latency and reactivation. Human Herpesviruses: Biology, Therapy, and Immunoprophylaxis. A. Arvin, G. Campadelli-Fiume, E. Mocarski et al. Cambridge.

Preston, V. G., J. A. Coates and F. J. Rixon (1983). "Identification and characterization of a herpes simplex virus gene product required for encapsidation of virus DNA." J Virol **45**(3): 1056-1064.

Qin, S., B. Zhang, W. Tian, L. Gu, Z. Lu and D. Deng (2015). "Kaiso mainly locates in the nucleus in vivo and binds to methylated, but not hydroxymethylated DNA." Chin J Cancer Res **27**(2): 148-155.

Radoshevich, L. and O. Dussurget (2016). "Cytosolic Innate Immune Sensing and Signaling upon Infection." Front Microbiol **7**: 313.

Raghav, S. K., S. M. Waszak, I. Krier, C. Gubelmann, A. Isakova, T. S. Mikkelsen and B. Deplancke (2012). "Integrative genomics identifies the corepressor SMRT as a gatekeeper of adipogenesis through the transcription factors C/EBPbeta and KAISO." Mol Cell **46**(3): 335-350.

Rahn, E., K. Thier, P. Petermann, M. Rubsam, P. Staeheli, S. Iden, C. M. Niessen and D. Knebel-Morsdorf (2017). "Epithelial Barriers in Murine Skin during Herpes Simplex Virus 1 Infection: The Role of Tight Junction Formation." J Invest Dermatol **137**(4): 884-893.

Rajcani, J., V. Andrea and R. Ingeborg (2004). "Peculiarities of herpes simplex virus (HSV) transcription: an overview." Virus Genes **28**(3): 293-310.

Ramchandani, M., M. Kong, E. Tronstein, S. Selke, A. Mikhaylova, et al. (2016). "Herpes Simplex Virus Type 1 Shedding in Tears and Nasal and Oral Mucosa of Healthy Adults." Sex Transm Dis **43**(12): 756-760.

Randall, R. E. and S. Goodbourn (2008). "Interferons and viruses: an interplay between induction, signalling, antiviral responses and virus countermeasures." J Gen Virol **89**(Pt 1): 1-47.

Rapicavoli, N. A., K. Qu, J. Zhang, M. Mikhail, R. M. Laberge and H. Y. Chang (2013). "A mammalian pseudogene lncRNA at the interface of inflammation and anti-inflammatory therapeutics." Elife **2**: e00762.

Rasmussen, S. B., L. N. Sorensen, L. Malmgaard, N. Ank, J. D. Baines, Z. J. Chen and S. R. Paludan (2007). "Type I interferon production during herpes simplex virus infection is controlled by cell-type-specific viral recognition through Toll-like receptor 9, the mitochondrial antiviral signaling protein pathway, and novel recognition systems." J Virol **81**(24): 13315-13324.

Rathinam, V. A. and K. A. Fitzgerald (2011). "Innate immune sensing of DNA viruses." Virology **411**(2): 153-162.

Read, G. S., B. M. Karr and K. Knight (1993). "Isolation of a herpes simplex virus type 1 mutant with a deletion in the virion host shutoff gene and identification of multiple forms of the vhs (UL41) polypeptide." J Virol **67**(12): 7149-7160.

Reikine, S., J. B. Nguyen and Y. Modis (2014). "Pattern Recognition and Signaling Mechanisms of RIG-I and MDA5." Front Immunol **5**: 342.

Reina, J., O. Gutierrez, E. Ruiz de Gopegui and E. Padilla (2005). "[Incidence of genital infections caused by herpes simplex virus type 1 (HSV-1) from 1995 to 2003]." Enferm Infecc Microbiol Clin **23**(8): 482-484.

Reinert, L. S., L. Harder, C. K. Holm, M. B. Iversen, K. A. Horan, et al. (2012). "TLR3 deficiency renders astrocytes permissive to herpes simplex virus infection and facilitates establishment of CNS infection in mice." J Clin Invest **122**(4): 1368-1376.

Reinert, L. S., K. Lopusna, H. Winther, C. Sun, M. K. Thomsen, et al. (2016). "Sensing of HSV-1 by the cGAS-STING pathway in microglia orchestrates antiviral defence in the CNS." Nat Commun **7**: 13348.

Remeijer, L., R. Duan, J. M. van Dun, M. A. Wefers Bettink, A. D. Osterhaus and G. M. Verjans (2009). "Prevalence and clinical consequences of herpes simplex virus type 1 DNA in human cornea tissues." J Infect Dis **200**(1): 11-19.

Renner, D. W. and M. L. Szpara (2018). "Impacts of Genome-Wide Analyses on Our Understanding of Human Herpesvirus Diversity and Evolution." J Virol **92**(1).

Renzette, N., C. Pokalyuk, L. Gibson, B. Bhattacharjee, M. R. Schleiss, et al. (2015). "Limits and patterns of cytomegalovirus genomic diversity in humans." Proc Natl Acad Sci U S A **112**(30): E4120-4128.

Riet, J., L. R. V. Ramos, R. V. Lewis and L. F. Marins (2017). "Improving the PCR protocol to amplify a repetitive DNA sequence." Genet Mol Res **16**(3).

Rinn, J. L. and H. Y. Chang (2012). "Genome regulation by long noncoding RNAs." Annu Rev Biochem **81**: 145-166.

Ritchie, M. E., B. Phipson, D. Wu, Y. Hu, C. W. Law, W. Shi and G. K. Smyth (2015). "limma powers differential expression analyses for RNA-sequencing and microarray studies." Nucleic Acids Res **43**(7): e47.

Robinson, M. D., D. J. McCarthy and G. K. Smyth (2010). "edgeR: a Bioconductor package for differential expression analysis of digital gene expression data." Bioinformatics **26**(1): 139-140.

Rock, D. L. and N. W. Fraser (1983). "Detection of HSV-1 genome in central nervous system of latently infected mice." Nature **302**(5908): 523-525.

Roest, R. W., W. I. van der Meijden, G. van Dijk, J. Groen, P. G. Mulder, G. M. Verjans and A. D. Osterhaus (2001). "Prevalence and association between herpes simplex virus types 1 and 2-specific antibodies in attendees at a sexually transmitted disease clinic." Int J Epidemiol **30**(3): 580-588.

Roifman, C. M., J. Zhang, D. Chitayat and N. Sharfe (2000). "A partial deficiency of interleukin-7R alpha is sufficient to abrogate T-cell development and cause severe combined immunodeficiency." Blood **96**(8): 2803-2807.

Roizmann, B., R. C. Desrosiers, B. Fleckenstein, C. Lopez, A. C. Minson and M. J. Studdert (1992). "The family Herpesviridae: an update. The Herpesvirus Study Group of the International Committee on Taxonomy of Viruses." Arch Virol **123**(3-4): 425-449.

Rosato, P. C. and D. A. Leib (2015). "Neurons versus herpes simplex virus: the innate immune interactions that contribute to a host-pathogen standoff." Future Virol **10**(6): 699-714.

Ross, M. T., D. V. Grafham, A. J. Coffey, S. Scherer, K. McLay, et al. (2005). "The DNA sequence of the human X chromosome." Nature **434**(7031): 325-337.

Rossi, S. L., R. B. Tesh, S. R. Azar, A. E. Muruato, K. A. Hanley, et al. (2016). "Characterization of a Novel Murine Model to Study Zika Virus." Am J Trop Med Hyg **94**(6): 1362-1369.

Rossini, G., C. Cerboni, A. Santoni, M. P. Landini, S. Landolfo, D. Gatti, G. Gribaudo and S. Varani (2012). "Interplay between human cytomegalovirus and intrinsic/innate host responses: a complex bidirectional relationship." Mediators Inflamm **2012**: 607276.

Rouse, B. T. and S. Sehrawat (2010). "Immunity and immunopathology to viruses: what decides the outcome?" Nat Rev Immunol **10**(7): 514-526.

Roved, J., H. Westerdahl and D. Hasselquist (2017). "Sex differences in immune responses: Hormonal effects, antagonistic selection, and evolutionary consequences." Horm Behav **88**: 95-105.

Russell, T., B. Bleasdale, M. Hollinshead and G. Elliott (2018). "Qualitative Differences in Capsidless L-Particles Released as a By-Product of Bovine Herpesvirus 1 and Herpes Simplex Virus 1 Infections." J Virol **92**(22).

Russell, T. A., T. Stefanovic and D. C. Tscharke (2015). "Engineering herpes simplex viruses by infection-transfection methods including recombination site targeting by CRISPR/Cas9 nucleases." J Virol Methods **213**: 18-25.

Russell, T. A. and D. C. Tscharke (2016). "Lytic Promoters Express Protein during Herpes Simplex Virus Latency." PLoS Pathog **12**(6): e1005729.

Rutkowski, A. J., F. Erhard, A. L'Hernault, T. Bonfert, M. Schilhabel, et al. (2015). "Widespread disruption of host transcription termination in HSV-1 infection." Nat Commun **6**: 7126.

Saddawi-Konefka, R. and J. R. Crawford (2010). "Chronic viral infection and primary central nervous system malignancy." J Neuroimmune Pharmacol **5**(3): 387-403.

Saffran, H. A., G. S. Read and J. R. Smiley (2010). "Evidence for translational regulation by the herpes simplex virus virion host shutoff protein." J Virol **84**(12): 6041-6049.

Sakabe, K., I. Kawashima, K. Seiki and H. Fujii-Hanamoto (1990). "Hormone and immune response, with special reference to steroid hormone. 2. Sex steroid receptors in rat thymus." Tokai J Exp Clin Med **15**(2-3): 201-211.

Sakaoka, H., K. Kurita, Y. Iida, S. Takada, K. Umene, Y. T. Kim, C. S. Ren and A. J. Nahmias (1994). "Quantitative analysis of genomic polymorphism of herpes simplex virus type 1 strains from six countries: studies of molecular evolution and molecular epidemiology of the virus." J Gen Virol **75 (Pt 3)**: 513-527.

Sanchez, J. G., J. J. Chiang, K. M. J. Sparrer, S. L. Alam, M. Chi, M. D. Roganowicz, B. Sankaran, M. U. Gack and O. Pornillos (2016). "Mechanism of TRIM25 Catalytic Activation in the Antiviral RIG-I Pathway." Cell Rep **16**(5): 1315-1325.

Sanchez, R. and I. Mohr (2007). "Inhibition of cellular 2'-5' oligoadenylate synthetase by the herpes simplex virus type 1 Us11 protein." J Virol **81**(7): 3455-3464.

Sandri-Goldin, R. M. and G. E. Mendoza (1992). "A herpesvirus regulatory protein appears to act post-transcriptionally by affecting mRNA processing." Genes Dev **6**(5): 848-863.

Sanjana, N. E., O. Shalem and F. Zhang (2014). "Improved vectors and genome-wide libraries for CRISPR screening." Nat Methods **11**(8): 783-784.

Sanjuan, R. and P. Domingo-Calap (2016). "Mechanisms of viral mutation." Cell Mol Life Sci **73**(23): 4433-4448.

Sato, A., M. M. Linehan and A. Iwasaki (2006). "Dual recognition of herpes simplex viruses by TLR2 and TLR9 in dendritic cells." Proc Natl Acad Sci U S A **103**(46): 17343-17348.

Savic, B., S. Stanojlovic, M. Stojkovic, M. Misic, B. Savic and V. Draganic (2019). "Potential role of folic acid and vitamin B12 in herpes simplex virus keratitis reactivation." Vojnosanitetski pregled: 37-37.

Sawyer, S. L. and N. C. Elde (2012). "A cross-species view on viruses." Curr Opin Virol **2**(5): 561-568.

Sawyer, S. L., M. Emerman and H. S. Malik (2004). "Ancient adaptive evolution of the primate antiviral DNA-editing enzyme APOBEC3G." PLoS Biol **2**(9): E275.

Sawyer, S. L., L. I. Wu, M. Emerman and H. S. Malik (2005). "Positive selection of primate TRIM5alpha identifies a critical species-specific retroviral restriction domain." Proc Natl Acad Sci U S A **102**(8): 2832-2837.

Schattgen, S. A. and K. A. Fitzgerald (2011). "The PYHIN protein family as mediators of host defenses." Immunol Rev **243**(1): 109-118.

Schindler, C., D. E. Levy and T. Decker (2007). "JAK-STAT signaling: from interferons to cytokines." J Biol Chem **282**(28): 20059-20063.

Schmidt, N., T. Hennig, R. A. Serwa, M. Marchetti and P. O'Hare (2015). "Remote Activation of Host Cell DNA Synthesis in Uninfected Cells Signaled by Infected Cells in Advance of Virus Transmission." J Virol **89**(21): 11107-11115.

Schmutzhard, E. (2001). "Viral infections of the CNS with special emphasis on herpes simplex infections." J Neurol **248**(6): 469-477.

Schneider, W. M., M. D. Chevillotte and C. M. Rice (2014). "Interferon-stimulated genes: a complex web of host defenses." Annu Rev Immunol **32**: 513-545.

Schoggins, J. W., D. A. MacDuff, N. Imanaka, M. D. Gainey, B. Shrestha, et al. (2014). "Pan-viral specificity of IFN-induced genes reveals new roles for cGAS in innate immunity." Nature **505**(7485): 691-695.

Schoggins, J. W. and C. M. Rice (2011). "Interferon-stimulated genes and their antiviral effector functions." Curr Opin Virol **1**(6): 519-525.

Schoggins, J. W., S. J. Wilson, M. Panis, M. Y. Murphy, C. T. Jones, P. Bieniasz and C. M. Rice (2011). "A diverse range of gene products are effectors of the type I interferon antiviral response." Nature **472**(7344): 481-485.

Searles, R. P., E. P. Bergquam, M. K. Axthelm and S. W. Wong (1999). "Sequence and genomic analysis of a Rhesus macaque rhadinovirus with similarity to Kaposi's sarcoma-associated herpesvirus/human herpesvirus 8." J Virol **73**(4): 3040-3053.

Sedarati, F., K. M. Izumi, E. K. Wagner and J. G. Stevens (1989). "Herpes simplex virus type 1 latency-associated transcription plays no role in establishment or maintenance of a latent infection in murine sensory neurons." J Virol **63**(10): 4455-4458.

Sekulovich, R. E., K. Leary and R. M. Sandri-Goldin (1988). "The herpes simplex virus type 1 alpha protein ICP27 can act as a trans-repressor or a trans-activator in combination with ICP4 and ICP0." J Virol **62**(12): 4510-4522.

Sen, J., X. Liu, R. Roller and D. M. Knipe (2013). "Herpes simplex virus US3 tegument protein inhibits Toll-like receptor 2 signaling at or before TRAF6 ubiquitination." Virology **439**(2): 65-73.

Sengupta, T. K., E. M. Schmitt and L. B. Ivashkiv (1996). "Inhibition of cytokines and JAK-STAT activation by distinct signaling pathways." Proc Natl Acad Sci U S A **93**(18): 9499-9504.

Senner, C. E. and N. Brockdorff (2009). "Xist gene regulation at the onset of X inactivation." Curr Opin Genet Dev **19**(2): 122-126.

Seo, J. Y., R. Yaneva and P. Cresswell (2011a). "Viperin: a multifunctional, interferon-inducible protein that regulates virus replication." Cell Host Microbe **10**(6): 534-539.

Seo, J. Y., R. Yaneva, E. R. Hinson and P. Cresswell (2011b). "Human cytomegalovirus directly induces the antiviral protein viperin to enhance infectivity." Science **332**(6033): 1093-1097.

Seton-Rogers, S. (2013). "Non-coding RNAs: The cancer X factor." Nat Rev Cancer **13**(4): 224-225.

Severa, M., E. M. Coccia and K. A. Fitzgerald (2006). "Toll-like receptor-dependent and -independent viperin gene expression and counter-regulation by PRDI-binding factor-1/BLIMP1." J Biol Chem **281**(36): 26188-26195.

Shackelton, L. A. and E. C. Holmes (2006). "Phylogenetic evidence for the rapid evolution of human B19 erythrovirus." J Virol **80**(7): 3666-3669.

Shackelton, L. A., C. R. Parrish, U. Truyen and E. C. Holmes (2005). "High rate of viral evolution associated with the emergence of carnivore parvovirus." Proc Natl Acad Sci U S A **102**(2): 379-384.

Sharma, S. and K. A. Fitzgerald (2011). "Innate immune sensing of DNA." PLoS Pathog **7**(4): e1001310.

Shaveta, G., J. Shi, V. T. Chow and J. Song (2010). "Structural characterization reveals that viperin is a radical S-adenosyl-L-methionine (SAM) enzyme." Biochem Biophys Res Commun **391**(3): 1390-1395.

Shen, G., K. Wang, S. Wang, M. Cai, M. L. Li and C. Zheng (2014). "Herpes simplex virus 1 counteracts viperin via its virion host shutoff protein UL41." J Virol **88**(20): 12163-12166.

Shimeld, C., S. Efstathiou and T. Hill (2001). "Tracking the spread of a lacZ-tagged herpes simplex virus type 1 between the eye and the nervous system of the mouse: comparison of primary and recurrent infection." J Virol **75**(11): 5252-5262.

Shrivastava, S., R. Steele, R. Ray and R. B. Ray (2015). "MicroRNAs: Role in Hepatitis C Virus pathogenesis." Genes Dis **2**(1): 35-45.

Simmons, A., D. Tscharke and P. Speck (1992). "The role of immune mechanisms in control of herpes simplex virus infection of the peripheral nervous system." Curr Top Microbiol Immunol **179**: 31-56.

Singh, T. D., J. E. Fugate, S. Hocker, E. F. Wijdicks, A. J. Aksamit, Jr. and A. A. Rabinstein (2016). "Predictors of outcome in HSV encephalitis." J Neurol **263**(2): 277-289.

Sinzger, C., M. Digel and G. Jahn (2008). "Cytomegalovirus cell tropism." Curr Top Microbiol Immunol **325**: 63-83.

Slabaugh, M. B., N. A. Roseman and C. K. Mathews (1989). "Amplification of the ribonucleotide reductase small subunit gene: analysis of novel joints and the mechanism of gene duplication in vaccinia virus." Nucleic Acids Res **17**(17): 7073-7088.

Slifer, C. M. and S. R. Jennings (2015). "Battling the spread: Herpes simplex virus and encephalitis." Immunol Cell Biol.

Sloan, D. D., G. Zahariadis, C. M. Posavad, N. T. Pate, S. J. Kussick and K. R. Jerome (2003). "CTL are inactivated by herpes simplex virus-infected cells expressing a viral protein kinase." J Immunol **171**(12): 6733-6741.

Smiley, J. R. (2004). "Herpes simplex virus virion host shutoff protein: immune evasion mediated by a viral RNase?" J Virol **78**(3): 1063-1068.

Smith, E. C. (2017). "The not-so-infinite malleability of RNA viruses: Viral and cellular determinants of RNA virus mutation rates." PLoS Pathog **13**(4): e1006254.

Smith, G. (2012). "Herpesvirus transport to the nervous system and back again." Annu Rev Microbiol **66**: 153-176.

Smith, K. O. (1964). "Relationship between the Envelope and the Infectivity of Herpes Simplex Virus." Proc Soc Exp Biol Med **115**: 814-816.

Smith, R. W., P. Malik and J. B. Clements (2005). "The herpes simplex virus ICP27 protein: a multifunctional post-transcriptional regulator of gene expression." Biochem Soc Trans **33**(Pt 3): 499-501.

Smyth, G. K. (2004). "Linear models and empirical bayes methods for assessing differential expression in microarray experiments." Stat Appl Genet Mol Biol **3**: Article3.

Sodeik, B., M. W. Ebersold and A. Helenius (1997). "Microtubule-mediated transport of incoming herpes simplex virus 1 capsids to the nucleus." J Cell Biol **136**(5): 1007-1021.

Souyris, M., C. Cenac, P. Azar, D. Daviaud, A. Canivet, et al. (2018a). "TLR7 escapes X chromosome inactivation in immune cells." Sci Immunol **3**(19).

Souyris, M., J. E. Mejia, J. Chaumeil and J. C. Guery (2018b). "Female predisposition to TLR7-driven autoimmunity: gene dosage and the escape from X chromosome inactivation." Semin Immunopathol.

Speer, S. D., Z. Li, S. Buta, B. Payelle-Brogard, L. Qian, et al. (2016). "ISG15 deficiency and increased viral resistance in humans but not mice." Nat Commun **7**: 11496.

Spolarics, Z. (2007). "The X-files of inflammation: cellular mosaicism of X-linked polymorphic genes and the female advantage in the host response to injury and infection." Shock **27**(6): 597-604.

Sridharan, H., C. Zhao and R. M. Krug (2010). "Species specificity of the NS1 protein of influenza B virus: NS1 binds only human and non-human primate ubiquitin-like ISG15 proteins." J Biol Chem **285**(11): 7852-7856.

Stanberry, L. R., S. L. Spruance, A. L. Cunningham, D. I. Bernstein, A. Mindel, et al. (2002). "Glycoprotein-D-adjuvant vaccine to prevent genital herpes." N Engl J Med **347**(21): 1652-1661.

Steffy, K. R. and J. P. Weir (1991). "Mutational analysis of two herpes simplex virus type 1 late promoters." J Virol **65**(12): 6454-6460.

Steiner, I. (2011). "Herpes simplex virus encephalitis: new infection or reactivation?" Curr Opin Neurol **24**(3): 268-274.

Steiner, I. and F. Benninger (2013). "Update on Herpes Virus Infections of the Nervous System." Current Neurology and Neuroscience Reports **13**(12).

Steiner, I., J. G. Spivack, R. P. Lirette, S. M. Brown, A. R. MacLean, J. H. Subak-Sharpe and N. W. Fraser (1989). "Herpes simplex virus type 1 latency-associated transcripts are evidently not essential for latent infection." EMBO J **8**(2): 505-511.

Stern, S. and W. Herr (1991). "The herpes simplex virus trans-activator VP16 recognizes the Oct-1 homeo domain: evidence for a homeo domain recognition subdomain." Genes Dev **5**(12B): 2555-2566.

Stevens, J. G. (1975). "Herpes simplex viral latency - a review." IARC Sci Publ(11 Pt 2): 67-72.

Stevens, J. G. and M. L. Cook (1971). "Latent herpes simplex virus in spinal ganglia of mice." Science **173**(3999): 843-845.

Stingley, S. W., J. J. Ramirez, S. A. Aguilar, K. Simmen, R. M. Sandri-Goldin, P. Ghazal and E. K. Wagner (2000). "Global analysis of herpes simplex virus type 1 transcription using an oligonucleotide-based DNA microarray." J Virol **74**(21): 9916-9927.

Stirnweiss, A., A. Ksienzyk, K. Klages, U. Rand, M. Grashoff, H. Hauser and A. Kroger (2010). "IFN regulatory factor-1 bypasses IFN-mediated antiviral effects through viperin gene induction." J Immunol **184**(9): 5179-5185.

Stow, N. D. (1982). "Localization of an origin of DNA replication within the TRS/IRS repeated region of the herpes simplex virus type 1 genome." EMBO J **1**(7): 863-867.

Stranden, A. M., P. Staeheli and J. Pavlovic (1993). "Function of the mouse Mx1 protein is inhibited by overexpression of the PB2 protein of influenza virus." Virology **197**(2): 642-651.

Strelow, L. I. and D. A. Leib (1995). "Role of the virion host shutoff (vhs) of herpes simplex virus type 1 in latency and pathogenesis." J Virol **69**(11): 6779-6786.

Su, C., G. Zhan and C. Zheng (2016). "Evasion of host antiviral innate immunity by HSV-1, an update." Virol J **13**: 38.

Su, C. and C. Zheng (2017). "Herpes Simplex Virus 1 Abrogates the cGAS/STING-Mediated Cytosolic DNA-Sensing Pathway via Its Virion Host Shutoff Protein, UL41." J Virol **91**(6).

Subramanian, S., K. Tus, Q. Z. Li, A. Wang, X. H. Tian, et al. (2006). "A Tlr7 translocation accelerates systemic autoimmunity in murine lupus." Proc Natl Acad Sci U S A **103**(26): 9970-9975.

Sun, L., J. Wu, F. Du, X. Chen and Z. J. Chen (2013). "Cyclic GMP-AMP synthase is a cytosolic DNA sensor that activates the type I interferon pathway." Science **339**(6121): 786-791.

Sun, N., G. Zhang and Y. Liu (2018). "Long non-coding RNA XIST sponges miR-34a to promotes colon cancer progression via Wnt/beta-catenin signaling pathway." Gene **665**: 141-148.

Sunil, M., E. Reid and M. J. Lechowicz (2010). "Update on HHV-8-Associated Malignancies." Curr Infect Dis Rep **12**(2): 147-154.

Supek, F., M. Bosnjak, N. Skunca and T. Smuc (2011). "REVIGO summarizes and visualizes long lists of gene ontology terms." PLoS One **6**(7): e21800.

Suzich, J. B. and A. R. Cliffe (2018). "Strength in diversity: Understanding the pathways to herpes simplex virus reactivation." Virology **522**: 81-91.

Syrett, C. M., V. Sindhava, S. Hodawadekar, A. Myles, G. Liang, et al. (2017). "Loss of Xist RNA from the inactive X during B cell development is restored in a dynamic YY1-dependent two-step process in activated B cells." PLoS Genet **13**(10): e1007050.

Szabo, A., K. Bene, P. Gogolak, B. Rethi, A. Lanyi, I. Jankovich, B. Dezso and E. Rajnavolgyi (2012). "RLR-mediated production of interferon-beta by a human dendritic cell subset and its role in virus-specific immunity." J Leukoc Biol **92**(1): 159-169.

Szomolanyi-Tsuda, E., X. Liang, R. M. Welsh, E. A. Kurt-Jones and R. W. Finberg (2006). "Role for TLR2 in NK cell-mediated control of murine cytomegalovirus in vivo." J Virol **80**(9): 4286-4291.

Szretter, K. J., J. D. Brien, L. B. Thackray, H. W. Virgin, P. Cresswell and M. S. Diamond (2011). "The interferon-inducible gene viperin restricts West Nile virus pathogenesis." J Virol **85**(22): 11557-11566.

Taddeo, B., W. Zhang and B. Roizman (2010). "Role of herpes simplex virus ICP27 in the degradation of mRNA by virion host shutoff RNase." J Virol **84**(19): 10182-10190.

Takaoka, A., Z. Wang, M. K. Choi, H. Yanai, H. Negishi, et al. (2007). "DAI (DLM-1/ZBP1) is a cytosolic DNA sensor and an activator of innate immune response." Nature **448**(7152): 501-505.

Takeda, K. and S. Akira (2004). "TLR signaling pathways." Semin Immunol **16**(1): 3-9.

Takeuchi, O. and S. Akira (2010). "Pattern recognition receptors and inflammation." Cell **140**(6): 805-820.

Takeuchi, O., K. Takeda, K. Hoshino, O. Adachi, T. Ogawa and S. Akira (2000). "Cellular responses to bacterial cell wall components are mediated through MyD88-dependent signaling cascades." Int Immunol **12**(1): 113-117.

Tan, K. S., F. Olfat, M. C. Phoon, J. P. Hsu, J. L. Howe, J. E. Seet, K. C. Chin and V. T. Chow (2012). "In vivo and in vitro studies on the antiviral activities of viperin against influenza H1N1 virus infection." J Gen Virol **93**(Pt 6): 1269-1277.

Tanaka, Y. and Z. J. Chen (2012). "STING specifies IRF3 phosphorylation by TBK1 in the cytosolic DNA signaling pathway." Sci Signal **5**(214): ra20.

Tang, H. B., Z. L. Lu, X. K. Wei, T. Z. Zhong, Y. Z. Zhong, et al. (2016). "Viperin inhibits rabies virus replication via reduced cholesterol and sphingomyelin and is regulated upstream by TLR4." Sci Rep **6**: 30529.

Tang, Y. D., L. Na, C. H. Zhu, N. Shen, F. Yang, et al. (2014). "Equine viperin restricts equine infectious anemia virus replication by inhibiting the production and/or release of viral Gag, Env, and receptor via distortion of the endoplasmic reticulum." J Virol **88**(21): 12296-12310.

Tangye, S. G., A. Ferguson, D. T. Avery, C. S. Ma and P. D. Hodgkin (2002). "Isotype switching by human B cells is division-associated and regulated by cytokines." J Immunol **169**(8): 4298-4306.

Teng, T. S., S. S. Foo, D. Simamarta, F. M. Lum, T. H. Teo, et al. (2012). "Viperin restricts chikungunya virus replication and pathology." J Clin Invest **122**(12): 4447-4460.

Termini, J. M., Z. A. Silver, B. Connor, A. Antonopoulos, S. M. Haslam, A. Dell and R. C. Desrosiers (2017). "HEK293T cell lines defective for O-linked glycosylation." PLoS One **12**(6): e0179949.

Thellman, N. M. and S. J. Triezenberg (2017). "Herpes Simplex Virus Establishment, Maintenance, and Reactivation: In Vitro Modeling of Latency." Pathogens **6**(3).

Thompson, R. L. and N. M. Sawtell (2000). "Replication of herpes simplex virus type 1 within trigeminal ganglia is required for high frequency but not high viral genome copy number latency." J Virol **74**(2): 965-974.

Tian, X., G. Devi-Rao, A. P. Golovanov and R. M. Sandri-Goldin (2013). "The interaction of the cellular export adaptor protein Aly/REF with ICP27 contributes to the efficiency of herpes simplex virus 1 mRNA export." J Virol **87**(13): 7210-7217.

Trapnell, C., D. G. Hendrickson, M. Sauvageau, L. Goff, J. L. Rinn and L. Pachter (2013). "Differential analysis of gene regulation at transcript resolution with RNA-seq." Nat Biotechnol **31**(1): 46-53.

Trapnell, C., A. Roberts, L. Goff, G. Pertea, D. Kim, et al. (2012). "Differential gene and transcript expression analysis of RNA-seq experiments with TopHat and Cufflinks." Nat Protoc **7**(3): 562-578.

Trapnell, C., B. A. Williams, G. Pertea, A. Mortazavi, G. Kwan, M. J. van Baren, S. L. Salzberg, B. J. Wold and L. Pachter (2010). "Transcript assembly and quantification by RNA-Seq reveals unannotated transcripts and isoform switching during cell differentiation." Nat Biotechnol **28**(5): 511-515.

Treangen, T. J., D. D. Sommer, F. E. Angly, S. Koren and M. Pop (2011). "Next generation sequence assembly with AMOS." Curr Protoc Bioinformatics **Chapter 11**: Unit 11 18.

Triezenberg, S. J., R. C. Kingsbury and S. L. McKnight (1988a). "Functional dissection of VP16, the trans-activator of herpes simplex virus immediate early gene expression." Genes Dev **2**(6): 718-729.

Triezenberg, S. J., K. L. LaMarco and S. L. McKnight (1988b). "Evidence of DNA: protein interactions that mediate HSV-1 immediate early gene activation by VP16." Genes Dev **2**(6): 730-742.

Tseng, Y. Y., G. R. Liao, G. C. Sen, F. Y. Lin and W. L. Hsu (2015). "Regulation of PACT-Mediated Protein Kinase Activation by the OV20.0 Protein of Orf Virus." J Virol **89**(22): 11619-11629.

Tsitoura, E., J. Thomas, D. Cuchet, K. Thoinet, P. Mavromara and A. L. Epstein (2009). "Infection with herpes simplex type 1-based amplicon vectors results in an IRF3/7-dependent, TLR-independent activation of the innate antiviral response in primary human fibroblasts." J Gen Virol **90**(Pt 9): 2209-2220.

Umbach, J. L., M. F. Kramer, I. Jurak, H. W. Karnowski, D. M. Coen and B. R. Cullen (2008). "MicroRNAs expressed by herpes simplex virus 1 during latent infection regulate viral mRNAs." Nature **454**(7205): 780-783.

Umene, K. and H. Sakaoka (1999). "Evolution of herpes simplex virus type 1 under herpesviral evolutionary processes." Arch Virol **144**(4): 637-656.

Unterholzner, L., S. E. Keating, M. Baran, K. A. Horan, S. B. Jensen, et al. (2010). "IFI16 is an innate immune sensor for intracellular DNA." Nat Immunol **11**(11): 997-1004.

Valentine, R. and G. L. Smith (2010). "Inhibition of the RNA polymerase III-mediated dsDNA-sensing pathway of innate immunity by vaccinia virus protein E3." J Gen Virol **91**(Pt 9): 2221-2229.

Van der Hoek, K. H., N. S. Eyre, B. Shue, O. Khantisitthiporn, K. Glab-Ampi, et al. (2017). "Viperin is an important host restriction factor in control of Zika virus infection." Sci Rep **7**(1): 4475.

van Genderen, I. L., R. Brandimarti, M. R. Torrisi, G. Campadelli and G. van Meer (1994). "The phospholipid composition of extracellular herpes simplex virions differs from that of host cell nuclei." Virology **200**(2): 831-836.

van Lint, A. L., M. R. Murawski, R. E. Goodbody, M. Severa, K. A. Fitzgerald, R. W. Finberg, D. M. Knipe and E. A. Kurt-Jones (2010). "Herpes simplex virus immediate-early ICP0 protein inhibits Toll-like receptor 2-dependent inflammatory responses and NF-kappaB signaling." J Virol **84**(20): 10802-10811.

Vastag, L., E. Koyuncu, S. L. Grady, T. E. Shenk and J. D. Rabinowitz (2011). "Divergent effects of human cytomegalovirus and herpes simplex virus-1 on cellular metabolism." PLoS Pathog **7**(7): e1002124.

Verhelst, J., E. Parthoens, B. Schepens, W. Fiers and X. Saelens (2012). "Interferon-inducible protein Mx1 inhibits influenza virus by interfering with functional viral ribonucleoprotein complex assembly." J Virol **86**(24): 13445-13455.

Verpooten, D., Y. Ma, S. Hou, Z. Yan and B. He (2009). "Control of TANK-binding kinase 1-mediated signaling by the gamma(1)34.5 protein of herpes simplex virus 1." J Biol Chem **284**(2): 1097-1105.

Vignuzzi, M., J. K. Stone, J. J. Arnold, C. E. Cameron and R. Andino (2006). "Quasispecies diversity determines pathogenesis through cooperative interactions in a viral population." Nature **439**(7074): 344-348.

Villacres, M. C., J. Longmate, C. Auge and D. J. Diamond (2004). "Predominant type 1 CMV-specific memory T-helper response in humans: evidence for gender differences in cytokine secretion." Hum Immunol **65**(5): 476-485.

Wadd, S., H. Bryant, O. Filhol, J. E. Scott, T. Y. Hsieh, R. D. Everett and J. B. Clements (1999). "The multifunctional herpes simplex virus IE63 protein interacts with heterogeneous ribonucleoprotein K and with casein kinase 2." J Biol Chem **274**(41): 28991-28998.

Wagner, H. J., M. Hornef, H. M. Teichert and H. Kirchner (1994). "Sex difference in the serostatus of adults to the Epstein-Barr virus." Immunobiology **190**(4-5): 424-429.

Wagner, M. J. and W. C. Summers (1978). "Structure of the joint region and the termini of the DNA of herpes simplex virus type 1." J Virol **27**(2): 374-387.

Wald, A. (2006). "Genital HSV-1 infections." Sex Transm Infect **82**(3): 189-190.

Walkin, L., S. E. Herrick, A. Summers, P. E. Brenchley, C. M. Hoff, R. Korstanje and P. J. Margetts (2013). "The role of mouse strain differences in the susceptibility to fibrosis: a systematic review." Fibrogenesis Tissue Repair **6**(1): 18.

Walsh, K. B., J. R. Teijaro, P. R. Wilker, A. Jatzek, D. M. Fremgen, et al. (2011). "Suppression of cytokine storm with a sphingosine analog provides protection against pathogenic influenza virus." Proc Natl Acad Sci U S A **108**(29): 12018-12023.

Wan, Y., D. W. Renner, I. Albert and M. L. Szpara (2015). "VirAmp: a galaxy-based viral genome assembly pipeline." Gigascience **4**: 19.

Wang, F., E. E. Zumbrun, J. Huang, H. Si, L. Makaroun and H. M. Friedman (2010a). "Herpes simplex virus type 2 glycoprotein E is required for efficient virus spread from epithelial cells to neurons and for targeting viral proteins from the neuron cell body into axons." Virology **405**(2): 269-279.

Wang, H., D. J. Davido and L. A. Morrison (2013a). "HSV-1 strain McKrae is more neuroinvasive than HSV-1 KOS after corneal or vaginal inoculation in mice." Virus Res **173**(2): 436-440.

Wang, H., W. Liu, S. Black, O. Turner, J. M. Daniel, W. Dean-Colomb, Q. P. He, M. Davis and C. Yates (2016a). "Kaiso, a transcriptional repressor, promotes cell migration and invasion of prostate cancer cells through regulation of miR-31 expression." Oncotarget **7**(5): 5677-5689.

Wang, J., S. H. Basagoudanavar, X. Wang, E. Hopewell, R. Albrecht, A. Garcia-Sastre, S. Balachandran and A. A. Beg (2010b). "NF-kappa B RelA subunit is crucial for early IFN-beta expression and resistance to RNA virus replication." J Immunol **185**(3): 1720-1729.

Wang, J., C. M. Syrett, M. C. Kramer, A. Basu, M. L. Atchison and M. C. Anguera (2016b). "Unusual maintenance of X chromosome inactivation predisposes female lymphocytes for increased expression from the inactive X." Proc Natl Acad Sci U S A **113**(14): E2029-2038.

Wang, J. P., E. A. Kurt-Jones, O. S. Shin, M. D. Manchak, M. J. Levin and R. W. Finberg (2005). "Varicella-zoster virus activates inflammatory cytokines in human monocytes and macrophages via Toll-like receptor 2." J Virol **79**(20): 12658-12666.

Wang, K., L. Ni, S. Wang and C. Zheng (2014). "Herpes simplex virus 1 protein kinase US3 hyperphosphorylates p65/RelA and dampens NF-kappaB activation." J Virol **88**(14): 7941-7951.

Wang, L., I. Tassiulas, K. H. Park-Min, A. C. Reid, H. Gil-Henn, J. Schlessinger, R. Baron, J. J. Zhang and L. B. Ivashkiv (2008a). "'Tuning' of type I interferon-induced Jak-STAT1 signaling by calcium-dependent kinases in macrophages." Nat Immunol **9**(2): 186-193.

Wang, N., Q. Dong, J. Li, R. K. Jangra, M. Fan, A. R. Brasier, S. M. Lemon, L. M. Pfeffer and K. Li (2010c). "Viral induction of the zinc finger antiviral protein is IRF3-dependent but NF-kappaB-independent." J Biol Chem **285**(9): 6080-6090.

Wang, S., K. Wang, R. Lin and C. Zheng (2013b). "Herpes simplex virus 1 serine/threonine kinase US3 hyperphosphorylates IRF3 and inhibits beta interferon production." J Virol **87**(23): 12814-12827.

Wang, W., L. Xu, J. Su, M. P. Peppelenbosch and Q. Pan (2017). "Transcriptional Regulation of Antiviral Interferon-Stimulated Genes." Trends Microbiol **25**(7): 573-584.

Wang, X., E. R. Hinson and P. Cresswell (2007). "The interferon-inducible protein viperin inhibits influenza virus release by perturbing lipid rafts." Cell Host Microbe **2**(2): 96-105.

Wang, Z., M. K. Choi, T. Ban, H. Yanai, H. Negishi, et al. (2008b). "Regulation of innate immune responses by DAI (DLM-1/ZBP1) and other DNA-sensing molecules." Proc Natl Acad Sci U S A **105**(14): 5477-5482.

Wang, Z., M. Gerstein and M. Snyder (2009). "RNA-Seq: a revolutionary tool for transcriptomics." Nat Rev Genet **10**(1): 57-63.

Watson, G., W. Xu, A. Reed, B. Babra, T. Putman, E. Wick, S. L. Wechsler, G. F. Rohrmann and L. Jin (2012). "Sequence and comparative analysis of the genome of HSV-1 strain McKrae." Virology **433**(2): 528-537.

Weaver, S. C., A. C. Brault, W. Kang and J. J. Holland (1999). "Genetic and fitness changes accompanying adaptation of an arbovirus to vertebrate and invertebrate cells." J Virol **73**(5): 4316-4326.

Weber, F., V. Wagner, S. B. Rasmussen, R. Hartmann and S. R. Paludan (2006). "Double-stranded RNA is produced by positive-strand RNA viruses and DNA viruses but not in detectable amounts by negative-strand RNA viruses." J Virol **80**(10): 5059-5064.

Webre, J. M., J. M. Hill, N. M. Nolan, C. Clement, H. E. McFerrin, et al. (2012). "Rabbit and mouse models of HSV-1 latency, reactivation, and recurrent eye diseases." J Biomed Biotechnol **2012**: 612316.

Weidberg, H. and Z. Elazar (2011). "TBK1 mediates crosstalk between the innate immune response and autophagy." Sci Signal **4**(187): pe39.

Weinheimer, S. P., B. A. Boyd, S. K. Durham, J. L. Resnick and D. R. O'Boyle, 2nd (1992). "Deletion of the VP16 open reading frame of herpes simplex virus type 1." J Virol **66**(1): 258-269.

Weller, S. K. and D. M. Coen (2012). "Herpes simplex viruses: mechanisms of DNA replication." Cold Spring Harb Perspect Biol **4**(9): a013011.

Wentworth, B. B. and E. R. Alexander (1971). "Seroepidemiology of infectious due to members of the herpesvirus group." Am J Epidemiol **94**(5): 496-507.

Westra, D. F., K. L. Glazenburg, M. C. Harmsen, A. Tiran, A. Jan Scheffer, G. W. Welling, T. Hauw The and S. Welling-Wester (1997). "Glycoprotein H of herpes simplex virus type 1 requires glycoprotein L for transport to the surfaces of insect cells." J Virol **71**(3): 2285-2291.

Whitley, R. J. (1988). "Herpes-Simplex Virus-Infections of the Central Nervous-System - a Review." American Journal of Medicine **85**(2a): 61-67.

Whitman, L., M. J. Wall and J. Warren (1946). "Herpes simplex encephalitis." J Am Med Assoc **131**: 1408-1411.

Whittaker, G. R. and A. Helenius (1998). "Nuclear import and export of viruses and virus genomes." Virology **246**(1): 1-23.

Wilcox, D. R. and R. Longnecker (2016). "The Herpes Simplex Virus Neurovirulence Factor gamma34.5: Revealing Virus-Host Interactions." PLoS Pathog **12**(3): e1005449.

Wilson, A. C., K. LaMarco, M. G. Peterson and W. Herr (1993). "The VP16 accessory protein HCF is a family of polypeptides processed from a large precursor protein." Cell **74**(1): 115-125.

Wisner, T., C. Brunetti, K. Dingwell and D. C. Johnson (2000). "The extracellular domain of herpes simplex virus gE is sufficient for accumulation at cell junctions but not for cell-to-cell spread." J Virol **74**(5): 2278-2287.

Wrzos, H., P. L. Abt and F. Rapp (1990). "Anti-interferon antibody inhibits natural killer cell activity in HSV-2 genital infection in C57BL/6J mice." Intervirology **31**(2-4): 230-240.

Wu, B. and S. Hur (2015). "How RIG-I like receptors activate MAVS." Curr Opin Virol **12**: 91-98.

Wu, D., E. Lim, F. Vaillant, M. L. Asselin-Labat, J. E. Visvader and G. K. Smyth (2010). "ROAST: rotation gene set tests for complex microarray experiments." Bioinformatics **26**(17): 2176-2182.

Wu, J. and Z. J. Chen (2014). "Innate immune sensing and signaling of cytosolic nucleic acids." Annu Rev Immunol **32**: 461-488.

Wu, J., L. Sun, X. Chen, F. Du, H. Shi, C. Chen and Z. J. Chen (2013). "Cyclic GMP-AMP is an endogenous second messenger in innate immune signaling by cytosolic DNA." Science **339**(6121): 826-830.

Wuest, T., B. A. Austin, S. Uematsu, M. Thapa, S. Akira and D. J. Carr (2006). "Intact TRL 9 and type I interferon signaling pathways are required to augment HSV-1 induced corneal CXCL9 and CXCL10." J Neuroimmunol **179**(1-2): 46-52.

Wysocka, J. and W. Herr (2003). "The herpes simplex virus VP16-induced complex: the makings of a regulatory switch." Trends Biochem Sci **28**(6): 294-304.

Xia, H. J., G. H. Zhang, R. R. Wang and Y. T. Zheng (2009). "The influence of age and sex on the cell counts of peripheral blood leukocyte subpopulations in Chinese rhesus macaques." Cell Mol Immunol **6**(6): 433-440.

Xiao, T. S. and K. A. Fitzgerald (2013). "The cGAS-STING pathway for DNA sensing." Mol Cell **51**(2): 135-139.

Xing, F., T. Matsumiya, K. Onomoto, R. Hayakari, T. Imaizumi, H. Yoshida, M. Yoneyama, T. Fujita and K. Satoh (2012a). "Foreign RNA induces the degradation of mitochondrial antiviral signaling protein (MAVS): the role of intracellular antiviral factors." PLoS One **7**(9): e45136.

Xing, J., L. Ni, S. Wang, K. Wang, R. Lin and C. Zheng (2013). "Herpes simplex virus 1-encoded tegument protein VP16 abrogates the production of beta interferon (IFN) by inhibiting NF-kappaB activation and blocking IFN regulatory factor 3 to recruit its coactivator CBP." J Virol **87**(17): 9788-9801.

Xing, J., S. Wang, R. Lin, K. L. Mossman and C. Zheng (2012b). "Herpes simplex virus 1 tegument protein US11 downmodulates the RLR signaling pathway via direct interaction with RIG-I and MDA-5." J Virol **86**(7): 3528-3540.

Xu, D., M. Holko, A. J. Sadler, B. Scott, S. Higashiyama, et al. (2009). "Promyelocytic leukemia zinc finger protein regulates interferon-mediated innate immunity." Immunity **30**(6): 802-816.

Xu, H., C. Su, A. Pearson, C. H. Mody and C. Zheng (2017). "Herpes Simplex Virus 1 UL24 Abrogates the DNA Sensing Signal Pathway by Inhibiting NF-kappaB Activation." J Virol **91**(7).

Yang, K., A. Puel, S. Zhang, C. Eidenschenk, C. L. Ku, et al. (2005). "Human TLR-7-, -8-, and -9-mediated induction of IFN-alpha/beta and -lambda Is IRAK-4 dependent and redundant for protective immunity to viruses." Immunity **23**(5): 465-478.

Yang, T. Y. and R. J. Courtney (1995). "Influence of the host cell on the association of ICP4 and ICP0 with herpes simplex virus type 1." Virology **211**(1): 209-217.

Yao, X. D. and K. L. Rosenthal (2011). "Herpes simplex virus type 2 virion host shutoff protein suppresses innate dsRNA antiviral pathways in human vaginal epithelial cells." J Gen Virol **92**(Pt 9): 1981-1993.

Ye, R., C. Su, H. Xu and C. Zheng (2017). "Herpes Simplex Virus 1 Ubiquitin-Specific Protease UL36 Abrogates NF-kappaB Activation in DNA Sensing Signal Pathway." J Virol **91**(5).

Yildirim, E., J. E. Kirby, D. E. Brown, F. E. Mercier, R. I. Sadreyev, D. T. Scadden and J. T. Lee (2013). "Xist RNA is a potent suppressor of hematologic cancer in mice." Cell **152**(4): 727-742.

Yirrell, D. L., W. A. Blyth and T. J. Hill (1987). "The influence of androgens on paralysis in mice following intravenous inoculation of herpes simplex virus." J Gen Virol **68 (Pt 9)**: 2461-2464.

Yokota, S., N. Yokosawa, T. Kubota, T. Suzutani, I. Yoshida, S. Miura, K. Jimbow and N. Fujii (2001). "Herpes simplex virus type 1 suppresses the interferon signaling pathway by inhibiting phosphorylation of STATs and janus kinases during an early infection stage." Virology **286**(1): 119-124.

Yoon, H. G., D. W. Chan, A. B. Reynolds, J. Qin and J. Wong (2003). "N-CoR mediates DNA methylation-dependent repression through a methyl CpG binding protein Kaiso." Mol Cell **12**(3): 723-734.

York, I. A., C. Roop, D. W. Andrews, S. R. Riddell, F. L. Graham and D. C. Johnson (1994). "A cytosolic herpes simplex virus protein inhibits antigen presentation to CD8+ T lymphocytes." Cell **77**(4): 525-535.

Yu, H., Y. Xue, P. Wang, X. Liu, J. Ma, et al. (2017). "Knockdown of long non-coding RNA XIST increases blood-tumor barrier permeability and inhibits glioma angiogenesis by targeting miR-137." Oncogenesis **6**(3): e303.

Yu, X. and S. He (2016). "The interplay between human herpes simplex virus infection and the apoptosis and necroptosis cell death pathways." Virol J **13**: 77.

Yu, X., Y. Li, Q. Chen, C. Su, Z. Zhang, et al. (2015). "Herpes Simplex Virus 1 (HSV-1) and HSV-2 Mediate Species-Specific Modulations of Programmed Necrosis through the Viral Ribonucleotide Reductase Large Subunit R1." J Virol **90**(2): 1088-1095.

Zabierowski, S. and N. A. DeLuca (2004). "Differential cellular requirements for activation of herpes simplex virus type 1 early (tk) and late (gC) promoters by ICP4." J Virol **78**(12): 6162-6170.

Zabolotny, J. M., C. Krummenacher and N. W. Fraser (1997). "The herpes simplex virus type 1 2.0-kilobase latency-associated transcript is a stable intron which branches at a guanosine." J Virol **71**(6): 4199-4208.

Zarember, K. A. and P. J. Godowski (2002). "Tissue expression of human Toll-like receptors and differential regulation of Toll-like receptor mRNAs in leukocytes in response to microbes, their products, and cytokines." J Immunol **168**(2): 554-561.

Zaritsky, L. A., J. R. Bedsaul and K. C. Zoon (2015). "Virus Multiplicity of Infection Affects Type I Interferon Subtype Induction Profiles and Interferon-Stimulated Genes." J Virol **89**(22): 11534-11548.

Zenner, H. L., R. Mauricio, G. Banting and C. M. Crump (2013). "Herpes simplex virus 1 counteracts tetherin restriction via its virion host shutoff activity." J Virol **87**(24): 13115-13123.

Zerbino, D. R. and E. Birney (2008). "Velvet: algorithms for de novo short read assembly using de Bruijn graphs." Genome Res **18**(5): 821-829.

Zhang, D., C. Su and C. Zheng (2016). "Herpes Simplex Virus 1 Serine Protease VP24 Blocks the DNA-Sensing Signal Pathway by Abrogating Activation of Interferon Regulatory Factor 3." J Virol **90**(12): 5824-5829.

Zhang, Q. and K. T. Jeang (2013). "Long non-coding RNAs (lncRNAs) and viral infections." Biomed Pharmacother **3**(1): 34-42.

Zhang, S. Y., E. Jouanguy, S. Ugolini, A. Smahi, G. Elain, et al. (2007). "TLR3 deficiency in patients with herpes simplex encephalitis." Science **317**(5844): 1522-1527.

Zhang, X., D. Bogunovic, B. Payelle-Brogard, V. Francois-Newton, S. D. Speer, et al. (2015). "Human intracellular ISG15 prevents interferon-alpha/beta over-amplification and auto-inflammation." Nature **517**(7532): 89-93.

Zhang, X., F. A. Castelli, X. Zhu, M. Wu, B. Maillere and L. BenMohamed (2008). "Gender-dependent HLA-DR-restricted epitopes identified from herpes simplex virus type 1 glycoprotein D." Clin Vaccine Immunol **15**(9): 1436-1449.

Zheng, C. and C. Su (2017). "Herpes simplex virus 1 infection dampens the immediate early antiviral innate immunity signaling from peroxisomes by tegument protein VP16." Virol J **14**(1): 35.

Zhenilo, S., I. Deyev, E. Litvinova, N. Zhigalova, D. Kaplun, A. Sokolov, A. Mazur and E. Prokhortchouk (2018). "DeSUMOylation switches Kaiso from activator to repressor upon hyperosmotic stress." Cell Death Differ.

Zhou, C. and D. M. Knipe (2002). "Association of herpes simplex virus type 1 ICP8 and ICP27 proteins with cellular RNA polymerase II holoenzyme." J Virol **76**(12): 5893-5904.

Zhou, Z. H., M. Dougherty, J. Jakana, J. He, F. J. Rixon and W. Chiu (2000). "Seeing the herpesvirus capsid at 8.5 A." Science **288**(5467): 877-880.

Zhu, H., J. P. Cong and T. Shenk (1997). "Use of differential display analysis to assess the effect of human cytomegalovirus infection on the accumulation of cellular RNAs: induction of interferon-responsive RNAs." Proc Natl Acad Sci U S A **94**(25): 13985-13990.

Zhu, L. and H. Zhu (2014). "Ocular herpes: the pathophysiology, management and treatment of herpetic eye diseases." Virol Sin **29**(6): 327-342.

Zolini, G. P., G. K. Lima, N. Lucinda, M. A. Silva, M. F. Dias, et al. (2014). "Defense against HSV-1 in a murine model is mediated by iNOS and orchestrated by the activation of TLR2 and TLR9 in trigeminal ganglia." J Neuroinflammation **11**: 20.

Zschaler, J., D. Schlorke and J. Arnhold (2014). "Differences in innate immune response between man and mouse." Crit Rev Immunol **34**(5): 433-454.

Zurcher, T., J. Pavlovic and P. Staeheli (1992a). "Mechanism of human MxA protein action: variants with changed antiviral properties." EMBO J **11**(4): 1657-1661.

Zurcher, T., J. Pavlovic and P. Staeheli (1992b). "Mouse Mx2 protein inhibits vesicular stomatitis virus but not influenza virus." Virology **187**(2): 796-800.

Zurcher, T., J. Pavlovic and P. Staeheli (1992c). "Nuclear localization of mouse Mx1 protein is necessary for inhibition of influenza virus." J Virol **66**(8): 5059-5066.